



HAL
open science

Optimization of coupling in near field by magnetic field steering

Jaafar Al-Sinayyid

► **To cite this version:**

Jaafar Al-Sinayyid. Optimization of coupling in near field by magnetic field steering. Electric power. Université Gustave Eiffel, 2022. English. NNT : 2022UEFL2081 . tel-04822625

HAL Id: tel-04822625

<https://theses.hal.science/tel-04822625v1>

Submitted on 6 Dec 2024

HAL is a multi-disciplinary open access archive for the deposit and dissemination of scientific research documents, whether they are published or not. The documents may come from teaching and research institutions in France or abroad, or from public or private research centers.

L'archive ouverte pluridisciplinaire **HAL**, est destinée au dépôt et à la diffusion de documents scientifiques de niveau recherche, publiés ou non, émanant des établissements d'enseignement et de recherche français ou étrangers, des laboratoires publics ou privés.



**UNIVERSITÉ GUSTAVE EIFFEL
ÉCOLE DOCTORALE MSTIC**

A thesis presented for the degree of
Doctor of Philosophy in Université Gustave Eiffel

**OPTIMIZATION OF COUPLING IN
NEAR FIELD BY MAGNETIC FIELD
STEERING**

Localization in Wireless Power Transfer and RFID

BY JAAFAR ALSINAYYID

Thesis supervisor :

Gaëlle Lissorgues Professeur de ESIEE PARIS, Directrice de l'École Doctorale MSTIC

Doctorate coordinator :

Hakim Takhedmit Maître de Conférences Laboratoire ESYCOM, Université Gustave Eiffel

Patrick Poulichet Enseignant-Chercheur Laboratoire ESYCOM, Université Gustave Eiffel

Reporters :

Christian Vollaire Professeur des Universités, École Centrale de Lyon

Eric Labouré Professeur des Universités, Université Paris-Saclay

Examiners :

Laurent Laguerre Directeur de Recherche, laboratoire GERS-GeoEND, Université Gustave Eiffel

Anne-Claude Tarot Maître de Conférences, Université Rennes 1

Marjorie Grzeskowiak-Lucas Maîtresse de Conférences , INSA Toulouse

Guest:

Antoine Diet Maître de Conférences , Geeps, Centrale Supélec

ESYCOM LABORATORY CNRS UMR 9007

UNIVERSITE GUSTAVE EIFFEL

France

2022

ABSTRACT

IPT (Inductive Power Transfer) is an approach based on magnetic coupling to realize a WPT (Wireless Power Transfer) system. In applications using IPT as a mean for transferring power, like RFID, it is of great interest to have a free positioning system, meaning without or at least fewer constraints on relative positioning and orientation between the sender and the receiver.

One of the problems which face the free positioning WPT by using IPT is the great sensitivity of the system to lateral and orientational misalignment between the sender and the receiver of power.

This could hugely reduce the efficiency of the whole system for certain lateral and orientational misalignments, resulting in null points for the coupling coefficient, therefore no power transfer in general or no detection in case of RFID (Radio Frequency Identification).

Another subject related to IPT is the ability to localize the receiver. The ability of the transmitter to localize the receiver could be interesting for applications such as IoT (Internet of Things).

In Qi standards for wireless power transfer, the localization is performed by using a coils array.

Here the resolution of localization is equal to the diameter of the coils in the transmitter array. Decreasing the diameter of coils in transmitters increases the resolution of localization but also reduces the range of power transfer. This in an inevitable trade-off.

In this work we tried to address these problems.

First We consider the problem of misalignment between the receiver and the transmitter.

For this we propose a reconfigurable antenna which changes its structure by turning on and off specific parts of itself. This will guarantee the effective power transfer in the range of interest, regardless of the lateral and orientational misalignments between the sender and the receiver. Experimental verification will shows the feasibility of this method.

Then we mention some of deficiency of the proposed method and try to enhance it furthermore. At this point we turn our intention to the subject of localization for enhancing the performance of the IPT system.

This will lead us to a system which is performing the localization in a fast and reliable way. In first step we will show the feasibility of the proposed method in general and it is not a practical system yet.

In this first step we assumed to have access to both transmitter and the receiver. This is what we call a two ports network. A real practical system should be an one port network in which we don't assume having access to the receiver.

To move from one port network to two port network is our next step. Here we learn that we need to work in resonance frequency for acceptable performance of the system.

In all these steps we start by explaining the main idea. Then we simulate the proposed

ideas. We will rely largely on MATLAB for our simulation and beside it we will use other software like Ansys Q3D.

Then we will run experiments for testing the proposed ideas and methods. The experimental results shows the feasibility of our methods. At each step we will discuss the errors in experimental results and its origin and how to reduce it. We will end our work by mentioning the limitation and shortcomings of our work and by mentioning the perspective of this work.

RESUME

L'IPT (Inductive Power Transfer) est une approche basée sur le couplage magnétique pour réaliser un système WPT (Wireless Power Transfer).

Dans les applications utilisant l'IPT comme moyen de transfert de puissance, comme la RFID, il est très intéressant d'avoir un système de positionnement libre, c'est-à-dire sans ou au moins avec moins de contraintes sur le positionnement et l'orientation relatifs entre l'émetteur et le récepteur. Ces contraintes sont là pour garantir une inductance mutuelle non nulle (ou un déficit d'inductance mutuelle).

L'un des problèmes auxquels est confronté le WPT à positionnement libre en utilisant l'IPT est la grande sensibilité du système au désalignement latéral et d'orientation entre l'émetteur et le récepteur de puissance.

Dans ce travail, nous essayons de résoudre le problème du transfert de puissance inductif (TPI) dû au manque d'inductance mutuelle entre le récepteur et l'émetteur.

En raison de la nature vectorielle du champ magnétique et du mécanisme de la loi de Faraday, il est possible que le récepteur se trouve dans des zones nulles.

Ce sont des endroits et des orientations du récepteur dans lesquels le récepteur n'a pas d'inductance mutuelle avec l'émetteur.

Lorsque l'inductance mutuelle est nulle ou très faible, il n'y a pas de transfert de puissance, ce qui constitue un échec pour les systèmes de transfert de puissance ou les applications qui utilisent l'idée de transfert de puissance de manière intégrée, comme la RFID.

La première méthode que nous proposons est basée sur les TLA (Twisted Loop Antenna) qui peuvent être considérées comme un réseau de bobines. Différentes structures des TLA créent en effet différents modèles de courant électrique.

À leur tour, les différents modèles de courant électrique créent différents modèles de champs magnétiques.

Par conséquent, cela nous donne un moyen de contrôler le champ magnétique en contrôlant quel TLA est excité et quel TLA ne l'est pas.

Cette méthode est très bien connue pour le rayonnement en champ lointain, et nous l'avons appliquée aux champs proches.

C'est l'idée principale qui se cache derrière le guidage du faisceau par champ magnétique. La même méthode pourrait être utilisée pour augmenter la portée du transfert d'énergie sans fil.

L'idée d'utiliser une structure de type réseau pour augmenter l'efficacité du transfert d'énergie a été proposée précédemment, mais nous avons adopté une nouvelle approche et proposé une application de cette méthode.

Cependant, nous avons adopté une nouvelle approche et proposé une application de ce principe, à savoir un système qui garantit le transfert de puissance indépendamment du désalignement entre l'émetteur et le récepteur.

La méthode suppose que le volume de l'espace dans lequel le récepteur est placé est donné à

l'avance et qu'il dépend de l'application en question. Elle suppose également que l'inductance mutuelle minimale requise est donnée à l'avance.

Cela dépend également de l'application à laquelle nous avons affaire et il n'est pas difficile de le déterminer.

Lorsque le volume d'intérêt et l'inductance mutuelle minimale requise sont donnés, nous divisons le volume d'intérêt en cellules.

Ensuite, chaque cellule est couverte en trois étapes. À chaque étape, on choisit une configuration du TLA qui crée un champ magnétique adapté à une orientation parallèle aux plans XY, XZ ou ZY. Ce faisant, nous libérons le récepteur de toute contrainte sur son orientation. Lorsque les cellules couvrent tout le volume d'intérêt, le récepteur peut se trouver n'importe où dans le volume d'intérêt. La simulation a été réalisée suivie de mesures.

Les mesures ont montré un bon accord entre les calculs et les valeurs mesurées pour les inductances mutuelles, ce qui confirme la faisabilité de la méthode.

Cette méthode est raisonnable s'il y a un bon nombre de récepteurs en même temps dans le volume d'intérêt.

Cependant, s'il y a quelques récepteurs ou même un seul d'entre eux (par exemple pour la recharge sans fil de robots, de voitures, de drones...), la méthode devrait quand même fonctionner, mais elle ne semble pas être une approche très efficace.

La raison en est que l'inductance mutuelle effective que la bobine réceptrice aura dans cette méthode est la moyenne des inductances mutuelles que la bobine réceptrice a à chaque étape. appropriée pour le récepteur, ce champ magnétique change à l'étape suivante et dans cette nouvelle étape, le champ magnétique n'est pas nécessairement approprié.

étape suivante et dans cette nouvelle étape, le champ magnétique n'est plus nécessairement adapté et le récepteur doit attendre jusqu'à ce que la répétition de la configuration qui génère le champ magnétique approprié.

récepteurs ou même un seul récepteur, ce n'est plus une méthode efficace.

Une meilleure solution possible est d'avoir une sorte de localisation. Lorsque la localisation est effectuée, le champ magnétique peut être dirigé de manière optimale pour la position et l'orientation particulières du récepteur.

Il convient de préciser que, bien que nous ayons mentionné ici la localisation comme méthode d'amélioration du couplage magnétique, la capacité de localisation en elle-même est un sujet intéressant à considérer.

Pour ce faire, nous avons proposé un algorithme basé sur la mesure de l'inductance mutuelle entre l'émetteur et le récepteur.

Dans ce cas, l'émetteur est une grille de bobines circulaires. Mais l'idée est générale et pourrait être appliquée à d'autres types de grilles d'émetteurs.

L'inductance mutuelle mesurée entre l'émetteur et le récepteur pourrait être utilisée pour la localisation du récepteur.

Cette méthode nécessite une connaissance a priori du volume d'intérêt. Il s'agit d'un regain autour de l'émetteur dans lequel le récepteur pourrait être localisé.

Dans cette méthode, nous divisons le volume d'intérêt en une grille de points en 3D. Ensuite, nous supposons que le centre du récepteur se trouve à l'un de ces points.

En général, nous pouvons supposer que le récepteur peut avoir n'importe quelle orientation et que cela ne changera rien à l'algorithme, mais pour simplifier, supposons que nous sommes intéressés par la recherche de la position du récepteur et que l'orientation du récepteur est fixe. Nous devons également calculer ce que nous appelons la matrice pré-calculée de l'inductance mutuelle.

Il s'agit de la valeur de l'inductance mutuelle entre le récepteur et l'émetteur si le récepteur

se trouvait en n'importe quel point des grilles 3D du volume d'intérêt.

Pour notre hypothèse selon laquelle le récepteur a une orientation fixe, il s'agit d'une matrice 3D.

Si nous ne voulons pas avoir de contrainte sur l'orientation, ce sera une matrice 5d.

Notre émetteur est une grille de bobines que nous pouvons choisir et exciter séparément. Nous commençons par choisir une bobine de la grille de l'émetteur puis nous mesurons l'inductance mutuelle entre le récepteur et l'émetteur.

Ensuite, nous comparons cette inductance mutuelle mesurée avec la matrice d'inductance mutuelle pré-calculée correspondant à la bobine excitée et nous en déduisons toutes les positions possibles du récepteur qui donnent lieu à l'inductance mutuelle mesurée.

Nous trouverons un ensemble de positions qui ont la même inductance mutuelle. La position n'est pas déterminée de manière unique.

Nous choisissons une autre bobine et procédons de la même manière. Encore une fois, nous ne trouverons pas de position unique comme réponse.

Mais si ce processus est rapide (ce qui est le cas en pratique) par rapport à la vitesse de déplacement du récepteur (s'il se déplace), nous pouvons supposer qu'au moment de la mesure, le récepteur se trouvait au même endroit.

Ainsi, la position réelle du récepteur devrait être l'intersection de deux ensembles possibles de positions du récepteur que nous avons calculés précédemment. Cela signifie que nous devons prendre l'intersection des deux.

Si leur intersection n'est pas encore unique, nous passons à la troisième bobine, puis à la quatrième et ainsi de suite, jusqu'à ce que nous ayons une position unique.

À ce stade, la localisation est terminée.

Les simulations ont été réalisées à l'aide d'un code MATLAB spécifique et son applicabilité a été démontrée par une série d'expériences.

Les résultats expérimentaux montrent que l'algorithme fonctionne comme prévu et qu'il est possible de localiser le récepteur en fonction de son couplage magnétique mutuel avec l'émetteur.

Si la même procédure est exécutée en continu, on peut suivre dynamiquement le mouvement du récepteur.

On a supposé que le récepteur se trouve dans une position inconnue mais toujours parallèle à l'émetteur. Cette hypothèse a été faite pour des raisons de simplicité et n'affecte pas le principe et l'utilité de l'algorithme.

L'algorithme pourrait être modifié pour localiser un récepteur dans une situation plus générale dans laquelle le récepteur pourrait avoir n'importe quelle orientation arbitraire, et cette modification sera l'une des perspectives de ce travail.

Cependant, cette hypothèse n'est pas une réelle limitation. La vraie limitation vient du fait de considérer plus d'un récepteur.

L'algorithme, dans son état actuel, est capable de localiser un seul récepteur dans le volume d'intérêt.

Si nous voulons localiser plus d'un récepteur, nous devons calculer la matrice d'inductance mutuelle pré-calculée pour chaque bobine de l'émetteur et toutes les combinaisons du récepteur dans leurs différentes positions possibles.

Comme le nombre de récepteurs est faible, le code peut être généralisé pour traiter ces situations. Mais si le nombre de récepteurs augmente, la mémoire et la puissance de calcul du système augmenteront et le code ne sera plus applicable (ou du moins pas en temps réel).

Il s'agit d'une réelle limitation et la surmonter est une autre des perspectives de ce travail.

Mais il ne faut pas oublier qu'en cas de présence d'un certain nombre de récepteurs dis-

tribués dans le volume d'intérêt, la méthode proposée au chapitre 2 devient plus pertinente et dans ce cas, la localisation n'est probablement pas nécessaire.

Après la localisation, on a également montré comment la connaissance de l'emplacement du récepteur pouvait être utilisée pour améliorer le couplage magnétique entre l'émetteur et le récepteur.

Au moyen d'une grille de bobines commutables, le champ magnétique est orienté correctement vers le récepteur.

Cette approche de formation de faisceau permet d'augmenter l'inductance mutuelle entre l'émetteur et le récepteur et d'accroître l'efficacité de ces systèmes de transfert de puissance par induction.

Pour faire cela systématiquement, nous divisons le volume d'intérêt en cellules, puis nous déterminons la configuration de l'émetteur qui convient à chaque cellule.

Lorsque nous découvrons (en exécutant l'algorithme de localisation) dans quelle cellule se trouve le récepteur, nous choisissons une configuration de la grille qui crée un champ magnétique adapté à cette cellule spécifique.

L'expérience montre la validité du calcul et de la simulation de la direction du faisceau en fonction de la position du récepteur.

Jusqu'à présent, nous travaillons avec un réseau à deux ports. C'est la même chose que de dire que nous avons accès à la fois à l'émetteur et au récepteur.

avoir accès à l'émetteur est simple mais avoir accès au récepteur n'est pas pratique dans la plupart des situations réalistes.

dans la plupart des situations réalistes. Dans l'étape suivante, nous avons montré que si nous ajoutons des éléments de résonance et d'adaptation à l'antenne de l'émetteur et à l'antenne du récepteur, il devient possible de déduire la valeur de l'inductance mutuelle entre l'émetteur et le récepteur en mesurant l'impédance d'entrée de l'émetteur sans avoir besoin de l'aide de l'émetteur.

l'impédance d'entrée de l'émetteur sans avoir besoin d'accéder au récepteur.

Pour ce faire, la valeur des autres éléments du système émetteur-récepteur doit être connue. Nous aurons une expression qui nous donnera l'impédance d'entrée en fonction de l'inductance mutuelle.

En mesurant l'impédance d'entrée, on peut déduire l'inductance mutuelle. Une fois cette opération effectuée, la suite est identique à ce que nous avons déjà expliqué. La valeur déduite de l'inductance La valeur de l'inductance mutuelle déduite peut être utilisée pour exécuter l'algorithme de localisation.

Dans ce cas également, les simulations ont été faites en utilisant un code MATLAB et son applicabilité a été démontrée en exécutant un ensemble de tests.

et son applicabilité a été démontrée en effectuant une série d'expériences. Les résultats expérimentaux montrent que l'algorithme fonctionne comme prévu. Dans les deux cas, nous avons une certaine erreur dans la localisation.

Comme on peut s'y attendre, l'erreur dans le réseau à un port est plus importante que celle dans les réseaux à deux ports. Cependant, même avec cette erreur, la méthode semble localiser le récepteur avec une précision plus ou moins acceptable. Cette précision peut être contrôlée pour correspondre à la précision requise pour des applications concrètes.

Acknowledgements

I would like to express my gratitude and my deep appreciation to my director and supervisors : Gaëlle LISSORGUES, Patrick POULICHET and Hakim TAKHEDMIT who guided me throughout this project.

I wish to extend my special thanks to Marjorie Grzeskowiak-Lucas and Antoine Diet for the assistance provided by them.

I also would like to thanks the reviewers and all the jury members.

I wish to acknowledge the help and support provided by all the staff in the ESYCOM laboratory.

I would also like to thank my friends and colleges for their support and help.

Contents

1	INTRODUCTION TO WIRELESS POWER TRANSFER AND RADIO FREQUENCY IDENTIFICATION IN NEAR FIELD	1
1.1	FAR-FIELD AND NEAR-FIELD IN WPT	1
1.2	TYPES OF WIRELESS POWER TRANSFER IN NEAR-FIELD	3
1.3	THE MAGNETIC INDUCTIVE COUPLING WPT	4
1.3.1	BASIC WPT SYSTEM	4
1.3.2	EFFICIENCY OF WPT	6
1.3.3	MOBIL RECEIVERS IN WPT	7
1.4	APPLICATIONS OF WPT IN MOBILE IPT	10
2	A RECONFIGURABLE ANTENNA FOR ENHANCING THE MAGNETIC COUPLING IN IPT AND RFID	13
2.1	INTRODUCTION	13
2.2	MAGNETIC FIELD AND BIOT-SAVART LAW	15
2.3	MAGNETIC FIELD BEAM STEERING	21
2.4	MUTUAL INDUCTANCE	32
2.5	A Reconfigurable Antenna for Enhancing the Magnetic Coupling	50
2.6	Measurement	66
3	A RECONFIGURABLE COIL GRID FOR RECEIVER LOCALIZATION IN INDUCTIVE POWER TRANSFER	77
3.1	INTRODUCTION	77
3.2	RECONFIGURABLE TRANSMITTER MULTI-COILS ANTENNA	85
3.3	LOCALIZATION METHOD IN NEAR FIELD	88
3.4	SIMULATION AND EXPERIMENTAL RESULT FOR LOCALIZATION	99
3.5	REDIRECTING THE MAGNETIC FIELD BY CHANGING THE CONFIGURATION OF THE TRANSMITTER BASED ON THE LOCALIZED RECEIVER AND EXPERIMENTAL RESULTS	116
3.6	CONCLUSION	122
4	ONE PORT RECONFIGURABLE COIL GRID FOR RECEIVER LOCALIZATION IN INDUCTIVE POWER TRANSFER	123
4.1	INTRODUCTION	123
4.2	MAGNETICALLY COUPLED RESONATOR	124
4.3	Integrability of the localization algorithm in in-use standards	137
4.4	LOCALIZATION BY MEASURING THE INPUT IMPEDANCE	145
4.5	CONCLUSION	160

CONTENTS

List of Figures

1.1	Near field and Far field around the source,[52].	2
1.2	Classification of WPT technologies,[51].	3
1.3	Diagrams of magnetic field coupling, magnetic resonance coupling, electric field coupling, and electric resonance coupling,[63].	5
1.4	Conceptual diagram of basic WPT system configuration,[63].	6
1.5	On left normal spiral coil for WPT. On the right a new design proposed in [15] to enhance the Q factor of the coils. For each turn of the coil the width of the coil reduces.[15].	7
1.6	In a two coil WPT system, which has low coupling coefficient, the intermediate coil boosts the self-inductance of the primary side at around the resonance frequency of the intermediate coil, so that the coupling coefficient is compensated.[56].	8
1.7	Three-orthogonal-coil topology for omnidirectional WPT systems,[71].	8
1.8	3D field orientation WPT system. By controlling the amplitude and the phase of current in each of the three coils, one could control the magnetic field in space around them [74].	9
1.9	Main features of WPT systems,[52]. What we will consider in this study is enclosed in black circles	10
1.10	Flying drone powered by IPT. The black circles indicate the position of receiver and the transmitter coils.[25].	11
1.11	A general classification of power transfer in terms of mobility, distance, and means of powering[60].	11
1.12	A free positioning IPT according to Qi [72]-[30].	12
2.1	When we have a surface S in a magnetic field, it could be divided in a number of infinitesimal surfaces. What is important here is the angle α_j between the norm vector of the surface and the direction of the magnetic field at the infinitesimal surfaces ΔS_j . [59]	14
2.2	Biot-Savart law [57]	15
2.3	The circle in the left is approximated by a polygon of 7 vertices, which is not a very good approximation. As we increase the number of vertices to 15 (in the middle) and 50 (on the right) for example, the polygon becomes better and better approximation of a circle. The polygon on the right is a good approximation and almost completely covers the circle underneath it.	16
2.4	Calculated magnetic field as vectors due to small straight line (shown in red) of electric current.	17

LIST OF FIGURES

2.5	Calculated magnetic field as line of field due to small straight line (shown in red) of electric current.	18
2.6	Current loop in a cylindrical coordinate system [57].	19
2.7	The magnetic field of a filamentary loop of one turn as vectors.	20
2.8	The magnetic field of a filamentary loop of one turn as field lines.	20
2.9	B_x component of the magnetic field of a loop carrying 1 A current. The magnetic field is in Tesla and the X,Y and Z axes in Meter.	21
2.10	B_y component of the magnetic field of a loop carrying 1 A current. The magnetic field is in Tesla and the X,Y and Z axes in Meter.	22
2.11	B_z component of the magnetic field of a loop carrying 1 A current. The magnetic field is in Tesla and the X,Y and Z axes in Meter.	22
2.12	B_x component of the magnetic field of a circular loop current of diameter of 10 cm carrying 10 mA current. The field is at a distances of 4 cm above the loop. The loop is shown in white. The magnetic field is in Tesla.	23
2.13	Absolute value of B_x component of the magnetic field of a circular loop current of diameter of 10 cm carrying 10 mA current. The field is at a distances of 4 cm above the loop. The loop is underneath the surface and could not be seen here. The magnetic field is in Tesla.	24
2.14	B_z component of the magnetic field of a circular loop current of diameter of 10 cm carrying 10 mA current. The field is at a distances of 4 cm above the loop. The loop is underneath the surface and could not be seen here. The magnetic field is in Tesla.	25
2.15	Commercial application of guided positioning. This is not a free positioning system. The receiver should be positioned by the user above the coil (shown on the left), otherwise the system will not work.[29].	26
2.16	a. The free positioning method based on a mechanically moveable primary coil is illustrated. The white circle is the receiver that could be anywhere in certain range. The transmitter, the blue circle, moves underneath to locate itself in better position. b. The method based on a selective excitation of a coil array is illustrated. [32]	26
2.17	When there is no phase difference between applied current to (for example) two coils, the resultant magnetic field (the black arrow) don't change the direction because the components always change in proportion (left panel) so the resultant vector remains in the same direction. When there is phase difference between applied current to two coils, the resultant magnetic field (the black arrow) changes the direction because the components are not any more changing in same proportion (right panel). blue arrows represent the magnetic field due to blue current in one coil in three instances of time, red arrows represent the magnetic field due to red current in second coil in three instances of time, and the black arrow is the final magnetic field.	27
2.18	Modifying the magnitude of magnetic field due to two different parts of the structure shown in blue vectors, enables us to control the direction of the total magnetic field in any direction. Two black lines in the right of the figure show the direction of the total magnetic field before and after of the rotation of the field. If the currents that generate B1 and B2 are in phase, the total magnetic field will always oscillate in the same direction.	28
2.19	3-D magnetic beam steering WPT system with a loaded receiver coil resonator[48].	29

LIST OF FIGURES

2.20	A twisted loop antenna in its simplest possible configuration. It is composed of two coplanar coils next to each other. Both coils are made of one turn, so the current is the same in both of them. The electric current in one loop is in clockwise direction and in the other loop in anti clockwise direction (shown by blue arrows). The diameter of each loop is 4 cm. The black lines are the magnetic field lines due to this configuration in space around the antenna.	29
2.21	A twisted loop antenna in a configuration consisting of four coils. The diameter of small coils are 4 cm and the diameter of larger coils are 8 cm. Coils are coplanar and each coil has one turn, so they have the same electric current. The electric current in one small and big loop is in clockwise direction, and in the other small and big loop in anti clockwise direction (shown by blue arrows). The black lines are the magnetic field due to this configuration in space around the antenna.	30
2.22	A twisted loop antenna in a more complicated configuration consisting of eight coils. This configuration is two copy of the configuration shown in Fig.2.21 with one of them rotated in respect to the other by 90 degree. The all structure is coplanar. The black lines are the magnetic field due to this configuration in space around the antenna.	30
2.23	The surface shows the value of B_x component of the field in a plane parallel to the plane on which the twisted loop antenna is placed (that is X-Y) and at 4 cm above the twisted loop antenna, for one possible configuration of a twisted loop antenna shown in Fig. 2.22. The white circle is our target point where we want to increase the value of B_x	32
2.24	The surface shows the value of B_x component of the field in a plane parallel to the plane on which the twisted loop antenna is placed (that is X-Y) and at 4 cm above the twisted loop antenna, for one possible configuration of a twisted loop antenna shown in Fig. 2.22. In comparison to Fig. 2.23, this configuration enhance the value B_x component of the field in the targeted point shown in white circle.	33
2.25	Self Inductance of a current loop [57].	33
2.26	Mutual inductance between two loops. $\Psi_1 = \Psi_2$ [57].	36
2.27	a. A receiver (tag) with multi turns coil(loop 1) b. A transmitter (reader) with multi turn coil (loop 2) [28].	37
2.28	A transmitter of 1 turn coil with 5 cm radius carrying 1 mA current placed in the origin of the coordinate system. A receiver of a 1 turn coil with 1 cm radius shown in black color placed at $(x,y,z)=(0\text{ cm},0\text{ cm},5\text{ cm})$. The receiver normal vector is $(n = -1j)$	39
2.29	The magnitude of each component of the magnetic field due to the transmitter are shown as we sweep along the X axis from $x=-20\text{ cm}$ to $x=20\text{ cm}$, for fixed $z=5\text{ cm}$ and fixed $y=0\text{ cm}$. The two black dashes show the border of region shown in Fig. 2.28, which expands from -10 to 10 cm. B_y is zero everywhere.	39
2.30	The mutual inductance between transmitter and receiver is shown as we sweep along the X axis from $x=-20\text{ cm}$ to $x=20\text{ cm}$, for fixed $z=5\text{ cm}$ and fixed $y=0\text{ cm}$. It is zero everywhere.	40
2.31	The magnitude of each component of the magnetic field due to the transmitter are shown as we sweep along the X axis from $x=-20\text{ cm}$ to $x=20\text{ cm}$, for fixed $z=5\text{ cm}$ and fixed $y=5\text{ cm}$	41

LIST OF FIGURES

2.32	The mutual inductance between transmitter and receiver is shown as we sweep along the X axis from $x=-20$ cm to $x=20$ cm, for fixed $z=5$ cm and fixed $y=5$ cm.	41
2.33	The mutual inductance between transmitter and receiver is shown for the same condition of Fig. 2.29 but this time increasing the diameter of the receiver loop by the factor of 4. This flatten the mutual inductance.	42
2.34	The variable that we use to rotate the receiver loop.	43
2.35	The variation of the mutual inductance of our example when we fix the position of the center of the coil to the ($x=0$ cm, $y= 0$ cm, $z= 5$ cm). This is an arbitrary position and the same figure could be plotted for any point.	44
2.36	The variation of the induced voltage in the receiver coil when we fix the position but change the orientation of the receiver coil. The receiver is in the plane parallel to the transmitter.	44
2.37	The variation of the induced voltage in the receiver coil when we fix the position but change the orientation of the receiver coil. The receiver has 30 degree angle with the plane parallel to the transmitter.	45
2.38	The variation of the induced voltage in the receiver coil when we fix the position but change the orientation of the receiver coil. The receiver has 65 degree angle with the plane parallel to the transmitter.	45
2.39	The variation of the induced voltage in the receiver coil when we fix the position but change the orientation of the receiver coil. The receiver has 90 degree angle with the plane parallel to the transmitter.	45
2.40	The volume of interest is a black rectangular cuboid extending 30 cm along X axis, 30 cm along Y axis and 20 cm along Z axis. The receiver is a loop of 1 cm radius in XZ plane. The transmitter is a circular coil of radius 10 cm placed on the XY plane with its center at the origin, carrying 1mA current. The planes show the value of mutual inductance with contours of equal values of mutual inductance.	47
2.41	The volume of interest is a black rectangular cuboid extending 30 cm along X axis, 30 cm along Y axis and 20 cm along Z axis. The receiver is a loop of 1 cm radius in XZ plane. The transmitter is a TLA of radius 10 cm which is placed in symmetrical way around the origin in the XY plane. Each loop of the TLA carry a current in 1 mA in opposite direction (one in clockwise other in anti clockwise). The planes show the value of mutual inductance with contours of equal values of mutual inductance.	48
2.42	The volume of interest is a black rectangular cuboid extending 30 cm along X axis, 30 cm along Y axis and 20 cm along Z axis. The receiver is a loop of 1 cm radius in XZ plane. The transmitter is a circular coil of radius 10 cm placed on the XY plane with its center at the origin, carrying 1mA current. Here we fix X coordinate to $X=0$, fix Z coordinate to $Z=10$ cm, then we sweep along Y axis. The blue curve shows the variation of the mutual inductance as we move along Y axis.	49

LIST OF FIGURES

2.43	The volume of interest is a black rectangular cuboid extending 30 cm along X axis, 30 cm along Y axis and 20 cm along Z axis. The receiver is a loop of 1 cm radius in XZ plane. The transmitter is a TLA of radius 10 cm which is placed in symmetrical way around the origin in the XY plane. Each loop of the TLA carry a current in 1 mA in opposite direction (one in clockwise other in anti clockwise). Here we fix X coordinate to X=0, fix Z coordinate to Z=10 cm, then we sweep along Y axis. The blue curve shows the variation of the mutual inductance as we move along Y axis.	49
2.44	A scenario for RFID application of the magnetic coupling for the shopping. A cart with a RFID reader implanted underneath it. This reader can read all the items and calculate the price automatically in the exit without the customer having to scan all of them one by one. Black circles show the receiver coils attached to each object. The cart is shown in blue and the volume of interest is a black box.	51
2.45	Each loop of the TLA is connected to next loop through a switch that connects pin C, to either pin A or B. Here we show 3 loops. The vertical distance between loops is exaggerated to make it easier to show the concept. These switches are controlled by a circuitry attached to the TLA.	53
2.46	Those are the three loops shown in Fig. 2.45. Here the switches state are chosen by controlling mechanism in a way that all three loops are connected and are part of the TLA. The loops that carry the electric current are shown in red.	54
2.47	Those are the three loops shown in Fig. 2.45. Here the switches state are chosen by controlling mechanism in a way that we disconnect the middle loop and it is not part of the TLA. The loops that are part of the TLA and conduct current are shown in red, and the loop that is excluded from TLA and does not conduct current is shown in green.	54
2.48	Connecting each loop to other through switches also enables us to change the direction of the current in each loop. If the current I enters the loop on the right in a anti clock wise direction by switching the switch connecting it to the loop on the left side we can control the direction of the current in the left side loop. There are two possible directions for current, clock wise and anti clock wise directions.	55
2.49	Here the cell-1 is a rectangular cuboid extending 4 cm along X axis, 8 cm along Y axis and 8 cm along Z axis. The cell-1 is shown in blue. The goal is to create a field which is suitable for the orientation of the receiver if it was parallel to the XY plane (shown by blue circle). On the left we see such configuration. The arrows show the direction of current in each loop. On the right, we see the Z component of the configuration. We can see it covers all the cell.	56
2.50	Here we still considering cell-1 which is shown in blue. The goal is to create a field which is suitable for the orientation of the receiver if it was parallel to the XZ plane (shown by blue circle). On the left we see such configuration. The arrows show the direction of current in each loop. The red loop are disconnected and are not part of the configuration. On the right we see the Y component of the configuration. We can see it cover all the cell.	57

LIST OF FIGURES

2.51	Here we are still considering cell-1 which is shown in blue. The goal is to create a field which is suitable for the orientation of the receiver if it was parallel to the YZ plane (shown by blue circle). On the left we see such configuration. The arrows show the direction of current in each loop. On the right we see the X component of the configuration. We can see it covers all the cell.	58
2.52	On the right we have the total magnetic field (in red) in a certain point due to the magnetic fields (dashed blue) of two different coils. If we want to rotate the field for example in the Y direction, we realize one possible way is to reverse the direction of the magnetic field due to coil 2, by changing the direction of current in it, and at the same time by increasing its strength, by increasing its turns. The results is shown on the left side of the figure with the total magnetic field in Y direction, which was our goal.	59
2.53	The volume of interest is a box extending in Y axis from -10 cm to 10 cm. In X extending from -6 cm to 6 cm. In Z from -6 cm to 6 cm. This volume is divided into three cells, shown here in three different colors. cell-1 in red, cell-2 in blue and cell-3 in black. The receiver coils could be anywhere in this volume of interest and it could have any orientation.	60
2.54	The structure of a TLA chosen for experimental verification of our method. The TLA is consisting of four loops. The two larger loops have diameter of 8 cm, one of the small loops has diameter of 6 cm and another small loop has the diameter of 5 cm. It is placed in the XY plane centered in the origin of the coordinate system, which is the center of the volume of interest.	61
2.55	The Y component of the Magnetic field across XY plane of the volume of interest for a fixed Z (Z= 6cm). Cell 1 and cell 3 are shown also, to emphasize the fact that TLA indeed creates a Y component of the field that increases in the position of cell 1 and cell 3.	63
2.56	The Y component of the Magnetic field across XY plane of the volume of interest for a fixed Z (Z= 6cm). Cell 2 is shown also, to emphasize the fact that TLA indeed create a Y component of the field that increases in the position of cell 2.	64
2.57	Representation of the mutual inductance. We fix Z and X component of receiver location and we move it along the Y axis. The receiver is in XZ plane. The TLA is shown in black. The arrows and the number next to each loop indicates the number of turns and the direction of current in each loop. The colour of these arrows corresponds to the same colour of mutual inductance curve, configuration 1 in blue and configuration two in red. Each configuration is suitable for a cell with the same colour. Here the Z axis is used to show two quantities at the same time: The vertical distance from the TLA, this is shown in meter. But also it is used to show the mutual inductance. The value of mutual inductance is not given here, what we want to show is the relative variation of mutual inductance in a way that it increases in the targeted cells as expected.	65
2.58	Circuit model of two magnetically coupled inductors (transmitter and receiver) in low frequency. L1 is the self inductance of the transmitter (TLA), L2 is the self inductance of the receiver and M represents the mutual inductance between transmitter and receiver.	67
2.59	Two-port network model of the transmitter (TLA) and the receiver.	68

LIST OF FIGURES

2.60	The fabricated TLA for the experiment. This TLA has the same property (size of each loop, number of turns,...) for which we did the simulation. . . .	70
2.61	The setup for the measurement. X,Y and Z axis are shown in black. The volume of interest is the blue box. The TLA is in the XY plane and is connected to port 1 of the VNA. The receiver is in XZ plane and connected to port 2.	71
2.62	The geometry of the setup shown in Fig. 2.61 is given here in schematics to make it easier to see the different components of the set up measurement. . .	72
2.63	Sweeping the receiver along Y axis, we move the receiver while keeping its orientation and X and Z coordinates fixed, step by step along the Y axis. In each step the new measurement is done and the value of mutual inductance between the transmitter and the receiver being at that particular position is measured. a) $y=8$ cm. b) $y=0$ cm. c) $y=-8$ cm.	73
2.64	The results of sweeping the receiver along Y axis, while keeping the orientation and X and Z coordinates of the receiver center fixed. The red curve shows the mutual inductance due to the first structure of the TLAs, which covers the cell 1 and cell 3, and the blue curve is the mutual inductance due to the second structure of the TLAs, which covers the cell 2.	74
2.65	The mutual inductance at the point $y=-0.045$ for the first configuration of the TLA is too low, it means if happened that the receiver was in this point and its orientation lays in XZ plane it would not receive any energy.	75
2.66	The mutual inductance at the point $y=-0.045$ for the second configuration of the TLA is 4 nH. We can see the mutual inductance at this point got increased considerably, it means if now it happened that the receiver was in this point it would receive sufficient energy.	76
3.1	Multiple transmitter coils over which a device or devices can be placed freely as long as the device or devices are in the volume of interest (Image via https://makezens.com/liberty-series/)	78
3.2	Electric circuit model of a receiver-transmitter system. L_1 and L_2 are the self inductances of the transmitter and the receiver. R_1 and R_2 are the internal resistances of the transmitter and the receiver. Z_L is the load connected to the receiver and V_s is the voltage source and V_L is the voltage across the load Z_L . M is the mutual inductance between the transmitter and receiver.	79
3.3	When there is two transmitters for example, and the receiver is closer to one of them, the reflected impedance will be higher in the transmitter closer to the receiver. By measuring the input impedance of each transmitter it is possible to deduce which transmitter is closer to the receiver. Then one conclude if the receiver is in area 1 or area 2, shown here by block boxes.	80
3.4	A situation which will lead to wrong localization if we follows the Qi standard naively. Due to the orientation of the receiver, though the receiver is closer to the Tx1, it will have higher mutual inductance with Tx2 (we discussed the raison in the previous chapter). In this case the Qi standard will conclude that the receiver is in area 2.	81
3.5	Range of detection is approximately equal to the inaccuracy in location. If the current method is applied in natural habitat of animals, one should increase the diameter of transmitter coil and that will increase the inaccuracy in the detection of the animal position.	82

LIST OF FIGURES

3.6	A diagram of the grid of coils that we use as a transmitter underneath the volume of interest (or the transmitter is placed at $Z < 0$). The green box is the volume of interest. The black circles are the coils of the transmitter. The switches between coils allow connecting or disconnecting each coil of the transmitter.	86
3.7	One possible configuration which is made of only one coil. In this configuration the switches are selected in a way that disconnect all the coils (shown in black color) except for one coil, shown in red color. In our method we will use configurations like this which are made of one active coil for localization.	87
3.8	Another possible configuration which is consisting of three active coils (shown in red) and other coils are turned of (shown in black). In our method we will use configurations like this which are made of more than one active coil for field steering.	87
3.9	The location of the receiver (the purple coil) is the location of the center of the circular receiver coil, shown in black dot and specified by (x, y, z) coordinates. The orientation of the circular receiver coil is the orientation of a vector perpendicular to the circular receiver coil (the blue arrow) and specified by (θ, ϕ) coordinates. This means the complete localization is finding out these five variables.	89
3.10	In this example the Transmitter is a circular coil of radius of 3.3 cm with one turn. We put the receiver which is a circular coil of radius of 1 cm with one turn in six different locations. To show these locations relative to the transmitter, the transmitter is shown in white circle. Each of these six locations is the center of each six spherical plots. If we assume the center of the transmitter is at $(x=0, y=0, z=0)$ cm, These locations are, 1: $(x=0, y=0, z=3)$ cm), 2: $(x=0, y=3.3, z=3)$ cm, 3: $(x=0, y=6, z=3)$, 4: $(x=4, y=0, z=3)$, 5: $(x=4, y=4, z=4)$ cm, 6: $(x=6, y=6, z=4)$ cm. The value of mutual inductance as a function of the location and orientation of the receiver is the radial distance from the center of each spherical plots to the surface shown for each orientation. To show the complete dependency of mutual inductance on location and orientation, one should imagine such spherical plots at all the points in space. The unit of the axes is in Henry. However the exact values of mutual inductance here is not important for us, we just want to show how it is a function of five variables.	90
3.11	A visualization of a pre-calculated mutual inductance matrix in which the transmitter is a circular coil of 3.3 cm radius with 6 turns and the receiver is a circular coil of 1 cm radius with 1 turn. The transmitter coil is centred at $X=10$ cm, $Y=10$ cm and $Z=0$ cm. This is one of the coils of our grid of coils shown in Fig.3.6. The pre-calculated mutual inductance matrix shows the mutual inductance between the transmitter and the receiver as a function of location in the volume of interest. These locations are distinct points. Each point represents one location at which the center of the receiver could be. The color of that point shows the value of mutual inductance. The positive and negative values refer to the direction of magnetic field passing through the receiver coil.	92

LIST OF FIGURES

3.12	A certain value of mutual inductance could be a result of large different numbers of positions of receiver determined by simulation. In this figure the grid box is the volume of interest. The transmitter coil (the white circle) of radius 3.3 cm is placed at ($x = 3.3$ cm, $y = 10$ cm, $z = 0$ cm), and the receiver coil is of radius 1 cm. The surface shows the positions of the receiver which yield in same mutual inductance. The value of 5 pH for mutual inductance is arbitrary chosen for the sake of demonstration.	93
3.13	A certain value of mutual inductance could be a result of large different numbers of positions of receiver determined by simulation. In this figure the grid box is the volume of interest. The transmitter coil (the white circle) of radius 3.3 cm is placed at ($x = 3.3$ cm, $y = 165$ cm, $z = 0$ cm), and the receiver coil is of radius 1 cm. The surface shows the positions of the receiver which yield in same mutual inductance. The value of 0.16 nH for mutual inductance is arbitrary chosen for the sake of demonstration.	94
3.14	The two surfaces show all the positions of the receiver according to each coil (shown in Fig.3.12 and Fig.3.13 determined by simulation. The real position of the receiver should belong to their intersection.	95
3.15	Procedure of localization.	98
3.16	The origin of the coordinate system, the position of each transmitter coil by its number (as in table 3.4), and how we assign a number to the position of the receiver. The green cuboid is the volume of interest.	100
3.17	The real transmitter fabrication (grid of red coils) and the set-up of the measurement, the volume of interest in shown as a black cuboid, and the receiver coil (red small coil) is placed in some arbitrary position in the volume of interest.	101
3.18	The pre-calculated mutual inductance matrix is a transmitter-coil specific 3D matrix of numbers which will be stored in the controlling circuitry of the transmitter.	103
3.19	The schematic that is used to model the measurement process in this chapter. It is a two port network. Later we will make our model more realistic, by moving from two port network to one port network, but not in this chapter. .	104
3.20	The measured value of mutual inductance (12.72 nH) could be a result of any positions of receiver belonging to the surface shown here. Till this step there are 7325 possible positions of the receiver which match the measured mutual inductance. The position is not unique and the localization process should continue.	105
3.21	The set of all possible positions of the receiver stored in MATLAB as a numerical matrix. First column indicates the X coordinate, the second column indicates the Y coordinate and the third column indicates the Z coordinate. In this step there are 2525 possible positions of the receiver which match the measured mutual inductance.	106
3.22	The measured value of mutual inductance (0.997 nH) could be a result of any positions of receiver belonging to the surface shown here. This is configuration (2).	106

LIST OF FIGURES

3.23	Left panel shows possible positions of the receiver due to the configuration 1 and configuration 2. Right panel shows their intersection. Intersection between surfaces belong to configuration 1 and configuration 2, reduces the set of possible positions of the receiver. The answer is still not unique. One should notice that the X, Y and Z axes in Right panel cover a small part of what is shown in Left panel. It means that the answer is converging toward small possible set of positions.	107
3.24	The measured value of mutual inductance (0.307 nH) could be a result of any positions of receiver belonging to the surface shown here.	108
3.25	Right panel shows possible positions of the receiver due to the configuration 3 and the possible positions of the receiver from previous steps. Left panel shows their intersections. Intersection between them reduces the set of possible positions of the receiver. The answer still is not unique.	109
3.26	The measured value of mutual inductance (0.997 nH) could be a result of any positions of receiver belonging to the surface shown here. This is for configuration 4.	110
3.27	Right panel shows possible positions of the receiver due to the configuration 4 and the possible positions of the receiver from previous steps. Left panel shows their intersection. Intersection between them reduces the set of possible positions of the receiver. The answer still is not unique.	111
3.28	The measured value of mutual inductance (0.920 nH) could be a result of any positions of receiver belonging to the surface shown here. This is configuration 5.	112
3.29	The intersection result now just contain six possible positions.	112
3.30	All the pre-calculated surfaces (due to the measurements of the mutual inductance) whose intersection leads to the localization of the receiver coil . . .	113
3.31	Two different configurations of transmitter lead to a magnetic field with different distributions in volume of interest. The upper part shows the magnetic field distribution of a configuration suitable for case in which the receiver is in the position shown by yellow circle and not suitable for case in which the receiver is in the position shown by white circle. The lower part shows the opposite (suitable for position shown by white circle and not yellow circle). Here the precise positions of the circles are not important and we just want to show the dependency of the magnetic field distribution in the volume of interest on the transmitter configuration.	117
3.32	The volume of interest is divided into sub volumes (green voxels). Depending on the result of localization of the receiver, a configuration of transmitter is selected corresponding to the magnetic fields that add constructively in a sub volume in which the receiver was found.	118
3.33	Part of the configuration table which is stored in the controlling system of the transmitter. "C" means connected, and "D" means disconnected.	118
3.34	The chart for the process of localization and power transfer.	119

LIST OF FIGURES

3.35 Calculation for z component of the magnetic for two different configurations of the transmitter suitable for (A panel) when the receiver is at the position $X = 12 \text{ cm}, Y = 12 \text{ cm}, Z = 4 \text{ cm}$ and (B panel) when the receiver is at the position $X = 6 \text{ cm}$ and $Y = 5 \text{ cm}, Z = 4 \text{ cm}$. The maximum of the generated field (z component) takes place at the position of the receiver. The black line in (B panel) is used to indicate the path along which measurement will be performed (shown in Fig.3.36) to compare the experimental results to the calculated results shown here. 120

3.36 Mutual inductance along the black line shown in Fig. 3.35. This line extends from point ($X=6 \text{ cm}, Y=-1 \text{ cm}, Z=4 \text{ cm}$) to point ($X=6 \text{ cm}, Y=30 \text{ cm}, Z=4 \text{ cm}$). The mutual inductance increases where the receiver is positioned and falls down in other locations. 121

4.1 The $L1$ and $R1$ are respectively the inductance of the transmitter and the resistance of the transmitter, the $L2$ is the inductance of the receiver, the $R2$ is the resistance of the receiver, $R3$ is R_{LOAD} which is the load connected to the receiver and the Mutual is M , the mutual inductance between the transmitter and the receiver. I_1 and I_2 are the currents in loop 1 and loop 2, and V_s is the voltage applied to the port 1, shown by Term1. 124

4.2 Simulation of real part of input impedance of a transmitter as a function of mutual inductance. The mutual inductance runs from zero to its maximum value of $1 \mu\text{H}$. One can see that the change in input impedance is very small to be measured. 126

4.3 Simulation of imaginary part of input impedance of a transmitter as a function of mutual inductance. The mutual inductance runs from zero to its maximum value of $1\mu\text{H}$. One can see that the change in input impedance is very small to be measured. 127

4.4 Parallel – Parallel transmitter-receiver magnetic resonance coupling schematic. V_s is the applied voltage and $I1, I2, I3, I4$ and $I5$ are the currents in each loop. 129

4.5 The real part of the input impedances of the circuit in Fig.4.4 as a function of the mutual inductance(M) and the frequency. This result shows what is known as frequency splitting. 130

4.6 The imaginary part of the input impedances of the circuit in Fig.4.4 as a function of the mutual inductance(M) and the frequency. This result shows what is known as frequency splitting. 131

4.7 The input impedances of the circuit in Fig.4.4 as a function of frequency with $M=0 \mu\text{H}$ 133

4.8 The input impedances of the circuit in Fig.4.4 as a function of frequency with $M=0.25 \mu\text{H}$ 134

4.9 The input impedances of the circuit in Fig.4.4 as a function of frequency with $M=0.5 \mu\text{H}$ 134

4.10 The input impedances of the circuit in Fig.4.4 as a function of frequency with $M=0.85 \mu\text{H}$ 135

4.11 Variation of input impedance, real part and imaginary part, as a function of the mutual inductance (M). These values becomes negative because the value of input impedance reduces. Weak coupling is when the M is small, and the strong coupling is when M is high. 138

LIST OF FIGURES

4.12	Real part of the input impedance of the circuit shown in Fig.4.4, as a function of M. Here the frequency is fixed at 125 kHz.	138
4.13	The imaginary part of the impedance of the circuit shown in Fig.4.4, as a function of M. Here the frequency is fixed at 125 kHz.. . . .	139
4.14	A generic antenna circuitry used in the near field magnetic coupling.	139
4.15	A generic antenna circuitry used in the near field magnetic coupling divided into four parts.	140
4.16	A generic receiver circuitry used in the near field magnetic coupling.	141
4.17	The Tx pin in Fig.4.15 is a current source. This current drives the transmitter. In these images the transmitter is in energy transmitting step. The voltage across the transmitter coil depends on the mutual inductance between transmitter and receiver. As the mutual inductance increases, for the same applied current, the voltage across the transmitter drops. The different voltages across the transmitter coil for different mutual inductances are what in-use protocols neglect and is what we use for deducing the mutual inductance. This measurement is performed on a HF RFID reader compatible with ISo 14443 Typ A standard using Agilent DSO-X 2002A oscilloscope.	142
4.18	The transmitter starts the communication. The data transmission from the transmitter to the receiver uses a 100% ASK modulation. Here we show the signal for just one value of M. If the value of M changes, the signal keeps it's shape, but the peak to peak values will change. This measurement is performed on a HF RFID reader compatible with ISo 14443 Typ A standard using Agilent DSO-X 2002A oscilloscope.	143
4.19	The data transmission from the tag back to the transmitter uses the principle of load modulation. This has a feedback effect as a voltage drop on transmitter side. For different coupling (different M) the signal keeps it's shape, but the peak to peak values will change. The in-use protocols only pay attention to the variation of this voltage to translate it into 0s or 1s (depending on certain coding)and the peak to peak value itself is neglected. It is this peak to peak value that we are going to use for localization method. This measurement is performed on a HF RFID reader compatible with ISo 14443 Typ A standard using Agilent DSO-X 2002A oscilloscope.	144
4.20	Transmitter antenna circuitry and receiver antenna circuitry that we are going to use has the main part of Fig.4.15 which is the matching and resonance circuitry part without getting us into unnecessary complication (like EMC) which are irrelevant to our work.	145
4.21	Transmitter antenna circuitry and receiver antenna circuitry that we are going to use. We want the relation between M and the input impedance of this circuit.	146
4.22	To design an inductor coils for the transmitter and the receiver that matches the capacitance of these commercially available capacitors and resonates at 125 kHz and be matched to 50 Ω we used software like FEEM (below) and Q3D Ansys (above)[26] [27].	149
4.23	The complete circuitry for the transmitter-receiver schematic	150
4.24	The fabrication of the transmitter antenna (right) and the fabrication of a receiver antenna (left). As we can see in the background of the picture both of them are tuned to resonate at 125 kHz. Measurements made by HP 4195.	150

4.25	The position of each transmitter coil in the volume of interest. The position of these coils depends on the The volume of interest. The choice of position of each coil is made in a way that guarantee that they cover all the volume of interest. The volume of interest is a cuboid shown in brown.	152
4.26	The measured value of mutual inductance ($M=0.205 \mu\text{H}$) could be a result of any position of receiver belonging to the surface shown here. The color just shows the Z component of the possible locations.	154
4.27	The measured value of mutual inductance ($M=0.417 \mu\text{H}$) could be a result of any positions of receiver belonging to the surface shown here.	155
4.28	The surface shows the intersection of possible positions according to coil 1 and coil 2.	155
4.29	The measured value of mutual inductance ($M=0.185 \mu\text{H}$) could be a result of any positions of receiver belonging to the surface shown here.	156
4.30	The measured value of mutual inductance ($M=0.383 \mu\text{H}$) could be a result of any positions of receiver belonging to the surface shown here.	157

List of Tables

2.1	A configuration which creates the desired magnetic field in Y direction in both cell 3 and cell 1 at the same time	62
2.2	A configuration which creates the desired magnetic field in Y direction in cell 2.	63
2.3	The self inductance of the TLA in its different configurations.	75
3.1	ERROR is the maximum difference between the actual position of RX and the determined position of RX.	84
3.2	Coordinates of each coil of the transmitter. Z coordinates for all coils are zero, (Z coordinate=0)	100
3.3	The self-inductances and quality factors of the transmitter coil(s) and the receiver coil, measured at a frequency of 100 kHz	102
3.4	Experimental results for localization.	114
3.5	Experimental results for localization that we will use for magnetic beam steering.	119
4.1	Properties of the transmitter(s) and the receiver.	150
4.2	Coordinates of each coil of the transmitter. Z coordinates for all coils could not be the same because they will intersect. However they are placed as close as possible to Z=0, in a range of (-2.5 cm, 2.5 cm).	151
4.3	Experimental results for localization.	158

BRIEF INTRODUCTIONS TO EACH CHAPTER

The main subject in this work is considering IPT (Inductive Power transfer). In particular enhancing the magnetic mutual coupling in IPT.

In chapter 1, we introduce the main concepts regarding the IPT. Here we will give a very brief summary about the state of arts concerning our target, which is enhancing the magnetic mutual coupling between the transmitter and the receiver. We will find that this enhancing is closely related to the localization of the receiver in respect to the transmitter. In chapter 2 we start by consider the problem of misalignment between the receiver and the transmitter.

In this chapter a reconfigurable antenna which changes its structure by turning on and off specific parts of itself is proposed. This will guarantee the effective power transfer in the range of interest, regardless of the lateral and orientational misalignments between the sender and the receiver. Experimental verification will shows the feasibility of this method. In chapter 3 we mention some deficiency of the method introduced in chapter 2. At this point we turn our intention to the subject of localization for enhancing the performance of the IPT system.

How ever in chapter 3 we will do so for a two ports network. This is a system in which we have access to both transmitter and the receiver. This is not a practical situation.

In chapter 4 we extend this method to a realistic one port network in which we do not need access to the receiver. In this chapter we will show that our proposed method is also compatible with currently in use system and could be integrated in them by miner modifications.

All these steps will be simulated first then measurements will be carried on. The measurements will conform the validity of proposed methods.

Chapter 1

INTRODUCTION TO WIRELESS POWER TRANSFER AND RADIO FREQUENCY IDENTIFICATION IN NEAR FIELD

1.1 FAR-FIELD AND NEAR-FIELD IN WPT

Wireless power transfer (WPT) describes the technology of transmitting electric power without using any wires which are normally used to transmit electric power.

Here the system which performs the Wireless power transfer is divided into two parts:

1. Transmitter or sender or primary side (in different literature it is called different names). This is the part of the system to which we apply the signal (or source of energy). We expect that the transmitter transfers this power to the second part of the system (receiver) without having them being connected by wires. This is the power-transmitting part of the system.
2. Receiver or tag or secondary side (in different literature it is called different names). This is the part of the system which we expect to receive the power of the transmitter without being connected by wires to it.

This is the power-receiving part of the system.

One could categorize different wireless power transfer technologies based on the mechanism by which they transfer the power:

1. Wireless power transfer operating in near-field or non-radiative propagation.
2. Wireless power transfer operating in far-field or radiative propagation.

By near-field we mean reactive fields. Those are the component of electric or magnetic

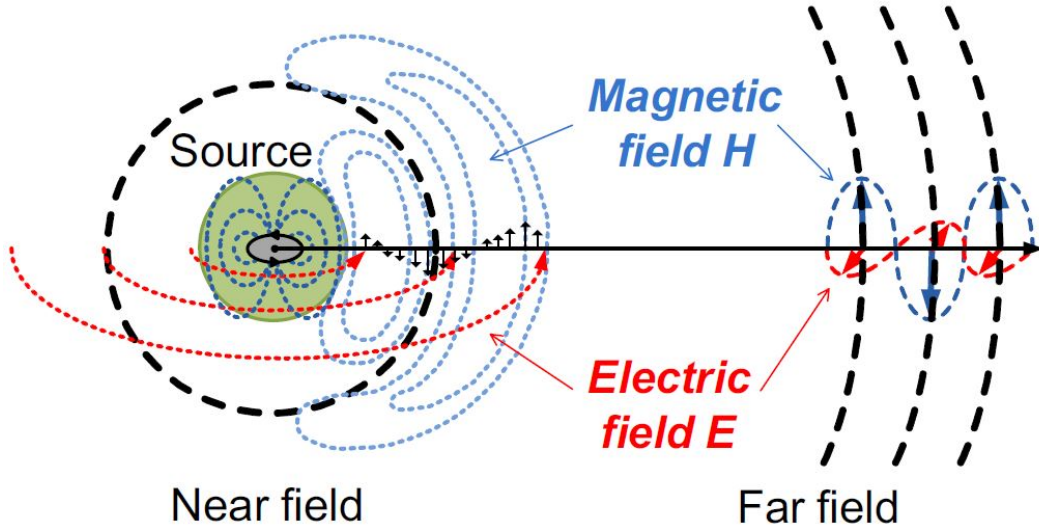


Figure 1.1: Near field and Far field around the source,[52].

fields which are dominant at small distance from the transmitter antenna and decay rapidly as we increase the distance from the transmitter.

Those fields also called reactive because they represent the stored energy in the field surrounding the transmitter antenna.

If we apply a certain frequency to the transmitter antenna in the half period of each time cycle, the transmitter sends energy into these fields but in the other half cycle these fields send back this energy to the transmitter.

So in one period (if we neglect the ohmic loss) there is no net energy (or power) transmitted (from the transmitter) to those fields. Energy (or power) goes back and forth between the transmitter and the fields all the time, hence the name reactive.

By far-fields we mean radiated fields. Those are the component of electric or magnetic fields which are dominant at large distance from the transmitter antenna and hence the name far-field.

The energy which is sent from transmitter to the far-fields will not return back to the transmitter and is transmitted in one direction away from the transmitter, hence the name radiated field.

It should be mentioned that the border between far-fields and the near-fields is not really sharp as our categorization suggests, but it is a gradual transition from reactive field being the dominant field to the radiated field being dominant (a very good distance approximation for border line between near-field and far-field is $\frac{\lambda}{2\pi}$).

So there is another category which operates in Mid-Range.

All these categorise are approximations. When we only consider the near field and neglect the far field (or vice versa), we are approximating a complicated situation into somewhat simpler situation.

Fig.1.1 summarizes what we have said.

A detailed analysis of Maxwell equations shows that for the near-field analysis, a good

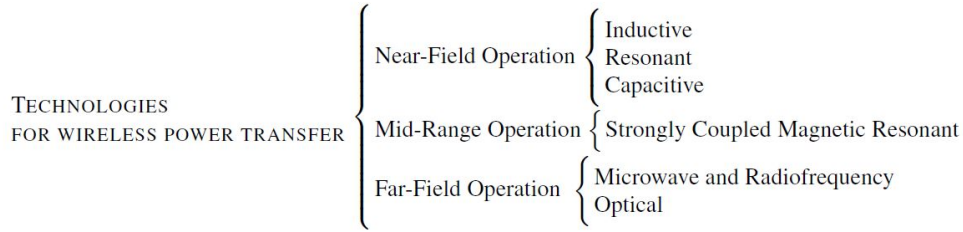


Figure 1.2: Classification of WPT technologies,[51].

approximation requires the following conditions:

1. The size of the transmitter is much smaller than the wavelength λ .
2. The distance between transmitter and the point in space which we are interested in analysing the field there, is much smaller than the wavelength λ .

And for the far-field analysis, a good approximation requires the following conditions:

1. The distance between transmitter and the point in space which we are interested in analysing the field there, is greater than the wavelength λ .
2. The size of the transmitter is more than 10 times greater than the wavelength λ [51].

There are numbers of WPT technologies which belong to these categories as shown in Fig4.5:

1. In the near-field there are the inductive, the resonant and the capacitive wireless power transfer.
2. Microwave-based or optical WPT are far-field technologies.

Because Maxwell's equation can be simplified in the near-field (by using quasi-static approximation) in a different way in comparison with, when we work in far-field, one should know to which group (far-field or near-field) a certain WPT technology belongs. So one can use the correct analyse tools and approximations.

As we will see later, in this work our interest is in magnetically coupled WPT system which operates in near-field. So we will use quasi-static approximation in this work.

1.2 TYPES OF WIRELESS POWER TRANSFER IN NEAR-FIELD

Figure 1.3 shows the types of wireless power transfer in near fields. The coupling type is categorized into two main categories. One is magnetic field coupling and the other is electric field coupling. This categorization depends on whether the coupling is achieved through a magnetic field or an electric field.

Each of these categories are further divided into two types based on the presence of the

resonance phenomenon or its absence.

1. The magnetic field coupling uses electromagnetic induction. Here the primary side and the secondary side are coupled by a magnetic field, and the phenomena of electromagnetic induction is used for power transfer.

We will explain it in more details later but it is enough for now to mention that as a result of the alternating magnetic field created by an alternating electric current in the primary side, energy is transmitted to the secondary side. In the magnetic field coupling the primary side and the secondary side are coils. In this work the magnetic field coupling is one of the wireless power transfer types which we are interested in.

2. The electric field coupling uses electric field instead of a magnetic field. (In this work we are not interested in studying the electric field coupling).

3. Magnetic resonance coupling. Introducing a resonant capacitor to the electromagnetic induction mentioned in group 1, will cause the primary side to resonate at a certain resonant frequency. If the secondary side also resonates at the same frequency (by introducing a resonant capacitor to it also), this enables the achievement of high efficiency and high power transfer.

In the magnetic resonance coupling the primary side and the secondary side both are resonators made of inductors (coils) and capacitors.

Magnetic resonance coupling will not work properly if the resonant conditions are not correct.

Having resonators on both side and working in resonance frequency, this as well let us to have a wireless power transfer system with relatively larger gap (gap is the physical distance between transmitter and the receiver) between the primary side and the secondary side in comparison to simple magnetic field coupling mentioned earlier.

Before magnetic resonance coupling, it was thought that wireless power transfer was realizable only over a distance of 1/10th of a coil diameter primary side; however, after the emergence of magnetic resonance coupling, it was found that power could actually be transmitted with high efficiency and high power over distances equal to or greater than a coil diameter [63]. This was a major boost for research and development in the field of wireless power technology [63]. In this work the magnetic resonance coupling is one of the wireless power transfer types which we are interested in.

4. Electric resonance coupling. This type uses electric field with the resonance phenomenon. This type follow the same logic (more or less) of magnetic resonance coupling in using the benefits of resonance for power transfer. Though the Electric resonance coupling and magnetic resonance coupling follow the similar logic, however because in electric resonance coupling we are dealing with electric field rather than magnetic field, these two types are suitable for different applications. (In this work we are not interested in studying the electric field coupling).

1.3 THE MAGNETIC INDUCTIVE COUPLING WPT

1.3.1 BASIC WPT SYSTEM

As we said in this work we are interested in wireless power transfer in magnetic field coupling (it's other name is inductive coupling). Although in this work we will concentrate on the coupling components, it is important to understand that such a system is much more

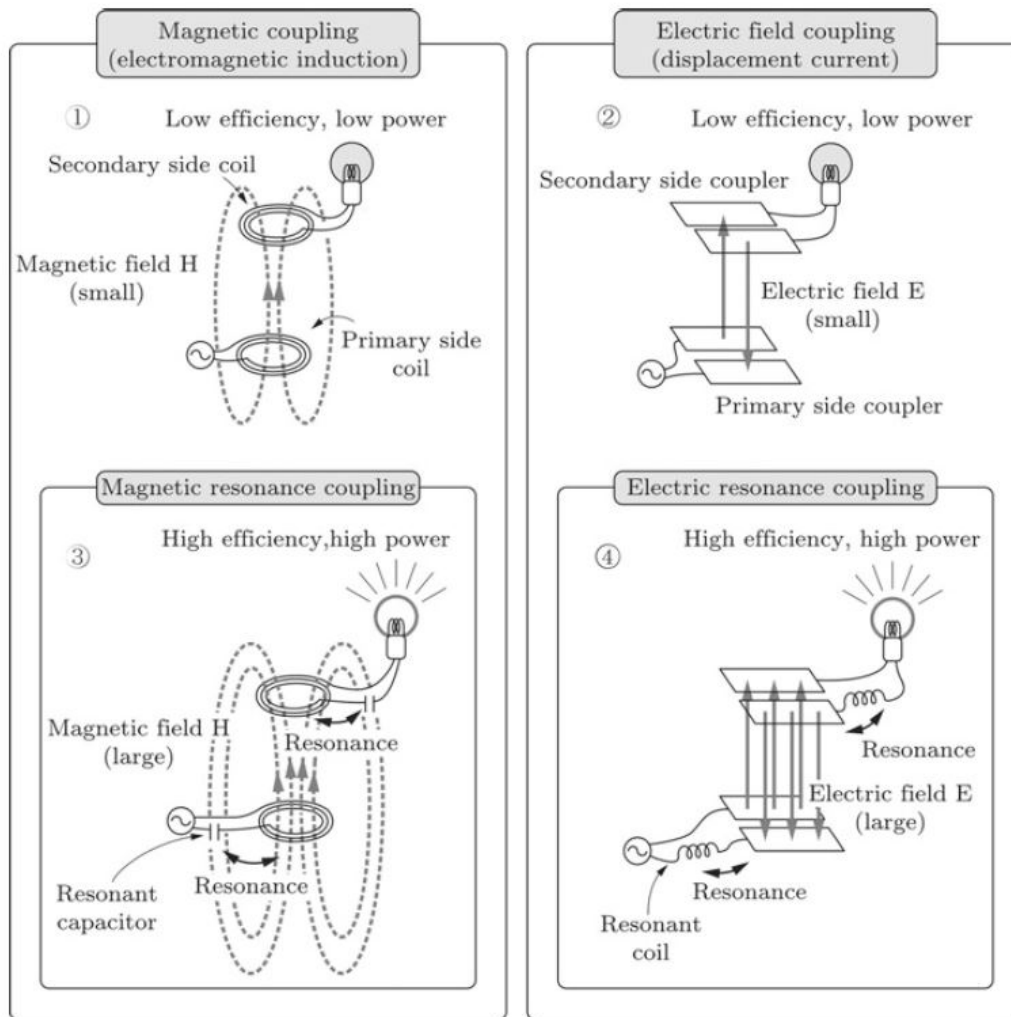


Figure 1.3: Diagrams of magnetic field coupling, magnetic resonance coupling, electric field coupling, and electric resonance coupling,[63].

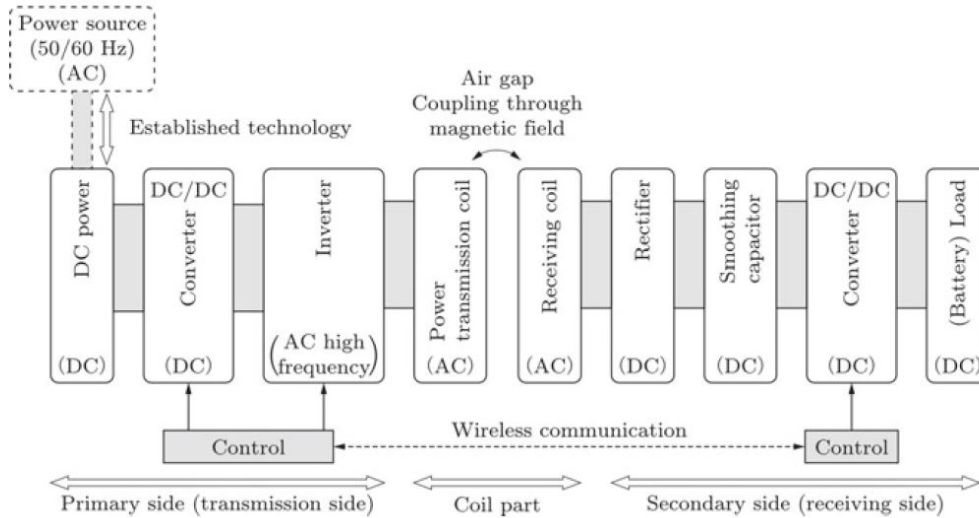


Figure 1.4: Conceptual diagram of basic WPT system configuration,[63].

than just coupling parts. It is a complete system consisting of many other parts beside the coupling elements.

Fig. 1.4 illustrates the conceptual diagram of the basic configuration of a wireless power transfer system. The main parts of any wireless power transfer in magnetic field coupling are([63],[24], [73], [3]-[71]):

1. DC generation: creating DC (most of the time from 50/60 Hz frequencies) with an AC/DC converter.
2. DC/AC transformation (inverter). The frequencies when the DC/AC transformation occurs are those used in wireless power transfer. Frequently used frequencies in wireless power transfer in magnetic field are 100–200 kHz, 6.78 MHz and 13.56 MHz.
3. Power transmission coils and receiving coils and an air gap between them in which wireless power transmission actually takes place.
4. AC/DC transformation (rectifier): The transferred power in AC is converted back to DC with a rectifier circuit.
5. DC/DC transformation (DC/DC converter): To reach a voltage and current ratio equal to the optimal load, some time it is called: Impedance adjustment.
6. Load components (resistance, battery, etc.)

1.3.2 EFFICIENCY OF WPT

There is an efficiency associated with each part of the wireless power transfer system shown in Fig.1.4 [55],[38]-[71].

There is the efficiency of inverter, the efficiency of converter and so on. What we are interested here is the efficiency of coupling. The efficiency of coupling is defined as the ratio of the applied power to the transmitter coil and the received power in the receiver coil [33].

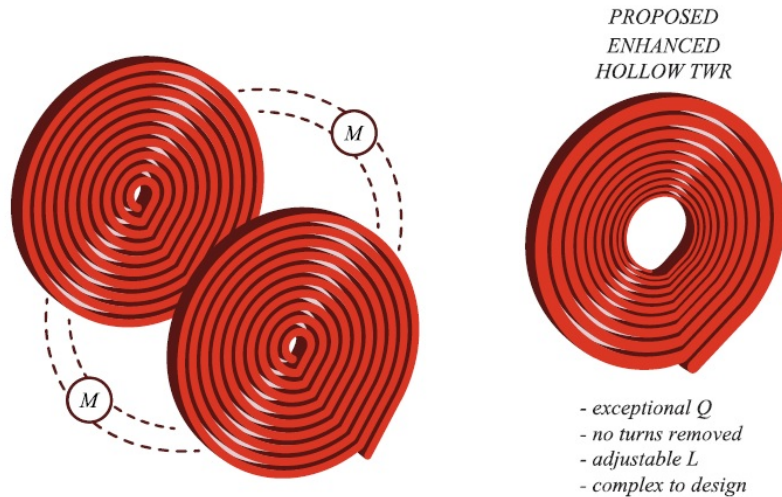


Figure 1.5: On left normal spiral coil for WPT. On the right a new design proposed in [15] to enhance the Q factor of the coils. For each turn of the coil the width of the coil reduces.[15].

One way to increase the efficiency of coupling is to enhance the Q factor of the transmitter coil and the receiver coil.

In [15], an improved planar spiral winding was proposed to improve the Q by using a Track-Width-Ratio geometry and increasing the inner radius of the winding.

In [56] an intermediate coil was utilized for WPT system which can enhance the self-inductance for the primary side at the resonant frequency, so effectively compensate the apparent coupling coefficient.

In [68], a new U-coil WPT system was proposed to improve the power transfer efficiency, ensure the suitability of the space in the path of power transmission direction, so increase the power density.

All these methods mentioned earlier (and some other not mentioned here) are suitable for applications in which the relative position of the transmitter and the receiver is fixed. There are other solutions which are suitable for cases in which the relative position of the transmitter and the receiver is not fixed.

1.3.3 MOBIL RECEIVERS IN WPT

In the case of the receiver not being in fixed position in respect to transmitter some new problems arise and need to be addressed. One of them is the receiver being in null areas. Those are positions with essentially zero coupling between receiver and the transmitter. This happens due to the vectorial nature of the magnetic field. If the receiver is in null position the efficiency practically reduces to zero, therefore such situations should be avoided. In [6],[22], [20] a structure is proposed (namely a twisted loop antenna) which reduces the

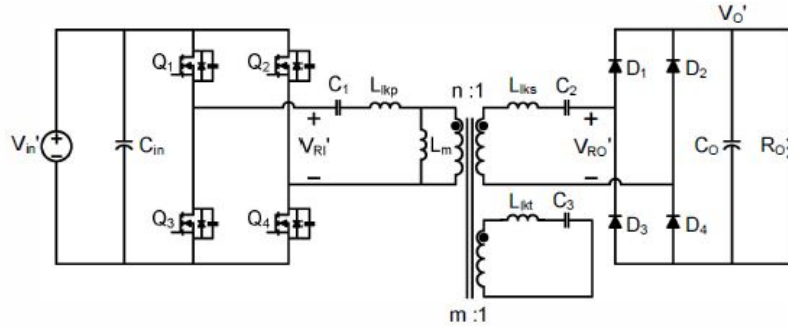


Figure 1.6: In a two coil WPT system, which has low coupling coefficient, the intermediate coil boosts the self-inductance of the primary side at around the resonance frequency of the intermediate coil, so that the coupling coefficient is compensated.[56].

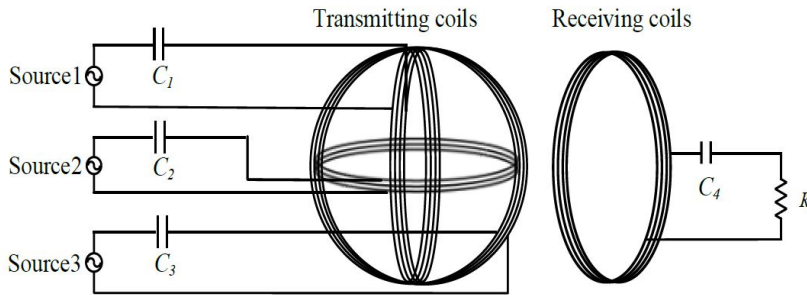


Figure 1.7: Three-orthogonal-coil topology for omnidirectional WPT systems,[71].

probability of receiver (when it is placed randomly close to the transmitter) being in null areas.

Another approach for dealing with the case of the receiver not being in fixed position in respect to transmitter is to create Omni-directional transmitters. This approach sometimes is called multi-objectives charging, which means having coupling between a transmitter and multiple receivers. The key of multi-objectives WPT system is to ensure the energy supply at an arbitrary spatial position [71].

For achieving Omni-directional transmitters, orthogonally-assembled coils has been increasingly studied by researchers since it can offer an enhanced flexible charging way for household appliances[71], as shown in Fig.1.7.

In [11], [14], [44] it is shown that, such an orthogonal topology (shown in Fig.1.7) is a promising approach for achieving Omni-directional transmitters.

Based on such an orthogonal topology, the current phase and amplitude modulation was proposed to spatially manipulate the electromagnetic field to be suitable for omnidirectional WPT systems.

In [48]- [49], the transmitter consisting of two vertical coils is proposed which is excited by current sources with adjusted amplitudes. This design aims to create a rotating electromagnetic field.

Beside manipulating the amplitude of the current exciting the transmitter, the effect of the

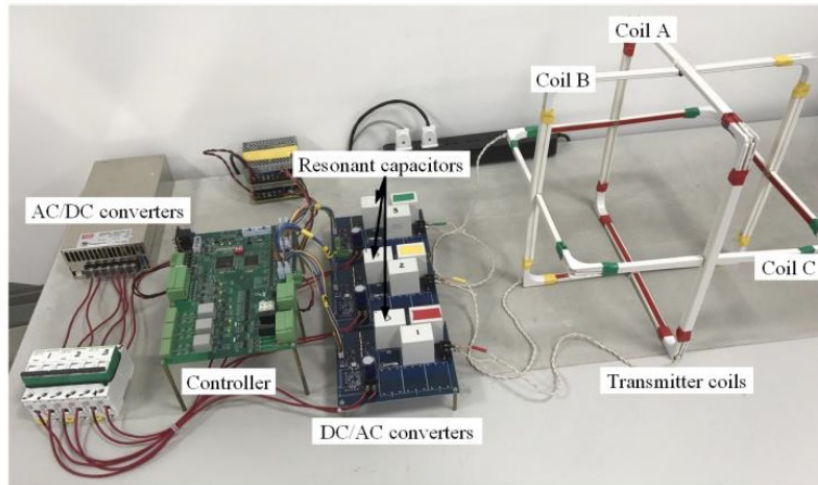


Figure 1.8: 3D field orientation WPT system. By controlling the amplitude and the phase of current in each of the three coils, one could control the magnetic field in space around them [74].

current phase was also studied for such a transmitter topology in [12], where the current applied to each coil has a phase difference of 90 degrees. This approach was adopted to verify the capability of power transfer to a moving receiver around the transmitter in a 2-dimensional space [71].

In [64], a new cubic transmitter was proposed to realize an omnidirectional WPT system by having just one single power source. This work can simplify the controlling system of WPT while its capability of 3-dimensional power transfer remains to be verified[71].

One notice that the created electromagnetic field can be not only distributed in a 3-dimensional space, but also concentrated to the loads directionally. This is the concept of magnetic field beam forming or sometimes called beam steering.

A 3-dimensional WPT system with a three orthogonal coils transmitter was proposed in [69] which is operated by the current amplitude controlling mechanism. In [47]-[46] a mathematical model for such system was put forth.

Such a coil topology is becoming one of the optimal technical solutions for omnidirectional WPT systems [71].

In this work there is a number of coils as transmitter. Having more than one coil brings its own issues (mainly coupling between transmitter coils instead of coupling between transmitter coils and the receiver).

In [39] a non-coupling coil pattern which can cancel the coupling between array components as the transfer coils is introduced. In [74], this problem is addressed by suitable placing of transmitter coil in respect to each other.

The possibility of having more than one receiver was addressed in other works. Several attempts were made to extend the magnetic induction WPT to a system with more than one receivers [8] or even multiple relays,[9]-[54]. For example in [41] magnetically coupled based networks with multiple transmitter-receiver and relays have been analysed for the underground Wireless sensor networks, [40].

In these works the optimal performance of the system is searched for by aiming at impedance

matching and tracking of the split frequencies beside the role of magnitude and phase of the input signal.

Also an implicit localization of the receiver is implemented in some of these works. For example in [69]-[65], [37] an omnidirectional scanning process for detecting the power transfer in a 3-dimensional space, then by monitoring the amount of power transfer and choosing its optimum values, the power flow is focused towards the targeted areas. Such principles could be applied to any WPT system comprising three orthogonal transmitter coils and multiple receivers with coil-resonators.

We call it implicit because there is no real knowledge involved in these approach about the position of the receiver.

However for example the system chooses the amplitude and the phase of the applied current to the transmitter in a way that effectively is suitable for the position of the receiver without knowing its position.

If this localization was explicit, it could increase the applicability of wireless power transfer to other application in which the explicit position of the receiver is a useful information, like internet of the things or animal tracking,[53],[43], [1], [2].

To summarize, in inductive wireless power transfer one way of improving the efficiency of the system is to improve the coupling between the receiver and the transmitter. One active field of this research is magnetic beam forming.

Magnetic beam forming is closely related to the localization. Though what we mentioned here did not included the explicit localization, later in chapter 3, before we explain our method for localization, we will mention works done in explicit localization in inductive power transfer to be in the right context.

To conclude this survey we say that in inductive wireless power transfer, a system can be investigated from different points of view. In this study we will be concerned with following features:

- Unidirectional or omnidirectional wireless power transfer. Here one can differentiate between WPT systems where the power is transferred to a fixed receiver where a load is connected. This is a uni-directional WPT. Alternatively, there are omnidirectional systems where the load does not need to be in a fixed position.
- Number of transmitters. The simplest topology for a WPT system consisting from one transmitter coil and one receiver coil is not the case all the time. In order to extend the WPT operability, several transmitters can be deployed in a region in order to transfer power to a load [7]-[31].
- Stationary/Mobile receiver. In some applications, WPT must be able to handle the receiver being placed in a random position before the charge starts. This is the case for dynamic EV (Electrical Vehicle) wireless charging.[36], [58], [70].
- Localization of the receiver.

Those are the main criteria we will consider in our work. There are other criteria like sensitivity of power transfer to the medium (being air, water,...) or the amount of power being transmitted and so on, which will not be considered here.

Fig.1.9 shows the main features of WPT systems including what we will consider in this

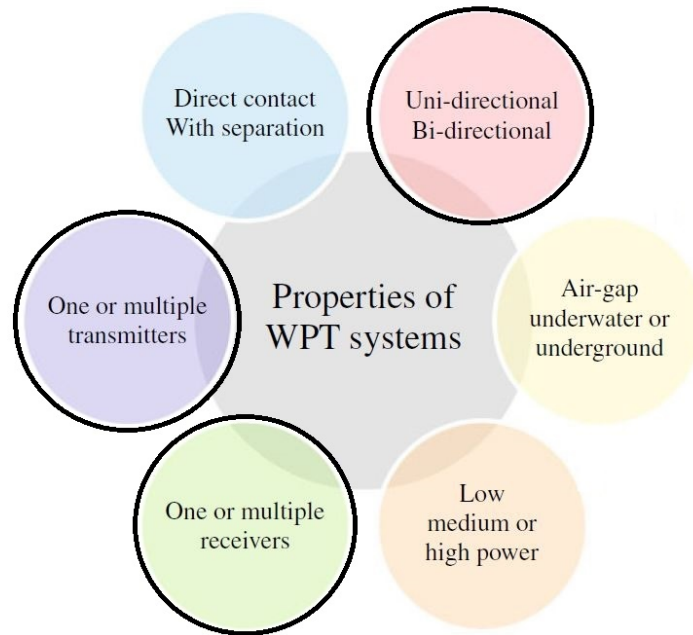


Figure 1.9: Main features of WPT systems,[52]. What we will consider in this study is enclosed in black circles .

work.[52].

1.4 APPLICATIONS OF WPT IN MOBILE IPT

The methods of power transfer for various sources and loads have evolved largely recently. There are many applications for inductive power transfer (IPT) and for WPT in general. However in this study we are interested in movable targets to be powered. Today more and more loads are movable and it is important to provide wireless power to moving things such as electric transportation, robots, and electric drones, Fig.1.10 shows IPT for flying drone. [60].

Currently, we mainly depend on electric wires and batteries to provide power to movables. As one can notice, some robots, smart phones, tablets, and desktop computers etc. should operate continuously even when they are not connected electrically to the power sources. It is not convenient to connect some movable devices always to the fixed power source. Batteries also has a limited time of powering and should be recharged. It is important to overcome these limitations for movable things. This is the motivation for mobile power electronics. The point is to supply electric energy to all movable things freely [60]-[35].

From this point of view power transfer can be classified as stationary and mobile based on the movement of power receiving device, this classification is shown in Fig.1.11.

Most application in WPT have been using SPT (Stationary Power Transfer), which includes fixed SPT of an unchanged configuration such as high-voltage power lines, street

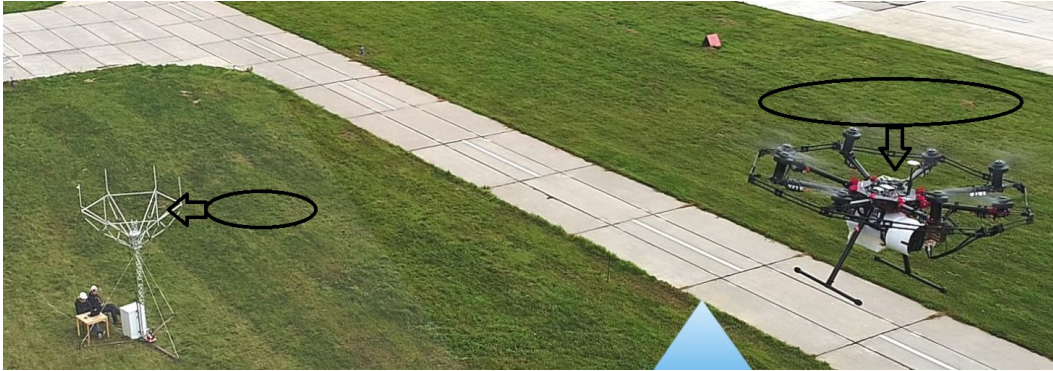


Figure 1.10: flying drone powered by IPT. The black circles indicate the position of receiver and the transmitter coils.[25].

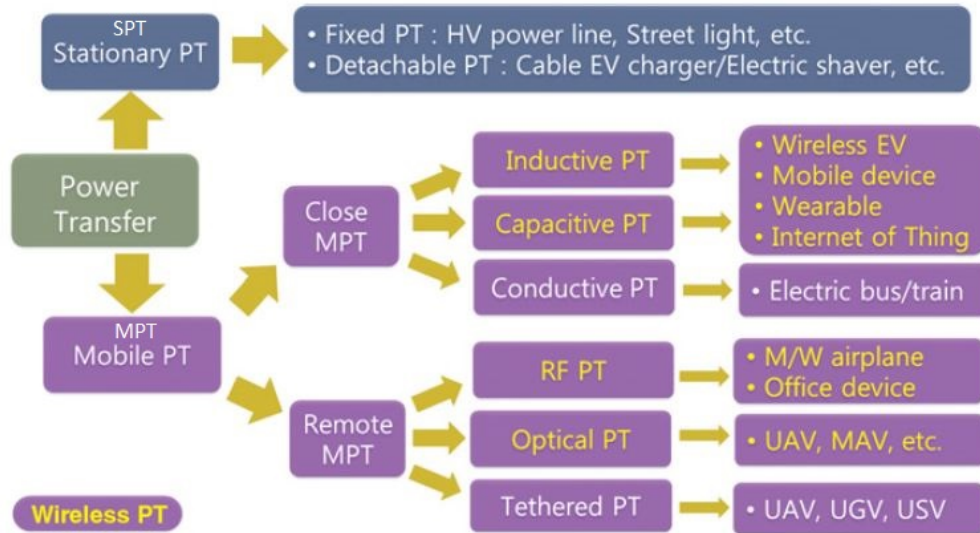


Figure 1.11: A general classification of power transfer in terms of mobility, distance, and means of powering[60].

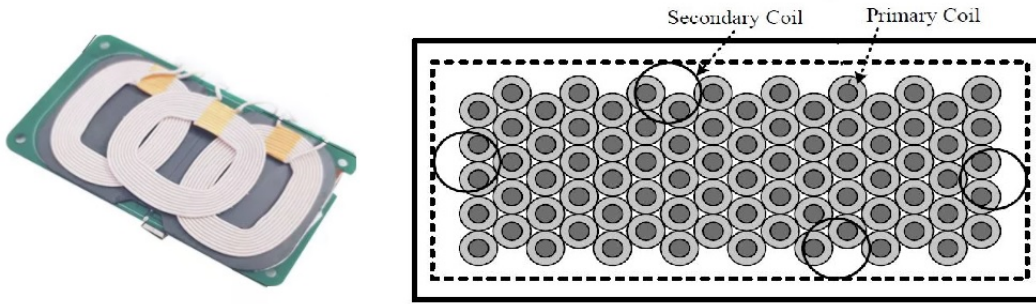


Figure 1.12: A free positioning IPT according to Qi [72]-[30].

lights, and home appliances like electric vehicles (EVs) and electric shavers etc...

To address the demand of mobility of receiver loads, various mobile power transfer (MPT) technologies have been studied [62]; they can be classified as close MPT and remote MPT. This depends on the range between the power transmitting source and the receiver loads. For the close MPT, the WPT range is from a few cm to a few m. Among the close MPTs, inductive power transfer (IPT) has been used largely because of its high power transfer capability at relatively low frequency, whereas capacitive power transfer (CPT) is not as commonly used because of its high operating frequency and small power transfer distance[42]-[13].

In 2008, the Wireless Power Consortium (WPC) was formed and in 2010 the first version of the wireless charging standard (Qi) was released [72]. By 2018, Qi standard has been supported by more than 600 companies and incorporated into more than 3000 products [66]. Adopting the principle of magnetic resonance coupling, Qi standard is based on a planar wireless charging technology with the free positioning and localized charging features [72]-[50].

As we said earlier free positioning means that the receiver coil can be positioned anywhere on the pad to receive energy. Fig. 1.12 shows the standard adopted by Qi and one commercial devices according to this standard. Later we will have more to say about these methods and their advantages and their disadvantages.

In This work we will concentrate on the free positioning inductive power transfer. According to Fig.1.11 this is the close mobile inductive power transfer system.

At the end it should be mentioned that one very important application of WPT is Radio Frequency Identifications (RFID). As WPT, RFID could operate in near field or far field. One category of RFID in near field uses the same mechanism which is used in IPT. Those are called RFID in low frequency (125 kHz-150 kHz) or high frequency (13.56 MHz) [18]-[17]. Having RFID with free positioning feature also is useful for some applications, like internet of things (IoT) etc. Because this kind of RFID uses the same mechanism which is used by IPT, whatever we are going to say on IPT also applies equally to this group of RFID.

Chapter 2

A RECONFIGURABLE ANTENNA FOR ENHANCING THE MAGNETIC COUPLING IN IPT AND RFID

2.1 INTRODUCTION

In this chapter we will have a more detailed look in the mechanism of magnetically coupled coils which is the main mechanism for Wireless Power Transfer (WPT) and the Radio Frequency Identification (RFID) in low and high frequency range. We will point out the problem of having null area which reduces the efficiency of WPT or failure of RFID systems. We will discuss the reason of the problem of null area and at the end we will propose a solution for this problem. We will start by explaining our method, then we check it by simulating the method in Matlab and finally we check it experimentally to see if theoretical results are in accordance with the theoretical and the simulated results. When we have the experimental results that show the applicability of the method our task is completed.

The magnetic coupling between reader and tag in LF RFID and HF RFID or in IPT is described in terms of Faraday's law of magnetic induction. According to this law which reads:

$$\frac{\partial \vec{B}}{\partial t} = -\nabla \times \vec{E} \quad (2.1)$$

any time-varying magnetic field, denoted by \vec{B} , will give rise to an electric field, denoted by \vec{E} , whose curl is equal to the rate of change in the magnetic field in respect to time. If it happens that in the location of created electric field \vec{E} there is a conductor, this \vec{E} will give rise to a voltage across this conductor according to:

$$V = - \int \vec{E} \cdot d\vec{l} \quad (2.2)$$

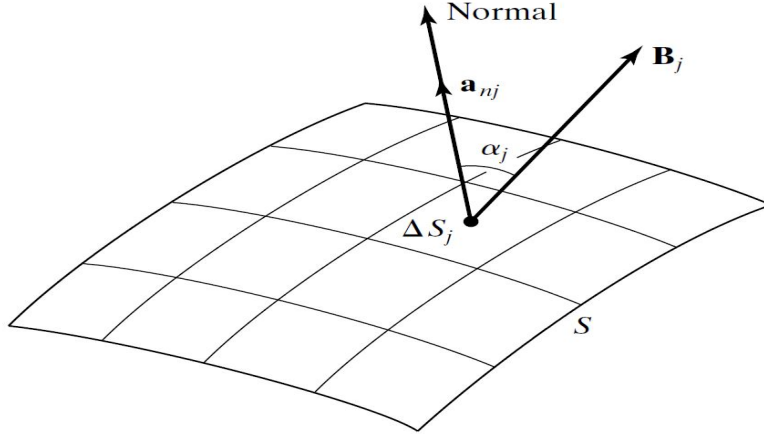


Figure 2.1: When we have a surface S in a magnetic field, it could be divided in a number of infinitesimal surfaces. What is important here is the angle α_j between the norm vector of the surface and the direction of the magnetic field at the infinitesimal surfaces ΔS_j . [59]

This induced voltage will create an electrical current in the conductor. Because in most practical situations in electronic we are working with closed circuits, it is more convenient to transform the equation 2.1 in its integral form which reads:

$$\oint \vec{E} \cdot d\vec{l} = -\frac{\partial \Phi}{\partial t} \quad (2.3)$$

Here Φ represents the magnetic flux passing through the closed conductor. From equations 2.2 and 2.3, we get:

$$V = -\frac{\partial \Phi}{\partial t} \quad (2.4)$$

This telling us that the induced voltage in a closed conductor is equal to the rate of change of the magnetic flux passing through it in respect to time.

To understand the magnetic flux Φ consider a surface S which is in a location where there is a magnetic field, as shown in Fig.2.1[59].

The magnetic flux passing through the surface S is found by dividing this surface in a number of infinitesimal parts, ΔS_j , represented by a vector normal to the ΔS_j . For each of these ΔS_j , we calculate its contribution to the total magnetic flux by:

$$d\Phi = \vec{B} \cdot \Delta\vec{S}_j \quad (2.5)$$

Applying the obtained result for each infinitesimal surface, and adding up the contributions of all these infinitesimal surfaces one get the total magnetic flux passing through the surface S .

The dot product in the equation 2.5, is given according to:

$$\vec{B} \cdot \Delta\vec{S}_j = B\Delta S_j \cos \alpha_j \quad (2.6)$$

The angle α , is the angle between the magnetic field and the vector normal to the ΔS_j as shown in the Fig.2.1.

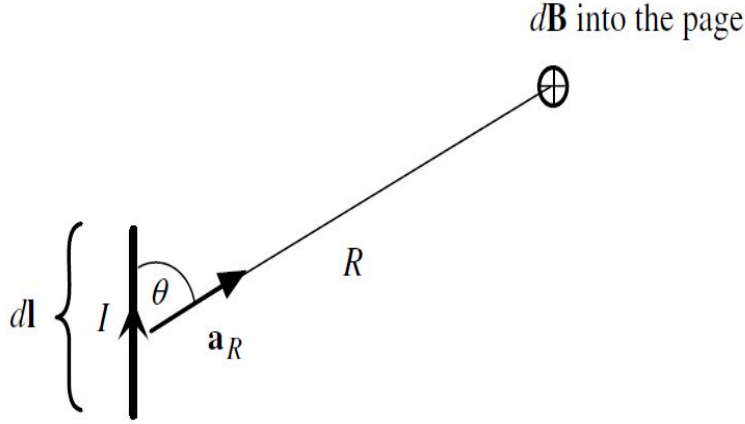


Figure 2.2: Biot–Savart law [57]

As one can see from the equation 2.6, the results of this product depends strongly on the direction of the magnetic field and the direction of the vector normal to the surface enclosed by the conductor or the orientation of the closed conductor in the magnetic field. For these reasons, we turn our attention more closely to the generated magnetic field and its property and the orientation of the closed conductor in which we will have induced voltage.

2.2 MAGNETIC FIELD AND BIOT-SAVART LAW

The fundamental law for the computation of the magnetic field is the Biot–Savart law. This law tells how a magnetic field is generated by electric current:

$$d\vec{B} = \frac{\mu_0 I}{4\pi R^2} d\vec{l} \times \vec{a}_R \quad (2.7)$$

Figure 2.2 shows the geometry associated with the variable of this law. Here it is assumed that the element carrying current is a filamentary element and the differential length vector $d\vec{l}$ is in the direction of current. R is the distance between differential length $d\vec{l}$ and the point where we want to calculate the magnetic field. The magnetic field depends on the cross product $d\vec{l} \times \vec{a}_R$, where \vec{a}_R is the unit vector from $d\vec{l}$ to the point where we want to calculate the magnetic field. It is this cross product that gives us the direction of the magnetic field. I is the DC current passing through the differential length $d\vec{l}$.

It should be mentioned here that this field is due to a DC current. Earlier we said that it is a time varying magnetic field that induces a voltage across a conductor. However, if we are working in regime in which the wavelength of the frequency of operation is very large in comparison to the sizes and distances we are interested in, we could assume that the results based on DC calculation are still very good approximation. This is the quasi-static approximation that is widely used and we are going to use here also. In terms of the angle θ in Fig. 2.2, we can rewrite the Biot–Savart law as:

$$d\vec{B} = \frac{\mu_0 I dl}{4\pi R^2} \sin \theta \vec{a}_n \quad (2.8)$$

CHAPTER 2. A RECONFIGURABLE ANTENNA FOR ENHANCING THE
MAGNETIC COUPLING IN IPT AND RFID

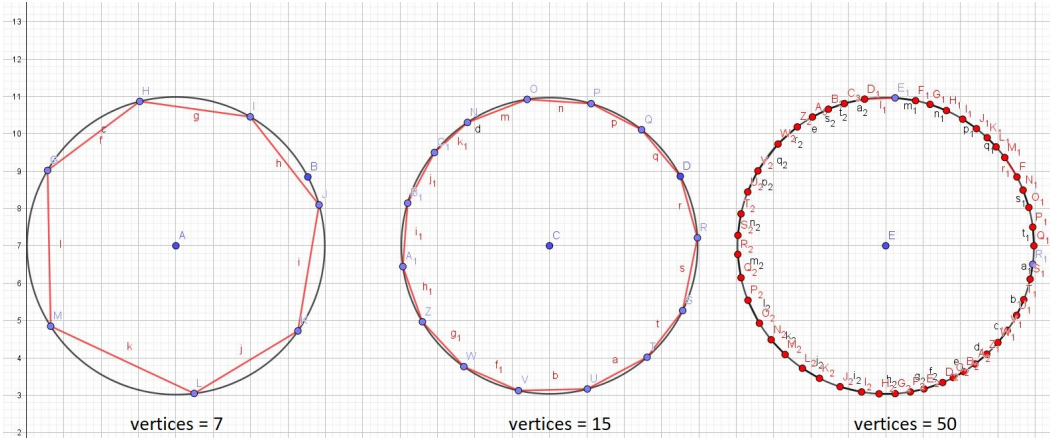


Figure 2.3: The circle in the left is approximated by a polygon of 7 vertices, which is not a very good approximation. As we increase the number of vertices to 15 (in the middle) and 50 (on the right) for example, the polygon becomes better and better approximation of a circle. The polygon on the right is a good approximation and almost completely covers the circle underneath it.

where \vec{a}_n , is a unit vector normal to the plane containing \vec{dl} and \vec{a}_R .

After determining the magnetic field due to a differential length vector \vec{dl} , one actually can determine the magnetic field due to any configuration of electric current, no important how complicated they are.

This is done in three steps:

1. Divide any structure into infinite number of infinitesimal differential lengths. This step is very common in calculus.
2. Use the Biot-Savart law (in equation 2.7 or 2.8) to calculate the magnetic field due to each infinitesimal differential length.
3. Add the magnetic field due to each infinitesimal differential length together to get the final magnetic field. This step which is summation over infinite elements in fact is taking the integral.

If this program could be carried out completely, one will end up with an analytical solution for a static magnetic field due to the DC current. But it turned out that it is a very complicated task and most of the time we could not solve it analytically even for very simple electric current carrying structure like a circular or rectangular coil. However these problem could be solved numerically. Here, we developed a Matlab code that approximates any electric current carrying structure into many elements (but not infinite number as demanded in step 1) and these elements are not of infinitesimal length (as demanded in step 1). However if these elements are small enough in comparison to the size of the structure that we study, the results are very good approximation of the analytical results. Further more these approximated results could be made, more accurate by decreasing the length of these elements (and at the same time increasing the number of these elements). This will increase the time of simulation and the required memory. At the end we have an optimization between required accuracy and the available memory and preferable calculation time.

Fig 2.3 shows these concepts for a circle.

Figure 2.4 shows the calculated magnetic field as vectors due to small straight line of

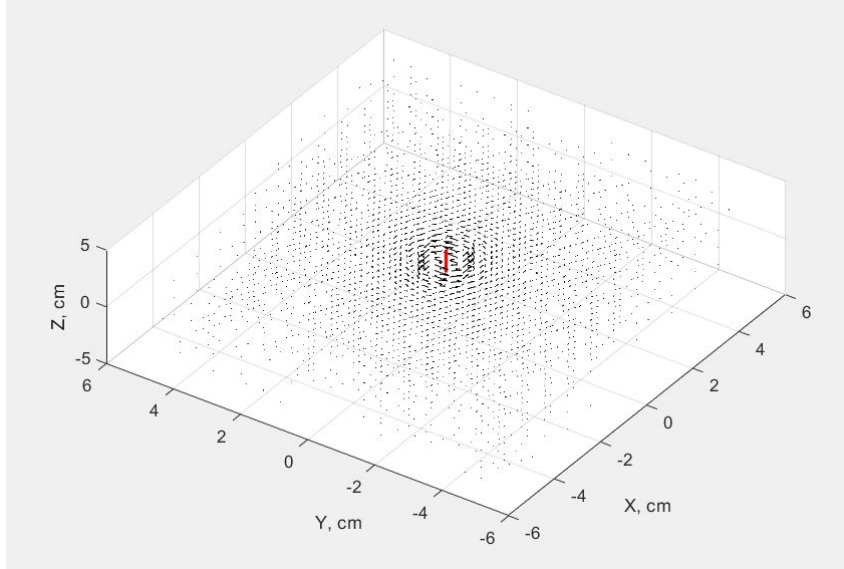


Figure 2.4: Calculated magnetic field as vectors due to small straight line (shown in red) of electric current.

electric current. Figure 2.5 shows the same results but instead of vector we are using field line to show the magnetic field.

Also there is another way for calculating magnetic field which could make it easier to calculate the magnetic field of a certain current distribution. It starts by noticing that:

$$\nabla \cdot \vec{B} = 0 \quad (2.9)$$

the divergence of the magnetic field is always zero. From vector calculus we know that the divergence of the curl of a vector field is always zero. This means that the magnetic field could be defined as a curl of another vector field, let's call this new vector field: \vec{A} that is called the vector magnetic potential

$$\vec{B} = \nabla \times \vec{A} \quad (2.10)$$

If we put this definition in the Amper law ¹

$$\nabla \times \vec{B} = \mu_0 \vec{J} \quad (2.11)$$

where \vec{J} is the current density, we get:

$$\nabla \times (\nabla \times \vec{A}) = \mu_0 \vec{J} \quad (2.12)$$

The equation 2.12 could be solved for $d\vec{l}$, a differential length of the line in the direction of the current of I, at a distance R from this differential current element[inductance book]:

$$\vec{A} = \frac{\mu_0}{4\pi} \int \frac{I}{R} d\vec{l} \quad (2.13)$$

¹In equation 2.11 we ignore the second term, namely time derivative of the electric field because we assume that we are working in quasi static regime. However it is shown in most text book about electromagnetism that even in general case this definition of \vec{A} , vector magnetic potential is still valid.

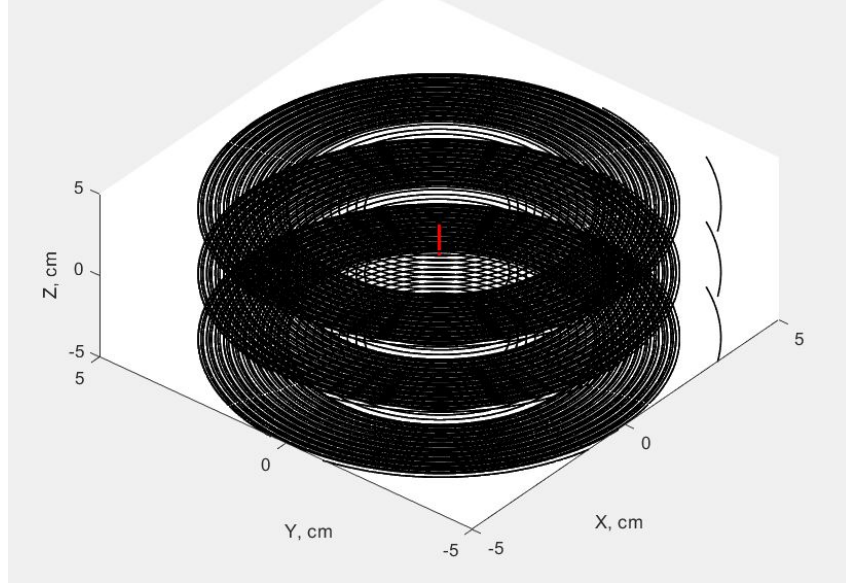


Figure 2.5: Calculated magnetic field as line of field due to small straight line (shown in red) of electric current.

When \vec{A} is calculated in this way, we could take its curl, according to the equation 2.10 to arrive at the magnetic field.

This method is more suitable for calculating the magnetic field of a current distribution which is more complicated than simple straight line. For example in the case of a current loop. Fig. 2.6 shows such a current loop lying in the xy plane and of the radius a in cylindrical coordinate system. In [57],[16], [34] it is shown that the vector magnetic potential \vec{A} of this current loop in a cylindrical coordinate system is calculated according to:

$$A_\phi = \frac{\mu_0 I}{2\pi} \int_{\phi=0}^{\phi=\pi} \frac{a \cos \phi}{\sqrt{a^2 + \rho^2 + z^2 - 2a\rho \cos \phi}} d\phi \quad (2.14)$$

Here A_ϕ is a component of \vec{A} which is in the ϕ direction, as shown in Fig. 2.6. Because the current is just in ϕ direction, according to equation 2.13, the only non zero component of \vec{A} is in ϕ direction, and other components are zero so we don't need to calculate them. ρ is the distance between the projection of the point at which we calculating \vec{A} on the xy plane and the origin of the current loop. z is the z component of the point at which we calculating \vec{A} if we assume the current loop center is at $z=0$.

Exact solution for the integral in equation 2.14 could be found in terms of the complete elliptic integrals [57],[16], [34] as follows:

$$A_\phi = \frac{\mu_0 I}{\pi k} \sqrt{\frac{a}{\rho}} \left[\left(1 - \frac{k^2}{2}\right) K - E \right] \quad (2.15)$$

where k^2 is defined to be:

$$k^2 = \frac{4a\rho}{(a + \rho)^2 + z^2} \quad (2.16)$$

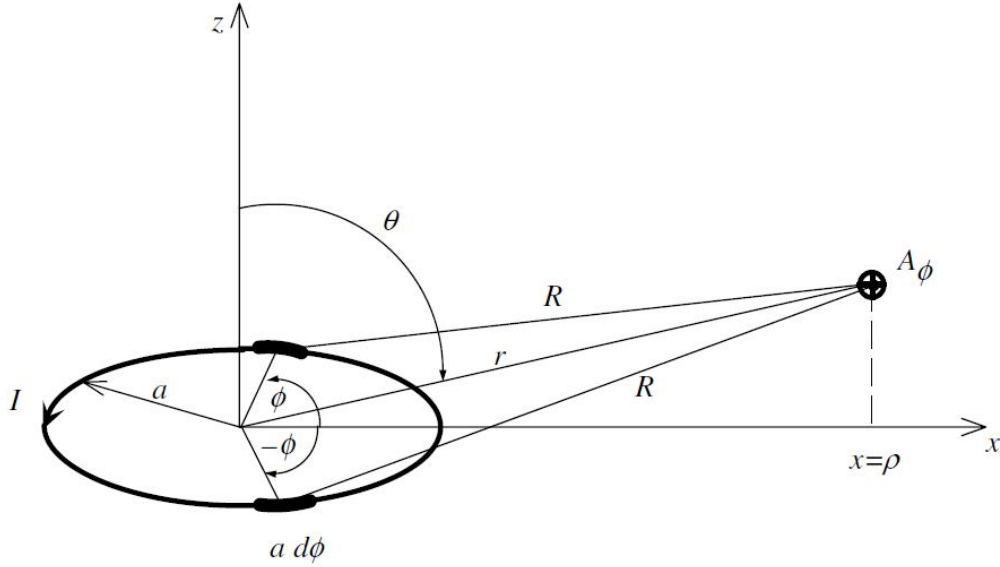


Figure 2.6: Current loop in a cylindrical coordinate system [57].

where K and E are the complete elliptic integrals of the first and second kind. If we take the curl of equation 2.15, we will have the following component for the \vec{B} in cylindrical coordinate:

$$B_\rho = \frac{\mu_0 I}{2\pi} \frac{z}{\rho \sqrt{(a+\rho)^2 + z^2}} \left[-K + E \frac{a^2 + \rho^2 + z^2}{(a-\rho)^2 + z^2} \right] \quad (2.17)$$

$$B_\phi = 0 \quad (2.18)$$

$$B_z = \frac{\mu_0 I}{2\pi} \frac{1}{\sqrt{(a+\rho)^2 + z^2}} \left[K + E \frac{a^2 - \rho^2 - z^2}{(a-\rho)^2 + z^2} \right] \quad (2.19)$$

These expressions for the magnetic field still are not in very clear and easy form but to our best knowledge, this is as far as one can go in getting analytical expressions.

However it is possible to evaluate these expressions numerically. We developed a Matlab code that evaluates these field components in a convenient and fast way.

Fig.2.7 show the magnetic field of a filamentary loop of one turn (that is a loop which is made of a wire of a thickness too small in respect to other physical sizes we are interested in, so we neglect it). The radius of this loop is 3 cm and each vector shows the magnitude and the direction of the magnetic field at certain point in space (field point). For getting better understanding of the shape of the magnetic field of a filamentary loop, it is more convenient to plot the magnetic field line instead of vectors.

In Fig.2.8, we clearly see that the loop carrying current creates magnetic field lines that form circles around the current carrying loop. The magnetic field lines are function of space, that is they change their value and direction from point to point in space. It is easier for us for the sake of future calculations and visualizations to work in Cartesian coordinate system. Transferring $\vec{\mathcal{A}}$ in cylindrical coordinate into \vec{A} in Cartesian coordinate system is a straight forward task. Later we will see that it is more important (due to the mechanism of mutual inductance) to pay attention to the different component of the magnetic field, namely

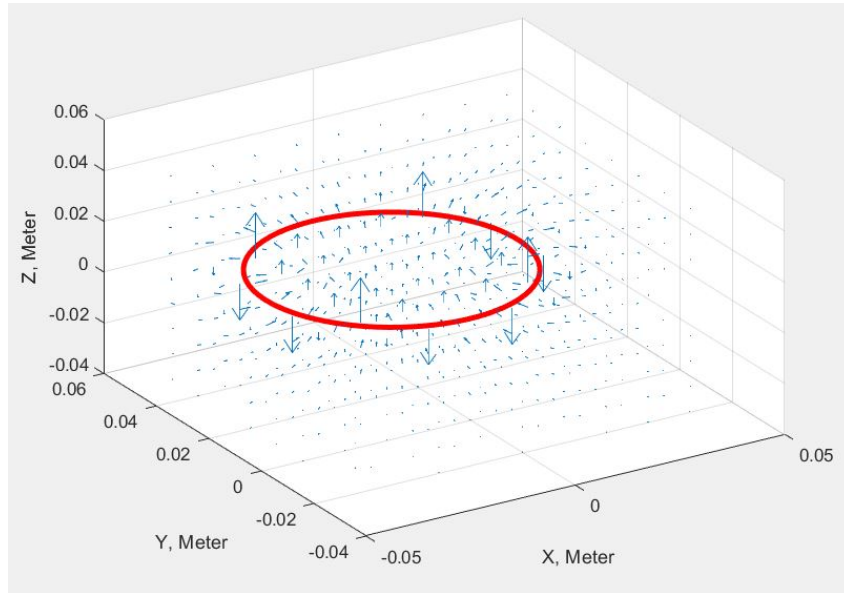


Figure 2.7: The magnetic field of a filamentary loop of one turn as vectors.

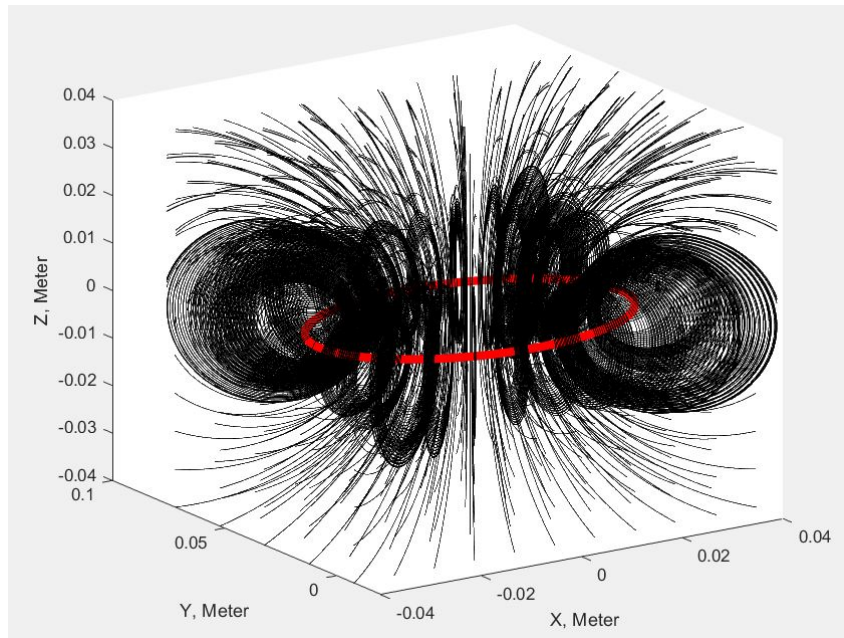


Figure 2.8: The magnetic field of a filamentary loop of one turn as field lines.

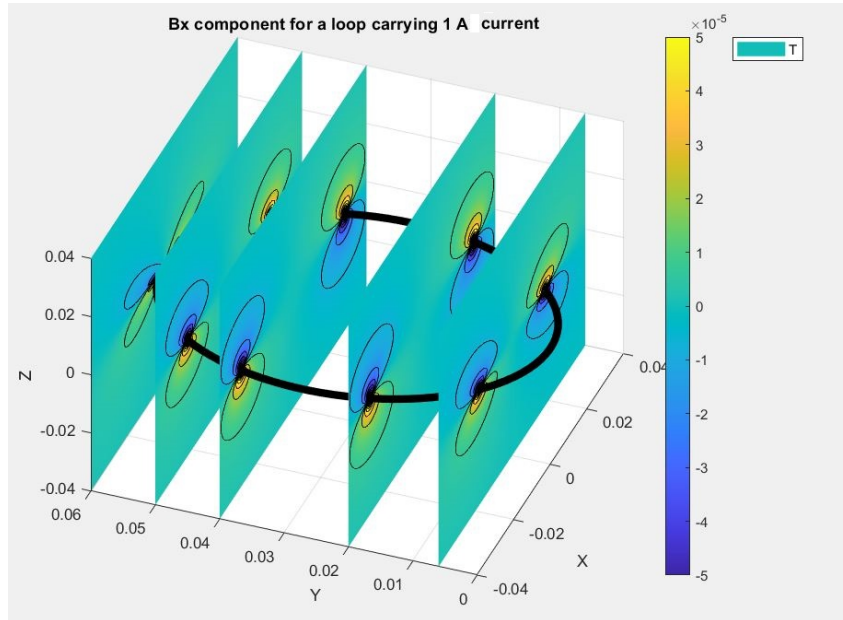


Figure 2.9: B_x component of the magnetic field of a loop carrying 1 A current. The magnetic field is in Tesla and the X,Y and Z axes in Meter.

B_x, B_y, B_z , at each point in space rather than to the whole magnetic field line. B_x, B_y, B_z are the magnetic field component along X, Y, Z axes. Figure 9-11 show those components for a loop carrying current.

Because these values are volume data (there is a certain value at each point) it is more convenient and easier to see if we plot them just in certain locations. Here we chose multiple plane cutting the loop to show the value of the magnetic field on these planes. The black lines on the planes are contours of equal values of the magnetic field components.

What we have being doing is this: we assume a certain current distribution is given, then from Biot-Savart law we calculates the magnetic field component due to this current distribution.

2.3 MAGNETIC FIELD BEAM STEERING

As we saw in equation 2.8, the Biot-Savart law is linear law in respect to current I. That makes it possible to use the principle of superposition with this law. The principle of superposition states that the final magnetic field of any configuration of electric current is simply the addition of the magnetic field due to each part of the electric current configuration. The magnetic field is a vector field, so the addition here means vectors addition.

In previous section we talked about the magnetic field of a current loop. By using the principle of superposition we could simply generalize the result we get in calculating the magnetic field of a single loop current, to any combination and configuration of a multiple loop current.

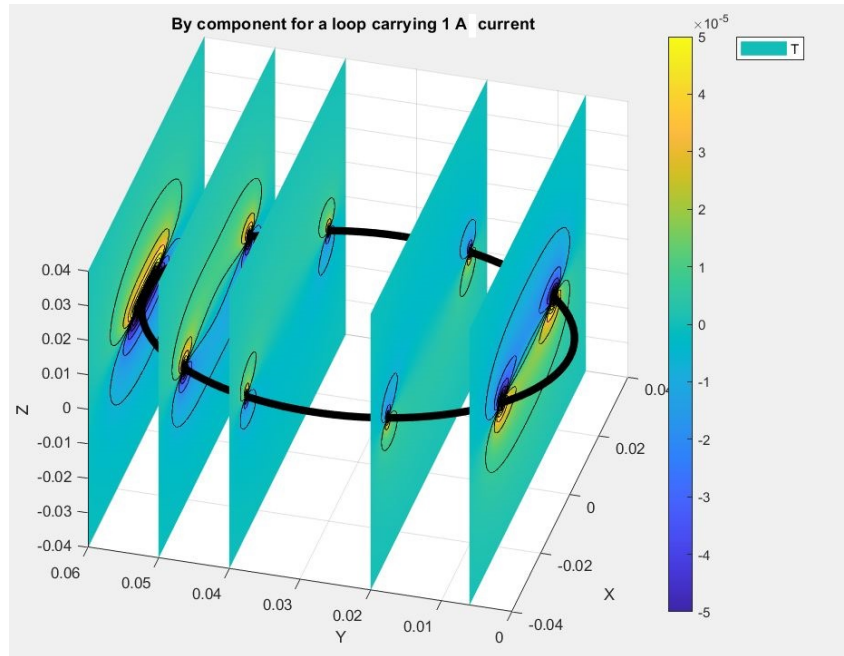


Figure 2.10: B_y component of the magnetic field of a loop carrying 1 A current. The magnetic field is in Tesla and the X,Y and Z axes in Meter.

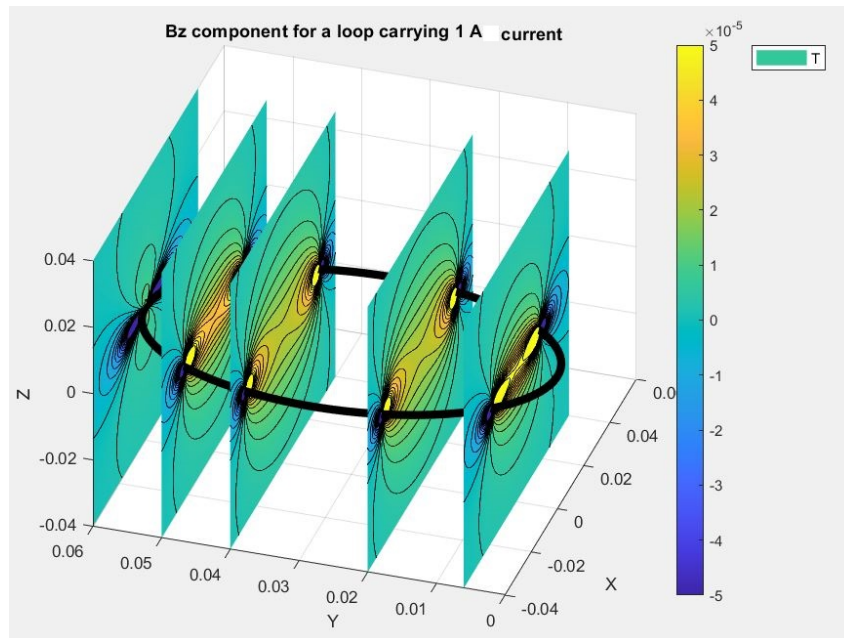


Figure 2.11: B_z component of the magnetic field of a loop carrying 1 A current. The magnetic field is in Tesla and the X,Y and Z axes in Meter.

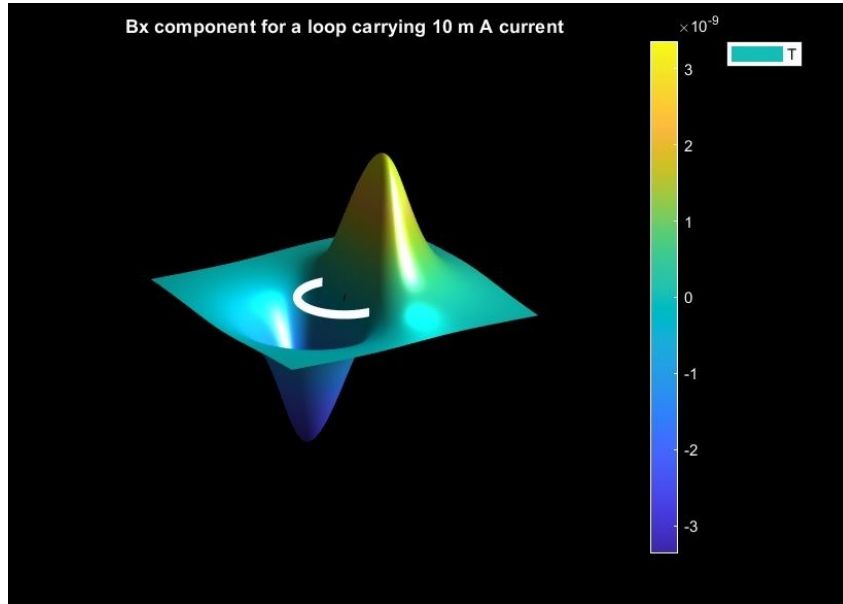


Figure 2.12: B_x component of the magnetic field of a circular loop current of diameter of 10 cm carrying 10 mA current. The field is at a distances of 4 cm above the loop. The loop is shown in white. The magnetic field is in Tesla.

The final magnetic field will be just the vector addition of the magnetic field due to each loop current.

Consider one loop current of diameter of 10 cm, carrying 10 mA of current in clockwise direction. As we said earlier talking about the components of the field is more useful than talking about the whole magnetic field line.

Fig 2.12 shows the B_x of this loop current at plane parallel to the plane of the loop current and at a distances of 4 cm above the loop. The loop current is in the X-Y plane and Z axis represents the distance above the loop current.

One can see that the value of B_x component in the center of the loop is zero in Fig. 2.12. To see it more clearly the absolute value of B_x is plotted in the Fig 2.13. The Fig.2.14 shows the B_z component of the magnetic field. We can see here that the B_z of the field in contrast to the B_x of the field, has its maximum in the center of the loop.

Now if for some reasons one is interested in having B_x component in a location, let say close to the center of the loop current, one could modify the magnetic field in that location by moving, for example, a second loop current next to the first loop current. As we said earlier the resultant magnetic field will be the superposition (vectorial addition) of these two magnetic fields due to the first and second loop.

Generating a magnetic field which is specially suitable for certain location of the receiver is the main objective of Localized WPT. There are different approaches for doing so which has been proposed in literature and find their way to industry. Here we mention some of them adopted by "Qi" standard[32]

Those include three WPT methods and include both guided and free positioning scenario.

1. Guided positioning. This is not a free positioning system. The receiver is forced to

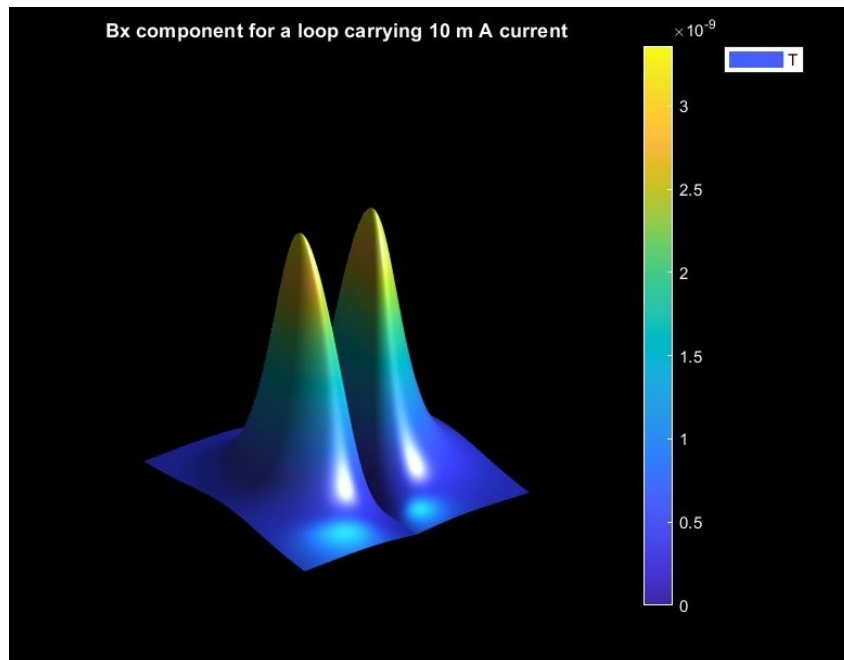


Figure 2.13: Absolute value of B_x component of the magnetic field of a circular loop current of diameter of 10 cm carrying 10 mA current. The field is at a distance of 4 cm above the loop. The loop is underneath the surface and could not be seen here. The magnetic field is in Tesla.

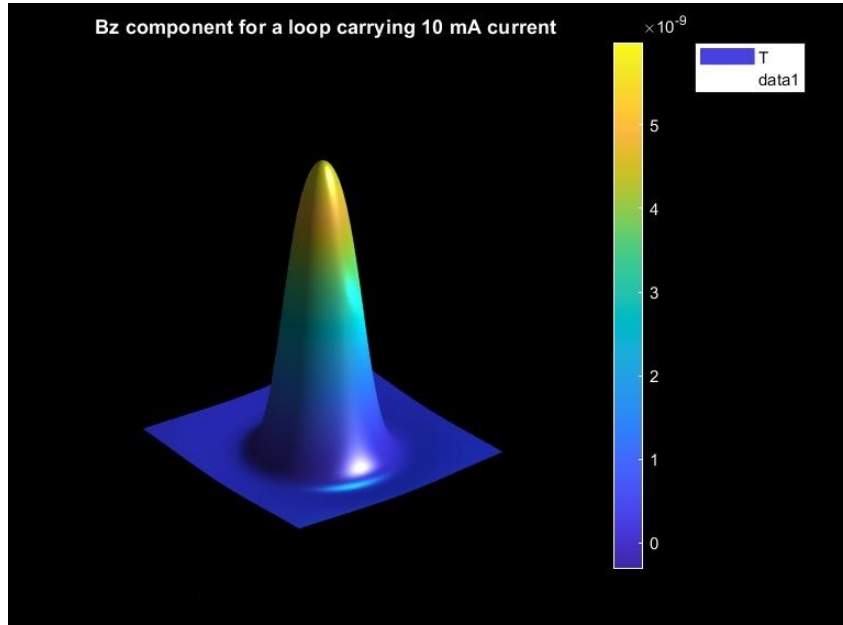


Figure 2.14: B_z component of the magnetic field of a circular loop current of diameter of 10 cm carrying 10 mA current. The field is at a distances of 4 cm above the loop. The loop is underneath the surface and could not be seen here. The magnetic field is in Tesla.

be in a certain location either by a frame that houses the receiver or any other attraction mechanism that force the receiver to certain location. This method is used in example for wireless charging of devices that could be positioned in a more or less precise location by the users, like mobile phone wireless charging, toothbrush wireless charging and so on. Fig.2.15 shows this guided positioning method which is currently one of the most used method in industry.

2. free-positioning charging by using a movable transmitter coil located under the charging surface. This method follows the logic we just mentioned, namely to enhance the magnetic field in the location of the receiver, the transmitter is moved to a position that generates suitable magnetic field for the receiver. This method needs some kind of localization, so the transmitter knows where to move.

3. free position for wireless power transfer using coils array without movable mechanical parts. In this method the receiver could have any location (in the certain range) and only transmitters close to the receiver will be energized. Fig.2.16 shows the principle of methods 2 and 3.

In this chapter the method that we want to explain does not fall clearly in any of these category but it has more in common with method 3.

In practice instead of moving the loop current around, it is much more convenient to have a circuit with capability to turn on or off the currents in its different parts. By controlling the value and the phase of current in different parts of the circuit, one controls the magnetic field generated by that part of the circuit. This give us a mean to control the total magnetic field of the circuit and enable us to generate (in certain realistic practical limits) any desired magnitude or rotate it to any desired direction. The structure of the electric

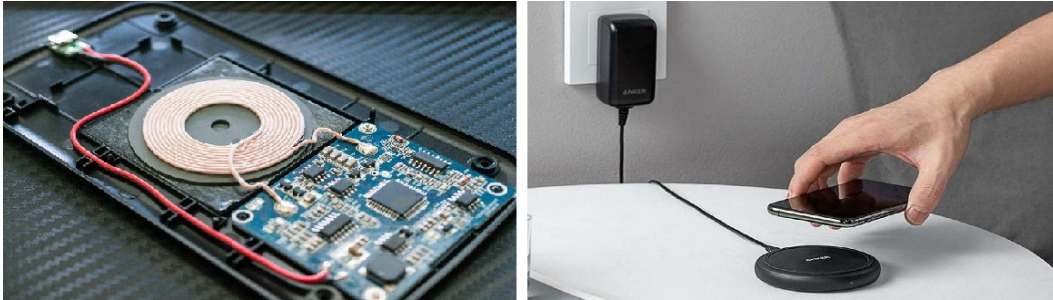


Figure 2.15: Commercial application of guided positioning. This is not a free positioning system. The receiver should be positioned by the user above the coil (shown on the left), otherwise the system will not work.[29]

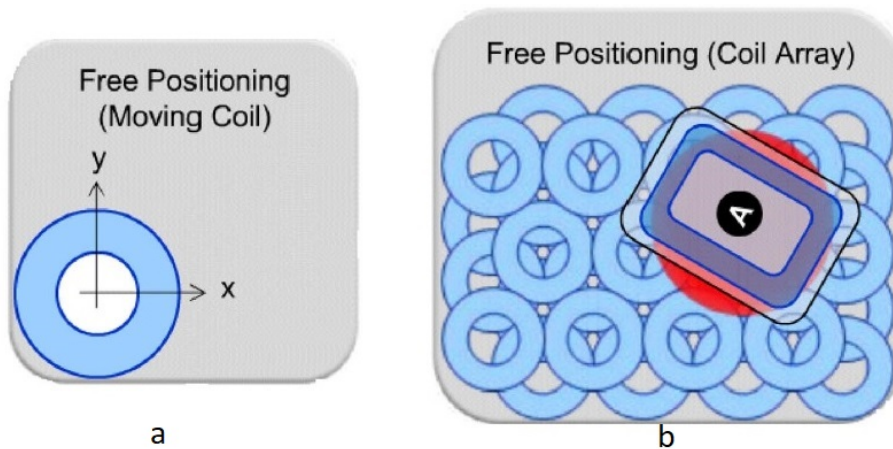


Figure 2.16: a. The free positioning method based on a mechanically moveable primary coil is illustrated. The white circle is the receiver that could be anywhere in certain range. The transmitter, the blue circle, moves underneath to locate itself in better position. b. The method based on a selective excitation of a coil array is illustrated. [32]

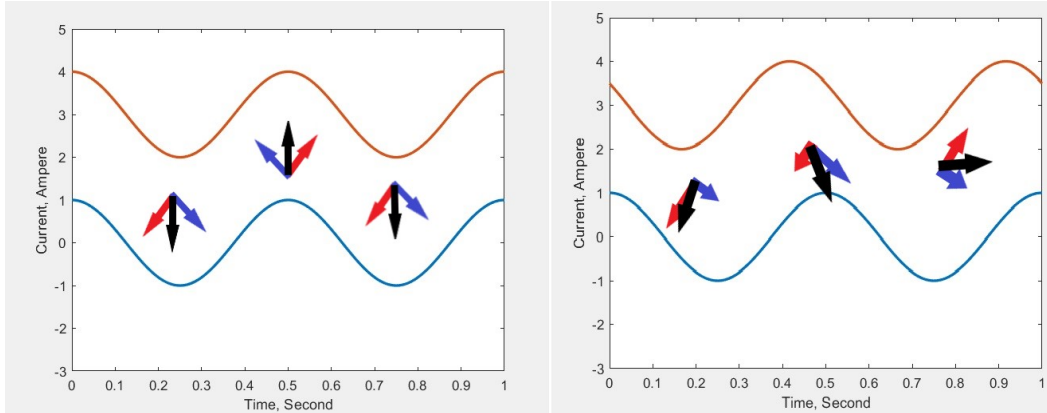


Figure 2.17: When there is no phase difference between applied current to (for example) two coils, the resultant magnetic field (the black arrow) don't change the direction because the components always change in proportion (left panel) so the resultant vector remains in the same direction. When there is phase difference between applied current to two coils, the resultant magnetic field (the black arrow) changes the direction because the components are not any more changing in same proportion (right panel). blue arrows represent the magnetic field due to blue current in one coil in three instances of time, red arrows represent the magnetic field due to red current in second coil in three instances of time, and the black arrow is the final magnetic field.

circuit that generates the magnetic field could be of any shape, it could be 3 dimensional or 2 dimensional (planar). One could control the magnitude of the current or its phase.

If the current in different parts of the structure of the electric circuit are not in phase, the magnetic field will change its direction while it oscillates, as shown in Fig. 2.17.

In this work we will not consider changing the phase, except by 180 degree which is equivalent to changing the direction of the current. Fig. 2.18 shows the main idea behind using the magnitude of the current in one part of the structure of the electric circuit to rotate the magnetic field in certain direction.

Assume that in a certain point in the space surrounding the structure of the electric circuit we have a total magnetic field shown by red vector. This total magnetic field is the result of vector addition of the magnetic field due to two different parts of the structure of the electric circuit, shown in dashed blue.

By modifying the magnitude of magnetic field due to these two different parts of the structure shown in blue vectors, one can have control on the direction of the total magnetic field. As we saw in equation 2.8 the magnitude of the field (hence each of its component) has linear relation to the electric current that generates them. So by increasing the electric current in one part of the circuit responsible for magnetic field of one of the dashed blue vector by a factor (n) one also increase the value of that field also by the factor of n .

Those current used should be alternating current, according to equation 2.4 otherwise DC current will not induce any voltage necessary for mechanism of magnetic induction. If current in different parts of the structure of the electric circuit are in phase, the magnetic field will oscillate while keeping its direction.

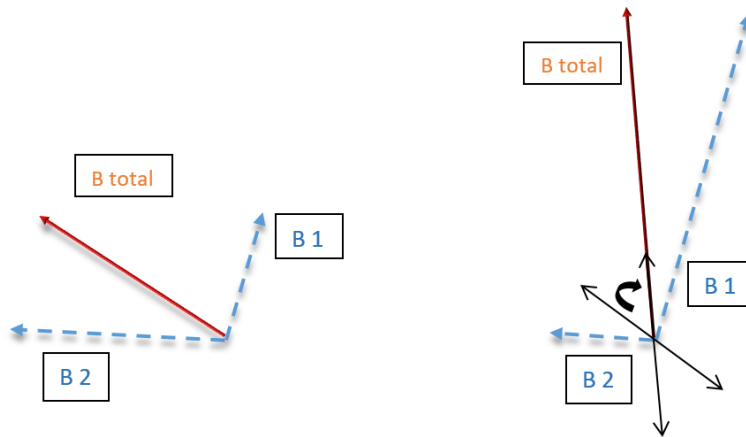


Figure 2.18: Modifying the magnitude of magnetic field due to two different parts of the structure shown in blue vectors, enables us to control the direction of the total magnetic field in any direction. Two black lines in the right of the figure show the direction of the total magnetic field before and after of the rotation of the field. If the currents that generate B1 and B2 are in phase, the total magnetic field will always oscillate in the same direction.

This is the foundation of magnetic beam steering.

To achieve magnetic field steering, different structures of the electric circuit have been proposed. Most such structures proposed for beam steering are 3D structures, composed of two (or three or even more) orthogonal coils. Fig.2.19 shows one of such structure composed of two orthogonal coils. It is true that having a 3D structure gives us more control, but having a 2D structure is more convenient for certain applications. 2D structures are plane structures that their physical size in one dimension is small and negligible to its size in other dimensions, hence we are going to call them two dimensional structures, or just 2D.

For this reason we chose a twisted loop antenna (TLA). In[23],[21] it was shown that a twisted loop antenna in general creates a magnetic field which is more suitable for the kind of magnetic field distribution required for the magnetic induction to work (we will explain the mechanism of magnetic field induction later and we will see why this is the case).

A twisted loop antenna is shown in Fig.2.20. It is composed of two coplanar coils next to each other. This is the simplest possible configuration of a twisted loop antenna. We could modify it by adding any number of coils to each side of it, Fig.2.21. We could change the diameters of these coils as we want and we could make two (or any number) of such twisted loop antenna and rotate them in respect to each other in any angle, Fig. 2.22.

As long as the structure is a 2D planar structure, we will call it a twisted loop antenna.

In fact we consider the twisted loop antenna as a set of coils that we could arrange in any way that is desirable for our work. It is a mat of coplanar coils.

The reason of using a twisted loop antenna instead of separated coils in this work is the simplicity of applying the signal to the structure. If we connect different loops via certain controlling mechanism, for example relay switch, one will need just one signal source for all the structure instead of a separate signal source for each coil.

Earlier we said the control of the magnetic field could be done by controlling the electric

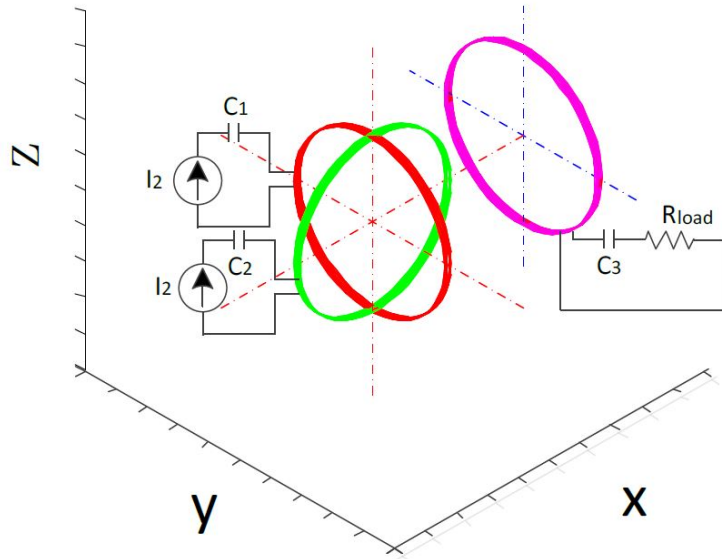


Figure 2.19: 3-D magnetic beam steering WPT system with a loaded receiver coil resonator[48].

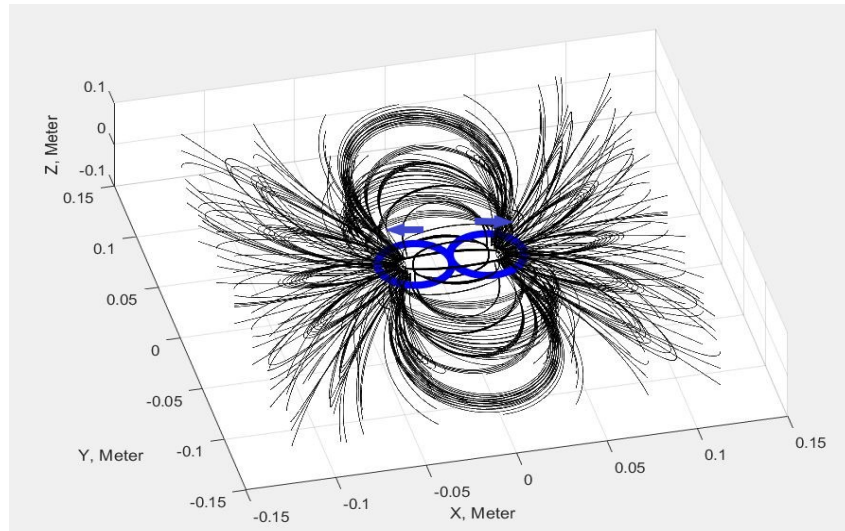


Figure 2.20: A twisted loop antenna in its simplest possible configuration. It is composed of two coplanar coils next to each other. Both coils are made of one turn, so the current is the same in both of them. The electric current in one loop is in clockwise direction and in the other loop in anti clockwise direction (shown by blue arrows). The diameter of each loop is 4 cm. The black lines are the magnetic field lines due to this configuration in space around the antenna.

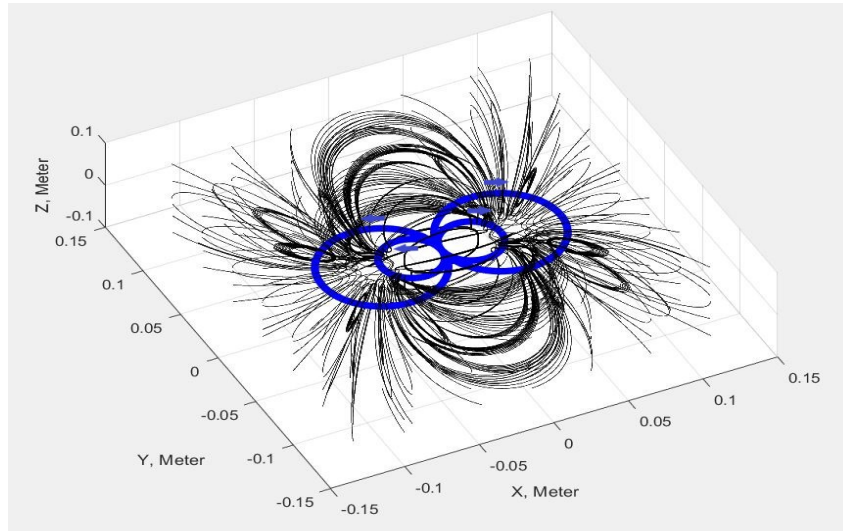


Figure 2.21: A twisted loop antenna in a configuration consisting of four coils. The diameter of small coils are 4 cm and the diameter of larger coils are 8 cm. Coils are coplanar and each coil has one turn, so they have the same electric current. The electric current in one small and big loop is in clockwise direction, and in the other small and big loop in anti clockwise direction (shown by blue arrows). The black lines are the magnetic field due to this configuration in space around the antenna.

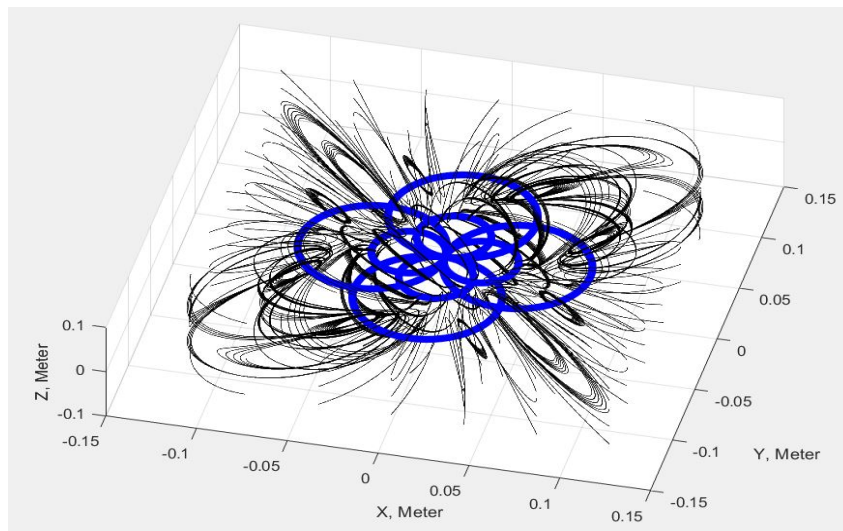


Figure 2.22: A twisted loop antenna in a more complicated configuration consisting of eight coils. This configuration is two copy of the configuration shown in Fig.2.21 with one of them rotated in respect to the other by 90 degree. The all structure is coplanar. The black lines are the magnetic field due to this configuration in space around the antenna.

current in coils. In a twisted loop antenna this task is done by keeping the same current flowing in the circuit, but by changing the number of turns in each coil, equivalently we are modifying the magnetic fields.

Again controlling of the number of turns in each coil is achieved by connecting them through for example relay switch, which enables us to connect or disconnect certain number of turn. This structure offers only 180 degree of phase change. Again its possible that through relay switch, one control the direction of current flow in each coil in two ways. One direction of the current circulating in the coil we call clockwise and the other we call anti clockwise.

The parameters that hard-wired in the structure and defined the structure of a twisted loop antenna and could not be controlled after fabrication of a twisted loop antenna are:

1. The number of coils and their relative position to each other.
2. Diameter of each coil

The parameters that could be changed and we have control on, are:

1. the number of turns in each coil. This number will effectively control the amount of electric current in the coil. Though in fact we are not changing the current, but increasing the number of turns will have the same effect on the magnetic field that increasing the current. For example, if we double the number of turns in a coil we also doubled the magnitude of the magnetic field due to that coil. Here we don't have continuous control and we can increase the number of turns (and eventually the magnitude of the magnetic field) by discrete number.
2. the direction of current in each coil in two discrete ways: clockwise and anti clockwise, which is equivalent to having current in 180 degree of phase difference.

When these parameters are chosen for a twisted loop antenna, we will say that twisted loop antenna is in a certain " configuration ", specified by the number of turn and the direction of current.

As we increase the range of discrete possibility the controlling system (the number of relay switches for example) became more and more complex and the justification we offered earlier for using a twisted loop antenna (which was essentially the ease of controlling its different parameters) is not truth any more.

However even within a limited number of parameters that could be changed, one could achieve sufficient number of configurations for dealing with practical situations.

Fig. 2.23 shows the generated magnetic field of one possible configuration of a twisted loop antenna shown in Fig. 2.22. The surface shows the value of B_x component of the field in a plane parallel to the plane on which the twisted loop antenna is placed (that is X-Y) and at 4 cm above the twisted loop antenna. The perpendicular axis here is not the vertical distance above the twisted loop antenna but the value of B_x component for different points with range of X and Y, but fixed Z, namely for Z=4 cm above the twisted loop antenna. The white circle is our target point where we want to increase the value of B_x .

Assume that first we have a certain configuration (certain number of turns for each coil and certain directions for current as explained earlier) of the twisted loop antenna shown in the Fig. 2.22 that creates the magnetic field component shown in the Fig. 2.23. Now assume that for some reason we want to create a magnetic field B_x component at the point shown by white circle.

By changing the configuration of the twisted loop antenna, one creates a magnetic field shown in the Fig. 2.24. Here as we can see, we increased the value of the magnetic field B_x component at that point (white circle) .

In doing so, we steered the magnetic field toward certain direction.

Later we will explain how to chose a suitable configuration for creating desired magnetic

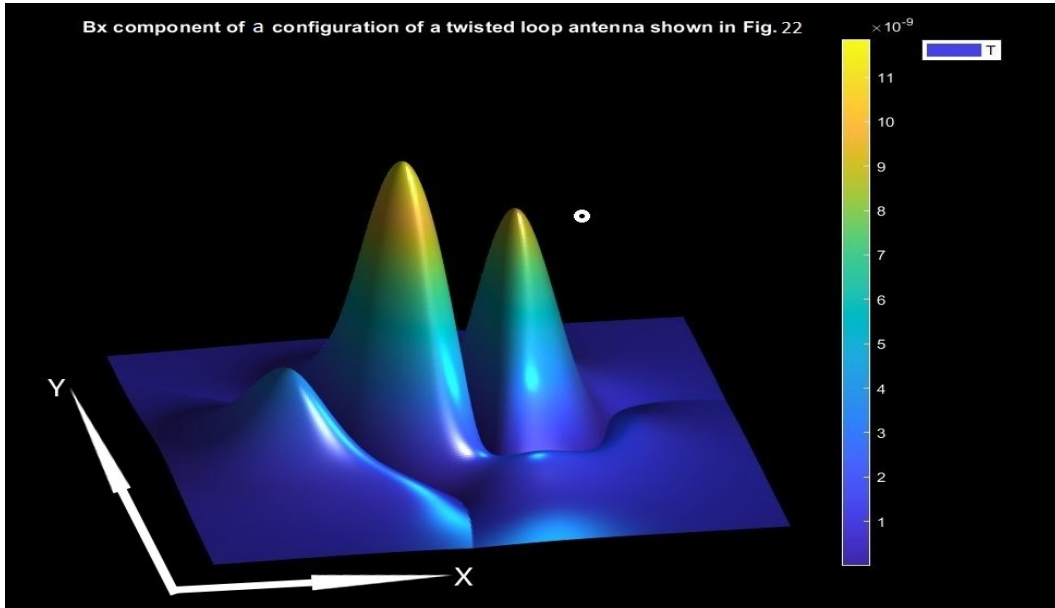


Figure 2.23: The surface shows the value of B_x component of the field in a plane parallel to the plane on which the twisted loop antenna is placed (that is X-Y) and at 4 cm above the twisted loop antenna, for one possible configuration of a twisted loop antenna shown in Fig. 2.22. The white circle is our target point where we want to increase the value of B_x .

field component at any point. It also should be mentioned that it is not always possible to create a local maxima in targeted point. However, we will later see that it is more important to create a local maxima in a vicinity of the targeted point, it is not necessary to create a local maxima exactly at the targeted point.

In this chapter, we will use different configurations of the twisted loop antenna as a mean to perform the magnetic beam steering.

Now that we know how to calculate the magnetic field and how to steer it, we should investigate the mechanism of magnetic induction more closely and see how it is affected by the distribution of the magnetic field lines.

2.4 MUTUAL INDUCTANCE

Faraday's law of induction is the fundamental mechanism of inductance. Assume we have a circular loop shown in Fig. 2.25. If we excite an electric current I in it so that the electric current flows in the counter-clockwise direction, this current will, by the Bio-Savart law, creates a magnetic field B which is passing through the surface that the current loop enclosed. We are assuming here that this surface is flat for simplicity, but any surface shape in fact gives the same results. For the counter-clockwise direction electric current as shown in Fig. 2.25 the magnetic field B , is upward passing through the surface enclosed by the

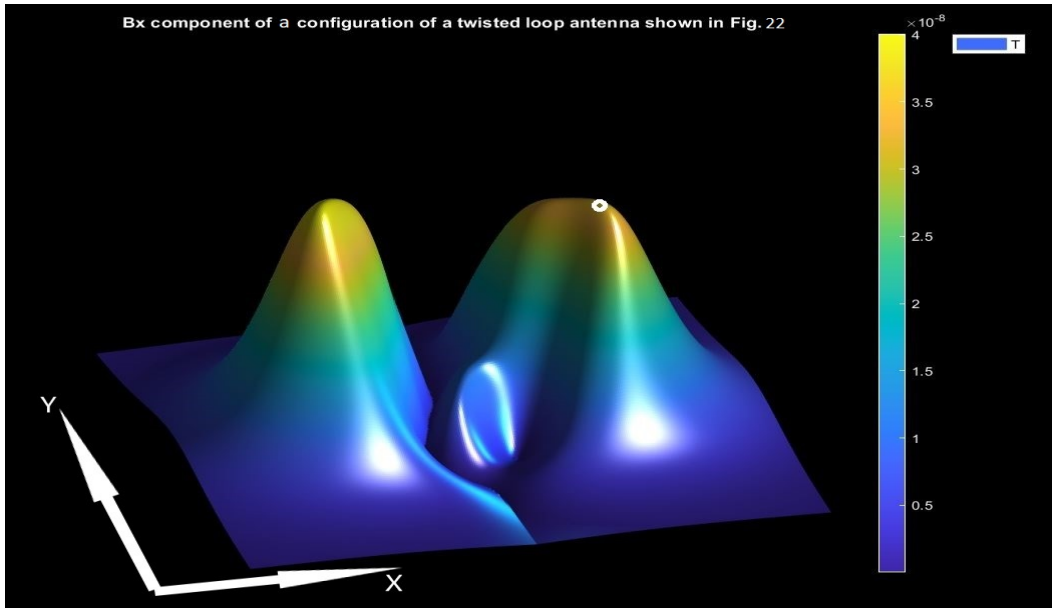


Figure 2.24: The surface shows the value of B_x component of the field in a plane parallel to the plane on which the twisted loop antenna is placed (that is X-Y) and at 4 cm above the twisted loop antenna, for one possible configuration of a twisted loop antenna shown in Fig. 2.22. In comparison to Fig. 2.23, this configuration enhance the value B_x component of the field in the targeted point shown in white circle.

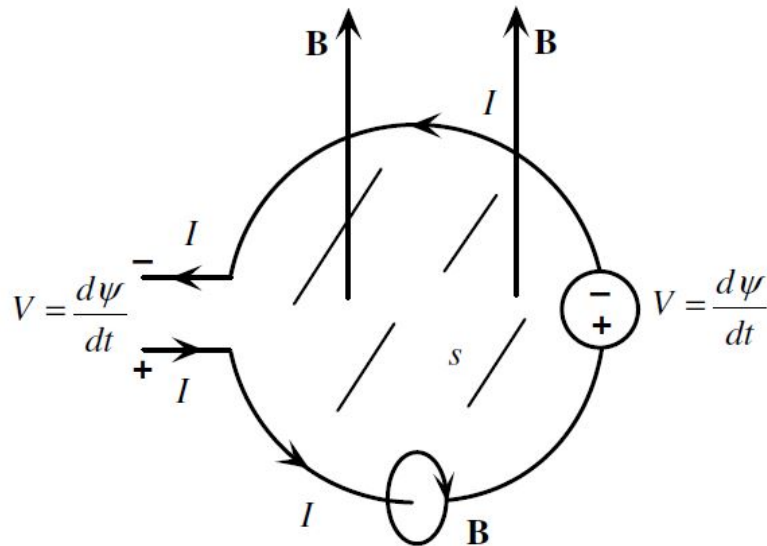


Figure 2.25: Self Inductance of a current loop [57].

loop. The total magnetic flux passing through the loop is shown by Ψ and is given by:

$$\Psi = \int \vec{B} \cdot d\vec{s} \quad (2.20)$$

$d\vec{s}$ is a differential part of the surface S which is the surface that the current loop encloses. If the electric current I, and its magnetic field B, is time dependent (that means we are applying an AC current and generating an alternating magnetic field), Faraday's law tells us this will induce a voltage around the current loop as in equation 2.21.

$$V = -\frac{\partial \Psi}{\partial t} \quad (2.21)$$

This voltage is not the voltage that we apply to the loop in order to excite the electric current I, this is a new voltage that rises across the loop as a consequence of applying an AC current to it and the total voltage across the loop is the externally applied voltage plus this induced voltage.

To quantify this voltage, we notice that according to equation 2.21, this voltage is equal to the rate of change of the magnetic flux. The magnetic flux has a linear relation to the magnetic field (magnetic flux is just summation through the value of magnetic field as indicated in the equation 2.20. It means that if we increase the value of the field by factor of 2 for example, the magnetic flux passing through a given area also will increase by the factor of 2. The magnetic field itself, as indicated in the equation 2.7, is proportional to the electric current I that generates it. It means that if we increase the value of the electric current I by factor of 2, the magnetic field also will increase by the factor of 2.

Now because the magnetic field and the magnetic flux are proportional to the electric current I, if we divide them by the electric current I, we will have a quantity, say L, which is independent of the electric current I, and connect the time varying current in the loop to the voltage induced across it as given in equation 2.22.

$$V = L \frac{\partial I}{\partial t} \quad (2.22)$$

This quantity L, is called self inductance and is a quantity that counts for the effect of Faraday's law in electric circuit. It is given in the unit of Henry in SI system.

The value of L is a function of geometry of the circuit elements and very often it is very difficult to calculate it analytically.

This procedure of calculating the inductance is called the method of Flux Linkages, because one calculates the magnetic flux that in a way "links" different part of a (in our case here) current loop together.

This is not the only possible way. There is another way for obtaining L by using the vector magnetic potential A instead of using B. For doing so we start by the equation 2.23,

$$\vec{B} = \nabla \times \vec{A} \quad (2.23)$$

from equation 2.20 we know that:

$$\Psi = \int \vec{B} \cdot d\vec{s} \quad (2.24)$$

If we substitute equation 2.23 in equation 2.24 we get:

$$\Psi = \int_s \vec{B} \cdot d\vec{s} = \int_s (\nabla \times \vec{A}) \cdot d\vec{s} \quad (2.25)$$

If we now use the Stokes's theorem, equation 2.25 becomes

$$\Psi = \oint_c \vec{\mathcal{A}} \cdot d\vec{l} \quad (2.26)$$

c in equation 2.26 is the closed contour that enclosed the surface s .

The self inductance again is obtained by dividing the equation 2.26 by the current I

$$L = \frac{\oint_c \vec{\mathcal{A}} \cdot d\vec{l}}{I} \quad (2.27)$$

Depending on the situation, sometimes it is more suitable and easier to use equation 2.27 for calculating L . However because in this work we ultimately interested in calculating the mutual inductance (to be defined later) and it is also easier to extend the method of Flux Linkages for calculating the mutual inductance, here we use the method of Flux Linkages for the rest of work.

It could be divided in four steps:

1. Excite an electric current I in the closed loop.
2. Calculate the magnetic field B at the surface enclosed by the loop.
3. Calculate the total magnetic flux passing through the surface enclosed by the loop.
4. Divide this flux by the electric current I .

Those physical principles are general principles. That means that if the time varying magnetic flux linkage is going to induce a voltage, it is going to induce voltage in any (for example) loop, in the loop that carries the electric current that give rise to the magnetic field in the first place call it loop 1), but as well to any other loops (call it loop 2,3,..) which have no connection to the excited loop, but the magnetic field of the first loop will pass through them.

In Fig. 2.26 the loop 1 is the primary loop to which we applied the time varying electric current I .

It creates the magnetic field B . This magnetic field B , penetrates the surface S_1 (enclosed by the loop 1) and will result in induced voltage determinable by the self inductance (L) of the loop 1.

However the magnetic field B is not confined to where just loop 1 is. It extends and distributes in all space around the loop 1. If we have loop 2 in vicinity of the loop 1, the magnetic field B will penetrate as well the surface 2, S_2 , enclosed by the loop 2.

So the magnetic flux in loop 2 due to the loop 1 will be:

$$\Psi_{21} = \oint_{s_2} \vec{B}_1 \cdot d\vec{s}_2 \quad (2.28)$$

in which B_1 is the magnetic field due to loop 1 in the infinitesimal surface area ds_2 , which is part of S_2 .

Similarity the magnetic flux in loop 1 due to the loop 2 will be:

$$\Psi_{12} = \oint_{s_1} \vec{B}_2 \cdot d\vec{s}_1 \quad (2.29)$$

in which B_2 is the magnetic field due to loop 2 in the infinitesimal surface area ds_1 , which is part of S_1 .

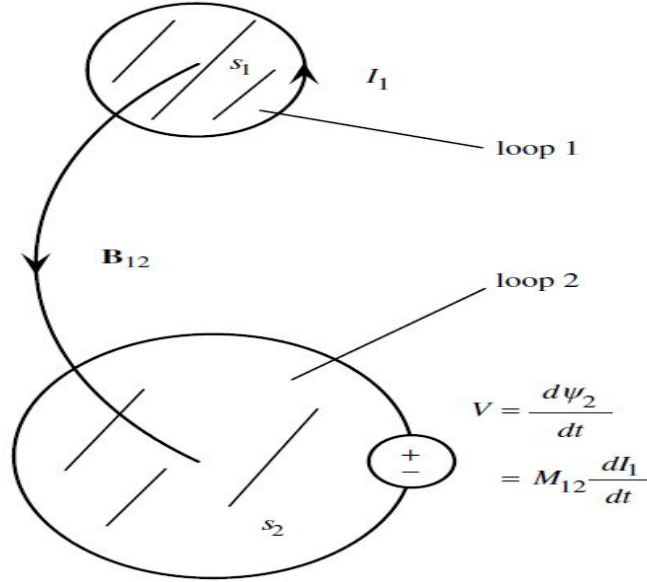


Figure 2.26: Mutual inductance between two loops. $\Psi_1 = \Psi_2$ [57].

This magnetic flux shown by Ψ_2 in Fig. 26 will induce the voltage V across the loop 2. As we did earlier in quantifying self inductance, here also we essentially because of linearity, could introduce a quantity that we call mutual inductance, or M , that quantifies this phenomena.

For doing so, we just have to divide the equation 2.28 and 2.29 by the current that generate them, I_1 in loop 1 for equation 2.28, and I_2 for loop 2 for equation 2.29:

$$M_{21} = \frac{\Psi_{21}}{I_1} \quad (2.30)$$

$$M_{12} = \frac{\Psi_{12}}{I_2} \quad (2.31)$$

Because of the symmetry, $\Psi_{21} = \Psi_{12}$ and by consequence $M_{12} = M_{21} = M$. As for self inductance (L) the mutual inductance (M) is independent of the value of the electric current in the loop 1. On the other hand unlike the self inductance of a loop which is fixed and only a function of its geometry (here we assume that circuits elements do not change their shape during their operation) the mutual inductance is a function of relative orientation and separation between different circuit elements.

In our example, in Fig. 2.26, it means that if we change the position or orientation of loop 1 or loop 2, their self inductance (L) will not change, but their mutual inductance (M) will change.

To avoid confusion from now, we will call the loop 1 in Fig. 2.26, that is the loop which we excite by applying the alternative electric current: the transmitter or reader or sender (in RFID and WPT literature these terms are used interchangeably). And the loop 2 in Fig. 2.26, that is the loop that does not have an independent source of energy and in which we induce a voltage, the receiver or the tag (in RFID and WPT literature these terms are used

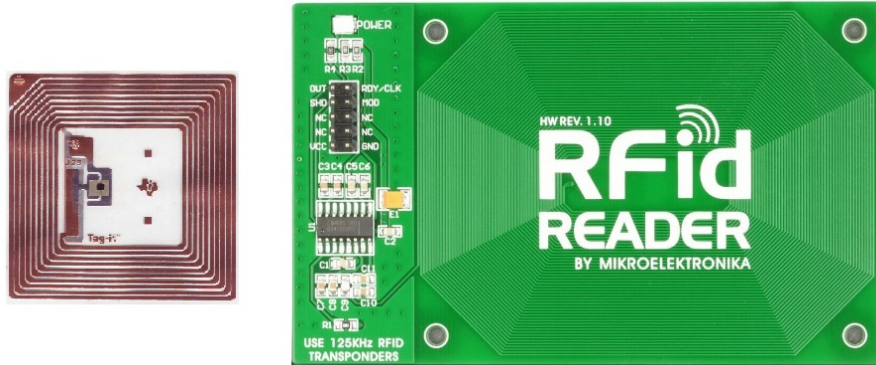


Figure 2.27: a. A receiver (tag) with multi turns coil(loop 1) b. A transmitter (reader) with multi turn coil (loop 2) [28].

interchangeably).

However one can increase the value of magnetic field by increasing the length of structure that carry electric current, for example in the case of a coil transmitter by increasing its diameter or by increasing the number of its turns. That is why in practice the transmitter coil used in RFID and WPT are multi turn coils transmitter, Fig. 2.27.

For the receiver, on the other hand for increasing the mutual inductance one could increase the size of the receiver coil for increasing the effective surface of the receiver. However a more practical solution is to increase the effective size of the receiver by increasing the number of turns of the receiver coil. That is why in practice the receiver coil used in RFID and WPT are multi turns coil receivers.

Because mutual inductance (M) is a result of a summation of magnetic flux over the surface enclosed by the receiver coil, it depends on number of variables, among which are the following:

1. The value of magnetic field generated by the transmitter coil in the position of receiver coil.

It is true that according to Bio-Savart law one can increase the value of magnetic field by increasing the current (for example by increasing the value of electric current by factor of 2, one will increase the value of magnetic field also by factor of 2), however we should also remember that the mutual inductance M , is a result of dividing the magnetic field by the current, so it is finally independent of the current.

What is important to notice also is the fact that the value of magnetic field for a given fixed current itself is a function of location and change from point to point in space. This means that if it happens that the receiver is placed in a position in which the magnetic field value is high, it will have large magnetic flux passing through it and if it happens that the receiver is placed in a position in which the magnetic field value is low it will have small magnetic flux passing through it.

2. The direction of magnetic field generated by the transmitter coil in the position of receiver coil.

The magnetic flux is a result of dot product of the magnetic field (which is a vector having both magnitude and direction) and the infinitesimal surface element vector (perpendicular to the surface of the receiver coil).

The result of this dot product depends strongly on the direction of these two vectors. It depends on the cosine of the angle between them. If the surface is perpendicular to the field the result of dot production is maximum ($\cos(0)=1$), and if the surface is parallel to the field the result of dot product is minimum ($\cos(90)=0$), even if the value of the magnetic field is high.

This will lead to dependency of the magnetic flux on 6 variables. The three components of the magnetic field (B_x, B_y, B_z) and the three components of the s vector: s_x, s_y and s_z .

$$\vec{B} \cdot \vec{s} = B_x s_x + B_y s_y + B_z s_z \quad (2.32)$$

Because the final result is addition of these three terms in equation 32, for calculating final magnetic flux for any arbitrary direction of receiver coil, it is easier to divide it into three steps.

In first step, we assume the receiver is perpendicular to say X axis. Then we scale the size of the coil by the cosine of the angle between the real direction of the receiver loop and the X axis. The same thing will be done for Y and Z axes. In doing so we project the receiver coil in three components along X, Y and Z axes. In second step, we just multiply the projected surface along X axis with the X component of the field, the projected surface along Y axis with the Y component of the field and the projected surface along Z axis with the Z component of the field. In third step, we add these results to get the final magnetic flux.

That is why we are more interested in the value of each component of the magnetic field in the location of the receiver more than actual direction of the magnetic field at that location.

To demonstrate this, consider the following situation shown in Fig. 2.28.

We have a transmitter of 1 turn coil with 5 cm radius carrying 1 mA current, shown in blue color in Fig. 2.28. We chose our coordinate system in a way that its origin is in the center of transmitter coil, and the transmitter coil is in the XY plane of our coordinate system.

The receiver is a 1 turn coil with 1 cm radius shown in black color in Fig. 2.28. In all this work when we talk about receiver loop we talk about circular loop. By doing so we do not lose any generality and the result could be applied to any shape of receiver. Further more by position of the receiver coil we mean the position of its center. Let assume the receiver coil position is at the beginning $(x,y,z)=(0 \text{ cm}, 0 \text{ cm}, 5 \text{ cm})$. To specify the direction of a coil, we need to specify the vector perpendicular to its surface. In this work we will call a vector perpendicular to the surface of a loop, the normal vector of that loop denoted by n. Let this vector in our example be $(n = 0i - 1j + 0k)$, where i, j and k are unit vectors along X, Y and Z axes.

Magnetic field is a 3D vector field. That means it has three outputs for each X, Y and Z in space. To be able to plot it in readable way here we fixed the Y and Z coordinate and sweep along X axis. Any value of Z and Y could be chosen, and we arbitrary chose $Y=0$, and $Z=5 \text{ cm}$, just for the sake of demonstration. In Fig. 2.29, the magnitude of each component of the magnetic field due to the transmitter are shown as we sweep along the X axis from $x=-20 \text{ cm}$ to $x=20 \text{ cm}$.

Now we sweep the receiver coil in the same way we did in Fig. 2.29 but this time for mutual inductance. The result is shown in Fig. 2.30. The results are zero everywhere along X axis for this particular orientation. After all these results are not very surprising. The orientation of the receiver loop that we choose (or in other words the normal vector

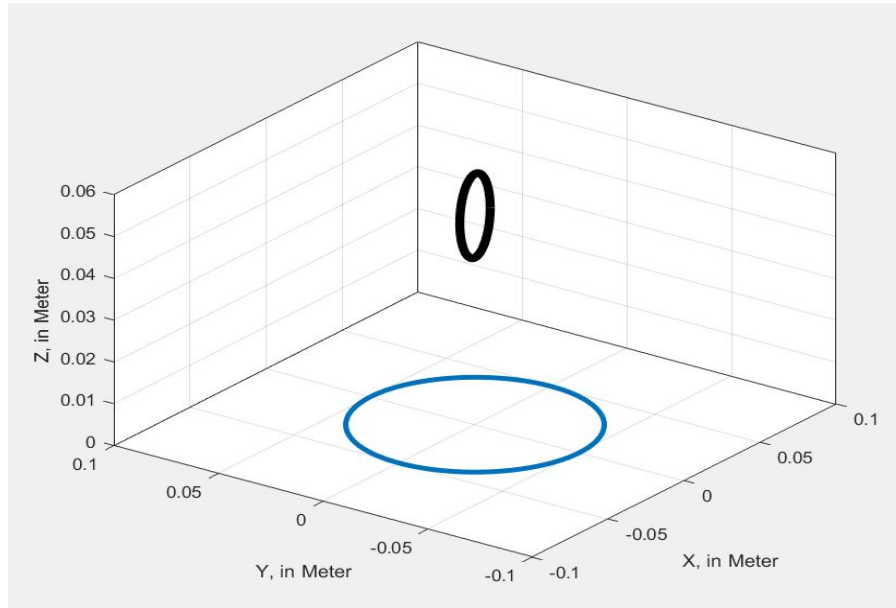


Figure 2.28: A transmitter of 1 turn coil with 5 cm radius carrying 1 mA current placed in the origin of the coordinate system. A receiver of a 1 turn coil with 1 cm radius shown in black color placed at $(x,y,z)=(0 \text{ cm},0 \text{ cm},5 \text{ cm})$. The receiver normal vector is $(n = -1j)$.

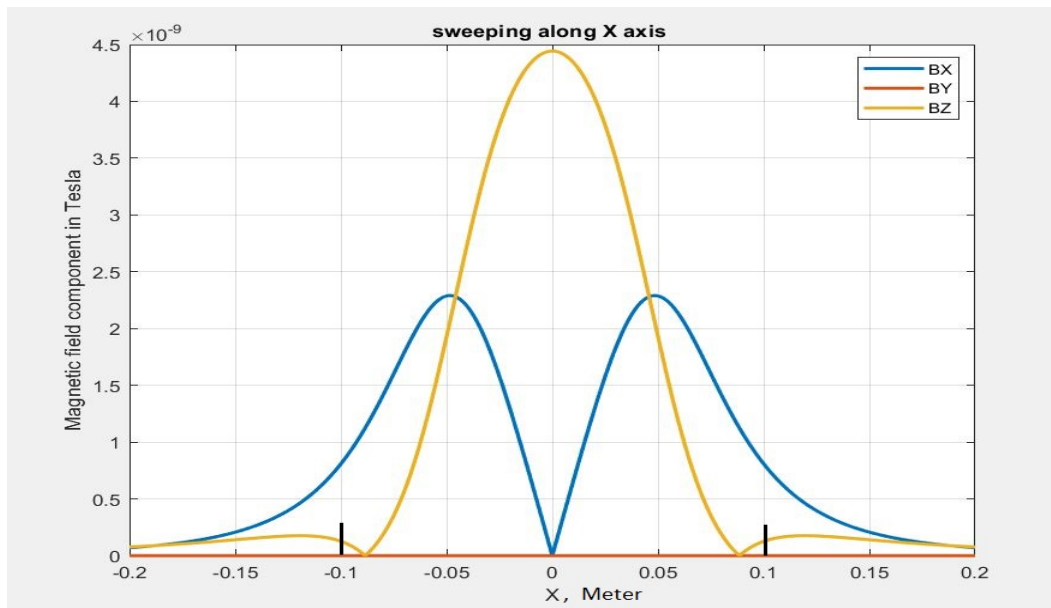


Figure 2.29: The magnitude of each component of the magnetic field due to the transmitter are shown as we sweep along the X axis from $x=-20 \text{ cm}$ to $x=20 \text{ cm}$, for fixed $z=5 \text{ cm}$ and fixed $y=0 \text{ cm}$. The two black dashes show the border of region shown in Fig. 2.28, which expands from -10 to 10 cm. B_y is zero everywhere.

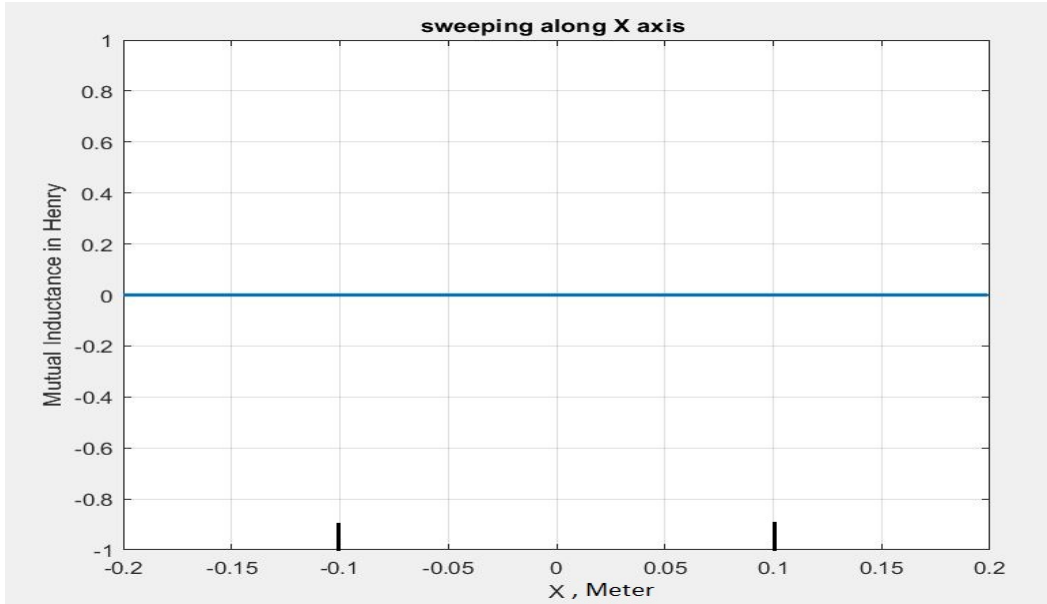


Figure 2.30: The mutual inductance between transmitter and receiver is shown as we sweep along the X axis from $x=-20$ cm to $x=20$ cm, for fixed $z=5$ cm and fixed $y=0$ cm. It is zero everywhere.

n) happens to be perpendicular to both X and Z axes. As we said earlier, this means that the projection of the surface of the loop is zero in YZ and XY plane. The surface of the loop just has projection on the ZX plane and the magnetic field component that result in magnetic flux for a surface in ZX plane is only the Y component of the field. We can see from Fig. 2.29 that the Y component of the field along the path that we swept along is zero everywhere, that is why the mutual inductance is also zero everywhere along that line.

Dividing the magnetic field to its component and the surface of the loop receiver in its projection on XY, ZX and YZ plane, makes the variation of the mutual inductance completely identical to the variation of the relevant component of the magnetic field (the component which is perpendicular to that particular plane). We can see that they are identical by comparing the mutual inductance in Fig. 2.30 to the B_y component in the Fig 2.29. To check this further more, we change the line along which we sweep the receiver coil and sweep along X axis from $X=-20$ cm to $X=20$ cm, but this time for fixed $y=5$ cm, and the $z=5$ cm, we get the magnetic field shown in the Fig. 2.31. Then we sweep the mutual inductance along the same line. If our logic is correct, we should see the identical variation as the variation of the B_y component. The result of this sweep for mutual inductance along the X axis from $X=-20$ cm to $X=20$ cm, with fixed $y=5$ cm, and the $z=5$ cm is shown in Fig. 2.32. As we can see the variation of the mutual inductance has similar shape as the variation of the B_y component and our method is verified.

It should be mentioned that the mutual inductance shows the same variation of the relevant magnetic field because the diameter of the receiver coil is small in respect to the scale of variation of the field. If the diameter of the receiver coil is bigger, the mutual inductance will be effected not just by the value of the magnetic field at the position of the receiver coil

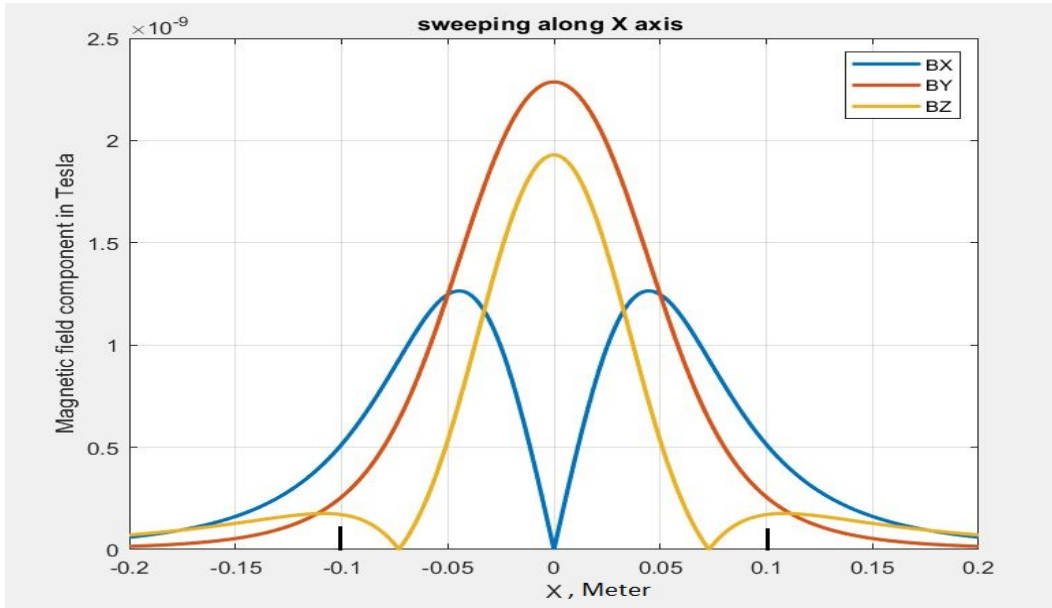


Figure 2.31: The magnitude of each component of the magnetic field due to the transmitter are shown as we sweep along the X axis from $x=-20$ cm to $x=20$ cm, for fixed $z=5$ cm and fixed $y=5$ cm.

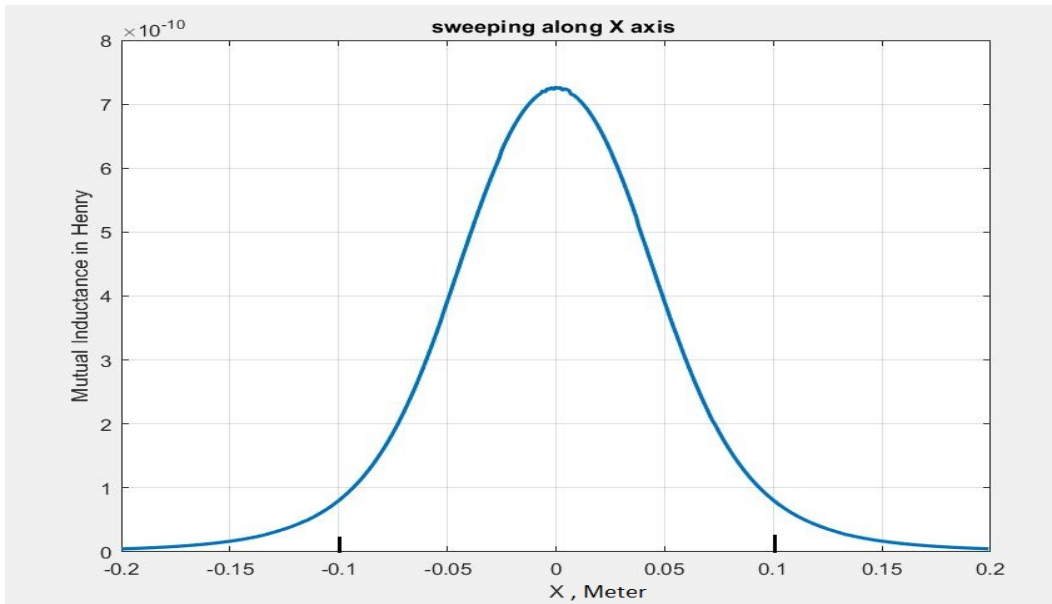


Figure 2.32: The mutual inductance between transmitter and receiver is shown as we sweep along the X axis from $x=-20$ cm to $x=20$ cm, for fixed $z=5$ cm and fixed $y=5$ cm.

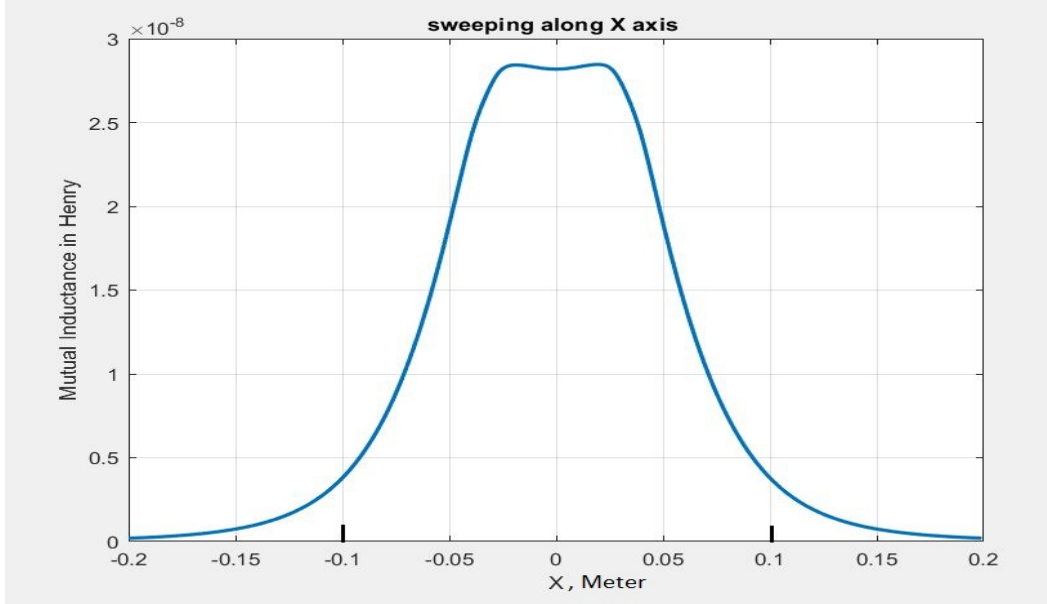


Figure 2.33: The mutual inductance between transmitter and receiver is shown for the same condition of Fig. 2.29 but this time increasing the diameter of the receiver loop by the factor of 4. This flattens the mutual inductance.

and its vicinity, but also by the value of relevant component of the magnetic field over a bigger area, namely the surface of the receiver coil. The effect of this is averaging over the variation of relevant component of the magnetic field.

If we do the same sweep whose result is shown in Fig. 2.32, for a receiver loop of radius 4 cm (increasing the diameter of receiver loop by factor of 4 in comparison to the first sweep), we will get the result shown in Fig. 2.33, which is a flattened version of the variation of the B_y component in Fig. 2.31. What should be noticed here, is that the mutual inductance for a certain fixed orientation of the receiver depends strongly on the position of the receiver coil in respect to the transmitter coil. There are certain positions where the mutual inductance between transmitter and receiver will be very small and practically zero.

The same thing happens if we fix the position and change the orientation of the receiver coil. When we change the orientation coil, we are changing the projection of the receiver loop onto the XY, YZ and ZX planes and consequently the relevant magnetic field component. The area of loop is weighted by the cosine of the angle between the receiver loop and each plane and that will give us the projected loop area on each plane. The magnetic flux will sum over all the three component of the magnetic field multiplied by the relevant projected area.

$$\begin{aligned} \Psi_B = & (\text{projection on } XY \text{ plane})B_z + (\text{projection on } ZY \text{ plane})B_x \\ & + (\text{projection on } XZ \text{ plane})B_y \end{aligned} \quad (2.33)$$

Fig. 2.34 shows the variables that we use to rotate the receiver loop (spherical coordinate). We rotate the loop by rotating the vector perpendicular to it (the normal vector). The direction of the vector is completely determined by two angles θ which runs in the range

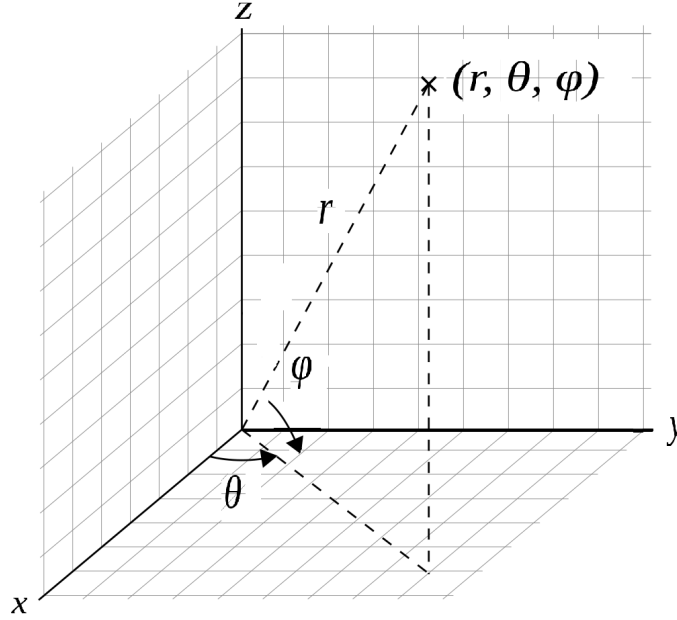


Figure 2.34: The variable that we use to rotate the receiver loop.

$[0, 2\pi]$ and Φ which runs in the range $[-\pi/2, \pi/2]$. \vec{r} is a unit vector (with its magnitude equal to one).

Fig.2.35 shows variation of the mutual inductance of our example when we fix the position to the $(x=0 \text{ cm}, y=0 \text{ cm}, z=5 \text{ cm})$. This is an arbitrary position and the same figure could be plotted for any point.

To see this effect of variation of the mutual inductance as a function of orientation of the receiver coil in practical cases, consider an RFID receiver (tag) which operates in 13.56 MHz frequency. We fix the position of the tag in respect to the transmitter, then we start to rotate it in different directions. Here we could not measure the mutual inductance directly, but what we could measure is the voltage (V) induced in the receiver coil. The voltage induced in the receiver is related to the mutual inductance (M) and the AC current (I) in the transmitter coil as:

$$V = j \omega M I \quad (2.34)$$

For an AC current source (fixed AC current), which is what drive the transmitter coil in practice, the induced voltage depends only on the mutual inductance between the receiver and the transmitter. Therefore, measuring the induced voltage in receiver coil is an indirect method for measuring the mutual inductance between the receiver and transmitter coils. Fig. 2.36 to Fig. 2.39 shows this effect.

In fact the final goal in WPT and a necessary step in RFID is this induced voltage in the receiver loop. It is this voltage (and the current it creates) that is the main mechanism of power transfer in WPT and RFID. What we saw is telling us that induced voltage is strongly depending on the mutual inductance, which in its turn depends strongly on the position and the orientation of the receiver in respect to the transmitter. That means the efficiency of the power transfer strongly depends on both the position and the orientation

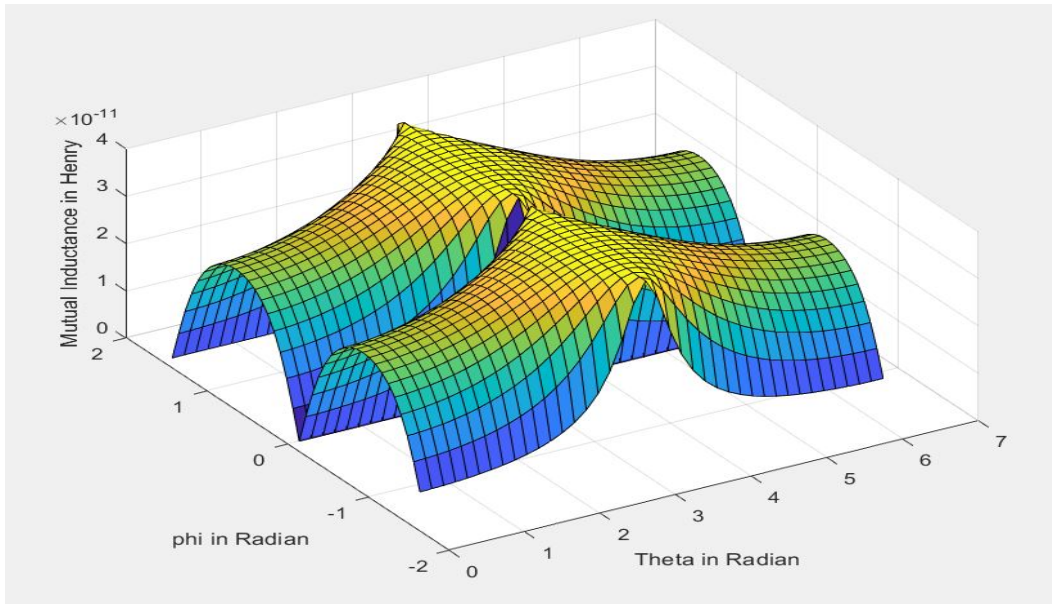


Figure 2.35: The variation of the mutual inductance of our example when we fix the position of the center of the coil to the $(x=0 \text{ cm}, y=0 \text{ cm}, z=5 \text{ cm})$. This is an arbitrary position and the same figure could be plotted for any point.

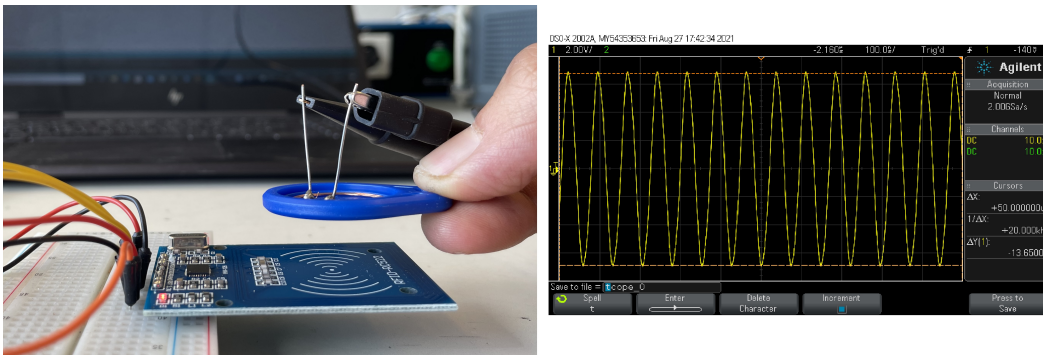


Figure 2.36: The variation of the induced voltage in the receiver coil when we fix the position but change the orientation of the receiver coil. The receiver is in the plane parallel to the transmitter.

CHAPTER 2. A RECONFIGURABLE ANTENNA FOR ENHANCING THE MAGNETIC COUPLING IN IPT AND RFID

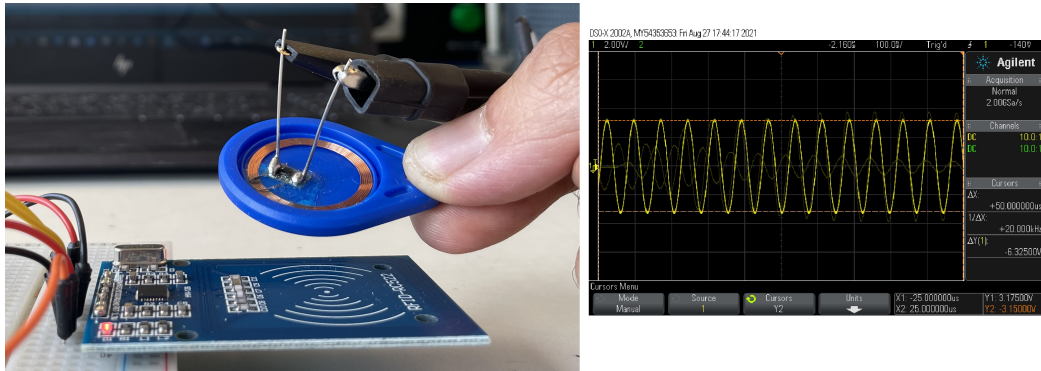


Figure 2.37: The variation of the induced voltage in the receiver coil when we fix the position but change the orientation of the receiver coil. The receiver has 30 degree angle with the plane parallel to the transmitter.

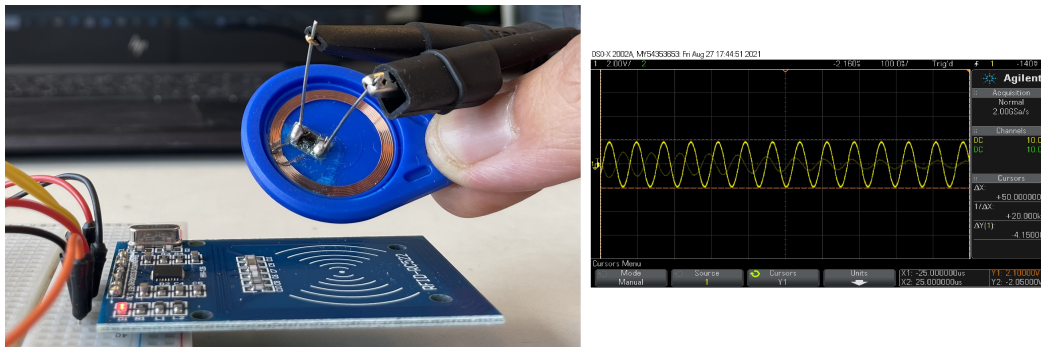


Figure 2.38: The variation of the induced voltage in the receiver coil when we fix the position but change the orientation of the receiver coil. The receiver has 65 degree angle with the plane parallel to the transmitter.

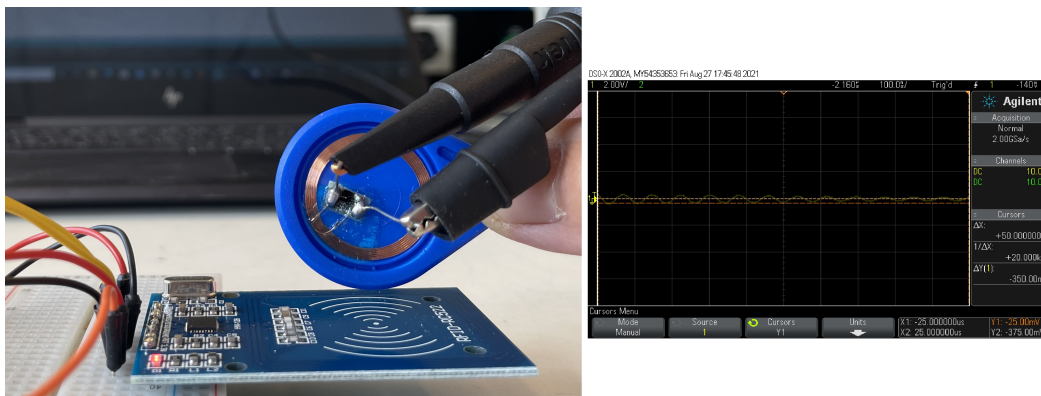


Figure 2.39: The variation of the induced voltage in the receiver coil when we fix the position but change the orientation of the receiver coil. The receiver has 90 degree angle with the plane parallel to the transmitter.

of the receiver in respect to the transmitter. If it happens that the receiver is in a position and an orientation that have large mutual inductance, the efficiency of the system will be high. If it happens that the receiver is in a position and an orientation that have low (or zero) mutual inductance the efficiency of the system will be low (or zero).

These positions where the mutual inductances are too low or fall practically to zero, are called null areas. Null areas are different for different orientations of receiver in respect to transmitter. These null areas are unavoidable due to vectorial nature of the magnetic field. They are unavoidable because it is always possible in a certain position to put that the receiver in a orientation parallel to the magnetic field. These null areas are dependant on both relative position and relative orientation of the receiver in respect to the transmitter. That means what is a null area for certain orientation of the receiver is not necessarily a null area to other possible orientations. Here our interest is related to small receiver coil relative to the size of the transmitter. When this is the case, the spatial variation of the magnetic field in general is smooth in comparison to the size of receiver . That is why the mutual inductance is largely the result of the magnetic field (both its magnitude and orientation) in region close to the center of receiver coil. Having small size receiver coil is more convenient in practice and in general for this reason it is more investigated in literature related to this subject (If we consider large receiver coil, it is possible to not have null area, but here we concern ourself with small receiver coil). As we said earlier the null area depends on both the orientation and position of the receiver in respect to the transmitter. To be more concrete we define the volume of interest. This is a volume inside which we want to investigate the behaviour of magnetic coupling. Instead of talking about the position of transmitter and receiver to each other, we will talk about absolute position of the receiver and transmitter in this volume of interest. We assign an origin of a Cartesian coordinate system inside this volume of interest then we define the position of receiver and transmitter in this coordinate system. In practice, because the magnetic field due to the current in the transmitter falls rapidly as we move away from transmitter, the dimensions of this volume of interest is roughly equal to the diameter of the transmitter size. It means that if we want to cover a larger volume of interest we need to use a larger transmitter. We also assume (for practical reason it is more convenient) that we do not have any control on the behaviour of the receiver coil. As long as it is in the volume of interest, it can have any position and orientation. Another practical assumption is that the size and the shape of the receiver coil is fixed and does not change. Here we are assuming it to be a circular loop of 1 cm radius. If the volume of interest is fixed, and the shape and the size of the receiver coil is fixed, and the position and the orientation of the receiver in the volume of interest is not controlled, the only thing that we have control on is the shape and the position of the transmitter in the volume of interest. The transmitter could have any shape but as we said earlier in practice it is much more convenient to have a 2 dimensional transmitter, it takes less space and could be embedded in the working environment easily. By changing the shape and the position of this 2D transmitter in the volume of interest, one could create different patterns of mutual inductance between the transmitter and the receiver in the volume of interest with maximum mutual inductance (desired) and minimal mutual inductance (not desired or null area) in different locations of the volume of interest (for certain orientation of the receiver). By changing the shape of the transmitter, we mean that we could chose a simple circular coil as a transmitter, or a TLA, or any other shapes. By changing its position we mean we could put it in different location in the volume of interest.

To give an example, assume the volume of interest is a rectangular cuboid extend:

- from $X=-15$ cm to $X=15$ cm

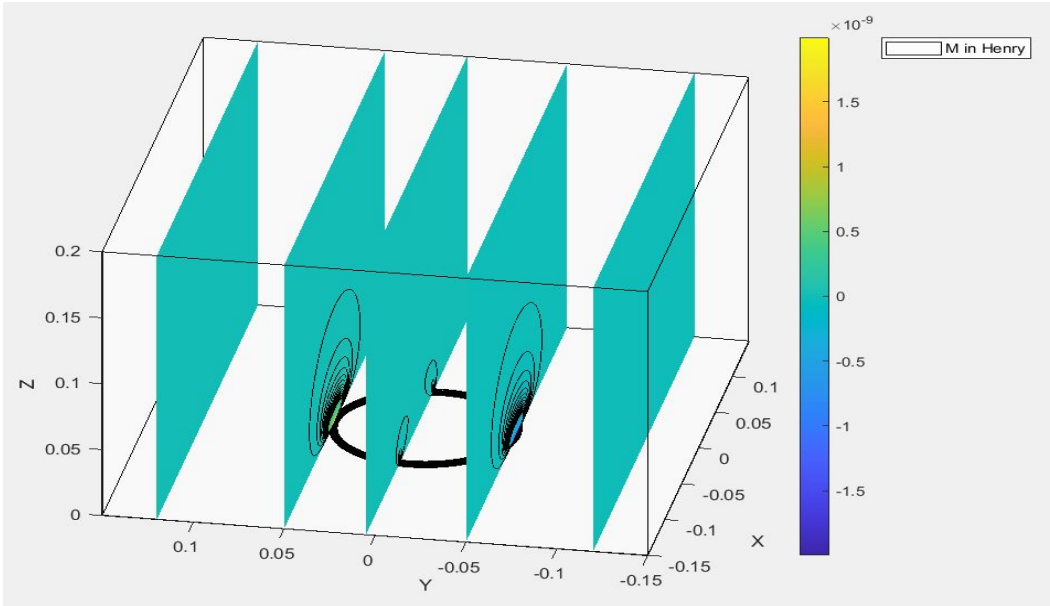


Figure 2.40: The volume of interest is a black rectangular cuboid extending 30 cm along X axis, 30 cm along Y axis and 20 cm along Z axis. The receiver is a loop of 1 cm radius in XZ plane. The transmitter is a circular coil of radius 10 cm placed on the XY plane with its center at the origin, carrying 1mA current. The planes show the value of mutual inductance with contours of equal values of mutual inductance.

- from $Y=-15$ cm to $Y=15$ cm
- from $Z=0$ cm to $Z=20$ cm.

The receiver coil could be at any location in this volume with an arbitrary orientation but it is a circular loop of 1 cm radius. For this example it is in XZ plane. If the transmitter was a circular coil of radius 10 cm placed on the XY plane with its center at the origin, it will create mutual inductance pattern shown in Fig. 2.40.

Now we change the shape of the transmitter. This time the transmitter is a TLA of radius 10 cm which is placed in symmetrical way around the origin in the XY plane. The magnetic mutual inductance of this configuration is shown in Fig. 2.41.

We plot the mutual inductance in 3D to show its volumetric nature. This means that it assigns a value to each point in space (specified by X,Y, and Z coordinate). However because there is a lot of information in the volumetric data, to get a better understanding of variation of the mutual inductance in the volume of interest, it is better to show just a part of the data. For doing so, we will fix one or more of the coordinates (X, Y or Z) and then sweep along the other coordinates. This way even if we don't show all the information but we present some of the information in the more readable way. Fig. 2.42 and Fig. 2.43 show the mutual inductance we already showed in Fig. 2.40 and Fig. 2.41 but in 2 dimensional way. Here we fix X and Z coordinate, then we sweep along the Y axis. For the rest of this work, we will use 2D plotting and keeping in mind that we have fixed some coordinates. Otherwise it will be mentioned.

The main point here is that for a certain volume of interest, the nulls depend on the

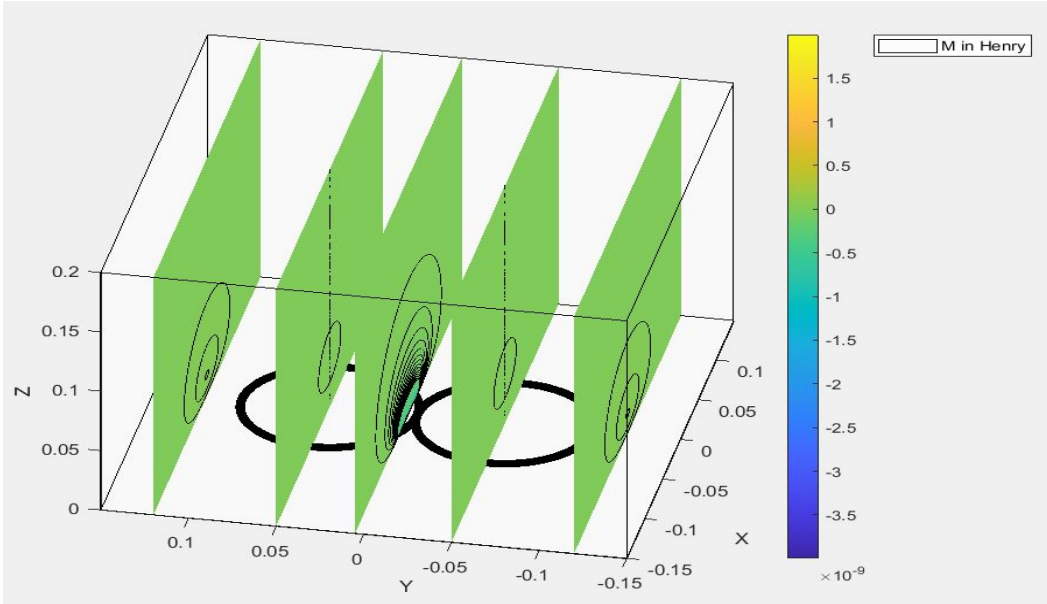


Figure 2.41: The volume of interest is a black rectangular cuboid extending 30 cm along X axis, 30 cm along Y axis and 20 cm along Z axis. The receiver is a loop of 1 cm radius in XZ plane. The transmitter is a TLA of radius 10 cm which is placed in symmetrical way around the origin in the XY plane. Each loop of the TLA carry a current in 1 mA in opposite direction (one in clockwise other in anti clockwise). The planes show the value of mutual inductance with contours of equal values of mutual inductance.

configuration of the transmitter. Having different transmitters configurations will lead to different distributions of null areas in the volume of interest. What is a null area in the the Fig. 2.42 (where we have shown the receiver coil at $X=0$, $Y=0$ and $Z=10$ cm) is not a null area in the Fig. 2.43 (where we have shown the receiver coil at $X=0$, $Y=0$ and $Z=10$ cm). In fact depending on the transmitter configuration, any point in the volume of interest could be in a range of maximum mutual inductance or practically zero mutual inductance (null area).

Fig. 2.42 and Fig. 2.43 show the nulls are due to different transmitters in the same volume of interest.

There are certain applications in which the null area are not a problem. For example if one uses magnetically coupled near field communication card, it is assumed that the user puts the cart in a certain well defined position (and with certain orientation) that is designed by the designer of the system to avoid null area, so the system will operate in the intended way. Those are constrained orientation and position situations, and they imply a-priori knowledge about orientation and the position of the receiver (or Tag in the RFID case).

But there are other many possible applications in which we don't know a-priori the position (as long as it in the volume of interest) and the orientation of the receiver.

Consider the following scenario for RFID application of the magnetic coupling. In a shopping center we could tag the objects by attaching a RFID tag to them. Then we could implement a RFID reader underneath the cart available in the shopping center. Then this

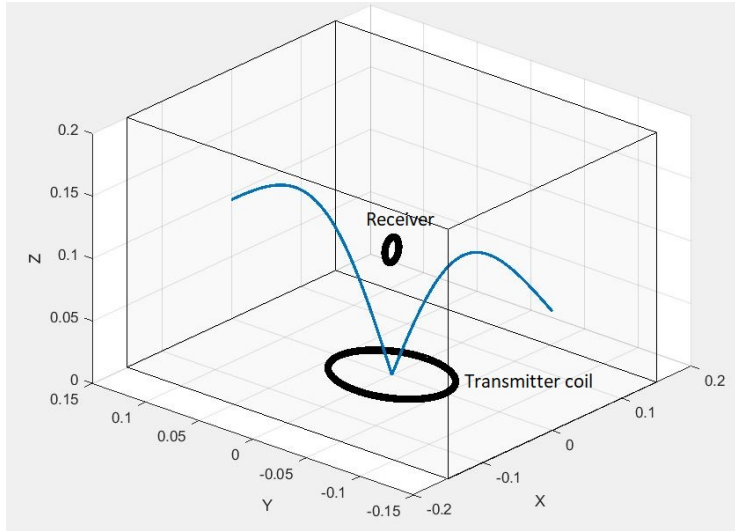


Figure 2.42: The volume of interest is a black rectangular cuboid extending 30 cm along X axis, 30 cm along Y axis and 20 cm along Z axis. The receiver is a loop of 1 cm radius in XZ plane. The transmitter is a circular coil of radius 10 cm placed on the XY plane with its center at the origin, carrying 1mA current. Here we fix X coordinate to X=0, fix Z coordinate to Z=10 cm, then we sweep along Y axis. The blue curve shows the variation of the mutual inductance as we move along Y axis.

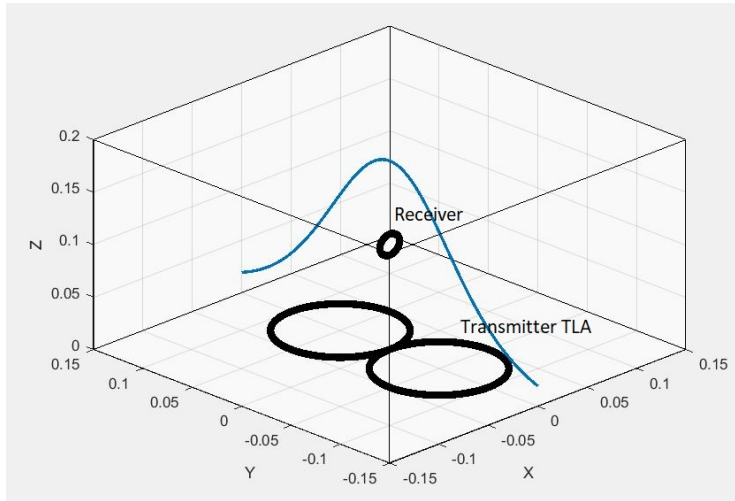


Figure 2.43: The volume of interest is a black rectangular cuboid extending 30 cm along X axis, 30 cm along Y axis and 20 cm along Z axis. The receiver is a loop of 1 cm radius in XZ plane. The transmitter is a TLA of radius 10 cm which is placed in symmetrical way around the origin in the XY plane. Each loop of the TLA carry a current in 1 mA in opposite direction (one in clockwise other in anti clockwise). Here we fix X coordinate to X=0, fix Z coordinate to Z=10 cm, then we sweep along Y axis. The blue curve shows the variation of the mutual inductance as we move along Y axis.

reader could read all the items and calculate the price automatically in the exit without the customer having to scan all of them one by one (by customer himself or the cashier). This could be easier and faster way of shopping.

Fig. 2.44 shows a demonstration of this scenario.

The positions of the objects (as long as they are in the volume of interest) is random. The orientation of the objects, and hence the orientation of the receiver coils, are also random. The problem with this scenario is this: if it happened that some objects are in null area, the chip on the tag will not have sufficiently high levels of power and voltage to operate the electronics implementing the given protocol and the tag (and the object) will not be detected.

To have more reliable systems that guaranty the detection of the receivers (tags) regardless of their positions and orientation, we want to address this problem. Currently this problem is addressed either by finding the most probable orientation of the receiver (tag) then designing a transmitter antenna in a way suitable for that particular orientation. Other methods of addressing this problem include attaching more than one receiver to the objects (multitagging) in different orientation (for example to different side of a box) so reducing the probability of not detecting the object. Other possible solution is having a 3D antenna (antenna which is not a planar), however those antenna are bulky and not suitable for all applications. Other applications in which this problem arises include Supply Chain and Inventory Control, keeping track of the identity of cattle and pets, Airline Luggage and so on. In all these applications though it is reasonable that the receiver tags are more likely to be in a certain orientation, one could not be sure about that in a-prior. Those are examples of use of magnetic coupling in RFID applications. Because RFID is essentially using the same mechanism as Wireless Power Transfer (WPT), the same problem arises in some WPT application in which it is hard to precisely control the position and the orientation of the receiver. This occurs more in movable WPT receiver (for example charging of robots and drone powered by WPT). It is possible to increase the complexity of these robots and drones so they will be positioned and orientated in desirable orientation, but that increase the cost of these systems.

Here we will introduce another kind of solution which does not need much of complicity to be added to the system and be easier to implement. This is a reconfigurable antenna which aimed to deal with null areas and eliminate them. This method is based on the concepts of magnetic field steering that we mentioned earlier, and will be described in next part.

2.5 A Reconfigurable Antenna for Enhancing the Magnetic Coupling

Before we proceed, we have to mention that what we are saying here holds truth for small receiver coil relative to the size of the transmitter. This is the case in many applications (for example in RFID applications of the magnetic coupling, it is more convenient to have small tags).

In the previous section we talked about null areas. To address this problem here we follow a step by step reasoning (from step 1 to step 4):

1. Any transmitter will have some null areas.

It is impossible to have a transmitter structure with no nulls for all possible orientations of the receiver. This happens because of the vectorial nature of the magnetic field. What-

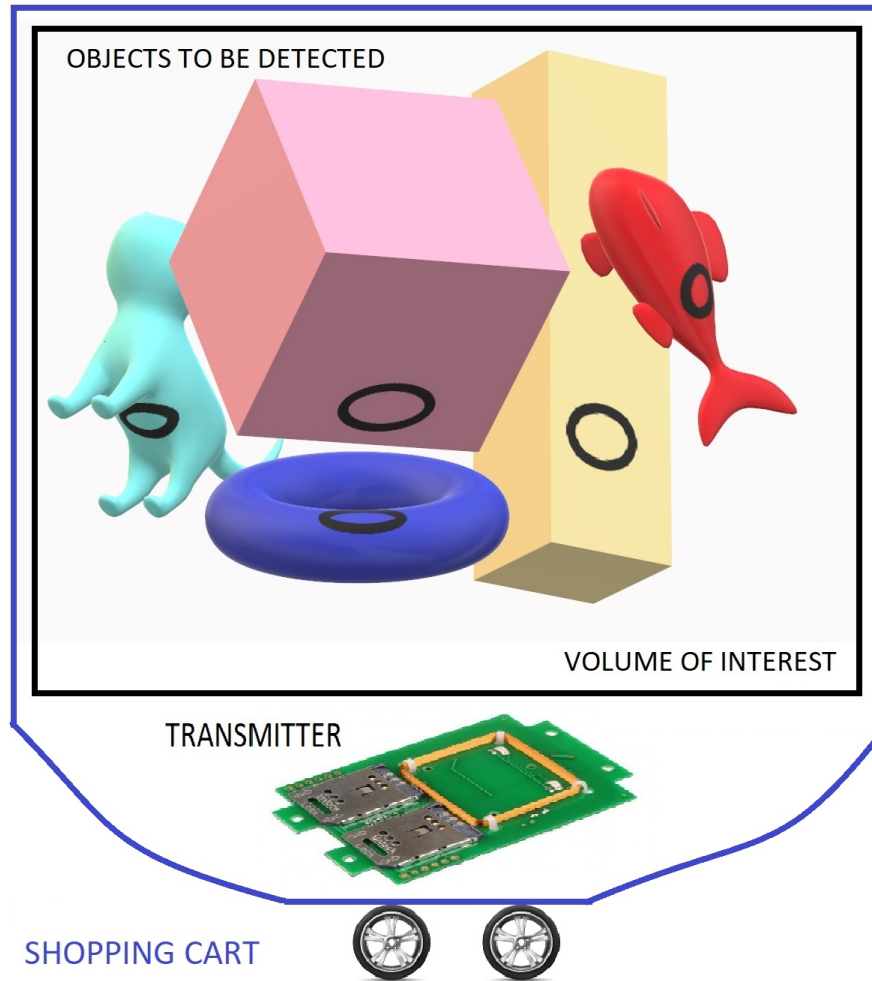


Figure 2.44: A scenario for RFID application of the magnetic coupling for the shopping. A cart with a RFID reader implanted underneath it. This reader can read all the items and calculate the price automatically in the exit without the customer having to scan all of them one by one. Black circles show the receiver coils attached to each object. The cart is shown in blue and the volume of interest is a black box.

ever the magnetic field distribution of a certain transmitter is, it is possible that we have a receiver which is parallel to the direction of the magnetic field. In this case the mutual inductance will be zero and that will be a null area. In other word eliminating all null area is not possible for any transmitter structure regardless of how its shape or how much complex it is. It should be mentioned that it is true as long as the phase of current is the same in all parts of the transmitter antenna. If it is not the case and each part of the transmitter is excited by its own current source, the direction of the field will rotate and what we said about null area is not correct any more. However here we are not taking this approach and we are considering a system which is excited and energized by a single current source.

2. Those null areas are unique to each transmitter structure in a given volume of interest. For example, if we are using a circular coil as a transmitter centered in the origin of the volume of interest, and the receiver coil has perpendicular orientation and is placed above the origin, as in Fig. 2.42, the receiver is in null area. Now if we replace the transmitter coil with a TLA, as in Fig. 2.43, the receiver coil is not any more in a null area for the same position of the tag.

3. Having more than one transmitter structure, energized at the same time is not a solution to eliminate these null areas, because the whole set of transmitters could be regarded as one more complicated structure with its own null area and it will bring us back to the point one. Now the point is to recognize that any transmitter structure which is fixed in time will have this problem. By fixed in time we mean that its structure (the shape of antenna, its position in respect to the volume of interest, etc..) does not change during the operation.

4. However if we change the structure of the transmitter antenna during its operation, each configuration will have its own null areas pattern. (from Fig. 2.42 and Fig. 2.43 we can see that different transmitters have a different null area pattern). That means if it happened, that the receiver coil is in null area for one transmitting antenna structure, it is possible that for another transmitter structure, it is not any more in a null area. Based on this, if we sweep through a set of different transmitter structures, one by one, at each time step, we could eliminate the null areas completely if this set of transmitter structures are chosen correctly. This is what we mean by a reconfigurable structure antenna. This idea will be used to optimize the magnetic coupling with switching between different transmitter structure as will be described in the next steps.

5. To change the structure it is practically inconvenient to physically remove on transmitter of certain shape and replace it by another transmitter of another shape. What is more convenient is to control it electronically by switching on or off certain parts of it, and it is effectively equivalent to changing the structure of the transmitter antenna.

6. In the section of the Magnetic field beam steering, we talked about Twisted loop antenna (TLA). There we said that a TLA is a 2D (planar) structure which could be regarded as a set of circular loops, arranged in a certain way. TLA provides us with a good candidate for constructing a reconfigurable transmitter antenna, which enables us to change its structure electronically.

7. Indeed in Fig. 2.21 and Fig. 2.22 we showed two possible examples of TLA. There are some variables that can be controlled :

A: Mechanical parameters: the positions of coils and their radius, which is not convenient and not considered in this study.

B-1: Electronic parameters: Disconnecting or connecting back each circular coil, or the number of turns in each coil. This could be done electronically easily by connecting each turn through switches (like relay switches) that could be controlled electronically. This is shown in Fig. 2.45.

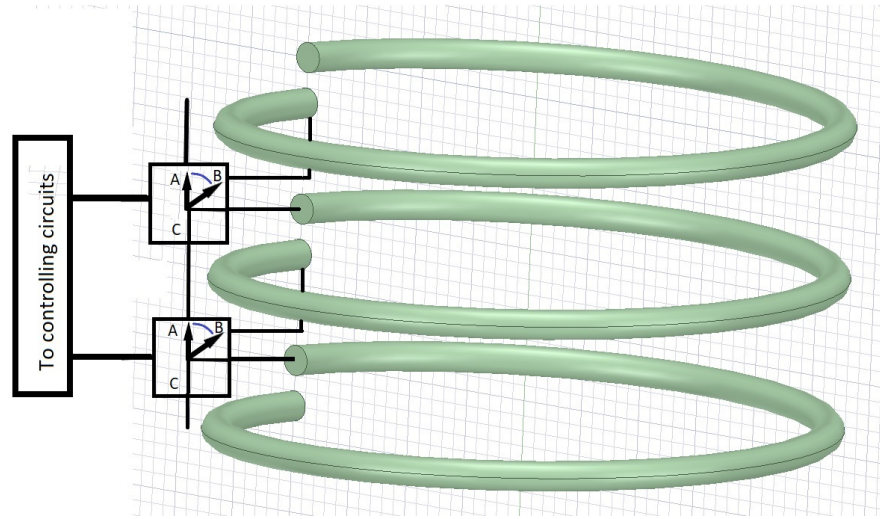


Figure 2.45: Each loop of the TLA is connected to next loop through a switch that connects pin C, to either pin A or B. Here we show 3 loops. The vertical distance between loops is exaggerated to make it easier to show the concept. These switches are controlled by a circuitry attached to the TLA.

Each loop of the TLA is connected to next loop through a switch that connects pin C, to either pin A or B. These switches are controlled by a circuitry attached to the TLA. In Fig. 2.46 we have an example in which the switches are connected in a way that all the loop are in series and the current passes through all the three loops.

The loops that are connected and conduct currents are shown in red. Now assume that we want to disconnect the loop in the middle. Fig. 2.47 shows the required switching that disconnect the middle loop and keep just two other loops connected.

The connected loop which conducts the current is shown here in red and the disconnected loop is shown in green. This way, we could connect or disconnect any loop and in doing so effectively change the structure of the TLA. We refer to each of these structures as one configuration and we will use this method to change the configuration of the TLA.

B-2: Electronic parameters: Connecting each loop to other through switches also enable us to change the direction of the current in each loop. By direction of the current we mean either it is clock-wise or anti clock-wise current.

Fig. 2.48 shows an example.

Assume that an electric current I enters the loop on the right side from its lower end and resulting in a circulation of the current which is anti clock wise. Now if this loop is connected to the other loop through a switch that could be in two state (connecting the C pin to either A or B pin), by controlling the state of the switch through controlling circuitry connected to the TLA we can control the direction of the current in the left side loop. If the switch is in state shown in blue, the current in left side loop will be in anti clock wise direction, shown by a blue circuit. If the switch is in state shown in purple, the current in left side loop will be in clock wise direction, shown by a purple circuit.

The idea described here could be done by any structure that has different parts. However one nice feature of the TLA is that it is relatively easy to control the structure collectively.

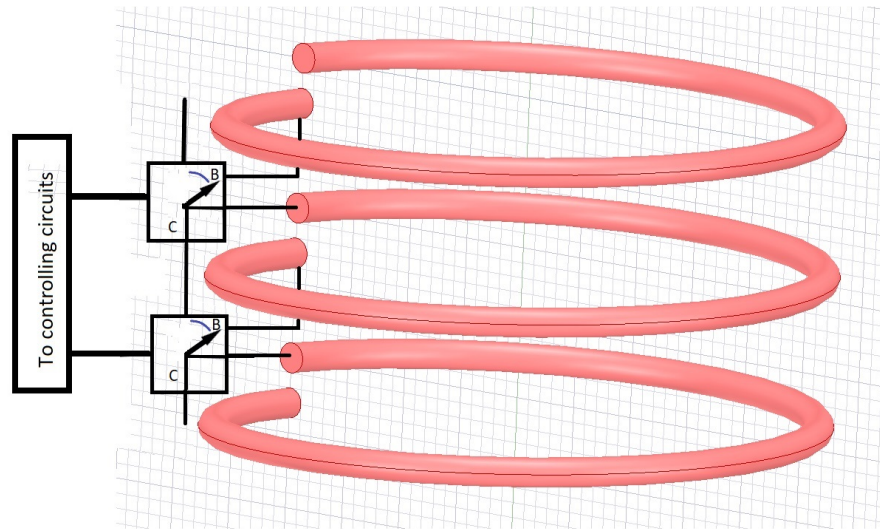


Figure 2.46: Those are the three loops shown in Fig. 2.45. Here the switches state are chosen by controlling mechanism in a way that all three loops are connected and are part of the TLA. The loops that carry the electric current are shown in red.

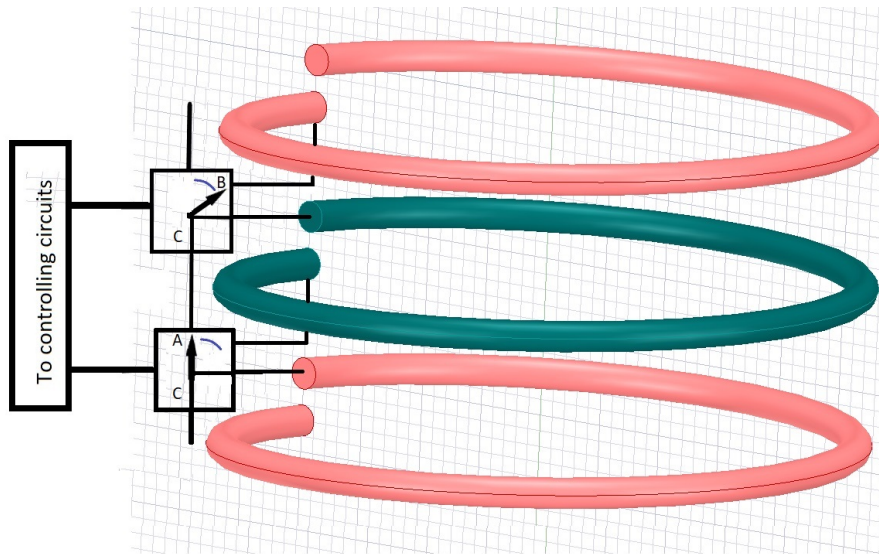


Figure 2.47: Those are the three loops shown in Fig. 2.45. Here the switches state are chosen by controlling mechanism in a way that we disconnect the middle loop and it is not part of the TLA. The loops that are part of the TLA and conduct current are shown in red, and the loop that is excluded from TLA and does not conduct current is shown in green.

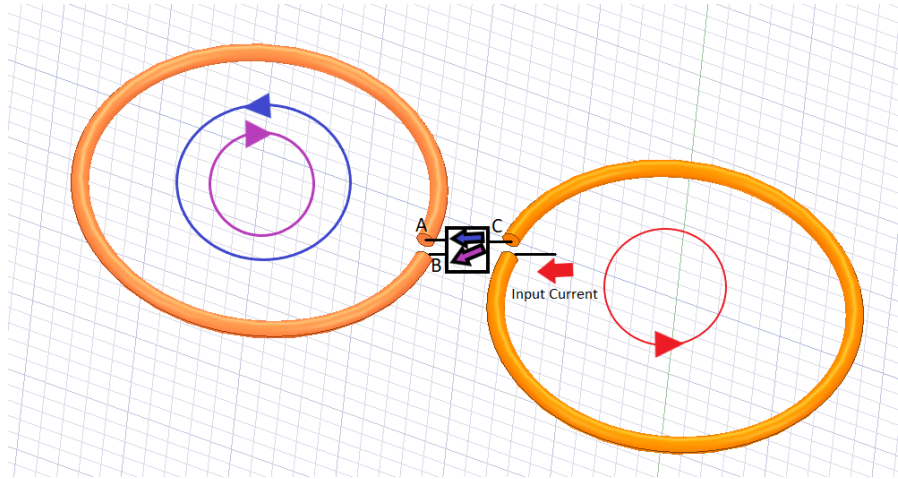


Figure 2.48: Connecting each loop to other through switches also enables us to change the direction of the current in each loop. If the current I enters the loop on the right in a anti clock wise direction by switching the switch connecting it to the loop on the left side we can control the direction of the current in the left side loop. There are two possible directions for current, clock wise and anti clock wise directions.

If it was not a TLA (for example a grid of disconnected coils), one have to control them one by one. But in the TLA case because different loops are already connected in a series, we don't need to instruct them to be connected to each other. We just need to tell which coil is disconnected (or in reverse direction for changing the direction of current), and the others are connected by default.

This simplifies the controlling circuits and uses less switches. This is another reason for using TLA in this chapter.

At the end we should mention that though these switches enable use to have large number of possible configurations, it does not give us complete controlling over TLA. Sometimes it is not possible to control the direction of current and disconnecting or connecting of each loop at the same time. However, the set of all possible configurations is huge and in practice it is often more than what we need.

8. The controlling mechanism stores the table information about the switching steps. The controlling mechanism goes through these switching steps one by one and each one of these steps are corresponding to one configuration. So the number of required TLA structures, is also the number of required steps.

9. We earlier mentioned that the region that we want to cover should be given in a prior. This volume of interest depends on particular application and could be determined easily depending on the specific application requirement. To proceed more systematically this volume of interest is divided into cells, say cell-1, cell-2, etc. Those cells are sub volumes of the volume of interest that together combine all the volume of interest. The number of cells depends on the volume to be covered, the size of transmitter, the minimum required mutual inductance between the transmitter and the receiver, etc.

10. Now our task is to make sure that if the receiver coil is in any position in any cells, having any random orientations, will have enough mutual inductance. To do so, we have to

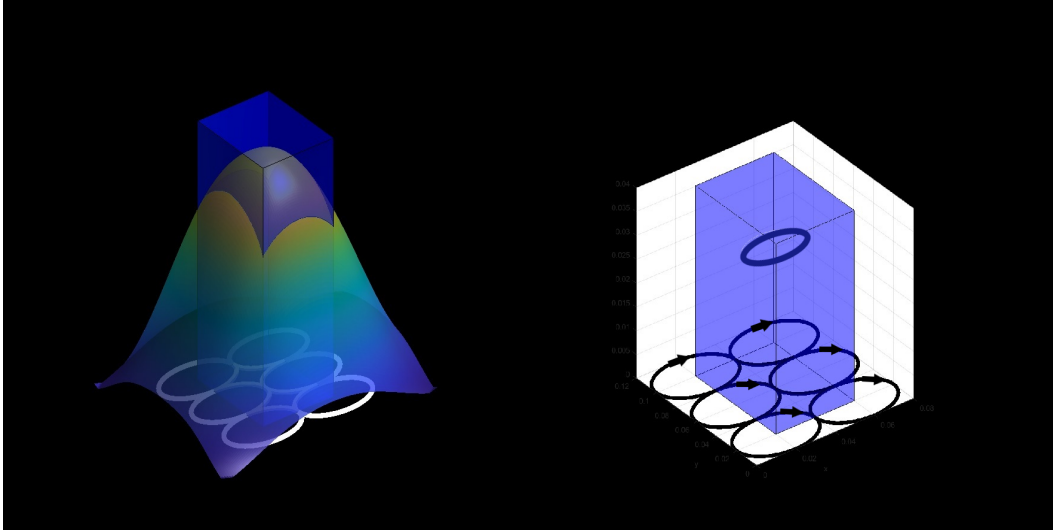


Figure 2.49: Here the cell-1 is a rectangular cuboid extending 4 cm along X axis, 8 cm along Y axis and 8 cm along Z axis. The cell-1 is shown in blue. The goal is to create a field which is suitable for the orientation of the receiver if it was parallel to the XY plane (shown by blue circle). On the left we see such configuration. The arrows show the direction of current in each loop. On the right, we see the Z component of the configuration. We can see it covers all the cell.

make sure that it is the case for any cell. So we consider each cell individually. When we are sure that for each individual cell all possible positions and orientations of the receiver are covered, we are sure that all the volume of interest is covered for any position in it with any possible orientation of the receiver.

11. To realize this in practice we first chose a configuration of the TLA in a way that creates suitable mutual inductance for the first cell. To cover all possible orientations of the receiver we do it in three steps. Earlier we said that any random orientation of the receiver coil could be resolved in three perpendicular orientations. In the first step, we chose a TLA configuration that creates a magnetic field which would give an acceptable mutual inductance if the receiver coil was in cell-1 and in XY plane. In the second step, we chose a TLA configuration that creates a magnetic field which would give an acceptable mutual inductance if the receiver coil was in cell-1 and in XZ plane. And in the third step we chose a TLA configuration that creates a magnetic field which would give an acceptable mutual inductance if the receiver coil was in cell-1 and in YZ plane. Hence, we insure that regardless of the orientation of receiver coil if it is in the cell-1, it will have good mutual inductance at least in one step.

The previous steps from 1 to 11, explain our approach, now we give an example.

Consider the Fig. 2.49.

Here the cell-1 is a rectangular cuboid extending 4 cm along X axis, 8 cm along Y axis and 8 cm along Z axis. The cell-1 is shown in blue. We are using 3 TLA next to each other (shown on the left side of the Fig. 2.49). In first step, we want to create a field which is suitable for the orientation of the receiver if it was parallel to the XY plane. This means we are interested in the Z component of the field, as we said earlier. To create such field in the

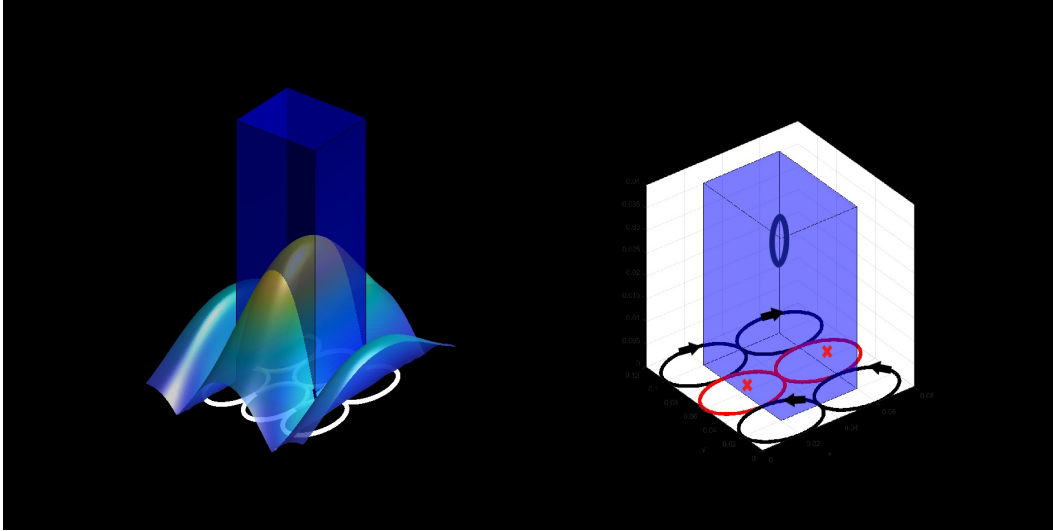


Figure 2.50: Here we still considering cell-1 which is shown in blue. The goal is to create a field which is suitable for the orientation of the receiver if it was parallel to the XZ plane (shown by blue circle). On the left we see such configuration. The arrows show the direction of current in each loop. The red loop are disconnected and are not part of the configuration. On the right we see the Y component of the configuration. We can see it cover all the cell.

cell-1 we set our switches in a way that all the loops carry current in the same direction. The resulted mutual inductance for such orientation of receiver coil is shown on the right side of the Fig. 2.49. If the receiver was at any point in this cell, it will have a mutual inductance above the minimum mutual inductance required by the specific application we are dealing with.

Now we assume that the receiver is in XZ plane. This time we are interested in the Y component of the field. We switch the configuration in a way shown in left side of the Fig. 2.50. This configuration results in mutual inductance shown on the right side of the Fig. 2.50.

Third step is concerning the case in which the receiver loop was to be in the YZ plane. This time we are interested in X component of the field. We switch the configuration in a way shown in left side of the Fig. 2.51. This configuration results in mutual inductance shown on the right side of the Fig. 2.51 as explained previously.

From Fig. 2.49 to Fig. 2.51, the unit of the volume of interest is length, but the unit of magnetic field component is Tesla. It is not very correct to show them on the same axis, but here we just want to show that there is no null area in the cell due to certain component of the magnetic field, rather than giving precise value of the field at each point in the volume of interest.

This will finish our steps for cell-1, and we move to next cell; cell-2, and then cell-3, and so on. When we are done we return to the cell-1, and continue in a loop.

The next logical step is to ask how we should choose the suitable configuration in each steps. This task is done based on the magnetic field steering that we mentioned earlier.

To see how this task is done in a real example consider the following situation. Assume we have a TLA structure, consisting of number of loops. We start by considering the magnetic

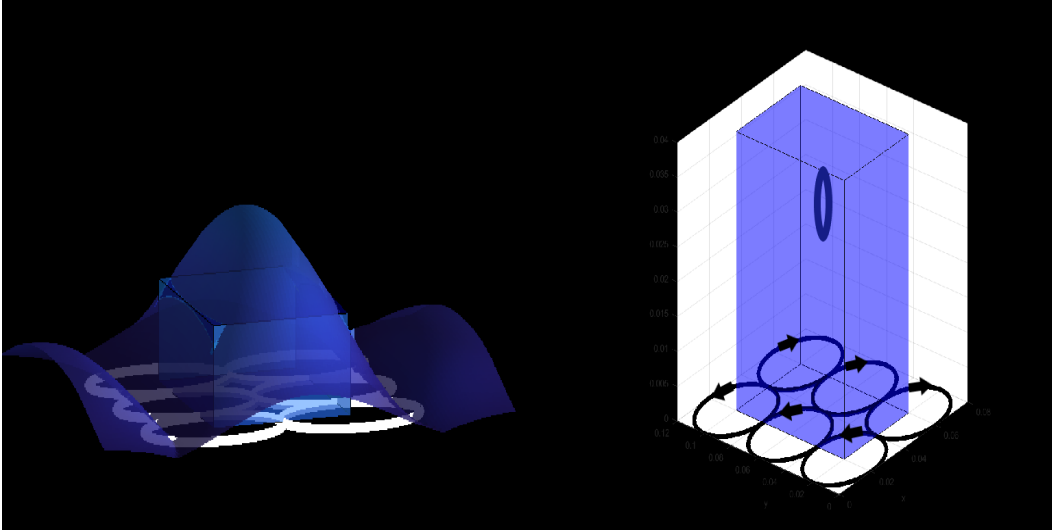


Figure 2.51: Here we are still considering cell-1 which is shown in blue. The goal is to create a field which is suitable for the orientation of the receiver if it was parallel to the YZ plane (shown by blue circle). On the left we see such configuration. The arrows show the direction of current in each loop. On the right we see the X component of the configuration. We can see it covers all the cell.

field created by each loop at a point of interest individually. Let say the point of interest is a center of a certain cell. This is shown in Fig. 2.52. The total magnetic field will be the vectorial addition of the contribution of each of this individual magnetic field.

Now if one is interested in having magnetic field which points mostly in say Y direction (suitable for a case in which the receiver coil is in XZ plane), one should manipulate the individual component in a way that their vector sum adds in Y direction and create a large magnetic field in Y direction. One could control the strength of the magnetic field due to a certain loop in the TLA by increasing the number of turns of that loop. The strength of the magnetic field is proportional to the number of turns in each loop.

If we want to multiply the strength of the magnetic field by say 3, we also increase the number of turns by the number of 3. Of course there is an upper limits for this which is the number of available turns. When we connect all available turns there is no more that we can do. However we choose the number of available turns with a priori knowledge about the volume of interest and the number of cells, so running short of the required number of turns is not a problem.

The direction of the magnetic field at the point of interest could be reversed by changing the direction of the current in the corresponding loop. Those two parameters are used (and often they are enough) to create total magnetic field with large component in the desired direction (as we already have seen in the Fig. 2.49 to Fig. 2.51).

So finding out the structure of TLAs that will give a suitable magnetic field for each step, is to find out the number of turns in each loop of the TLAs and the direction of the current in them. Then by switching on and off some turns of the TLAs, we will have different structures in each step, which in its turn give rise to different magnetic field orientations in each step.

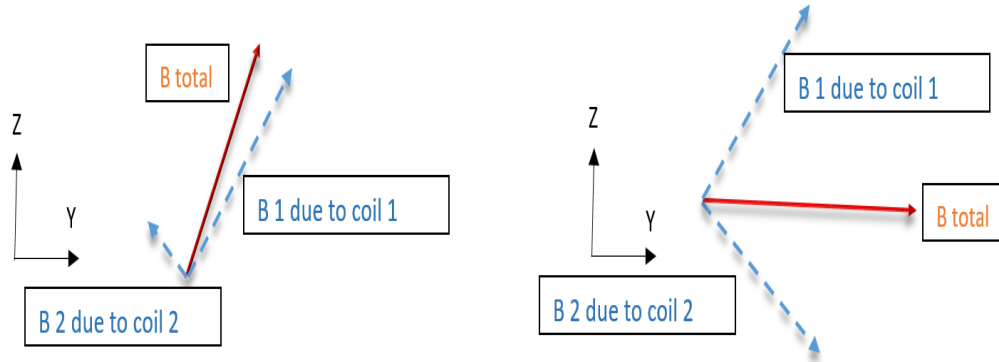


Figure 2.52: On the right we have the total magnetic field (in red) in a certain point due to the magnetic fields (dashed blue) of two different coils. If we want to rotate the field for example in the Y direction, we realize one possible way is to reverse the direction of the magnetic field due to coil 2, by changing the direction of current in it, and at the same time by increasing its strength, by increasing its turns. The results is shown on the left side of the figure with the total magnetic field in Y direction, which was our goal.

Before we move on, one should mention that it happens some times that the TLA structure suitable for one step is also suitable for another step. That means we don't need 3N steps for sweeping along all the necessary steps. In practice this is very help full and reduce the complexity of the controlling circuitry and the number of required steps.

This information about the required structure for each step and how to change the number of turns and the direction of current in them, can be stored in a micro controller to repeatedly run through them one by one. In doing so, we cover the whole volume of interest for all the possible orientations.

Before we go to experimental verification of this idea, it should be mentioned that in our calculation of the magnetic field (in order to choose which configuration is suitable for each step) we calculated magneto static fields due to constant current. Clearly as we mentioned earlier the induction of voltage due to mutual inductance needs an AC current and it could not be produced due to a DC current. However if the signal wavelength that drives the TLA is large in respect to the TLA antenna length, we could assume we have a quasi-static magnetic field which is approximated very well by the calculated static field. For this reason, the measurement will be done at low frequencies (from 100 kHz and 125 kHz).

For experimental verification, we assume that the given volume of interest spans for 20 cm in the Y direction, centred at the origin, 12 cm in the Z direction, and 12 cm along X axis. These might seen small ranges, but the point here is that the range that one could cover in magnetic coupling is roughly equal to the size of the transmitter. This means that the system is easily scalable and for covering larger volume of interest one should just increases the size of transmitters (according to the application on hand).

The goal here is this: We want our system guarantees that inside the volume of interest there is no null area, and furthermore regardless of the position of receiver coil, the mutual inductance of sender and receiver is at least 3 nH. Here we choose this value depending on the minimum requirement of our experimental tools, for other systems this value is calculated depending on the minimum power required to be transferred to the receiver [6].

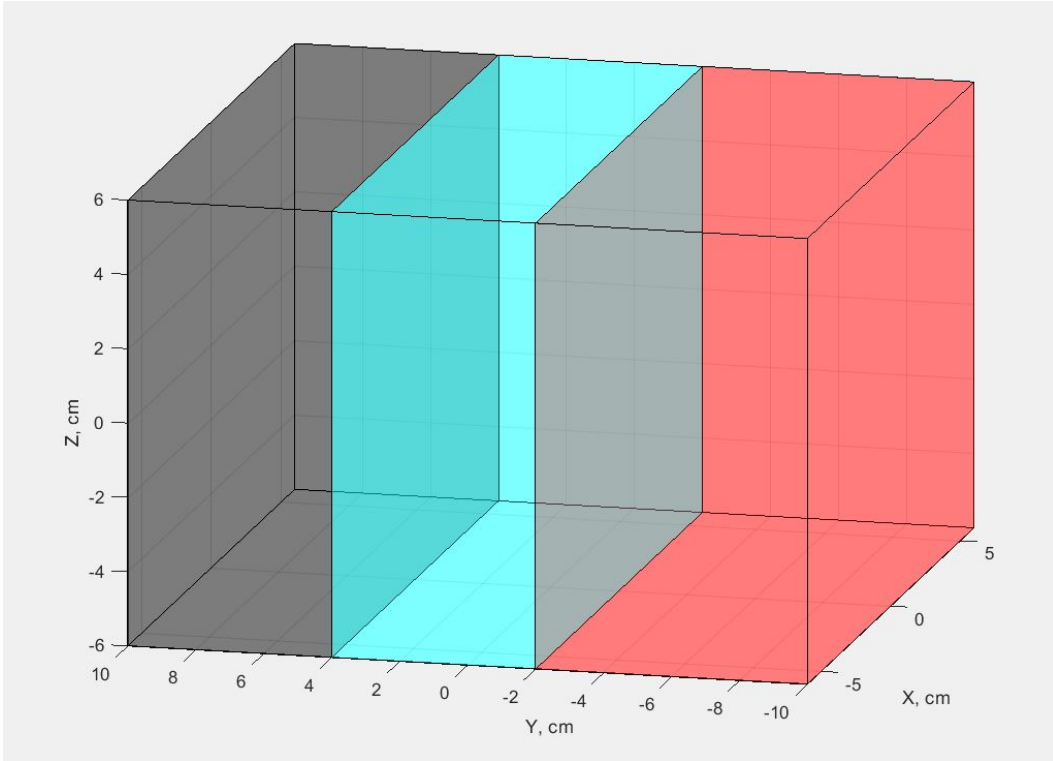


Figure 2.53: The volume of interest is a box extending in Y axis from -10 cm to 10 cm. In X extending from -6 cm to 6 cm. In Z from -6 cm to 6 cm. This volume is divided into three cells, shown here in three different colors. cell-1 in red, cell-2 in blue and cell-3 in black. The receiver coils could be anywhere in this volume of interest and it could have any orientation.

The number of cells depends mainly on the volume to be covered and the minimum mutual inductance required, as we mentioned earlier.

For our example we divide the volume of interest into three cells:

1. cell-1 from -10 cm to -2 cm along Y axis, from -6 cm to 6 cm along X axis, from -6 cm to 6 cm along Z axis.
2. cell-2 from -2 cm to 4 cm along Y axis, from -6 cm to 6 cm along X axis, from -6 cm to 6 cm along Z axis.
3. cell-3 from 4 cm to 10 cm along Y axis, from -6 cm to 6 cm along X axis, from -6 cm to 6 cm along Z axis.

This is shown in Fig. 53.

However as we mentioned earlier, sometimes it's possible to cover more than one cell by just one excitation, though this might result in having little area with mutual inductance less than required mutual inductance, which is in our case 3 nH.

We start by covering the case in which the receiver loop is in XZ plane. That means we are interested in the Y component of the field. From desired field for each step, we deduce the required structure that will produce that desired field. For doing so, we chose one of the easiest possible of TLA structure. Though this is an arbitrary choose, certain criteria

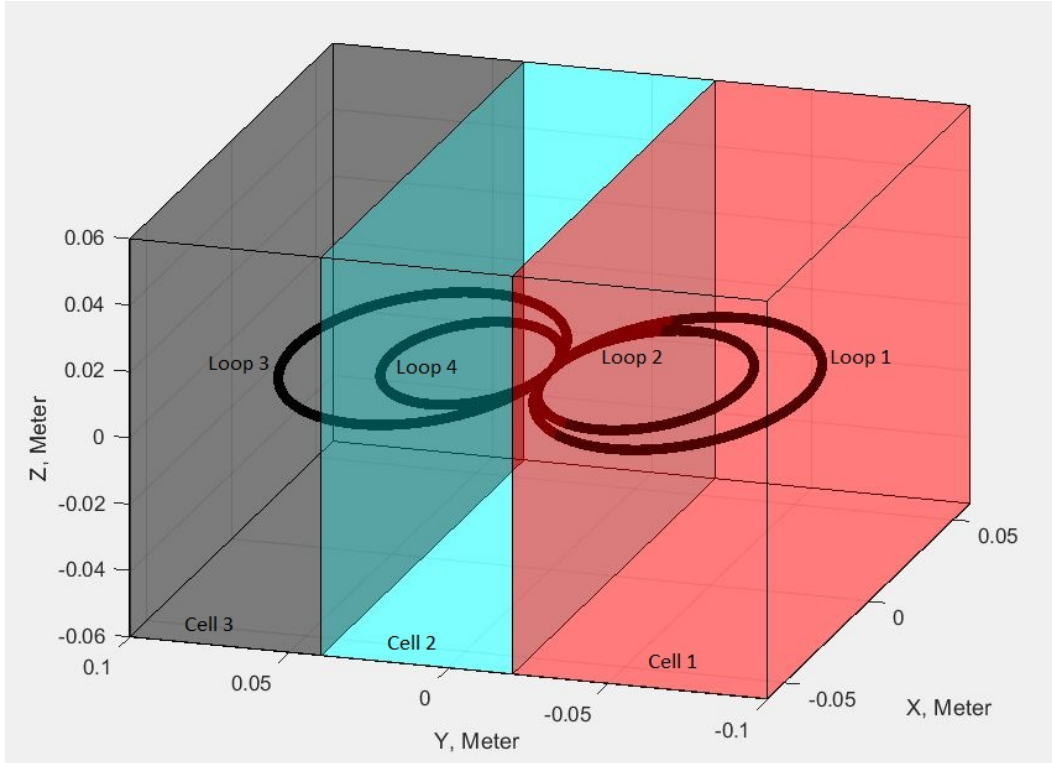


Figure 2.54: The structure of a TLA chosen for experimental verification of our method. The TLA is consisting of four loops. The two larger loops have diameter of 8 cm, one of the small loops has diameter of 6 cm and another small loop has the diameter of 5 cm. It is placed in the XY plane centered in the origin of the coordinate system, which is the center of the volume of interest.

should be taken in our consideration. Among them, the size of the TLA should be more or less the same size of volume of interest. Another thing is that for controlling the field component say Y component of the magnetic field, it is a good idea to have a structure which extends along Y axis. This makes the controlling easier. We start by choosing an arbitrary structure of a TLA (that means the size, the number of turns,...) but we check it if it fulfils the requirement and see if different configurations the chosen TLA could generate required magnetic field component. If the chosen TLA configuration could not do the job, we change it and check it again, till we have suitable TLA structure. Here we chose a TLA structure that is consisting of four loops. It is shown in Fig. 2.54.

The two larger loops have diameter of 8 cm, one of the small loops have diameter of 6 cm and another small loop has the diameter of 5 cm. It is placed in the XY plane centered in the origin of the coordinate system.

To find out what is the suitable configuration in this example, we start by last cell, cell-3, when the receiver loop is in the XZ plane. We should consider the Y component of the magnetic field in cell-3. We chose the center of the cell-3 and see what is the direction of the magnetic field in the centre of cell-3.

CHAPTER 2. A RECONFIGURABLE ANTENNA FOR ENHANCING THE
MAGNETIC COUPLING IN IPT AND RFID

Loop	Number of turns	Direction of current
The loop number 1 in Fig. 2.53	11 turns	clock wise current
The loop number 2 in Fig. 2.53	2 turns	anti clock wise
The loop number three in Fig. 2.53	1 turns	anti clock wise
The loop number four	9 turns	clock wise

Table 2.1: A configuration which creates the desired magnetic field in Y direction in both cell 3 and cell 1 at the same time

It is sufficient that in the beginning we just consider the center because in general the spatial variation of the field are not so fast if we chose the small size for the cell. Any way after we fixed the required configuration of the TLA to have suitable field in the center of the cell, we could check to see if it is the case for all cells. If the configuration is generating a desired magnetic field direction in whole the cell, the task is done, if not we have to change the configuration.

First, we check the direction of the magnetic field due to each individual loop in the center of the cell-3 (in each loop having a 1 turn and clock wise current). The vector sum of these will be the final magnetic field which in general is not in the desired direction to create acceptable mutual inductance. To rotate the field in Y direction (creating large Y component is desirable because we assumed the receiver loop is in XZ plane) we see which magnetic field should change its direction (we do so by changing the direction of the current in corresponding loop) and which magnetic field should become stronger by increasing the number of turns (or weaker by reducing the number of turns); so their vector sum will have larger component in Y direction. Though the configuration of the TLA that do the job is not unique, it is a good idea to chose one (if it is possible) that creates a suitable magnetic field for more than one cell. This will reduces the number of required steps. One could go through the all possible configurations of TLA one by one and pick the best result. This task maybe time consuming, but it is one time mission and don't need to be repeated. The configuration then will be stored in the memory of the controlling mechanism of the system. Here we chose a configuration which creates the desired magnetic field in Y direction in both cell 3 and cell 1 at the same time .

This configuration suitable for Y component of the magnetic field in cells 1 and 3 is shown in Table ??.

Fig.2.55 shows the result (the Y component of the Magnetic field) across XY plane of the volume of interest for a fixed Z. In this figure, we fixed z to be 6 cm above the TLA. Cell 1 and cell 3 are shown also, to emphasize the fact that TLA indeed creates a Y component of the field that increases in the position of cell 1 and cell 3.

Now in next step, we have to chose a configuration of the remaining cell, which is cell 2. The configuration suitable for Y component of the magnetic field in cells 2 is shown in Table 2.5.

Notice the only thing we have changed is the number of turns and the direction of current (electrically changeable parameter), and the radius and position of TLA has not changed (those are not electrically changeable parameter).

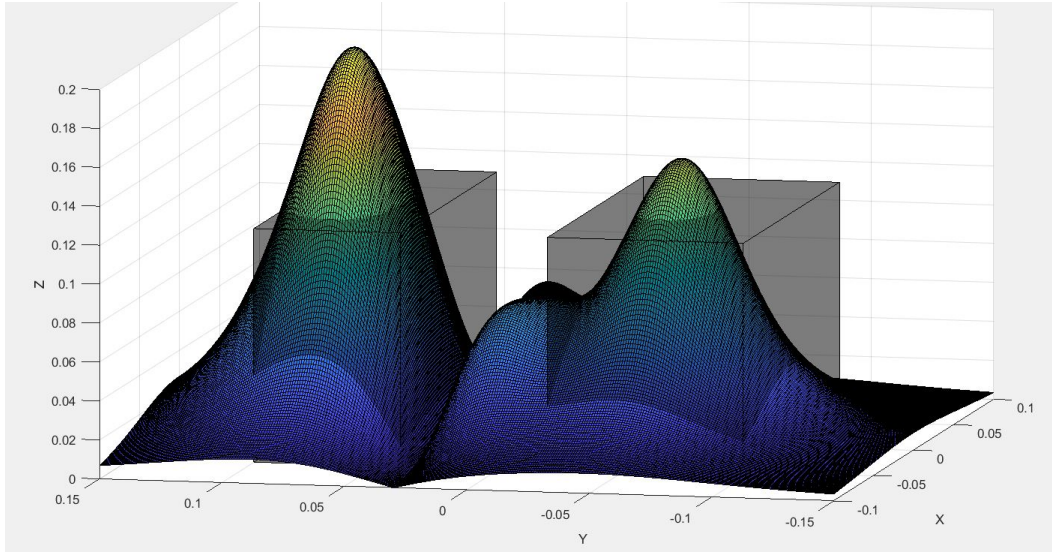


Figure 2.55: The Y component of the Magnetic field across XY plane of the volume of interest for a fixed Z ($Z= 6\text{cm}$). Cell 1 and cell 3 are shown also, to emphasize the fact that TLA indeed creates a Y component of the field that increases in the position of cell 1 and cell 3.

Loop	Number of turns	Direction of current
The loop number 1 in Fig. 2.53	2 turns	clock wise current
The loop number 2 in Fig. 2.53	4 turns	clock wise
The loop number three in Fig. 2.53	4 turns	anti clock wise
The loop number four	7 turns	anti clock wise

Table 2.2: A configuration which creates the desired magnetic field in Y direction in cell 2.

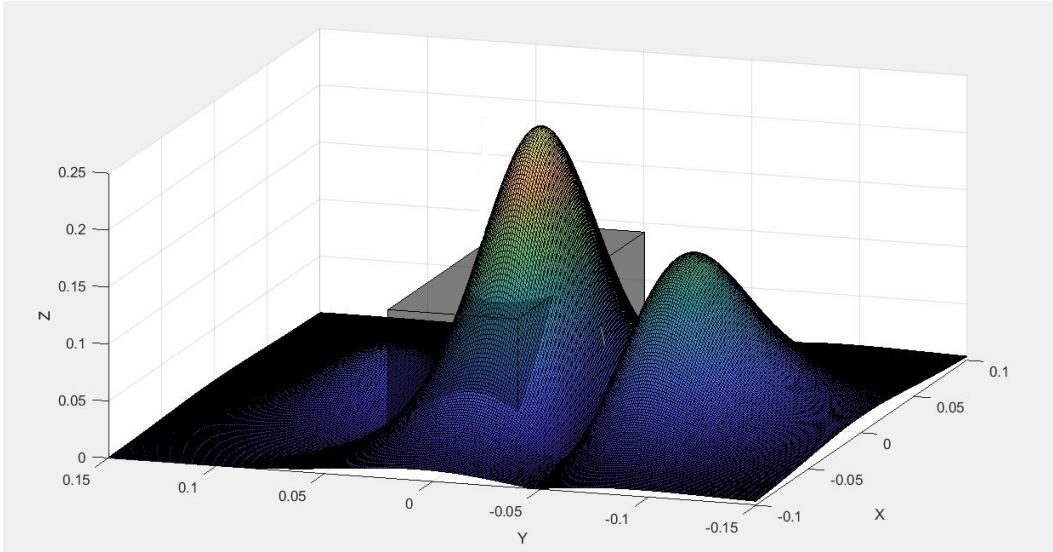


Figure 2.56: The Y component of the Magnetic field across XY plane of the volume of interest for a fixed Z ($Z=6\text{cm}$). Cell 2 is shown also, to emphasize the fact that TLA indeed create a Y component of the field that increases in the position of cell 2.

Fig.2.56 shows the result (the Y component of the magnetic field) across X and Y extension of the volume of interest for a fixed Z. In this figure, we fixed Z to be 6 cm above the TLA. Cell 2 is shown in gray, to emphasize the fact that TLA indeed creates a Y component of the field that increases in the position of cell 2.

Those were the Y component of the magnetic field. At the end we are interested in the mutual inductance.

In Fig.2.57 we put every thing together. To see better the mutual inductance we fix Z and X component of receiver location and we move it along the Y axis. The receiver is in XZ plane as we said and it is a circular loop of 2 cm diameter with one turn. The TLA is shown in black. The arrows and the number next to each loop indicates the number of turn and the direction of current in each loop. The colour of these arrows corresponds to the same colour of mutual inductance curve, configuration one in blue and configuration 2 in read. Each configuration is suitable for a cell with the same colour.

The same idea and same procedure will be done for the case in which we assume the receiver is in YZ plane (here we will be interested in magnetic field in X direction) and when we assume the receiver is in the XY plane (here we will be interested in magnetic field in Z direction). For directing field in X direction from symmetry one could deduce that what is needed is a another TLA which is in the same plane like the first one but rotated by 90 degrees, so what was true for Y in the first TLA structure will be true for the X in second structure. These two TLA along X and Y axes are shown in Fig.2.22. If we assume the receiver coil is in XY plane, this means we are interested in Z component of the field. This could easily be done if we choose all directions of currents in all loops to be in same direction.

In this section we presented a method for avoiding null area. In this method we divide the volume of interest in different cells then we use the beam forming to make sure that there

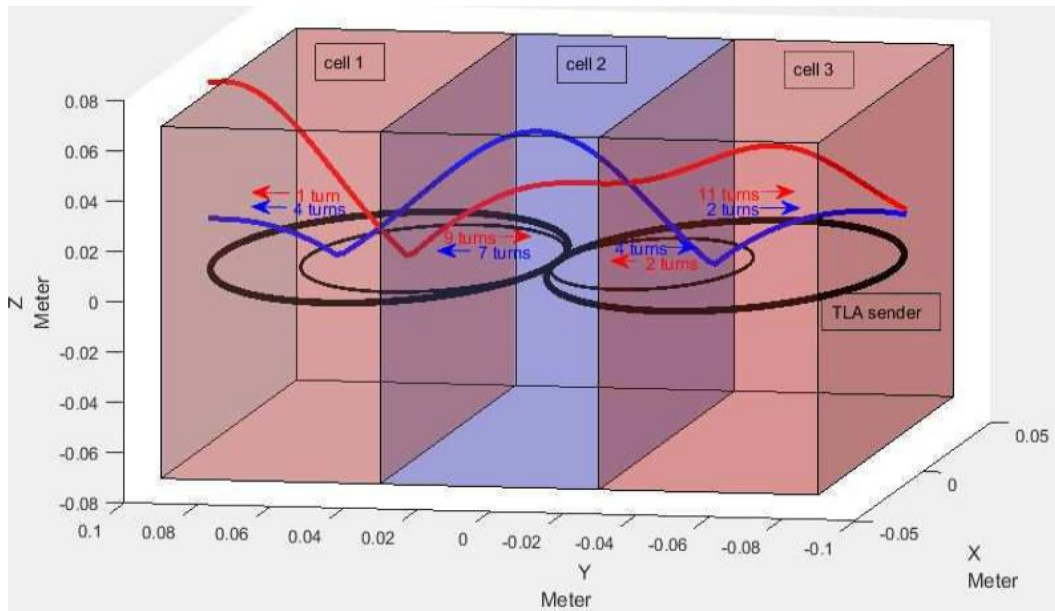


Figure 2.57: Representation of the mutual inductance. We fix Z and X component of receiver location and we move it along the Y axis. The receiver is in XZ plane. The TLA is shown in black. The arrows and the number next to each loop indicates the number of turns and the direction of current in each loop. The colour of these arrows corresponds to the same colour of mutual inductance curve, configuration 1 in blue and configuration two in red. Each configuration is suitable for a cell with the same colour. Here the Z axis is used to show two quantities at the same time: The vertical distance from the TLA, this is shown in meter. But also it is used to show the mutual inductance. The value of mutual inductance is not given here, what we want to show is the relative variation of mutual inductance in a way that it increases in the targeted cells as expected.

is no such nulls area in any cells for all possible orientation of the receiver.

2.6 Measurement

Till now we were trying to control the magnetic field created by the transmitter to overcome the null areas between transmitter and the receiver. Measuring the magnetic field directly is not an easy task, but measuring the consequence of this field, namely the mutual inductance between the transmitter and the receiver is a much more easier and more practical task.

It also should be mentioned that the same mechanism that gives rise to the mutual inductance between two electric circuits (say two loops) gives rise to other property of the circuit, namely self inductance. The reason is that, as any change in magnetic field induces an electric field, the change in magnetic field due to different parts of a transmitter will induce an electric field in other parts of transmitter itself. This is self inductance of any electric circuit. The self inductance of any electric circuits is constant as long as the shape and the structure of the circuits is constant. It will not change if we move the transmitter from one place to another, or if we rotate the transmitter. The same concepts apply to the receiver circuit also.

Another point that should be mentioned is that the transmitter and the receiver have their own resistivity (they are made of conductor with finite conductivity) and their own capacitance (they are made of conductors separated by insulators and that create a capacitor).

To measure the mutual inductance between receiver coil and the transmitter coil, we need to model the TLA (transmitter) and the receiver. We will do this by the following steps:

1. Transmitter could be modelled by an electrical circuit with self inductance L_1 . The resistivity is neglected due to its small value and the capacitance is neglected because we are working in relatively low frequency.
2. The receiver could be modelled by an electrical circuit with self inductance L_2 . The resistivity and the capacitance are neglected for the same reason as sender. However if we are going to work in high frequency we should keep in mind that these assumptions become inappropriate.
3. Both transmitter and receiver are inductors and both are two-terminal elements.
4. The mutual inductance between the transmitter and the receiver M_1 and the mutual inductance between the receiver and the transmitter M_2 are equal; we will simply call it M .
5. The induced voltage $M di/dt$, however, appears as a positive or a negative, based on the increasing current or decreasing current at a certain instant in time. We determine the sign of the induced voltage by using "dot convention", see Fig.2.58
6. We use transfer model, for modelling two magnetically coupled inductors (transmitter and receiver).

When we put all these steps together we get the model shown in the Fig.2.58. This is a two-ports network that can be fully characterize by different parameters, like S parameters, Z parameters and so on. We are going to use a VNA (Vector Network Analyser) for studying this two-ports network by measuring its S parameters. This could be done easily by using available VNA in the lab. The S matrix for a two port network has four components : S_{11}, S_{12}, S_{21} and S_{22} . What we need is to find the relation between these components and the parameters of the network shown in the Fig. 58, namely L_1, L_2 and M .

For doing this first, we measure the S parameters matrix. Then we convert this S matrix to

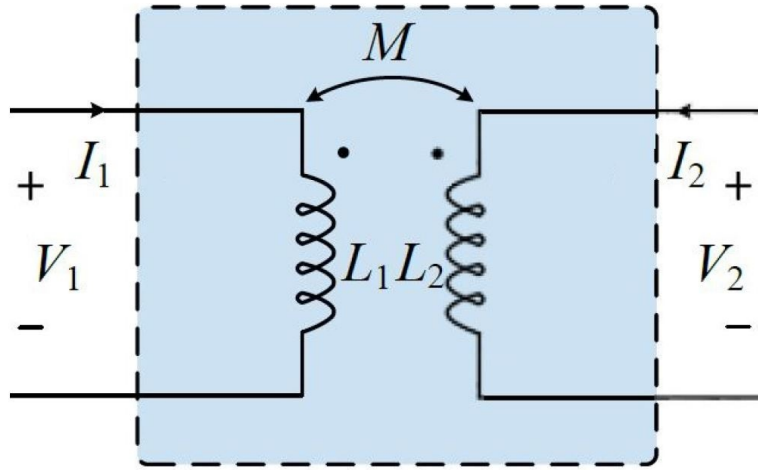


Figure 2.58: Circuit model of two magnetically coupled inductors (transmitter and receiver) in low frequency. L_1 is the self inductance of the transmitter (TLA), L_2 is the self inductance of the receiver and M represents the mutual inductance between transmitter and receiver.

the impedance matrix (Z matrix). Z matrix for two port network also has four components and is connected to S matrix components by:

$$Z_{11} = Z_0 \frac{(1 + S_{11})(1 - S_{22}) + S_{12}S_{21}}{(1 + S_{11})(1 - S_{22}) - S_{12}S_{21}} \quad (2.35)$$

$$Z_{12} = Z_0 \frac{2S_{12}}{(1 + S_{11})(1 - S_{22}) - S_{12}S_{21}} \quad (2.36)$$

$$Z_{21} = Z_0 \frac{2S_{21}}{(1 + S_{11})(1 - S_{22}) - S_{12}S_{21}} \quad (2.37)$$

$$Z_{22} = Z_0 \frac{(1 - S_{11})(1 + S_{22}) + S_{12}S_{21}}{(1 + S_{11})(1 - S_{22}) - S_{12}S_{21}} \quad (2.38)$$

In our measurement the Z_0 (characteristic impedance) is 50 Ohm.

Now we have the Z matrix representation of our network. In fact we chose to convert S matrix to Z matrix, because it enables us to connect it to the parameters of our network. To do so we refer to Fig.2.59. The impedance matrix relates the voltage and current in port 1 (let say it is the transmitter), V_1 and I_1 , to the voltage and current in port 2 (let say it is the receiver), V_2 and I_2 . In our case of two port network the Z matrix has four components. These components relate the voltages and currents in each port as follows:

$$\begin{bmatrix} V_1 \\ V_2 \end{bmatrix} = \begin{bmatrix} Z_{11} & Z_{12} \\ Z_{21} & Z_{22} \end{bmatrix} \begin{bmatrix} I_1 \\ I_2 \end{bmatrix} \quad (2.39)$$

Now we develop the circuit equation in frequency domain of the circuit in Fig. 2.59 and we get:

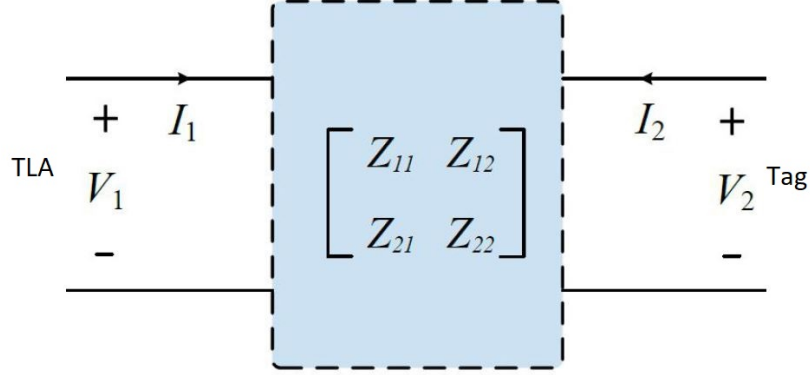


Figure 2.59: Two-port network model of the transmitter (TLA) and the receiver.

$$V_1 = j\omega L_1 I_1 + j\omega M I_2 \quad (2.40)$$

$$V_2 = j\omega M I_1 + j\omega L_2 I_2 \quad (2.41)$$

Now we put equation 2.40 and 2.41 in matrix form and we get:

$$\begin{bmatrix} V_1 \\ V_2 \end{bmatrix} = \begin{bmatrix} j\omega L_1 & j\omega M \\ j\omega M & j\omega L_2 \end{bmatrix} \begin{bmatrix} I_1 \\ I_2 \end{bmatrix} \quad (2.42)$$

If we compare the equation 42 to equation 39 we conclude:

$$\begin{bmatrix} j\omega L_1 & j\omega M \\ j\omega M & j\omega L_2 \end{bmatrix} = \begin{bmatrix} Z_{11} & Z_{12} \\ Z_{21} & Z_{22} \end{bmatrix} \quad (2.43)$$

Or in components form:

$$Z_{11} = j\omega L_1 \quad (2.44)$$

$$Z_{12} = j\omega M \quad (2.45)$$

$$Z_{21} = j\omega M \quad (2.46)$$

$$Z_{22} = j\omega L_2 \quad (2.47)$$

This means by measuring the Z_{12} and Z_{21} , and from given frequency we could deduce the mutual inductance. It also should be mentioned that our calculation was based on the Biot-Savart law which is a magneto static law. However working in low frequency should not bring a big change from magneto static. For this reason we are performing our measurement at 100 kHz frequency.

In short we measure the S parameters, convert them to Z parameters, and from Z parameter deduce the mutual inductances according to equations 45 and 46.

To do the measurement, we want to check the scenario for which we did the simulation, the

scenario whose final result are shown in Fig.2.59.

It was a case in which we have a volume of interest as a box extending in Y axis from -10 cm to 10 cm, in X extending from -6 cm to 6 cm and in Z from -6 cm to 6 cm.

The receiver coils could be anywhere in this volume of interest and it could have any orientation and our objective is to guarantee that the mutual inductance between the transmitter and the receiver is at minimum 3 nH whatever the position (within the volume of interest) and whatever the orientation of the receiver is. Here we choose this value of minimum mutual inductance arbitrary for the sake of demonstration, in practice this value should be calculated depending on the minimum power required to be transferred to the receiver [6]. We said that we divide the volume of interest into three cells then cover these cells for the three possibility of the receiver being in XY or XZ or YZ plane. Then we detailed simulation just for the case where the receiver was in the XZ plane, and we said that the other steps will follow the exactly same logic. This case will be tested in experiment to see whether or not the measurement confirm the simulations and the results obtained earlier. The final result of this simulation is shown in Fig.2.57.

In fact there is a small area (for Y from 0.03 to 0.06m) with mutual inductance less than aimed 3 nH in cell-3 but it's just a result of covering three cells by two structures, and could be easily solved by increasing the number of cells. Here we are interested in demonstrating the applicability of the idea of reconfigurable antenna in general and we will neglect this small null area and as we said it could be solved easily in any practical system.

For measuring the mutual inductances between the transmitter and the receiver, we recreate the conditions for which we did the simulation shown in Fig. 2.57.

1. We have the same volume of interest as in Fig.2.54.
 2. We divide the volume of interest into three cells as in Fig. 2.54.
 3. We fix the receiver orientation in the XZ plane, as in the simulation in Fig.2.57.
 4. We fix the X and Z coordinate of the receiver to X=0, and Z=6 cm as in the simulation in Fig. 2.57. The X coordinate is arbitrary and any value for it could be chosen but we chose the Z = 6cm for the following reason: Z = 6cm is the upper boundary of the volume of interest. For the lower boundary at Z=-6 cm, because of symmetry we will have the same results. We do the measurement in the boundary of the cell, because the mutual inductance becomes smaller as the distance from sender increases, so the lowest value of mutual inductance in a cell is at its boundary. If we guarantee the mutual inductance in the boundary of the cell is more than 3nH, we could be sure it is also higher than 3nH everywhere in that cell.
 5. We set the Y coordinate of the receiver at the edge of the volume of interest, then we move the receiver along the Y axis step by step, from the beginning of the volume of interest till its end and at each different position, we measure the S parameters, and from S parameters we deduce the mutual inductance as explained earlier.
- The Fig. 2.57 shows the result of the simulation for this set up and now we want to compare the experimental results with the results of the simulation.
6. For measuring the S parameters we use a ROHDE and SCHWARZ ZNB 8 Vector Network Analyser.
 7. We do the measurement at 100 kHz for the raison mentioned earlier, simply for the quasi-static assumptions to be valid.
 8. We fabricate TLA with the same property that we earlier calculated its property (radius of loops and number of turns) and did the simulation for.
 9. The receiver is a circular coil of radius of 1 cm.

The set up and the procedure are shown in Fig.2.60 to Fig.2.63. Fig2.64 shows the results.

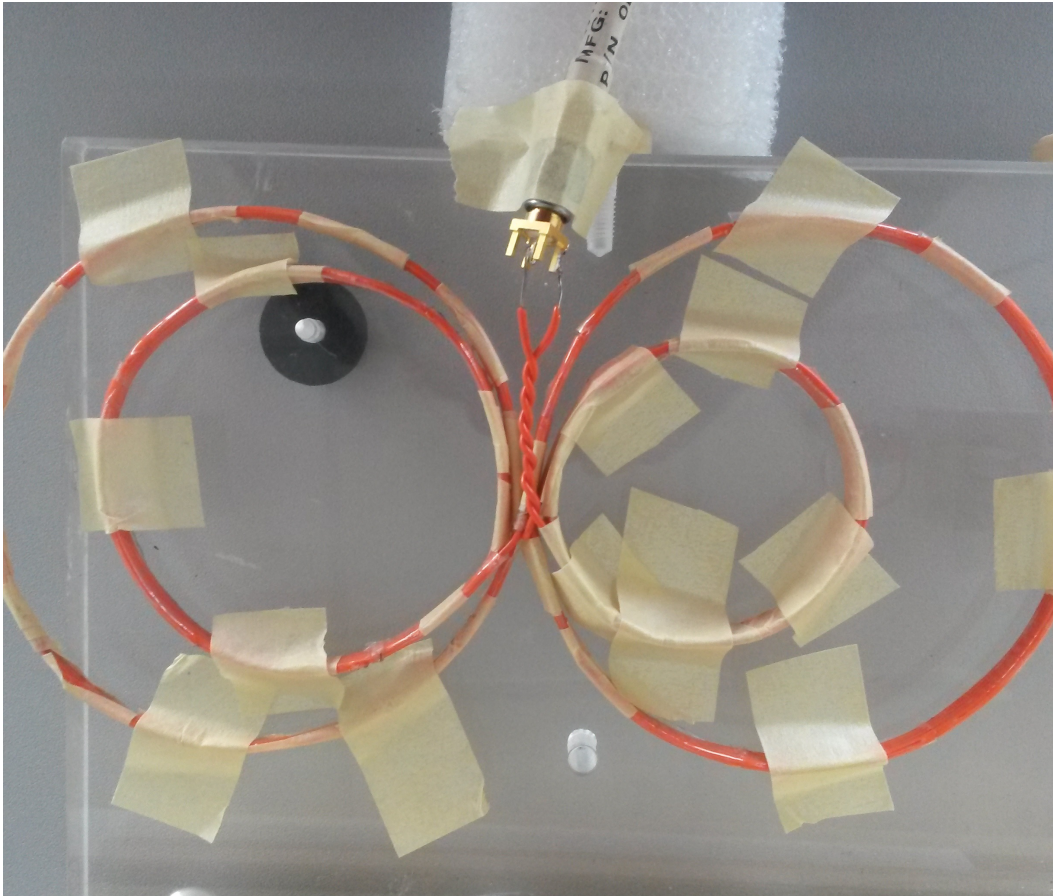


Figure 2.60: The fabricated TLA for the experiment. This TLA has the same property (size of each loop, number of turns,...) for which we did the simulation.

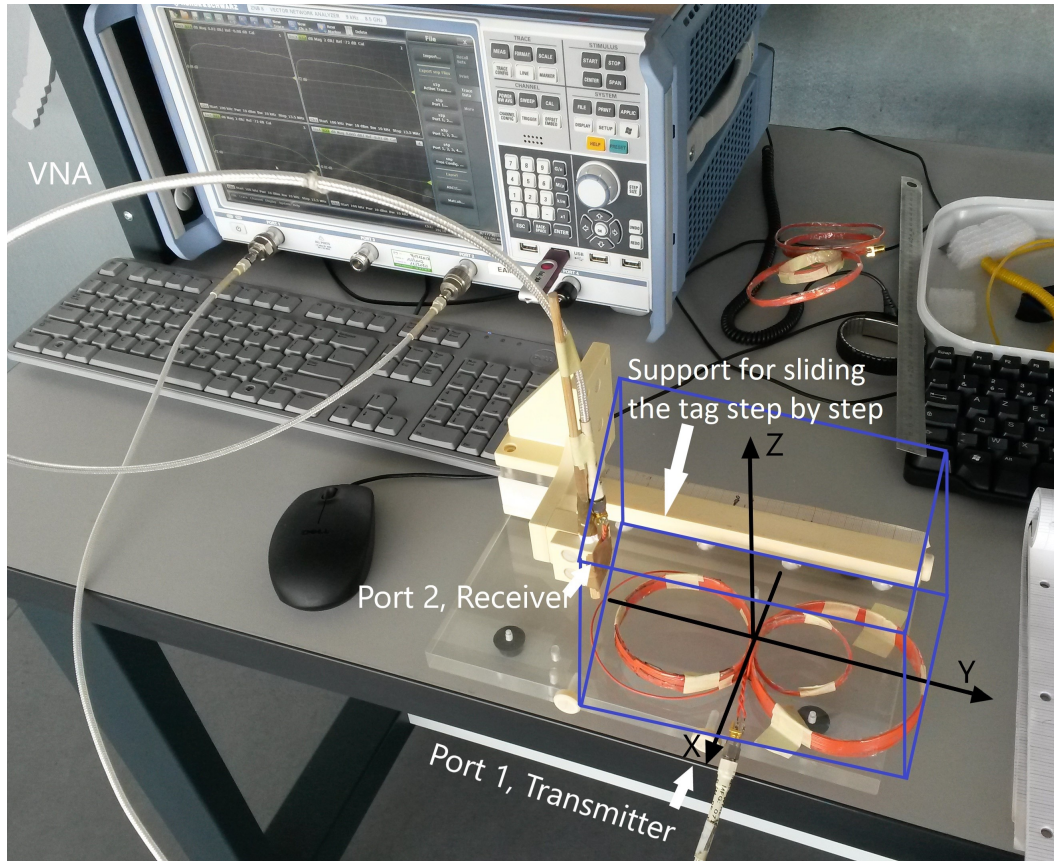


Figure 2.61: The setup for the measurement. X,Y and Z axis are shown in black. The volume of interest is the blue box. The TLA is in the XY plane and is connected to port 1 of the VNA. The receiver is in XZ plane and connected to port 2.

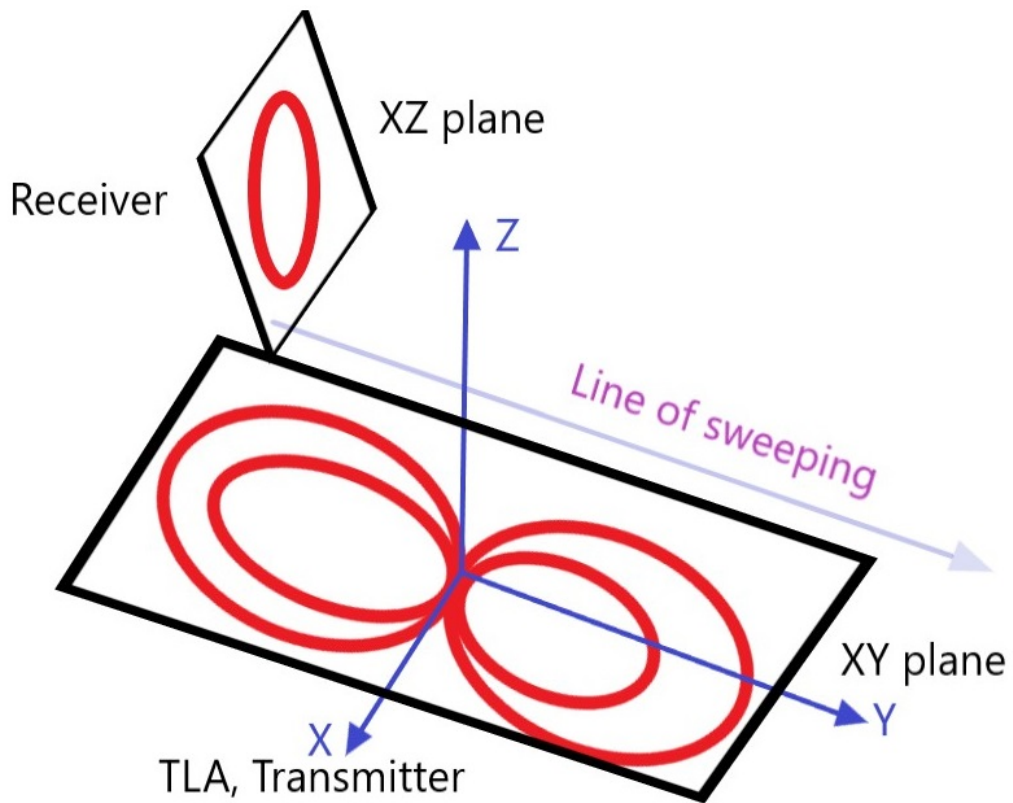


Figure 2.62: The geometry of the setup shown in Fig. 2.61 is given here in schematics to make it easier to see the different components of the set up measurement.

CHAPTER 2. A RECONFIGURABLE ANTENNA FOR ENHANCING THE MAGNETIC COUPLING IN IPT AND RFID

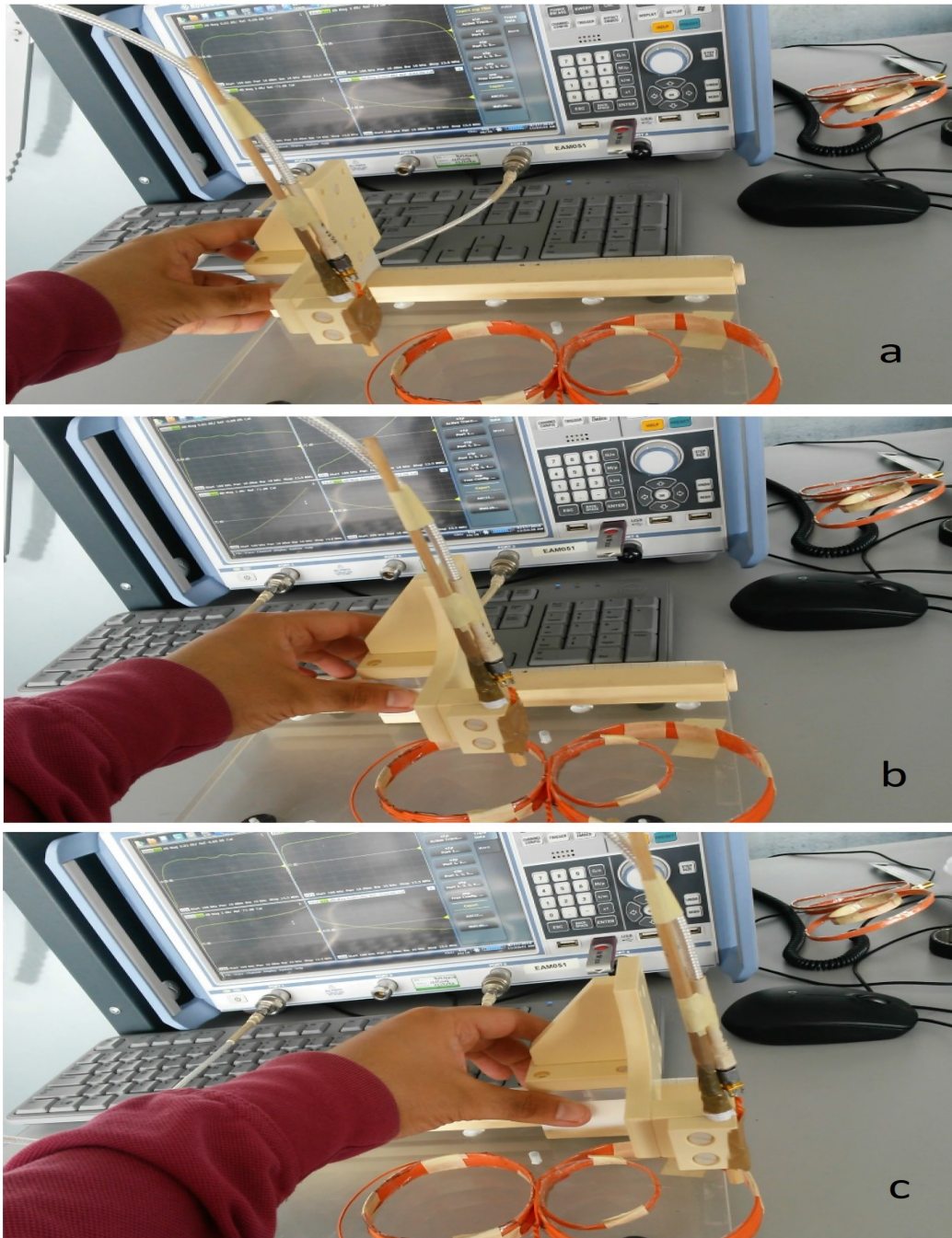


Figure 2.63: Sweeping the receiver along Y axis, we move the receiver while keeping its orientation and X and Z coordinates fixed, step by step along the Y axis. In each step the new measurement is done and the value of mutual inductance between the transmitter and the receiver being at that particular position is measured. a) $y=8$ cm. b) $y=0$ cm. c) $y=-8$ cm.

The red curve shows the mutual inductance due to the first structure of the TLAs, which

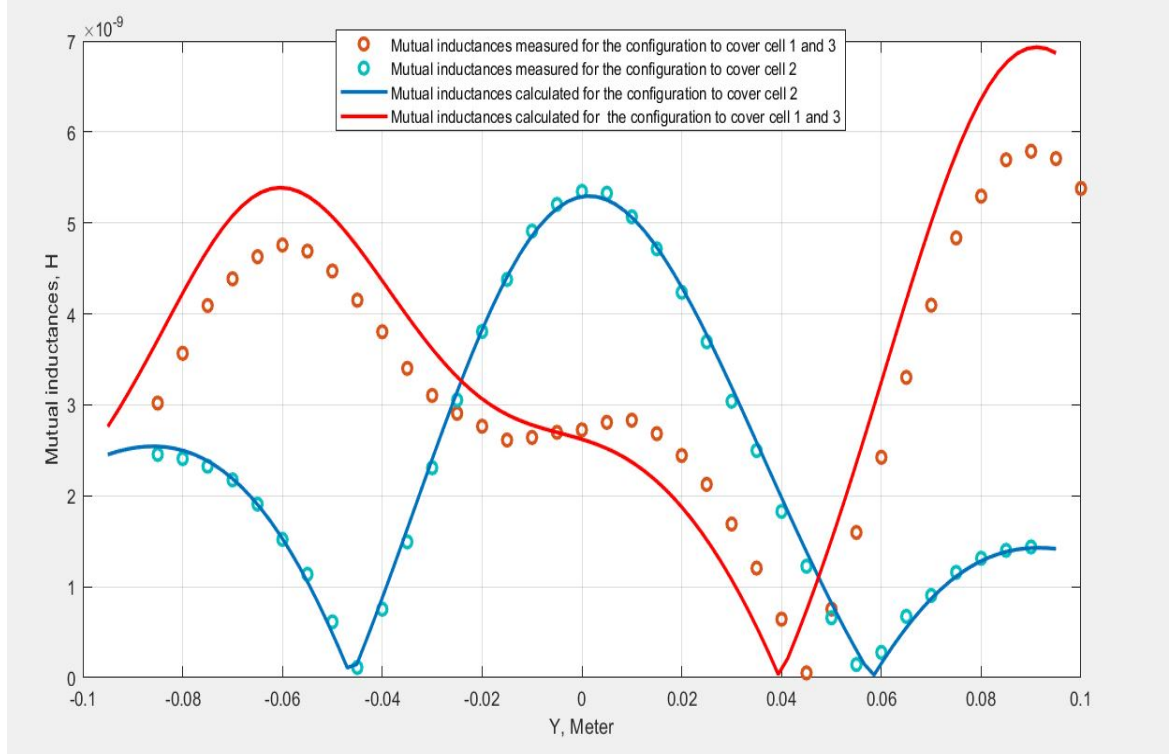


Figure 2.64: The results of sweeping the receiver along Y axis, while keeping the orientation and X and Z coordinates of the receiver center fixed. The red curve shows the mutual inductance due to the first structure of the TLAs, which covers the cell 1 and cell 3, and the blue curve is the mutual inductance due to the second structure of the TLAs, which covers the cell 2.

covers the cell 1 and cell 3, and the blue curve is the mutual inductance due to the second structure of the TLAs, which covers the cell 2.

For the first case, we have an average difference between calculated and measured values of 13%, and for the second case, it is 1%. The better agreement between measured results and calculated values for second structure in comparison to the first structure are probably due to second structure being better fabricated in term of better resemblance with the simulated structure.

Though the self inductance of the TLA in its different configurations is not very relevant to our mechanism, for the sake of completeness we are including them in the Table 2.6.

We said earlier that the mutual inductance profile between the receiver and any transmitter has an acceptable value in some points and very low value in other points. The points in which we do not have sufficient mutual inductance reduce the efficiency of the system.

On other hand when the parameters of our transmitter structure do not change, the mutual inductance profile of that structure also does not change. For changing the mutual inductance profile we should change the parameters of our structure. Changing these parameters will change the magnetic field produced by the TLA, and it is this changed magnetic field

CHAPTER 2. A RECONFIGURABLE ANTENNA FOR ENHANCING THE MAGNETIC COUPLING IN IPT AND RFID

Structure (covering cell)	Self-inductances
First structure (1, 3)	24.0 uH
Second structure (2)	15.0 uH

Table 2.3: The self inductance of the TLA in its different configurations.

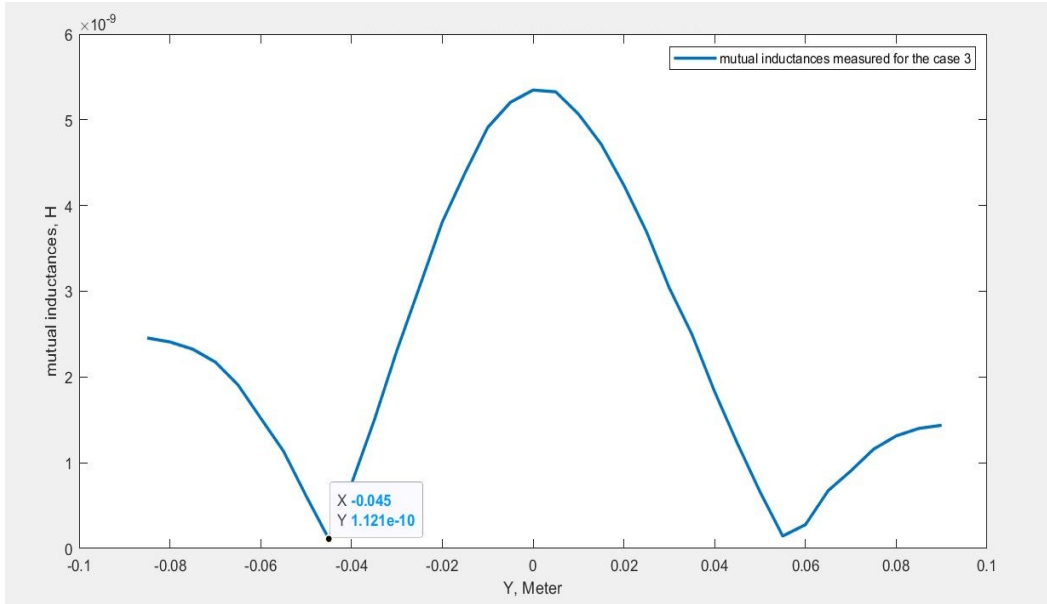


Figure 2.65: The mutual inductance at the point $y=-0.045$ for the first configuration of the TLA is too low, it means if happened that the receiver was in this point and its orientation lays in XZ plane it would not receive any energy.

that will change the mutual inductances. To enhance the performance of the system, the idea here was to change the parameter of our TLA in a way to change its mutual inductance profile in certain steps to ensure that all the points with low mutual inductance in certain configuration of TLA will have a good mutual inductance in the other configuration.

To see this in our simulation and measurement, consider the mutual inductance at the point $Y=-0.045$ is too low, it means if happened that the receiver was in this point and its orientation lays in XZ plane it would not receive any energy. It is shown in Fig2.65. At this point the mutual inductance is 0.1 nH.

We will change the parameters of our TLA structure in a way to increase the mutual inductance at the mentioned point. It is shown in Fig2.66. At this point the mutual inductance is 4 nH.

We can see the mutual inductance at the point $y=-0.045$ (just an arbitrary point chosen for sake of demonstration) got increased considerably (by the factor of 30), it means if happened that the receiver was in this point it would receive reasonable energy.

This process should be done quickly for the receiver to receive stable power. Hence for being practical these parameters should be parameters that are changeable electronically. The parameters of TLA that we could change by using electronics circuits are the current in

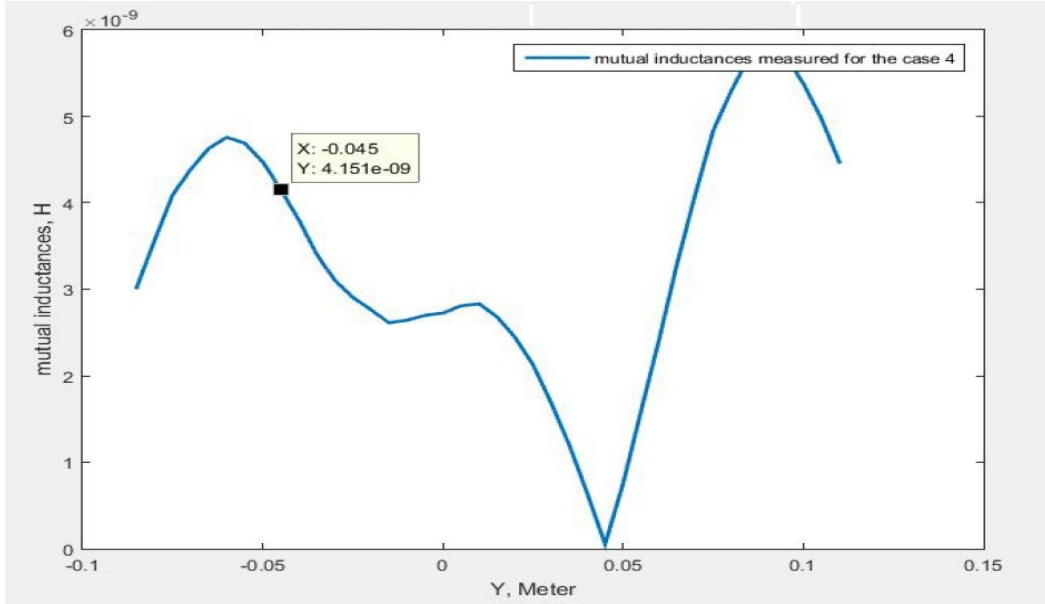


Figure 2.66: The mutual inductance at the point $y=-0.045$ for the second configuration of the TLA is 4 nH. We can see the mutual inductance at this point got increased considerably, it means if now it happened that the receiver was in this point it would receive sufficient energy.

each loop (could be done by changing the number of turns in each loop using switches) and the direction of the current in the loops (which again could be done using switches) other parameters (like the radius of each TLA, and their physical positions are not changeable electronically).

To summarize, the TLAs could be considered as an array of coils and different combinations of these coils create different structures which in its turn create different magnetic field patterns around the TLA. When a magnetic field of certain strength in certain direction is required, this could be done by choosing correct configuration of the TLA. This works essentially because field due to each coils add to the fields of other coils in a liner way. In some locations in the space around the TLA, they cancel each other and in other location they enhance each other. Manipulating fields by having more than one antenna (in our case transmitter) is very well known method for far-field system (like array of antenna). However, in far field most of the time the interest is in electric field rather than magnetic field. Here we applied this method to near-fields and magnetic fields. The same method could be used to increase the range of wireless power transfer. We followed a new approach and proposed an application of this principle, namely a system which guarantees power transfer regardless of misalignment between sender and receiver. The measurement showed agreement between calculation and the measured values for the mutual inductances, which confirms the feasibility of the method. This system could be more developed to obtain the ability to localize the position of the receiver coil by monitoring how the input impedance of the sender changes in each step.

Chapter 3

A RECONFIGURABLE COIL GRID FOR RECEIVER LOCALIZATION IN INDUCTIVE POWER TRANSFER

3.1 INTRODUCTION

The main subject which was discussed in the previous chapter was the realization of free positioning inductive power transfer system. We talked about a system which does not have any requirement on the receiver position and orientation, as long as the receiver is in a pre-given well defined volume, which we called volume of interest.

There we saw that one possible solution is to sweep along a set of configurations of a reconfigurable transmitting coil that will eliminate the null areas in the volume of interest. This solution is relevant when there is possibility of several receivers, in IPT - WPT or tags in RFID at the same time in the volume of interest. However if there are few of them or even just one of them (for example for wireless charging of robots, cars, drones,...) though the method still should work, but it does not seem to be a very efficient approach. The reason is that the effective mutual inductance the receiver coil has in the method of chapter two is the average of mutual inductances the receiver coil have in each step. This happens because if in one step we have a magnetic field which creates suitable mutual inductance for the receiver, that magnetic field will change in the next step and in this new step the magnetic field is not necessarily suitable any more and the receiver should wait till the repetition of the configuration that generates suitable magnetic field. If there is a few receivers or just even one receiver, it is not any more an efficient way.

One better possible solution is to have some kind of localization.

When the localization is done, the magnetic field could be steered in a way which is optimal for the particular position and the orientation of the receiver.

Though we here mentioned localization as a method for enhancing magnetic coupling, the



Figure 3.1: Multiple transmitter coils over which a device or devices can be placed freely as long as the device or devices are in the volume of interest (Image via <https://makezens.com/liberty-series/>)

ability of localization by itself is an interesting subject to be considered.

In Qi standards for wireless power transfer that we mentioned earlier the localization is performed by using a coil array. In the Qi standard the basic mechanism of localization is based on the coil array structure. A commercially available example is shown in Fig. 3.1. The system shown allows the users to place one or more portable electronic devices on the charging surface regardless of their positions. This freedom of positioning (as long as it is in the volume of interest) is achieved by having multiple transmitter coils over each other and any of them could be energized independently from others. The controlling circuitry of this wireless power transfer charging system then detects which coil (or coils) is best suited for the power transfer and then apply electric current only to it. It is also possible to apply electric current to multiple coils at the same time if there is more than one receiver.

The localization is performed by detecting which single coil or coils are more affected by the presence of the receiver due to the reflected impedance. In general, the receiver (or the tag in RFID case) causes higher reflected impedances in the transmitter coil which is closer to it than other coils of transmitter. Then the location of the coil with higher reflected impedance is used to estimate the location of receiver. Then power transfer is performed by exciting the coil or coils close to the receiver.

To understand this mechanism better and to see its advantages and drawbacks it is necessary to investigate reflected impedance concept.

We start by modelling the receiver-transmitter system as shown in Fig. 3.2. Again we assume here that we are working in low-frequency regime so the Quasi-static approximation is valid.

When we measure the impedance of the uncoupled transmitter, we will have (in frequency domain):

$$V_s = R_1 I_1 + j\omega L_1 I_1 \quad (3.1)$$

That means the impedance seen from voltage source is:

$$Z_{11} = \frac{V_s}{I_1} = R_1 + j\omega L_1 \quad (3.2)$$

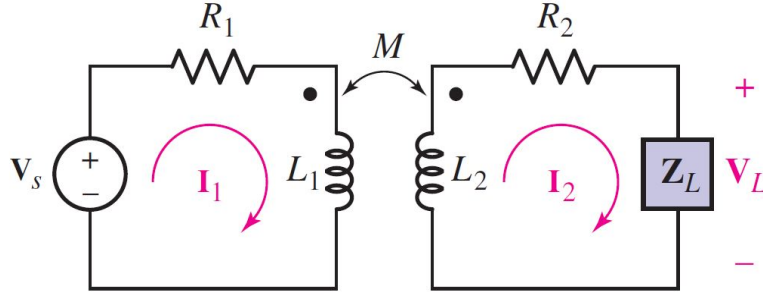


Figure 3.2: Electric circuit model of a receiver-transmitter system. L_1 and L_2 are the self inductances of the transmitter and the receiver. R_1 and R_2 are the internal resistances of the transmitter and the receiver. Z_L is the load connected to the receiver and V_s is the voltage source and V_L is the voltage across the load Z_L . M is the mutual inductance between the transmitter and receiver.

Z_{11} is the impedance of uncoupled transmitter.

Now if we take the mutual magnetic coupling in the Fig. 3.2 we will have:

$$V_s = I_1 R_1 + I_1 j\omega L_1 - I_2 j\omega M \quad (3.3)$$

$$0 = -j\omega M I_1 + (R_2 + j\omega L_2 + Z_L) I_2 \quad (3.4)$$

If we now simplify by substituting for Z_{11} and defining Z_{22} to be:

$$Z_{22} = R_2 + j\omega L_2 + Z_L \quad (3.5)$$

we get:

$$V_s = Z_{11} I_1 - j\omega M I_2 \quad (3.6)$$

$$0 = -j\omega M I_1 + Z_{22} I_2 \quad (3.7)$$

The input impedance of the transmitter is the ratio of the voltage applied to it to the current it drives from voltage source, $Z_{in} = \frac{V_s}{I_1}$, if we solve equations 3.6 and 3.7 for getting this ratio we get:

$$Z_{in} = \frac{V_s}{I_1} = Z_{11} - \frac{(j\omega)^2 M^2}{Z_{22}} \quad (3.8)$$

We note in equation 3.8 that the input impedance Z_{in} is simply Z_{11} (as we expect) if the M is zero, which is the case for uncoupled transmitter-receiver. As the coupling is increased from zero to another value, the input impedance differs from Z_{11} proportional to the squared of M . The constant of proportionality as we can see from equation 3.8 is $\frac{(j\omega)^2}{Z_{22}}$.

It is this term $\frac{(j\omega)^2 M^2}{Z_{22}}$, the difference in input impedance between uncoupled transmitter and coupled transmitter that we call reflected impedance.

To make connection between the reflected impedance and the localization one just should remember that mutual inductance itself is a consequence of relative position between transmitter and receiver. This means if we have two transmitters and the receiver happened to be closer to one of them, the mutual inductance between the receiver and the closer transmitter will be bigger than the inductance between the receiver and the other transmitter.

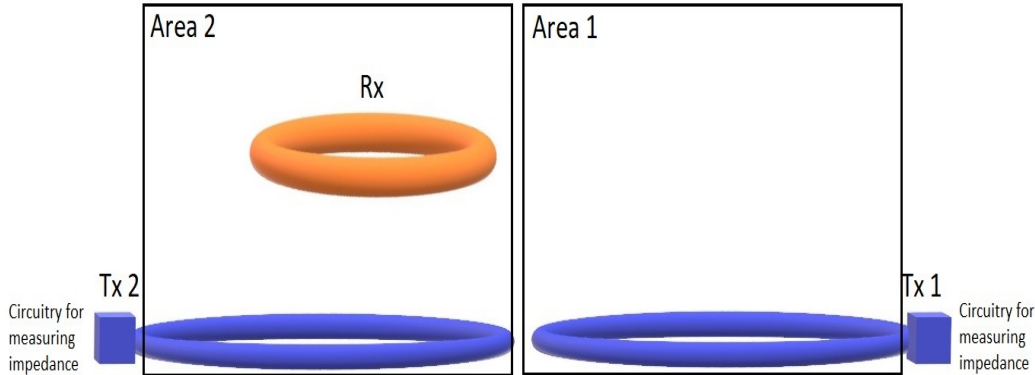


Figure 3.3: When there is two transmitters for example, and the receiver is closer to one of them, the reflected impedance will be higher in the transmitter closer to the receiver. By measuring the input impedance of each transmitter it is possible to deduce which transmitter is closer to the receiver. Then one conclude if the receiver is in area 1 or area 2, shown here by block boxes.

This means the closer transmitter will undergo higher deviation in its input impedance due to the its reflected impedance.

By turning this logic in reverse, if we have two transmitters and a receiver, if the input impedance of one transmitter changes more than the other, we could conclude that the receiver is closer to the transmitter with higher reflected impedance.

As one can see from Fig.3.3 this method essentially divides the volume of interest in numbers of areas, each area is corresponding to one transmitter coil. Then from known location of each transmitter coil the location of the receiver coil is deduced.

This method of localization in which instead of precise location of receiver, its approximate to a reference transmitter is evaluated, are called pseudo-localization method. Though we here just mentioned the Qi standard of industry and its mechanism based on reflected impedances, in recent years different methods in the same frame work of coils grid and reflected impedance have been proposed to enhance the accuracy of localization.

For example, in [45] the proposed system will choose a coil from the TX coil matrix as the signal emitting antenna and it will choose another coil beside as the receiving antenna. Whenever the RX coil is closed to a signal antenna, the receiving antenna will return a signal that is determined by the relative position between the RX and TX coils.

In [4] another method for localization in near field suitable for movable transmitter is proposed. This method depends on fixed reference receivers placed in known positions (or reference tags in RFID case). In RFID application of this method the transmitter reads the closest tags and from the data base containing the position of each tag, the position of the transmitter is deduced.

In [5] for increasing the accuracy of localization of a movable reader, it proposes a new design of transmitter antenna that divides the reading area of the transmitter into several parts. Other enhancement techniques for localization were proposed in [19], [61].

All these approaches (if we exclude the reference tags with known position) could be under-

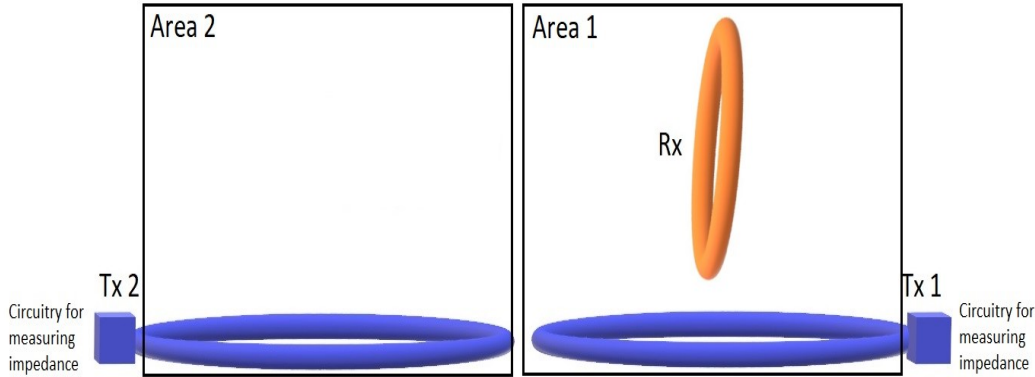


Figure 3.4: A situation which will lead to wrong localization if we follow the Qi standard naively. Due to the orientation of the receiver, though the receiver is closer to the Tx1, it will have higher mutual inductance with Tx2 (we discussed the reason in the previous chapter). In this case the Qi standard will conclude that the receiver is in area 2.

stood as some sort of variations on main method of Qi standard we explained earlier, and all of them have the same drawbacks. Here we mention three of such disadvantages.

1. It is true that in general the mutual inductance between a receiver and two (or more) transmitters is higher between a receiver and the closest transmitter to it, but it is not always the case.

To see this we should remember that the mutual inductance is not only a result of relative positions of transmitter and receiver, but it is also effected by the relative orientation between transmitter and receiver. Fig. 3.4 shows a situation which will lead to wrong localization if we follow the Qi standard naively. However Qi standard is aware of this disadvantage, and that is why Qi standard (like the charging panel in Fig. 3.1) requires also that the receiver should always be placed (by the users) in horizontal orientation to avoid this problem.

The conclusion is that though there is no constrain on the position of the receiver as long as it is in the volume of interest, there is a constrain on the orientation of the receiver.

This is not a problem for charging pad (because the user could make sure that this is the case by placing the receiver in a correct way) but this constrain make this method not very suitable for other applications in which one doesn't have complete control on the orientation of the receiver.

2. The resolution of these methods is equal to the diameter of coils constituting the array of transmitters. So, it is possible to increase the accuracy of localization by reducing the diameter of the transmitter coils. However, it is known that the effective power transfer takes place within the separation between transmitter and receiver which is not larger than the diameter of the transmitter coil. Therefore, decreasing the diameter of each coil although increases the resolution of localization but also reduces the range of effective power transfer. So, there is a trade-off between resolution of localization and maximum permitted distance between transmitter and receiver. In RFID applications for localization, this problem shows

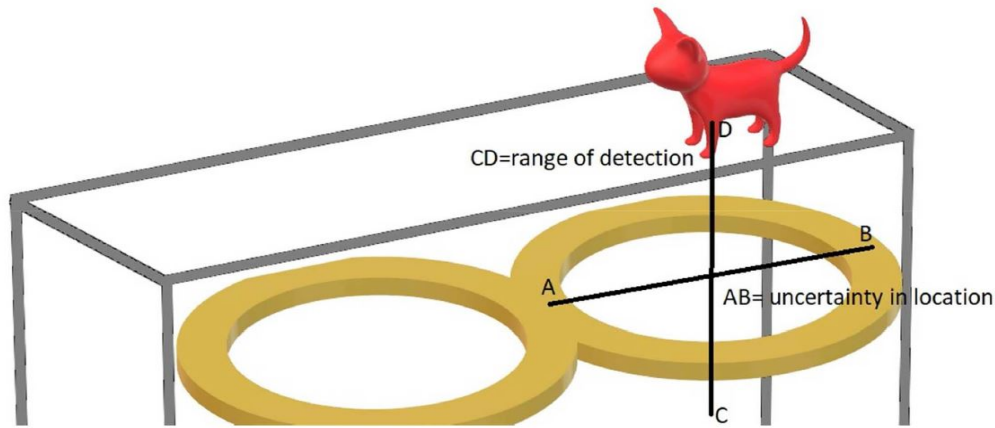


Figure 3.5: Range of detection is approximately equal to the inaccuracy in location. If the current method is applied in natural habitat of animals, one should increase the diameter of transmitter coil and that will increase the inaccuracy in the detection of the animal position.

up as a trade-off between resolution of localization and read range.

To give an example, consider using this method with inductive RFID for indoor tracking of small animals [10]. In such cases, a grid of transmitter antenna is placed directly underneath the cage of the small animal to be studied. However, if one wants to apply this set-up to free living animals, it is not always possible to place the transmitter coils close enough below the animals. It is then desirable to increase the range of detection above the transmitter coil. One option is to increase the diameter of the transmitter coil. But the above-mentioned trade-off between accuracy and range of detection will show up again.

Fig. 3.5 illustrates an example of this problem. The line segment CD shows the distance between the transmitter coil and the tag carried by the animal. As it was mentioned earlier, increasing the range of detection in RFID requires increasing the diameter of the transmitter coil, represented by the line segment AB in Fig. 3.5, to be equal to the line segment CD. In this example when the tag is detected by the transmitter, it can be anywhere along AB line segment and it is not possible to determine the location of the tag with a higher accuracy.

3. The third problem is not a problem but more a property of the earlier proposed solutions for overcoming what we mentioned in point 1 and point 2. The earlier proposed solutions involve additional complementary devices to be added to the system which increases the complexity and cost of the transmitter or the reader in RFID case. For example, for the method used in [4], to increase the accuracy of localization of movable reader it is necessary to increase the number of reference tags and use a denser grid of reference tags.

In this chapter a new solution is proposed to address these problems and associated issues. Namely we propose a method that:

1. Eliminates the false localization we mentioned earlier (the problem illustrated in Fig. 3.4). In other word we do not have as a requirement that the receiver should be in horizontal orientation in respect to the transmitter coils.
2. Makes it possible to modify the resolution and the distance of operation independently and achieve better localization accuracy (the problem shown in Fig. 3.5).
3. We offer to do so not by adding additional complementary devices (for example by in-

creasing the required coils or reference tags) but rather by proposing a new algorithm based on a data base stored in the memory of the control module of the transmitter. In other word instead of increasing the hardware complexity we increase the software complexity, which in most cases is more convenient and flexible.

Table 3.1 shows a brief comparison between the method proposed in this work and other methods proposed in the state of the art that try to enhance the localization in the framework of Qi standards.

After localization is done then, it is possible to use the obtained information about the location of the receiver to solve the classic problem of coils misalignment.

Indeed, the transmitter antenna is excited in a way that generates a magnetic field which can guarantee that the receiver is not in the null detection area. So, the proposed system is a reconfigurable transmitter antenna that localizes the receiver and then enhances the power transfer performance by beam steering according to the detected position and orientation of the receiver.

This method could be useful for example in applications such as charging table or the detection and data exchange with medical implants (in-body). All the calculations, simulations and the algorithm in this work were performed in MATLAB software. Furthermore, experimentations are presented to validate the proposed method.

In the next sections we will discuss a multi coils antenna as a tool for localization, after showing the experimental validation of the developed method, we end by using the results of localization in beam forming for WPT enhancement.

CHAPTER 3. A RECONFIGURABLE COIL GRID FOR RECEIVER LOCALIZATION
IN INDUCTIVE POWER TRANSFER

COMPARATIVE STUDY OF DIFFERENT LOCALIZATION TECHNIQUES IN NEAR FIELD RFID AND WPT					
METHOD/WORK	ADVANTAGE	DISADAVANTAGE	FREQUENCY BAND	PARAMETERS OF TX AND RX	ERROR
Magnetic attraction (Qi standard)	Low cost	Unable to localize	-	-	-
Movable primary coil (Qi standard)	Efficient power transfer	Mechanically moving parts high cost	-	-	-
Jianchao Li [45]	No need for reference tags	Range of detection decrease by increasing the accuracy of localization, not suitable for small size RX	HF	TX= 7 turns spiral coils Inner radius of TX = 10 mm, Outer radius of TX = 50 mm RX= 7 turns spiral coils Inner radius of RX = 80 mm, Outer radius of RX = 120 mm	1.22 cm
M. Y. Ahmad [4]	Suitable for tracking movable reader	Need for reference tags. Increasing accuracy of detection needs more tag	HF	TX= triangular-loop-bridge reader using multiple triangular loops RX= standard commercially available passive tags	4.05 cm
D. Fortin-Simard [19]	No need for reference tags	Without modification could not address of three-dimensional localization	HF	TX= commercially available reader A-PATCH-0025 RX= standard commercially available passive tags	14.1 cm
Lei Yang [67]	Suitable for tracking movable reader	Need for reference tags	HF	TX= commercially available reader RX= standard commercially available passive tags	18.6 cm
Proposed solution	Range of detection is independent of accuracy of localization. no need for reference tags.	Needs higher memory	LF	TX= 6 turns coil of radius 3.3 cm. RX=1 turn coil of radius 1 cm	4 mm

Table 3.1: ERROR is the maximum difference between the actual position of RX and the determined position of RX.

3.2 RECONFIGURABLE TRANSMITTER MULTI-COILS ANTENNA

Before we explain our method we should talk about the antenna structure and the hardware that makes the implementation of our method possible.

To do the localization and the power transfer we propose a 2D grid of coils. Where we say it is a 2D structure we mean that the height of the antenna structure is negligible to its other dimensions. This will be something like the mat shown in the Fig. 3.1. Though the method we are going to explain is general and the antenna structure really does not need to be a 2D structure, a 2D structure is much more convenient in practice, at least in many applications. It is not bulky and it could be regarded as a thin sheet which could be easily placed where ever it is required to be placed (underneath a table, behind the walls,...).

This 2D structure is in fact a grid of a coils all of them laying in the same plane. We call it a reconfigurable antenna because all coils have switches connected to them and these switches make it possible to either connect or disconnect each coil from the whole structure of the transmitter, or inverting the current direction in each coil. It means in one instance of time one could by turning off all the switches except one switch, turn off all the coils except one and thus transform the whole structure in just one coil. We could do this for any coil separately. Of course we could have two or any other number of coils as we wish at the same time. When just one coil (or any number of desired coils) is turned on, other coils are just sitting there as open circuits and they don't play any role (which means there is no coupling between them and other transmitter coils or receiver coil)

Though the transmitter coils could be of any shape, we here chose our transmitter to be a grid of circular coils. The number of circular coils and their diameter and the number of turns of each coil depend on the volume of interest. As we said earlier the volume of interest is the region of space that we assume that the receiver is located somewhere in it and the power transfer (in WPT) or the detection (in the RFID) case, takes place inside this volume of interest. The volume of interest is depending on the particular application and varies from one application to another. What is important for us is this: the volume of interest should be pre given, and it should be guaranteed that the receiver is indeed inside this volume of interest. Determining the volume of interest should not be a problem, when we have a practical application on our hands.

The number of circular coils and their diameter and the number of turns of each coil beside its dependency on volume of interest, also depends on the sensitivity of devices we use for measuring Z parameters of the transmitter-receiver system. In fact as we explain later it is these measured Z parameters that will be used to deduce the coupling coefficient (k) between receiver and transmitter.

This (k) will then be used for localization. To ensure that the coupling coefficient (k) is not too small to be measured, the number and the diameter of each coil should be chosen in a way that regardless of the position of the receiver in the volume of interest, there is always a number of transmitter coils that are close enough to the receiver to have mutual inductance strong enough to be measured.

In this chapter we chose the volume of interest to be a box of the dimensions: $x = 20$ cm, $y = 20$ cm and $z = 10$ cm. The volume of interest in this study is chosen arbitrary just to validate the idea. The transmitter antenna which we said is a grid of circular coils is placed underneath the volume on interest.

To make sure that regardless of the position of the receiver in the volume of interest, there is a number of transmitter coils close to it, a grid of coils consisting of 9 coils of radius 3.3

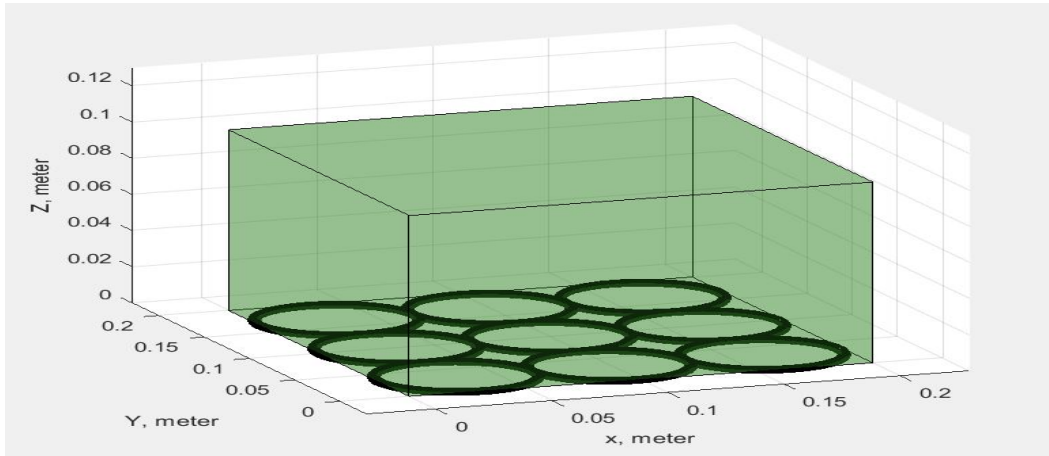


Figure 3.6: A diagram of the grid of coils that we use as a transmitter underneath the volume of interest (or the transmitter is placed at $Z < 0$). The green box is the volume of interest. The black circles are the coils of the transmitter. The switches between coils allow connecting or disconnecting each coil of the transmitter.

cm and each one of 6 turns, is chosen as transmitter antenna.

Fig. 3.6 shows a diagram of this grid of coils that we use as a transmitter underneath the volume of interest (the real transmitter is shown in the Fig. 3.17).

The green box is the volume of interest. It means that the receiver (if there is any receiver) is somewhere inside this box and its position has to be determined.

The black circles are the coils of the transmitter. The switches between coils (are not shown in the Fig. 3.6) allow connecting or disconnecting each coil of the transmitter, in a very similar way to what we explained in previous chapter for changing the configuration of TLAs. When these switches are selected in a way that particular coils are turned on and other coils are turned off, we say that we have chosen a certain configuration. By saying the coil is turned on we mean that it is connected to the power source and there is a current passing through it. In contrast when a coil is off it is not connected to the power source. Each possible combination of on and off coils, we will refer to as one configuration (or one structure).

Fig. 3.7 shows one possible configuration which is made of only one coil. In this configuration the switches are selected in a way that disconnect all the coils (shown in black colour) except for one coil, shown in red colour.

Of course the configuration of the transmitter does not have to consist of one coil, the Fig. 3.8 shows a configuration consisting of three active coils (shown in red) and others are turned off. However in our method we will use configurations made of one active coil for localization and configurations made of more than one active coil for field steering.

The switching is done by a circuitry connected to the transmitter. This is why we call the transmitter a reconfigurable transmitter.

At the end, one should mention that the size of the volume of interest we chose might look small, but it is in fact completely rescale-able. If one is interested in bigger volume of interest suitable for specific application, one just has to increase the dimension of all the components by the same scale. This is so because we are working in near field and in

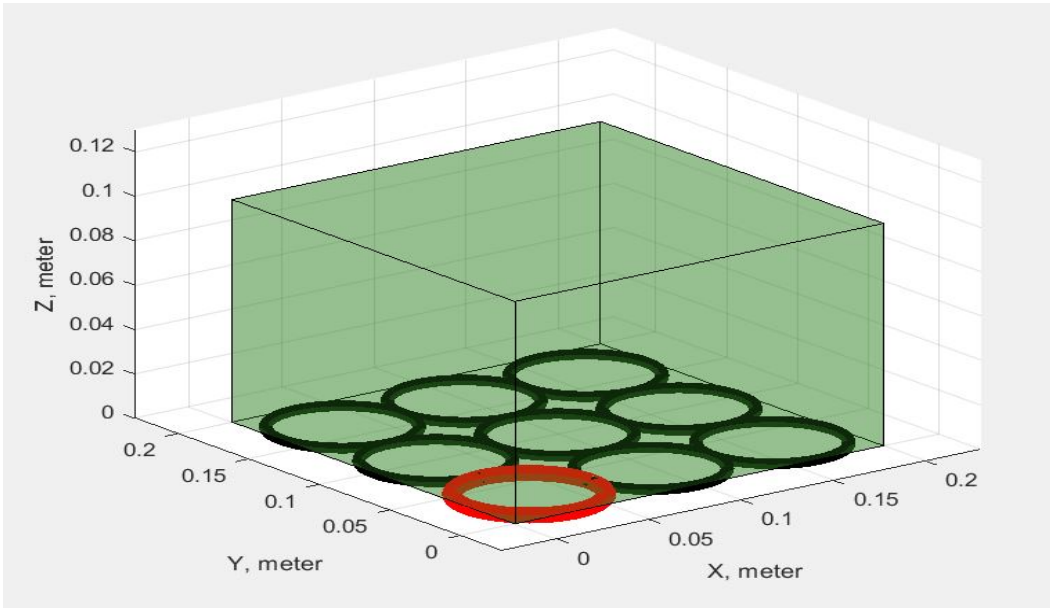


Figure 3.7: One possible configuration which is made of only one coil. In this configuration the switches are selected in a way that disconnect all the coils (shown in black color) except for one coil, shown in red color. In our method we will use configurations like this which are made of one active coil for localization.

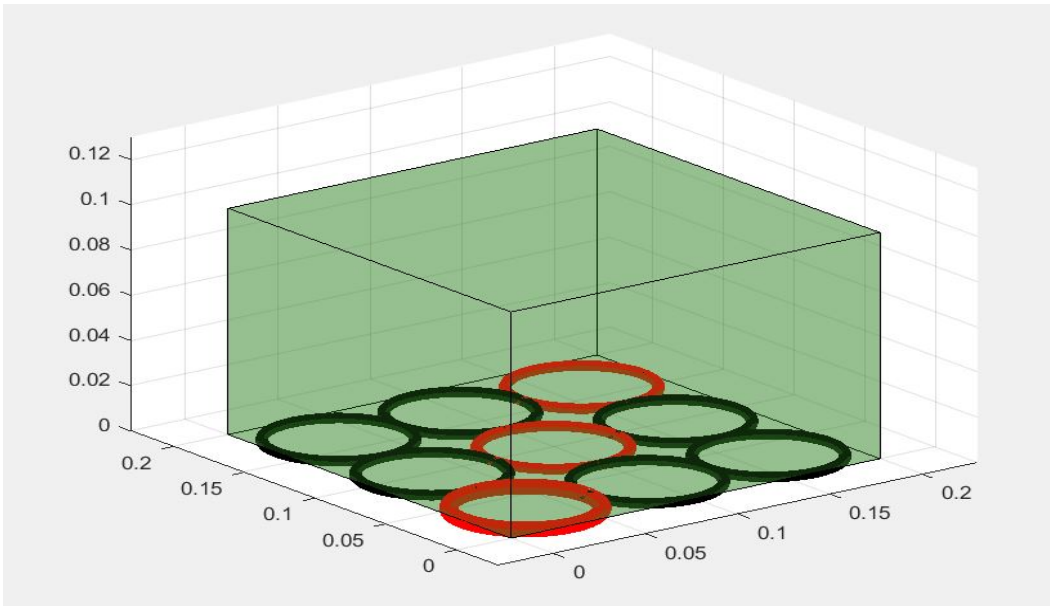


Figure 3.8: Another possible configuration which is consisting of three active coils (shown in red) and other coils are turned of (shown in black). In our method we will use configurations like this which are made of more than one active coil for field steering.

quasi-static approximation, in which the wavelength of the signal does not play any role.

3.3 LOCALIZATION METHOD IN NEAR FIELD

To do localization one should search for parameters that are affected by the relative position and the relative orientation between the transmitter and the receiver. When we have such parameters it might be possible by measuring them, working out in a reverse way the relative locations and the orientation of the transmitter and the receiver.

Another important feature that we would like is that these parameters should be accessible from inside the system. This means that these parameters should be a part of the mechanism of wireless power transfer (or RFID), and not some other added features to the system. For example it is possible to put a camera which detects the position of the receiver. We are not interested in this kind of solutions (that are in principle possible but which increase the complexity, size and the price of the system) instead we are interested in solutions that take benefit of the mechanism of the wireless power transfer (or RFID) itself.

The main parameter that plays a very important role in the wireless power transfer is the mutual inductance. It is this parameter that determine the efficiency of the system. In the previous chapter we saw that one property of this mutual inductance is to be a function of the relative position and the relative orientation between the transmitter and the receiver. We also recognized this property as a problem that could give rise to what we called null areas. However this property of mutual inductance provides us with what we are searching for. Namely a parameter that depends on the the relative position of transmitter and the receiver (so we could use it as an equivalent sensor for localization) and at the same time being a part of the main mechanism of the wireless power transfer (so we could perform localization without adding much to the complexity and the cost of the system).

We start by the observation that the mutual inductance between the transmitter and the receiver is a function of:

1. The geometry and size of transmitter.
2. The geometry and size of receiver.
3. The relative position and the relative orientation of transmitter and the receiver.

If we assume that the geometry and the size of the transmitter and the receiver are fixed and don't change (which is for many applications, a reasonable assumption) the mutual inductance is just a function of the relative position and the relative orientation of transmitter and the receiver. This suggests that if we could, somehow, measure the mutual inductance between the transmitter and the receiver (M), we should be able to deduce the location and the orientation of the receiver in respect to transmitter.

From now on, when we talk about the receiver, we have in our mind a circular planar receiver (which is very common in the industry).

By the location of the receiver we mean the location of the center of this circular coil.

When we talk about the orientation of the receiver we talk about the angle between the vector perpendicular to the transmitter and the vector perpendicular to the receiver. We will chose to put our transmitter on the XY plane and this means the vector perpendicular to the transmitter will be in the direction of the Z axis. This choice, will make the orientation of the receiver, the orientation of the vector perpendicular to the receiver with the Z axis. This is the well known spherical coordinates that we use to specify the orientation of the receiver. Fig.3.9 shows these parameters.

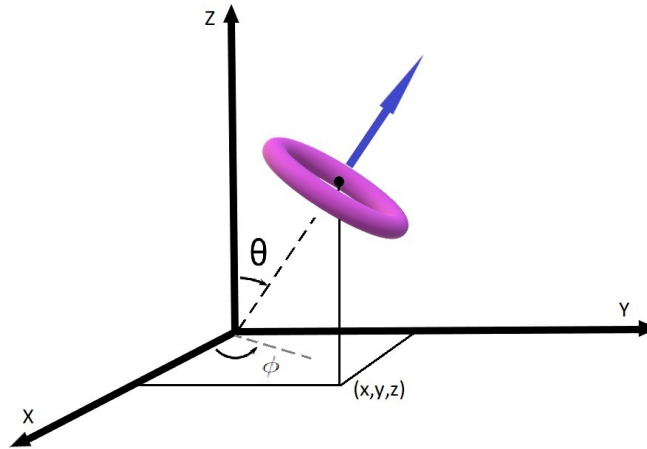


Figure 3.9: The location of the receiver (the purple coil) is the location of the center of the circular receiver coil, shown in black dot and specified by (x, y, z) coordinates. The orientation of the circular receiver coil is the orientation of a vector perpendicular to the circular receiver coil (the blue arrow) and specified by (θ, ϕ) coordinates. This means the complete localization is finding out these five variables.

Our first step will be this: we calculate the mutual inductance between the transmitter and the receiver, for any possible location of the receiver (as long as it is in the volume of interest) and for any possible orientation of the receiver.

We will call this the pre-calculated matrix. It assigns to any of possible combinations of the locations and the orientations of the receiver, a certain value of mutual inductance. Then when the mutual inductance between receiver and the transmitter is measured, one could compare this measured value of mutual inductance to the pre-calculated matrix of mutual inductances to determine which location(s) and orientation(s) of the receiver could possibly lead to the measured value of the mutual inductance.

Calculating and visualizing this pre-calculated matrix pose two problem.

1. To show this pre-calculated matrix in its complete form, one should imagine a five dimension space. Each axes of this five dimensions space will represent one of the five variables that specify the position and the orientation of the receiver (the variable shown in the Fig. 3.9).

To each point in this five dimensional space, a value will be assigned that represents the mutual inductance if the receiver had the position and the orientation specified by that point in the five dimensional space.

For example the point $(X1, Y1, Z1, \theta1, \phi1)$ in this five dimensional space, will have the value $M1$ which means if the receiver is located in point with coordinate $X1, Y1$ and $Z1$, and if the receiver has the orientation specified by $\theta1$ and $\phi1$, the mutual inductance between the receiver and the transmitter is $M1$. The same thing for the point $(X2, Y2, Z2, \theta2, \phi2)$ will have the value $M2$ and so on.

Though it is easy to realize the mutual inductance being as a function of five variables, it is not easy to visualize this dependency on five variables, because it needs a five dimensional space. In Fig. 3.10 we attempt to do so.

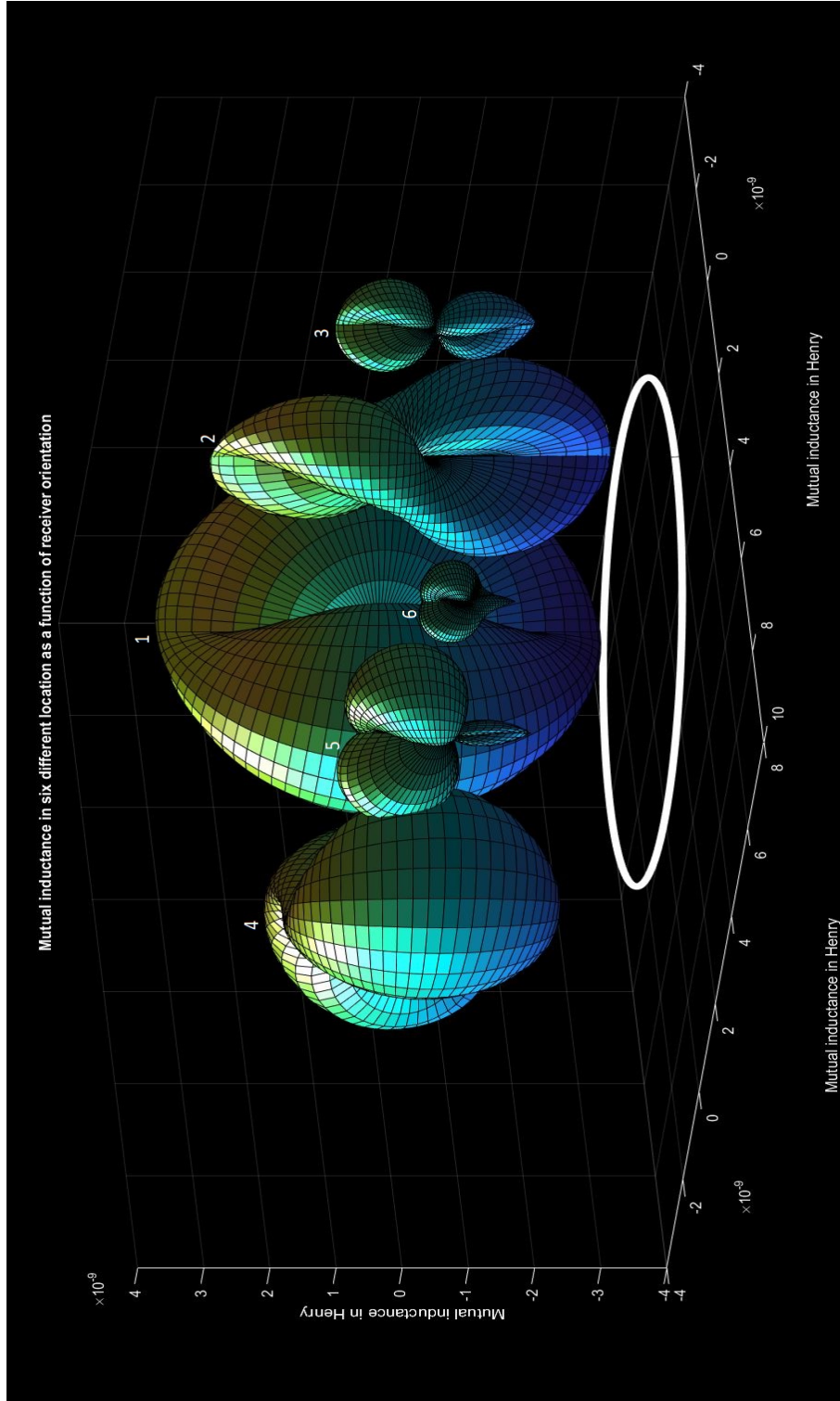


Figure 3.10: In this example the Transmitter is a circular coil of radius of 3.3 cm with one turn. We put the receiver which is a circular coil of radius of 1 cm with one turn in six different locations. To show these locations relative to the transmitter, the transmitter is shown in white circle. Each of these six locations is the center of each six spherical plots. If we assume the center of the transmitter is at $(x=0, y=0, z=0)$ cm, These locations are, 1: $(x=0, y=0, z=3)$ cm, 2: $(x=0, y=6, z=3)$, 4: $(x=4, y=0, z=3)$, 5: $(x=4, y=4, z=4)$ cm, 6: $(x=6, y=6, z=4)$ cm. The value of mutual inductance as a function of the location and orientation of the receiver is the radial distance from the center of each spherical plots to the surface shown for each orientation. To show the complete dependency of mutual inductance on location and orientation, one should imagine such spherical plots at all the points in space. The unit of the axes is in Henry. However the exact values of mutual inductance here is not important for us, we just want to show how it is a function of five variables.

In Fig.3.10 we have showed the value of mutual inductance in six different points. The Transmitter is a circular coil of radius of 3.3 cm consisting of one turn, and the receiver is a circular coil of radius of 1 cm consisting of one turn. The exact values of mutual inductance here are not important for us, we just want to show how it is a function of five variables. Each of these six points shown in Fig. 3.10 have certain X, Y and Z components which refer to the coordinates of the center of the receiver (the variable shown in the Fig. 3.9). The mutual inductance when the receiver is in a certain X, Y and Z coordinates also depends on the receiver orientation. This is shown in the Fig.3.10 by a spherical plot. The radial magnitude of this spherical plot (that is the length of a segment line connecting the center of the spherical plot to its surface) is the value of mutual inductance as a function of the orientation of the receiver when its center has the coordinates X, Y and Z. The orientation of the receiver is specified by the two angles ϕ and θ as shown in Fig. 3.9.

This difficulty of dealing with five dimensions function going to make the visualization of our method a little bit hard. To get around this problem we will assume that the receiver is always in a plane parallel to the transmitter and this orientation is not going to change. It makes the whole visualization possible and the whole process easier to perform. However it is not really a constraint and the algorithm that we are going to explain could be repeated easily without this constraint.

When we assume the orientation is fixed and there is no need to find it out (we don't have θ and ϕ as variables any more) our five dimensional space becomes a three dimensional space consisted only of X, Y and Z variables, each one denoted by one axis. Now each point in this three dimensional space corresponds directly to a point in the physical space.

2. The mutual inductance is a function of continuous variables (namely the X, Y and Z coordinates) which specify the location of the receiver. It means there are infinite points in the volume of interest for which the mutual inductance should be calculated. Instead we will divide the volume of interest in a set of discrete points distributed evenly in the volume of interest. We will calculate the mutual inductance between the receiver and the transmitter only for the cases in which the receiver is located at these points.

Going from continues three dimensional volume of interest to a discrete three dimensional volume of interest is justified by noticing that, the mutual inductance is a smooth function and it does not change very rapidly from point to point. This means that the value of mutual inductance in a certain point is more or less close to the values of mutual inductance in neighbouring points. This justify replacing the continues three dimensional volume of interest with a set of discrete points distributed in a three dimensional volume of interest.

From now we will call this set of discrete points distributed evenly in a three dimensional volume of interest as 3D grid of points.

The distance between the points of this 3D grid will be the limit of accuracy of the localization method. If we divide the volume of interest in a 3D grid consisting of points closer to each other the accuracy of localization will be higher. For this work as we said earlier the volume of interest is a box of the dimensions: X = 20 cm, Y = 20 cm and Z = 10 cm. Then we chose the spacing between the points of the 3D grid to be 1 mm along each axis, that means that we divide the volume of interest along X axis into 200 points, along Y axis into 200 point and along Z axis into 100 points. This will result in a 3D grid of (200*200*100) points, at any of which we will calculate the value of the mutual inductance. This will lead to the pre-calculated matrix of mutual inductance values that we talked about before.

Before we move on it should be mentioned that here we chose the distance between each point of the 3D grid of the pre-calculated mutual inductance matrix to be 1 mm just for the sake of demonstration. In practice this value should be chosen based on the required

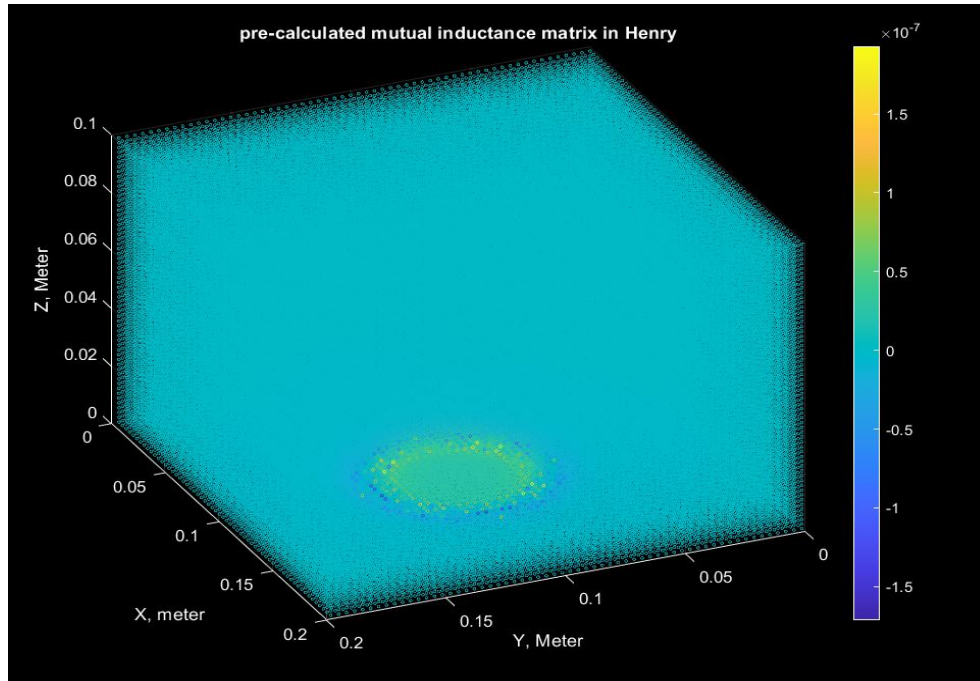


Figure 3.11: A visualization of a pre-calculated mutual inductance matrix in which the transmitter is a circular coil of 3.3 cm radius with 6 turns and the receiver is a circular coil of 1 cm radius with 1 turn. The transmitter coil is centred at $X=10$ cm, $Y=10$ cm and $Z=0$ cm. This is one of the coils of our grid of coils shown in Fig.3.6. The pre-calculated mutual inductance matrix shows the mutual inductance between the transmitter and the receiver as a function of location in the volume of interest. These locations are distinct points. Each point represents one location at which the center of the receiver could be. The color of that point shows the value of mutual inductance. The positive and negative values refer to the direction of magnetic field passing through the receiver coil.

accuracy of localization and the availability of memory of the electronic circuits which will control the grid of antenna which we mentioned in the previous section. Because as we will see later this pre-calculated mutual inductance matrix should be stored in the memory. Reducing the spacing between each points of pre-calculated mutual inductance matrix will increase its size, and we will need more memory in the controlling mechanism. The size of memory required for storing this pre-calculated mutual inductance matrix will be proportional to the cube of the number of points in it. An optimization should be performed between available memory and the required accuracy. The required precision of localization and available data storage capability will determine the maximum spacing between the points of the pre-calculated mutual inductance matrix.

Fig. 3.11 shows a visualization of such pre-calculated mutual inductance matrix.

In this figure the mutual inductance between the transmitter and the receiver as a function of location in the volume of interest is shown. These locations are distinct points of our 3D grids. Each point represents one location at which the center of the receiver could be. A numerical version of this pre-calculated mutual inductance matrix will be stored in the

memory .

Now with this pre-calculated mutual inductance matrix at hand we return to the process of the localization.

The idea is this: when we measure the mutual inductance between the receiver and the transmitter, for example we get the value M_1 , we compare this measured mutual inductance to the pre-calculated mutual inductance matrix. In doing so, we could find which position of the receiver could result in the measured mutual inductance M_1 .

The problem that arises is this: the mutual inductance (M) between the transmitter and the receiver could not be mapped to a unique position of the receiver. Indeed, it could be mapped to a set of positions of the receiver. If the receiver was at any of these positions, it will yield the same mutual inductance value.

This is shown in Fig. 3.12. Assume a certain value of mutual inductance between receiver and the transmitter is measured. Of course we already know the position of the transmitter in the volume of interest because we put it there. What we does not know is the position of the receiver. We compare this measured mutual inductance with the pre-calculated mutual inductance matrix to find out the possible position(s) of receiver that could result in the measured mutual inductance. We find out that the measured mutual inductance in fact could be a result of large different numbers of positions of receiver. The surface shown in Fig. 3.12 shows the set of all possible positions of the receiver in the volume of interest where all of them will have the same mutual inductance (we should remember that we fixed the orientation of the receiver to be parallel to the plane in which the transmitter is).

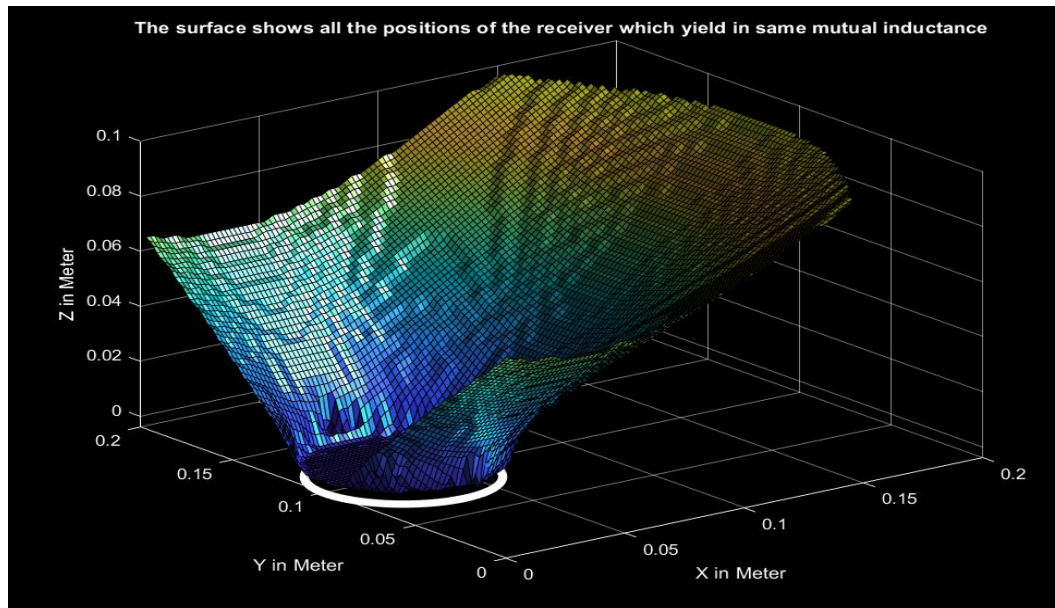


Figure 3.12: A certain value of mutual inductance could be a result of large different numbers of positions of receiver determined by simulation. In this figure the grid box is the volume of interest. The transmitter coil (the white circle) of radius 3.3 cm is placed at $(x = 3.3$ cm, $y = 10$ cm, $z = 0$ cm), and the receiver coil is of radius 1 cm. The surface shows the positions of the receiver which yield in same mutual inductance. The value of 5 μH for mutual inductance is arbitrary chosen for the sake of demonstration.

Though the value of measured mutual inductance does not lead to a unique position, it leads to a set of positions in the volume of interest which fits the obtained value of mutual inductance and eliminating other positions which do not fit the measured value of mutual inductance. Now the set of all possible positions of the receiver is smaller than the set of all possible positions of the receiver before this comparison was performed.

Indeed, instead of directly finding the right position of the receiver, the possible positions of the receiver in the volume of interest that are not consistent with the measured value of mutual inductance are eliminated.

What we need next is to keep eliminating more possible positions of the receiver and reduce the size of the set of all possible positions of the receiver in the volume of interest further more. But we could not proceed more by having just one transmitter coil.

But if we have another transmitter coil with known position in the volume of interest with its pre-calculated mutual inductance matrix calculated, we could proceed further more. That is why we chose our transmitter to be consisted of grids of coils instead of one coil.

Now we neglect the transmitter coil that we have been working with until now and assume that there is another transmitter coil with known position and with its pre-calculated mutual inductance matrix for the same volume of interest. The position of this second coil is not the same position of the first coil but the position of the receiver coil is still the same. We again measure the mutual inductance between the second coil and the receiver.

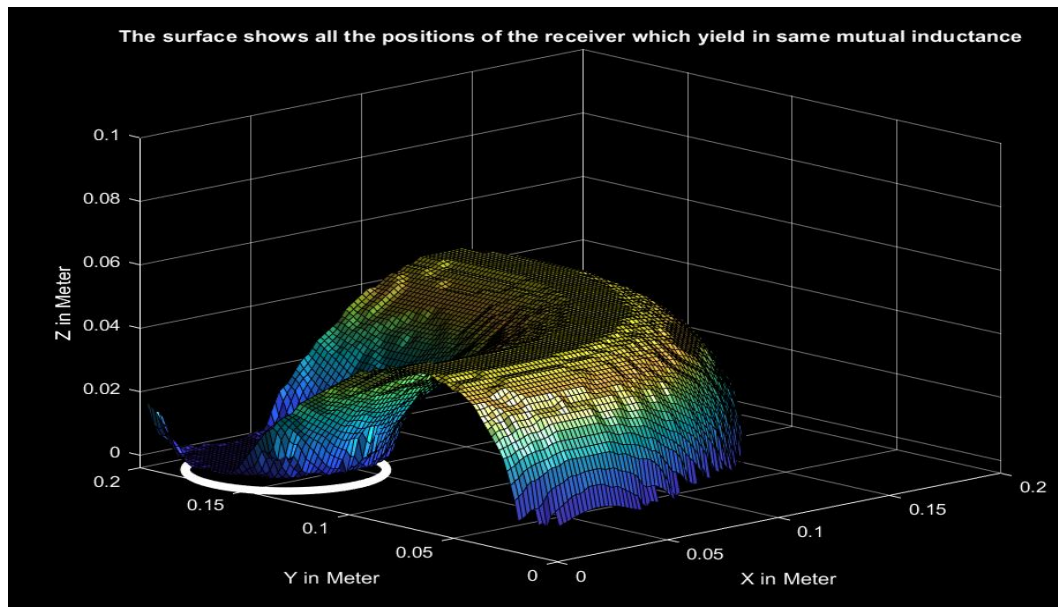


Figure 3.13: A certain value of mutual inductance could be a result of large different numbers of positions of receiver determined by simulation. In this figure the grid box is the volume of interest. The transmitter coil (the white circle) of radius 3.3 cm is placed at $(x = 3.3$ cm, $y = 165$ cm, $z = 0$ cm), and the receiver coil is of radius 1 cm. The surface shows the positions of the receiver which yield in same mutual inductance. The value of 0.16 nH for mutual inductance is arbitrary chosen for the sake of demonstration.

This second mutual inductance (between the second transmitter coil and the receiver) is not the same as the first measured mutual inductance (which was between the first transmitter coil and the receiver). But in both cases the position of the receiver coil is the same. Here we assume that in the time between first and second measurement the receiver coil does not change its position. Even if the receiver coil is moving, the time interval between these two measurements is so short that for any practical and realistic velocity of the receiver one could safely assume that the receiver occupies the same position during both measurements. When the second measurement is done we could use its pre-calculated mutual inductance matrix to find out all the possible position(s) that could lead to the second measured mutual inductance between the receiver and the (second) transmitter coil.

Fig. 3.13 shows the result of localization according to the second coil.

Now one should understand that because the position of the receiver did not changed in both measurements, it should at the same time belong to both subsets of possible positions according to pre-calculated mutual inductance matrix of first coil and the pre-calculated mutual inductance matrix of the second coil (shown in Fig.3.12 and Fig.3.13). To find the set of possible positions which is in the first set of possible positions and in the second set of possible positions, one should take the intersection of these two sets. Therefore, the positions that do not match the two measured values of coupling at the same time, are ruled out.

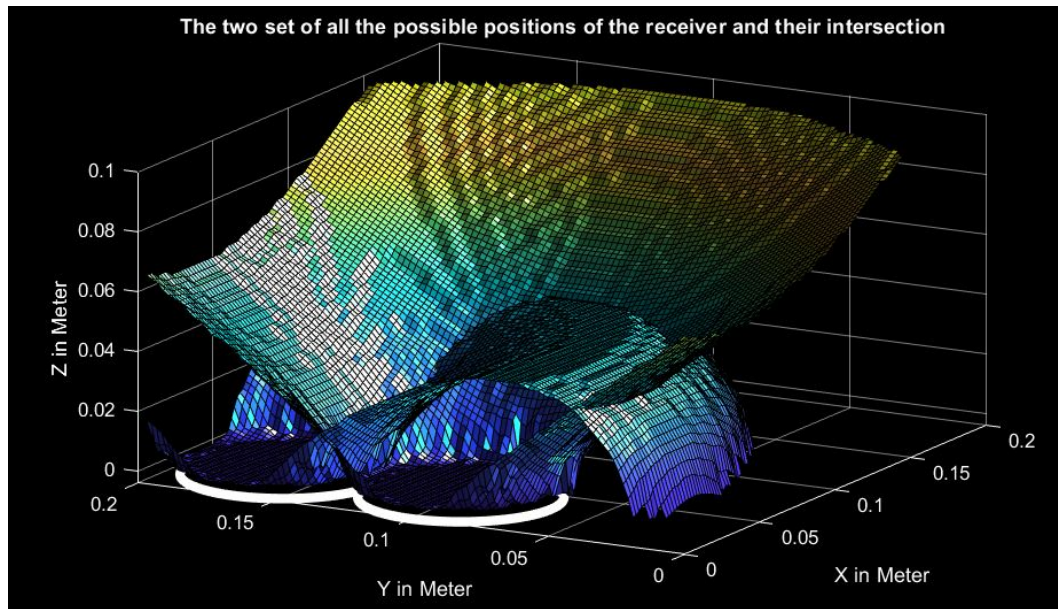


Figure 3.14: The two surfaces show all the positions of the receiver according to each coil (shown in Fig.3.12 and Fig.3.13 determined by simulation). The real position of the receiver should belong to their intersection.

Thus we further more reduced the set of possible positions to yet smaller subset. Now the new set is smaller because unlike the first two sets which each of them has to satisfy one condition (namely fitting the pre-calculated mutual inductance matrix for each of them separately), this new set has to satisfy two conditions at the same time (fitting both pre-

calculated mutual inductance matrix at the same time).

When there are more conditions to satisfy, there are fewer solutions that could do that. That is why the new set of possible positions is a subset and smaller set of the two set of possible positions that we started with.

Fig. 3.14 shows this operation.

To summarize:

- The localization procedure starts by choosing a configuration of the transmitter grid in which only one coil is connected to the power source (say coil number one) and other coils are disconnected (this means the transmitter is consisted only of coil number one).
- The mutual inductance between the coil number 1 of transmitter grid and the receiver is measured.
- From this measured mutual inductance, by a method explained earlier, all possible positions of the receiver according to the pre-calculated mutual inductance matrix of coil number 1 are calculated.
- To reduce this set of all possible positions of the receiver to its real position, we change the configuration of the transmitter grid to another configuration in which the coil number 2 is connected and all other coils are disconnected (this means the transmitter is consisted only of coil 2).
- By measuring the mutual inductance between the coil number 2 and the receiver and following the same principle described earlier, it is possible to find another subset of possible positions which fits the obtained value of mutual inductance between the coil 2 and the receiver.
- Because the real position of the receiver should at the same time belong to both subsets of possible positions (according to coil 1 and coil 2), the intersection of these two subsets is taken as a new and more reduced subset of possible positions of the receiver.
- Then an iterative approach is launched for coil number three, fourth,... and so on.
- This iteration is continued till a position or a small set of very closed points for the position of the receiver are obtained and the localization is finished.

Here we chose a grid of coils as a transmitter to demonstrate the applicability of this idea, but it really does not have to be a grid of coils. Any system that has the following feature could implement this method:

1. Having a reconfigurable transmitter (that means transmitter with more than one possible configuration). One could chose the desired configuration if it is needed.

2. Being able to measure the mutual inductance between the selected configuration of the transmitter and the receiver.

3. Having a tool to obtain all possible positions of the receiver based on the measured mutual inductance between the transmitter and the receiver.

It is to full fill the point number one that we have chosen a grid of coils with the ability to connect and disconnect any of them as a transmitter.

If this method was to be implemented in a stand alone device, it should be supplied by a mechanism of measuring the mutual inductance between the transmitter and the receiver. In our experimental verification we will use a VNA (Vector Network Analyzer) to deduce the mutual inductance between the transmitter and the receiver. We will talk more about this point later and distinguish between two ports and one port network in experimental verification and the practical scenario.

It is to full fill the point number three that we have chosen the approach of creating the pre-calculated mutual inductance matrix to map the measured mutual inductance between the transmitter and the receiver to all the possible position(s). The approach of creating the pre-calculated mutual inductance matrix to map the measured mutual inductance to the possible position(s), of course is not the only possible approach and we will talk more about other possible approaches later, namely developing an analytical solution for the mutual inductance as a function of the parameters describing the position of the receiver (parameter shown in the Fig. 3.9).

Fig. 3.15 summarizes our method.

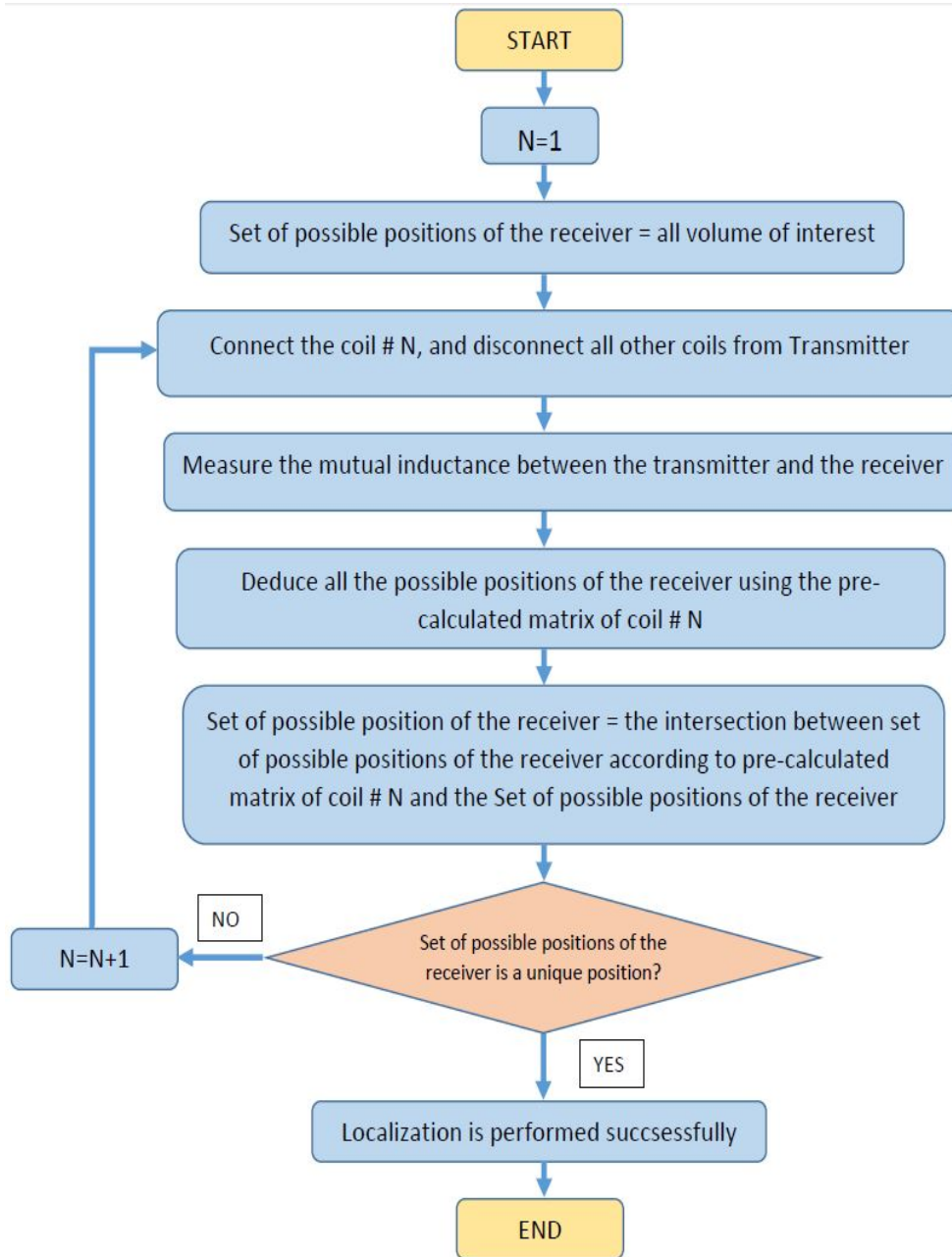


Figure 3.15: Procedure of localization.

3.4 SIMULATION AND EXPERIMENTAL RESULT FOR LOCALIZATION

By simulation in the title of this section we actually mean performing the algorithm for localization in near field. As we explained earlier the method is composed of measurement of mutual inductance then running an algorithm for deducing the location of the receiver. The algorithm is performed in conjunction with the measurement. The algorithm moves from one step to the next one, based on the measurement. Because of this we could not do a simulation first then compare the results with the experimental results as in conventional approach we did in the previous chapter.

It is for this reason that we do the simulation (performing the algorithm) and the measurement at the same time.

The algorithm is performed in a MATLAB code. No special function of MATLAB is used, we just used simple command like "for" loop or simple matrix creation and matrix comparisons. So the code could be implemented in a straight way in any other programming code or any micro-controller, provided enough memory. MATLAB is not necessary, we just use it for its convenience.

The measured data are imported to the MATLAB code, then MATLAB process these data for getting the desired answer.

As we said the volume of interest is the space where the receiver is somewhere in it. The objective is to find the location of the receiver in the volume of interest. The volume of interest is application-specific.

Here for the sake of demonstration (as we said earlier) we chose the volume of interest to be a cuboid of the dimensions : $\Delta X = 20$ cm, $\Delta Y = 20$ cm, $\Delta Z = 10$ cm.

The receiver is a circular coil with 10 mm radius and 1 turn. The transmitter consists of 9 circular coils. Each coil is of 3.3 cm radius and 6 turns. We chose these properties of transmitter (the number of coils and the number of turns in each coil) depending on the volume of interest to be covered. Because the method depends on the measured mutual inductance between the transmitter coils and the receiver, it is important to make sure that the mutual inductance between the transmitter and the receiver is high enough to be measured even if the receiver is placed at the frontier of the volume of interest and it has the smallest mutual inductance (as the receiver is farther from the transmitter the mutual inductance reduced). By increasing the number of turns, one actually increases the value of the mutual inductance leading to it being more easily measurable within the sensitivity of the measuring equipment.

It is for these reasons that we chose the transmitter that we have already mentioned. However the algorithm does not require this specific transmitter and any other transmitter with the previously mentioned features (being reconfigurable,...et.) does the job.

To quantify the position of the receiver, we will assign the origin of a Cartesian coordinate system to one of the volume of interest lower corner. The coordinate of the receiver (more precisely: the coordinates of the receiver center) will be measured in respect to this origin. For example if we say the receiver is in the X=12 cm, Y=12 cm and Z=4 cm, we mean that the center of the receiver is 12 cm away from the origin in the X direction, 12 cm away from the origin in the Y direction and 4 cm away from the origin in the Z direction.

The transmitter is placed underneath of the volume of interest. Each transmitter coil center has the coordinates given in Table 3.4.

CHAPTER 3. A RECONFIGURABLE COIL GRID FOR RECEIVER LOCALIZATION IN INDUCTIVE POWER TRANSFER

Coil	X coordinate	Y coordinate
The coil number 1 in Fig. 3.16	3.3 cm	3.3 cm
The coil number 2 in Fig. 3.16	9.9 cm	3.3 cm
The coil number 3 in Fig. 3.16	16.5 cm	3.3 cm
The coil number 4 in Fig. 3.16	3.3 cm	9.9 cm
The coil number 5 in Fig. 3.16	9.9 cm	9.9 cm
The coil number 6 in Fig. 3.16	16.5 cm	9.9 cm
The coil number 7 in Fig. 3.16	3.3 cm	16.5 cm
The coil number 8 in Fig. 3.16	9.9 cm	16.5 cm
The coil number 9 in Fig. 3.16	16.5 cm	16.5 cm

Table 3.2: Coordinates of each coil of the transmitter. Z coordinates for all coils are zero, (Z coordinate=0)

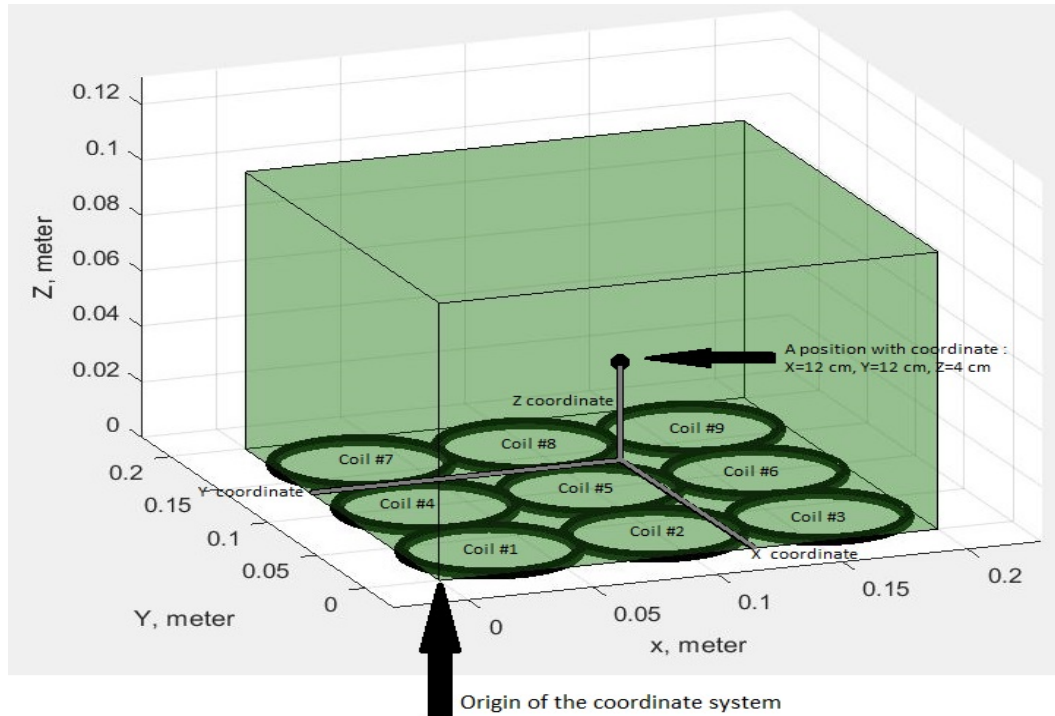


Figure 3.16: The origin of the coordinate system, the position of each transmitter coil by its number (as in table 3.4), and how we assign a number to the position of the receiver. The green cuboid is the volume of interest. 100

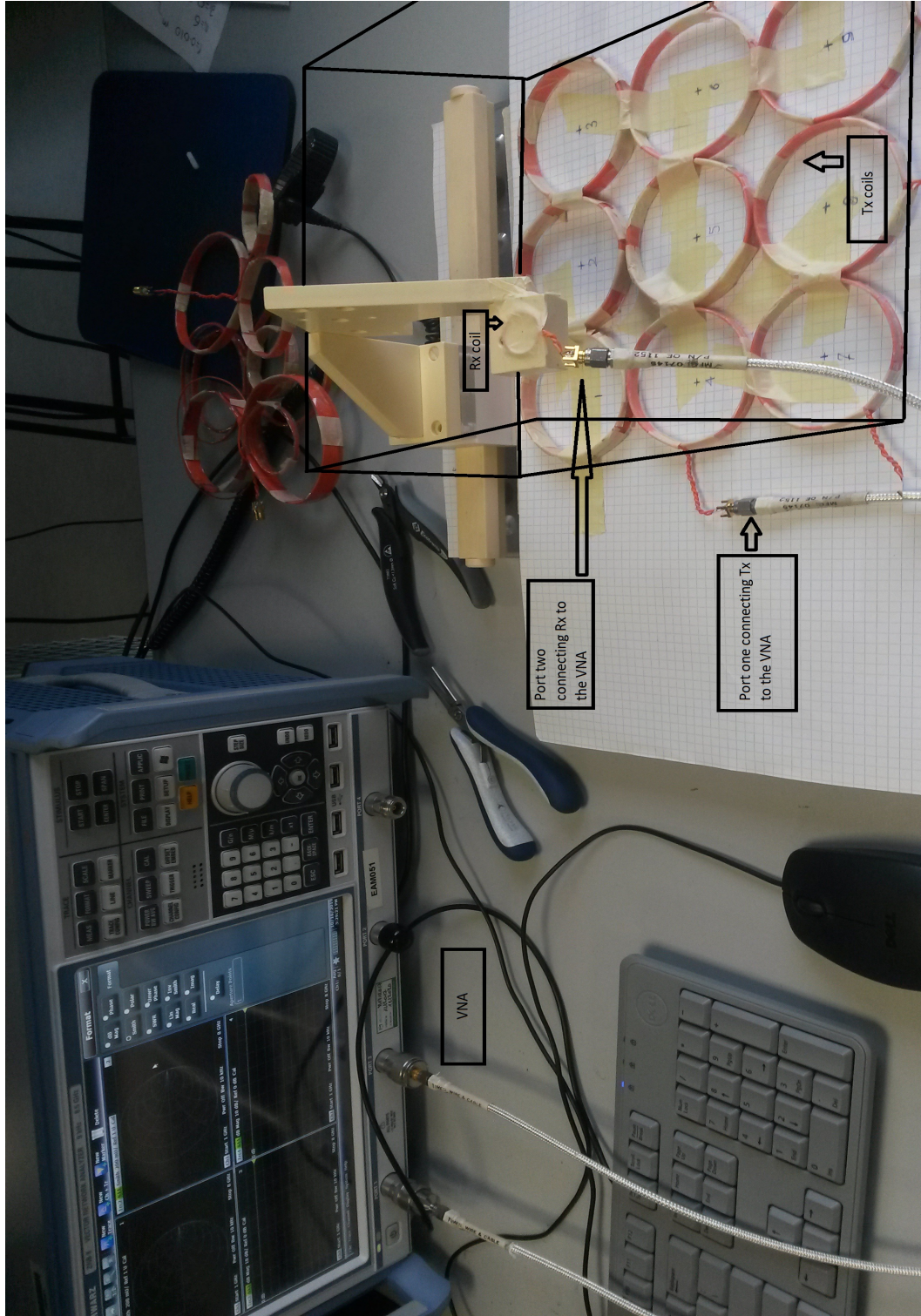


Figure 3.17: The real transmitter fabrication (grid of red coils) and the set-up of the measurement, the volume of interest is shown as a black cuboid, and the receiver coil (red small coil) is placed in some arbitrary position in the volume of interest.

Symbol	Quantity	Value in SI
L_1	Self-Inductance of 6 turns coil of radius 3.3 cm (TX)	4.58 μ H
Q1	Unloaded Quality factor of TX at 100 kHz	29.39
L2	Self-Inductance of 1 turn coil of radius 1 cm (RX)	59.65 nH
Q2	Unloaded Quality factor of RX at 100 kHz	3.75

Table 3.3: The self-inductances and quality factors of the transmitter coil(s) and the receiver coil, measured at a frequency of 100 kHz

All these geometric parameters, the origin of the coordinate system, the position of the transmitter coil and how we assign a number to the position of the receiver, are shown in Fig. 3.16.

Fig. 3.17 shows the real transmitter fabrication and the set-up of the measurement, the volume of interest in augmented manner, and the receiver coil placed in some arbitrary points in the volume of interest.

Table 3.4 shows the self-inductances and quality factors of the transmitter coil(s) and the receiver coil, measured at 100 kHz (to avoid inter-turns capacitance influence at this step of the work). The Unloaded Quality factor is defined as in Eq. 3.9 :

$$Q = \frac{\omega L}{R} \quad (3.9)$$

Where Q is Unloaded Quality factor of coil, L is its self-inductance, R is its resistance and ω is the angular frequency of operation.

The input power level of the VNA is fixed to 10 dBm. For experiments, a ROHDE & SCHWARZ ZNB 8 Vector Network Analyser (VNA) is used to measure the scattering parameters. The measurement was always done at 100 kHz to avoid considering parasitic capacitance. The measured data were transferred to a computer running the MATLAB algorithm, then the deduced locations based on our algorithm will be compared to the real positions of the receiver to validate the proposed technique of localization.

With this set up we start the localization process. The receiver is placed in a known arbitrary position in the volume of interest. We will pretend that we don't know the position of the receiver, then the goal is to deduce this position of the receiver by only using our knowledge about the mutual inductance between the transmitter and the receiver. If the method works as it is expected, this deduced position of the receiver should be the correct position of the receiver which is known for us. The difference between the real position of the receiver and the deduced position of the receiver is regarded as error in localization.

To be more clear we will proceed in steps.

1. The volume of interest is divided into a 3D grid of points, each point represents one

CHAPTER 3. A RECONFIGURABLE COIL GRID FOR RECEIVER LOCALIZATION
IN INDUCTIVE POWER TRANSFER

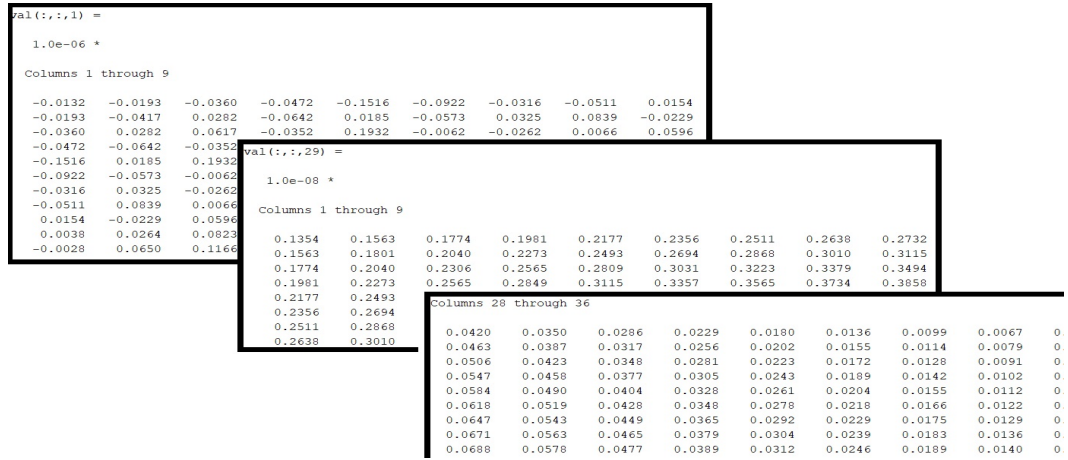


Figure 3.18: The pre-calculated mutual inductance matrix is a transmitter-coil specific 3D matrix of numbers which will be stored in the controlling circuitry of the transmitter.

possible location of the receiver. The distance between the points will be the limit of accuracy of the localization method.

The mutual inductance between each coil of the transmitter (each coil of the transmitter has a known position in the volume of interest mentioned in the table 3.4) and the receiver coil is calculated as if the receiver center was to be at any of the points of the 3D grid mentioned above. This is the pre-calculated mutual inductance matrix mentioned earlier. Each coil of the transmitter has its own pre-calculated mutual inductance matrix, because each coil of the transmitter is in a different locations in the volume of interest. So the relative position of the receiver coil (when it is in a certain position) and each coil of the transmitter will be different. The pre-calculated mutual inductance matrix is a transmitter-coil specific 3D matrix. In Fig. 3.11 we see a visual representation of one such matrix. In reality it is a 3D matrix of numbers. Fig. 3.18 shows part of one such matrix as it is seen in MATLAB. These matrices will be stored in the controlling circuitry of the transmitter. The size of storage required for storing each of these matrices will be proportional to the cube of number of points in the 3D grid by which we mapped the continuous volume of interest into a set of discrete points. In this study the spacing between the points of the 3D grid is 1 mm along each axis. In a real practical system, the required precision of localization and available data storage capability will determine the maximum spacing between the points of the grid. With nine such pre-calculated mutual inductance matrix for each coil of the transmitter calculated and stored in our algorithm we move to next step. Calculating this pre-calculated mutual inductance matrix takes time. In our case each pre-calculated mutual inductance matrix has (200*200*100) entries which equals 4 millions entries. In our work calculating each of these pre-calculated mutual inductance matrix took several hours. However it is not important, because we calculate pre-calculated mutual inductance matrix just one time then it is stored. It will not be calculated again. It is a calculation that is performed just one time.

2. We put the receiver center in the known location of X=5 cm, Y=5 cm and Z=2 cm, in the volume of interest. Our goal is to deduce this position by running our algorithm.

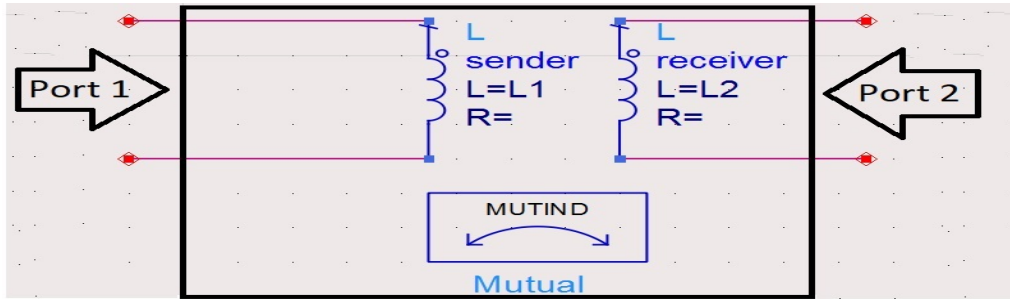


Figure 3.19: The schematic that is used to model the measurement process in this chapter. It is a two port network. Later we will make our model more realistic, by moving from two port network to one port network, but not in this chapter.

3. The circuit shown in the Fig. 3.19 is used to model the measurement process. It consists of a transmitter coil with its self-inductance $L1$, a receiver coil with its self-inductance $L2$. These parameters ($L1$ and $L2$) which are independent from the relative positions between the transmitter and the receiver, are known. What is unknown is the mutual inductance between the receiver and the transmitter, which depends on the position of the receiver. In this set up we treat the (Transmitter coil-Receiver coil) system as a two-port network. This means that for doing this measurement we assumed we have access to the transmitter and the receiver as well. This is clearly not a practical scenario. In reality we have access to the transmitter but we do not have any access to the receiver. In WPT and RFID we don't have any control on the receiver. The realistic model of this situation in the WPT and RFID is a one port network with the realistic assumption of not having access to the receiver. However this is not a problem for us at the moment. We will proceed with the unrealistic assumption of having two-port network for the sake of measurement and we later will face this problem and find solution for it in the next chapter. The main point here is to show that by measuring the mutual inductance between the receiver and the transmitter one can deduce the position of the receiver.

When we accept the circuit model in Fig. 3.19 the measurement is done in a same way as it was mentioned in the previous chapter:

- VNA measures the S parameters of the (Transmitter coil-Receiver coil) network (S_{11} , S_{12} , S_{21} , S_{22}).
- S parameters are converted to Z parameters according to the Eq. 35-38.
- Mutual inductance is deduced from Z parameters according to Eq. 44-47.

4. The localization process is initiated by choosing a configuration of the transmitter in which all the coils are disconnected except coil number 1. This means in this configuration the transmitter is consisted only of coil number 1. Lets call it configuration 1.

5. We measure the mutual inductance between the transmitter in configuration 1 and the receiver coil (as mentioned in the step 3) and we find the mutual inductance between the transmitter in configuration 1 and the receiver coil to be:

$$M=12.72 \text{ nH}$$

6. This value of the mutual inductance is compared with the pre-calculated mutual in-

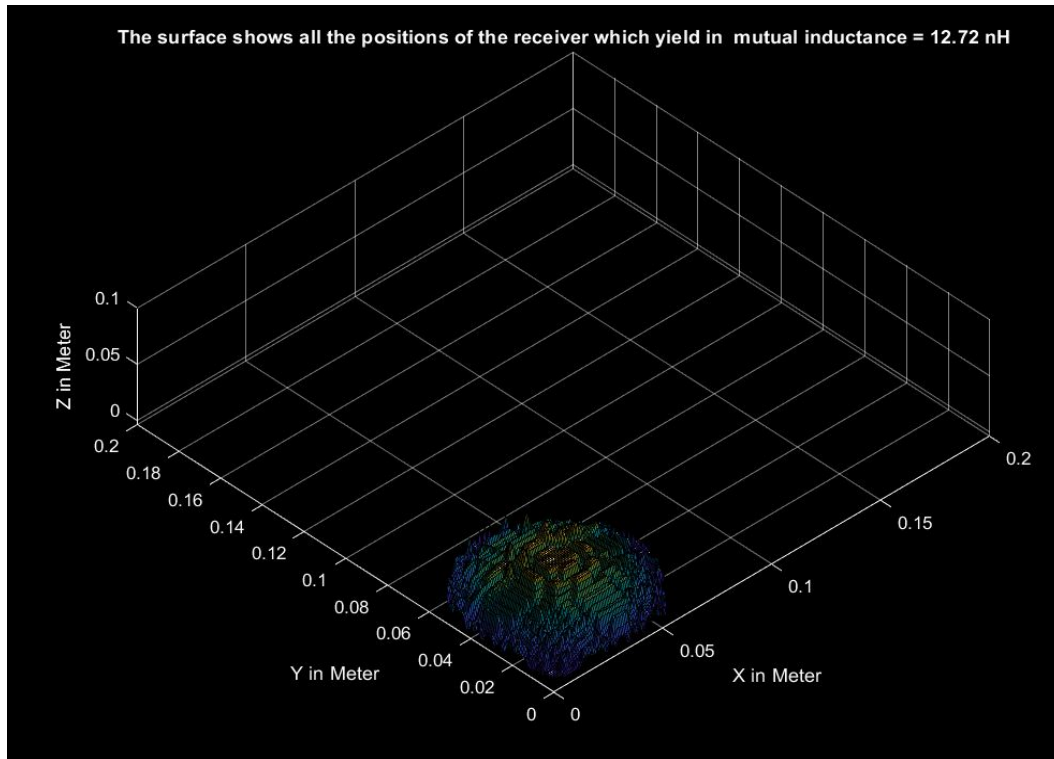


Figure 3.20: The measured value of mutual inductance (12.72 nH) could be a result of any positions of receiver belonging to the surface shown here. Till this step there are 7325 possible positions of the receiver which match the measured mutual inductance. The position is not unique and the localization process should continue.

ductance matrix of the coil 1 (corresponding to the configuration 1 of the transmitter) and all the possible positions of the receiver that would lead to the same measured mutual inductance in the volume of interest are determined. There are 4317 such possible positions. Fig. 3.20 shows the results.

7. The Fig. 3.20 is a visual representation of the results. MATLAB provides the result as a large set of points part of which is shown in Fig. 3.21. From now we just show the visual representation and keep in mind that each such surface (like the one shown in the Fig. 3.20) is just a large set of numerical values indicating the possible position of the receiver stored in MATLAB as a numerical matrix.

8. To reduce further more the number of possible positions and find the real position of the receiver, the configuration of the transmitter is changed. We disconnect the coil number 1 and connect only coil number 2. Now we are in a configuration in which the transmitter is consisting of only coil number two. Lets call it the configuration (2) of the transmitter.

9. We measure the mutual inductance between the transmitter in configuration 2 and the receiver coil (as mentioned in the step 3) and we find the mutual inductance between

CHAPTER 3. A RECONFIGURABLE COIL GRID FOR RECEIVER LOCALIZATION
IN INDUCTIVE POWER TRANSFER

2525x3 double

	1	2	3	4
1	1.0000e-07	0.0250	1.0000e-07	
2	1.0000e-07	0.0283	1.0000e-07	
3	1.0000e-07	0.0350	1.0000e-07	
4	1.0000e-07	0.0417	1.0000e-07	
5	1.0000e-07	0.0283	0.0017	
6	1.0000e-07	0.0383	0.0017	
7	1.0000e-07	0.0283	0.0033	
8	1.0000e-07	0.0383	0.0033	
9	0.0033	0.0050	1.0000e-07	
10	0.0033	0.0083	1.0000e-07	
11	0.0033	0.0117	1.0000e-07	
12	0.0033	0.0150	1.0000e-07	
13	0.0033	0.0183	1.0000e-07	

Figure 3.21: The set of all possible positions of the receiver stored in MATLAB as a numerical matrix. First column indicates the X coordinate, the second column indicates the Y coordinate and the third column indicates the Z coordinate. In this step there are 2525 possible positions of the receiver which match the measured mutual inductance.

the transmitter in configuration 1 and the receiver coil to be:
M=0.997 nH

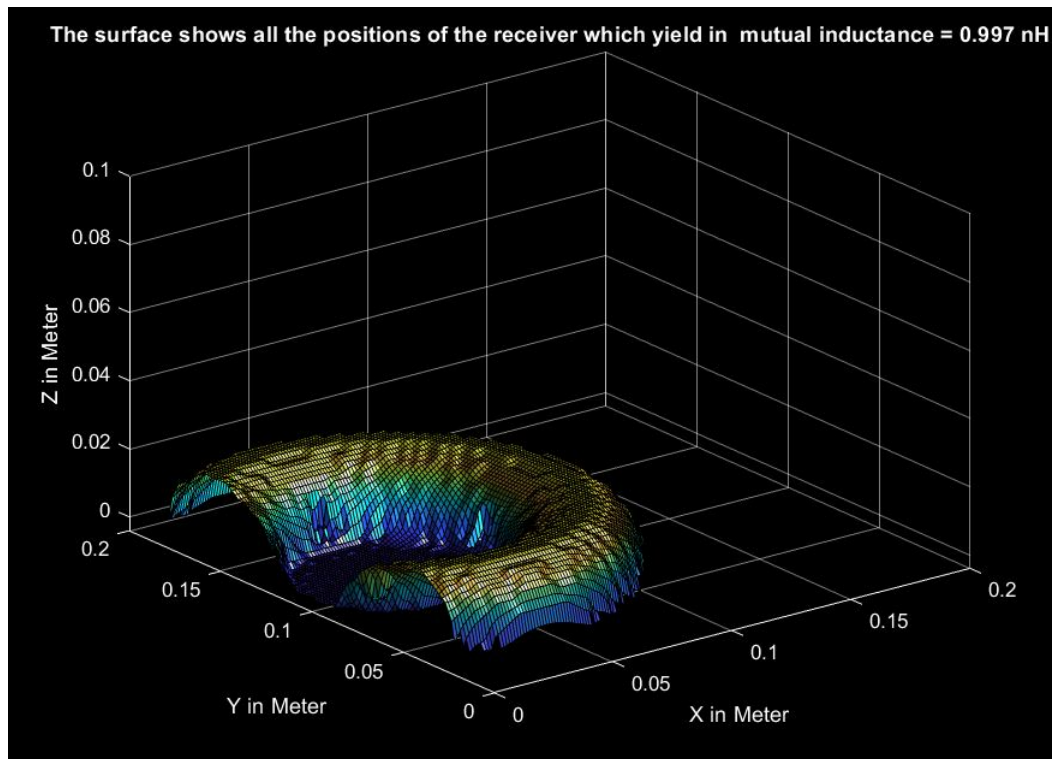


Figure 3.22: The measured value of mutual inductance (0.997 nH) could be a result of any positions of receiver belonging to the surface shown here. This is configuration (2).

10. This value of the mutual inductance is compared with the pre-calculated mutual inductance matrix of the coil 2 (corresponding to the configuration 2 of the transmitter) and all the possible positions of the receiver that would lead to the same measured mutual inductance in the volume of interest are determined. Fig. 3.22 shows the results.

11. We did not say it before but it should be mentioned that in order for taking the intersection between two possible set of positions of the receiver (that is what we got in steps 6 and 10) to be meaningful, the receiver coil should be at the same place in both of them. After we did the first measurement (in step 5) we switch off the coil number 1, then we switch on the coil number 2. This takes some time. We assume that the receiver coil does not change its position during this time. In fact we assume that receiver coil does not change its position during the whole process of the localization. However electronic switches are very fast in respect to possible movement of the receiver coil in real application and the assumption that the receiver coil dose not change its position during the localization process is justified. In our case the time required for measuring the mutual inductance and deducing its corresponding possible positions take few milliseconds. In real life scenarios the receivers (if moving), moving with much smaller speed that they could be assumed to be stationary if we consider their position during just few milliseconds.

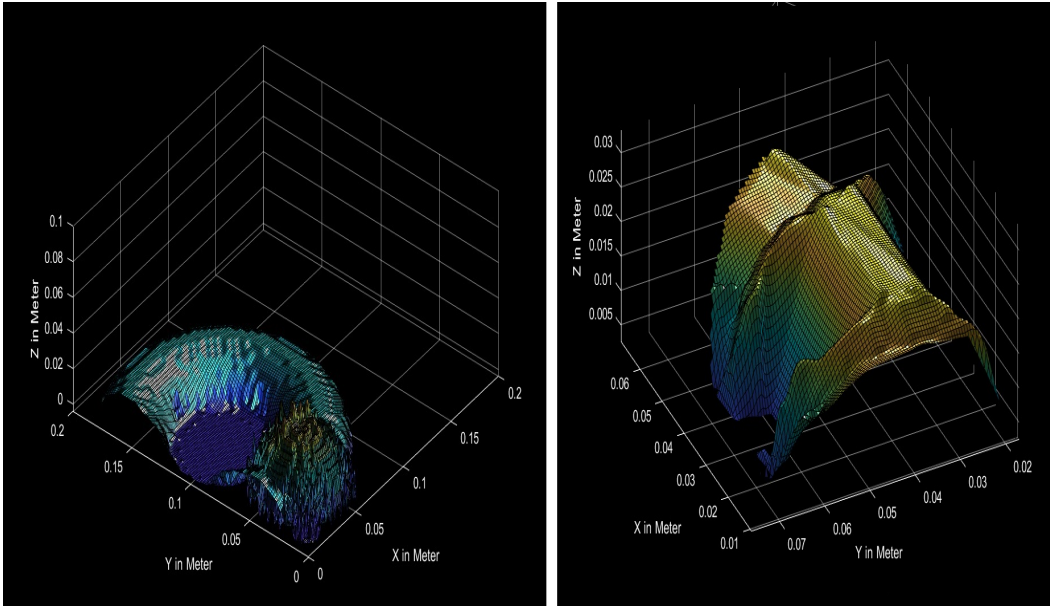


Figure 3.23: Left panel shows possible positions of the receiver due to the configuration 1 and configuration 2. Right panel shows their intersection. Intersection between surfaces belong to configuration 1 and configuration 2, reduces the set of possible positions of the receiver. The answer is still not unique. One should notice that the X, Y and Z axes in Right panel cover a small part of what is shown in Left panel. It means that the answer is converging toward small possible set of positions.

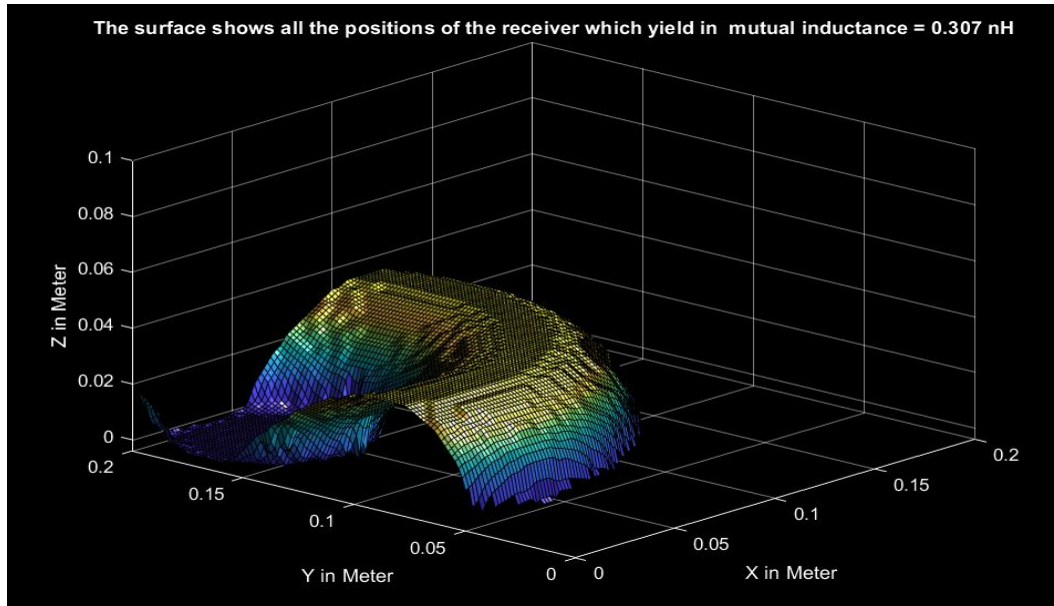


Figure 3.24: The measured value of mutual inductance (0.307 nH) could be a result of any positions of receiver belonging to the surface shown here.

12. Based on the possible positions of the receiver due to the configuration 1 and configuration 2, the answer which belongs to both should be retained. It represents their intersections. With such intersections the number of possible positions of the receiver is reduced further more. Fig. 3.23 shows the results.

13. The intersection derived in last stage contains 813 different locations. The answer is still not be unique. We again change the configuration of the transmitter. We disconnect the coil number 2 and connect only coil number 3. Now we are in a configuration in which the transmitter is consisting of only coil number three. Lets call it the configuration (3) of the transmitter.

14. We measure the mutual inductance between the transmitter in configuration 3 and the receiver coil. We find the mutual inductance between the transmitter in configuration 3 and the receiver coil to be:
 $M=0.307 \text{ nH}$

15. This value of the mutual inductance is compared with the pre-calculated mutual inductance matrix of the coil 3 (corresponding to the configuration 3 of the transmitter) and all the possible positions of the receiver that would lead to the same measured mutual inductance in the volume of interest are determined. Fig. 3.24 shows the results.

16. We again take the intersection between what we get in step 12 (the possible positions according to configurations 1 and 2) and the possible positions according to configuration 3. Intersection between them reduces the set of possible positions of the receiver. Fig. 3.25

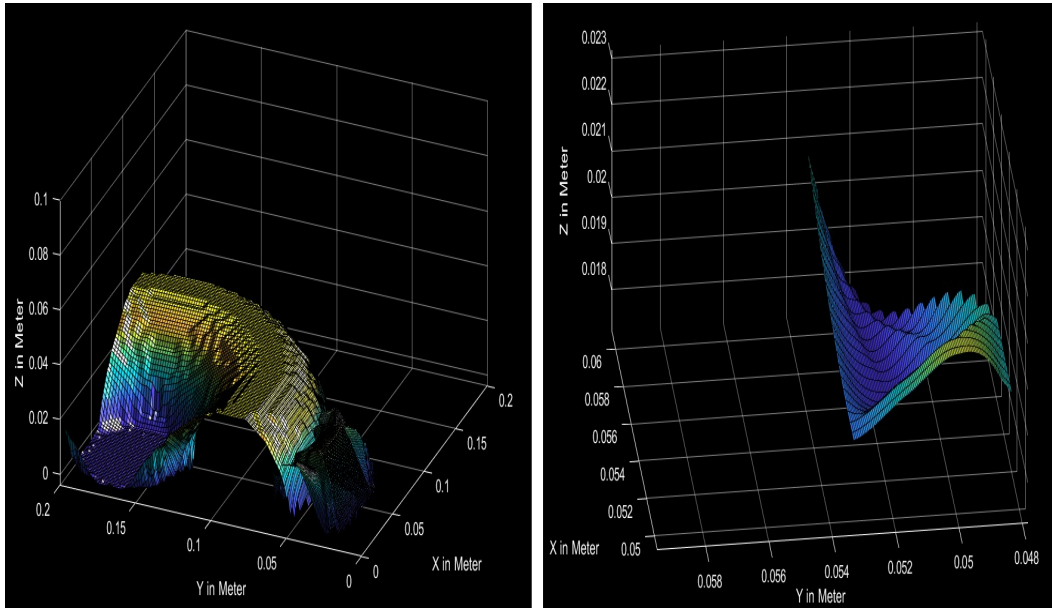


Figure 3.25: Right panel shows possible positions of the receiver due to the configuration 3 and the possible positions of the receiver from previous steps. Left panel shows their intersections. Intersection between them reduces the set of possible positions of the receiver. The answer still is not unique.

shows the results.

17. The intersection derived in last stage contains 107 different positions. Here we see the reduction! Before we had 813 different positions. The answer still is not unique. We again change the configuration of the transmitter. We disconnect the coil number 3 and connect only coil number 4. Now we are in a configuration in which the transmitter is consisting of only coil number four. Lets call it the configuration (4) of the transmitter.

18. We measure the mutual inductance between the transmitter in configuration 4 and the receiver coil. We find the mutual inductance between the transmitter in configuration 4 and the receiver coil to be:

$$M=0.997 \text{ nH}$$

19. This value of the mutual inductance is compared with the pre-calculated mutual inductance matrix of the coil 4 (corresponding to the configuration 4 of the transmitter) and all the possible positions of the receiver that would lead to the same measured mutual inductance in the volume of interest are determined. Fig. 3.26 shows the results.

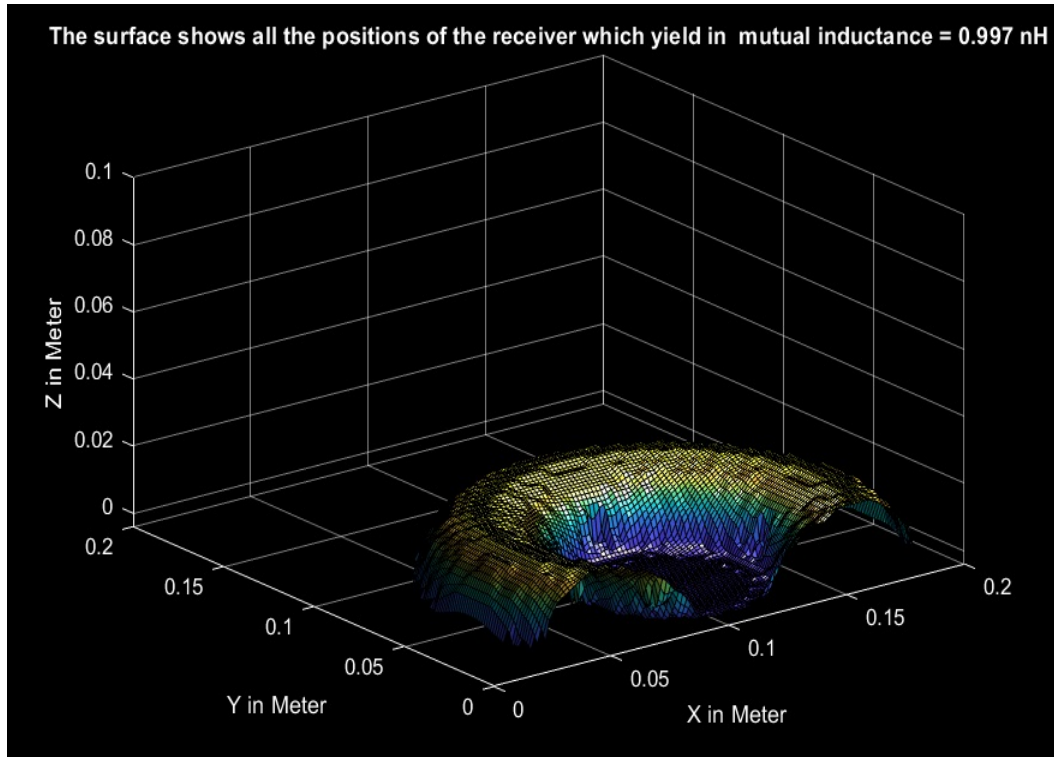


Figure 3.26: The measured value of mutual inductance (0.997 nH) could be a result of any positions of receiver belonging to the surface shown here. This is for configuration 4.

20. We again take the intersection between what we get in step 16 (the possible positions according to configuration 1, 2 and 3) and the possible positions according to configuration 4. Intersection between them reduces the set of possible positions of the receiver to 51 possible positions. Fig. 3.27 shows the results.

21. The intersection derived in last stage contains many possible positions and the answer still is not unique. We again change the configuration of the transmitter. We disconnect the coil number 4 and connect only coil number 5. Now we are in a configuration in which the transmitter is consisting of only coil number five. Lets call it the configuration (5) of the transmitter.

22. We measure the mutual inductance between the transmitter in configuration 5 and the receiver coil. We find the mutual inductance between the transmitter in configuration 5 and the receiver coil to be:
 $M=0.920$ nH

23. This value of the mutual inductance is compared with the pre-calculated mutual inductance matrix of the coil 5 (corresponding to the configuration 5 of the transmitter) and all

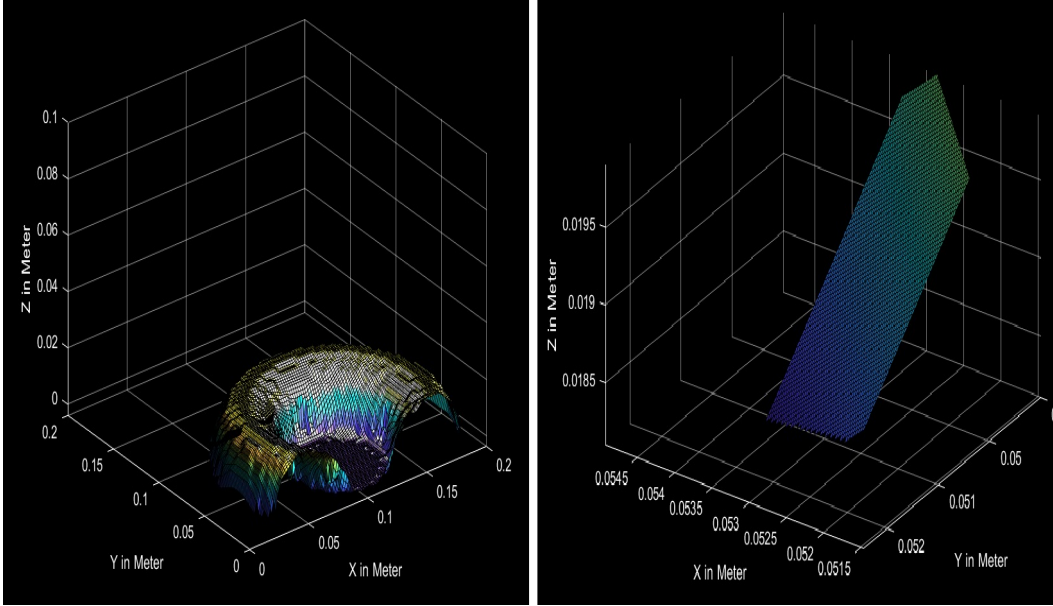


Figure 3.27: Right panel shows possible positions of the receiver due to the configuration 4 and the possible positions of the receiver from previous steps. Left panel shows their intersection. Intersection between them reduces the set of possible positions of the receiver. The answer still is not unique.

the possible positions of the receiver that would lead to the same measured mutual inductance in the volume of interest are determined. Fig. 3.28 shows the results.

24. We take the intersection between what we get in step 16 (the possible positions according to configuration 1, 2, 3 and 4) and the possible positions according to configuration 5. Intersection between them reduces the set of possible positions of the receiver.

25. We will not show here the results because the resultant number of possible positions are too small to be seen. The intersection result just contain six possible positions shown in the Fig. 3.29.

26. When we check these result we realize that they are very close to each other, that means the set of possible positions converged to a unique position. At this point the localization is done and there is no more need to chose next configuration for the transmitter.

27. The average of these six points is $X=0.0514$, $Y=0.0506$, $Z=0.0199$. When we compare this result to the real position of the receiver (mentioned in the step 2) we find them to match very well. We take it as approval for the feasibility of our proposed method.

28. Fig. 3.30 shows all the pre-calculated surfaces (due to the measurements of the mutual inductance) whose intersection leads to the localization of the receiver coil.

In our example it just happened that we needed five configurations of the transmitter to have the set of all possible positions of the receiver to converge to a single position. Some time it takes more, some other time it takes less.

To make sure that we were not just lucky in getting results and the algorithm is reliable, we

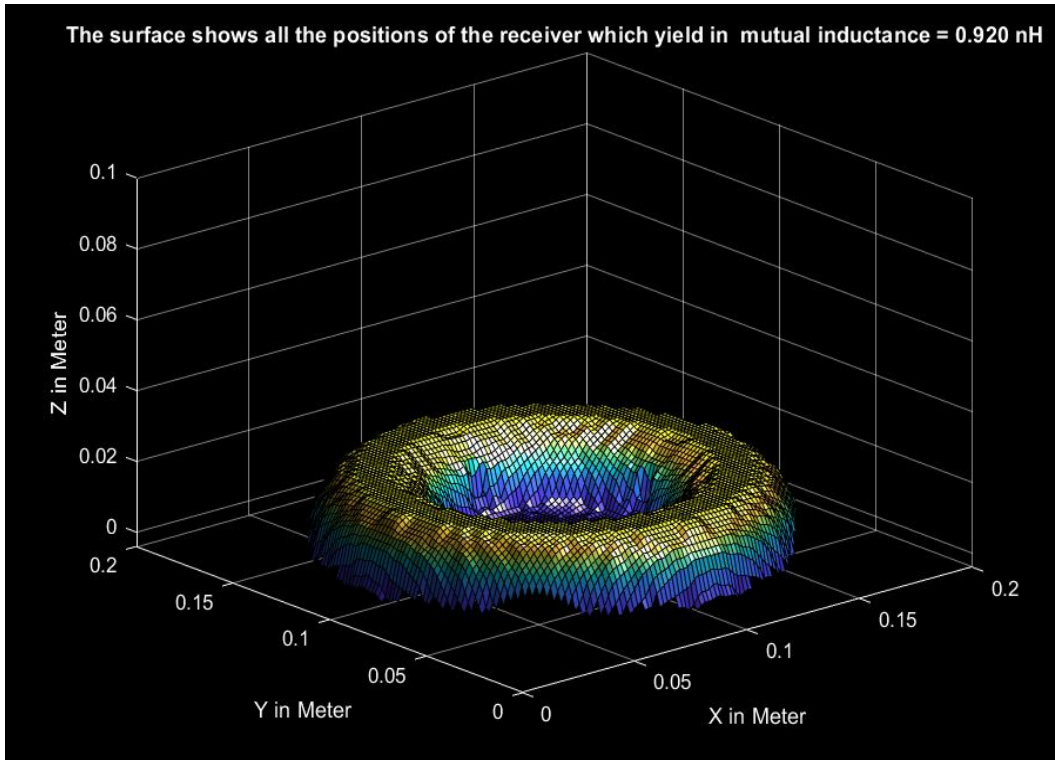


Figure 3.28: The measured value of mutual inductance (0.920 nH) could be a result of any positions of receiver belonging to the surface shown here. This is configuration 5.

locatione			
6x3 double			
	1	2	3
1	0.0500	0.0500	0.0208
2	0.0500	0.0517	0.0200
3	0.0500	0.0533	0.0192
4	0.0517	0.0500	0.0200
5	0.0533	0.0483	0.0200
6	0.0533	0.0500	0.0192
7			
8			

Figure 3.29: The intersection result now just contain six possible positions.

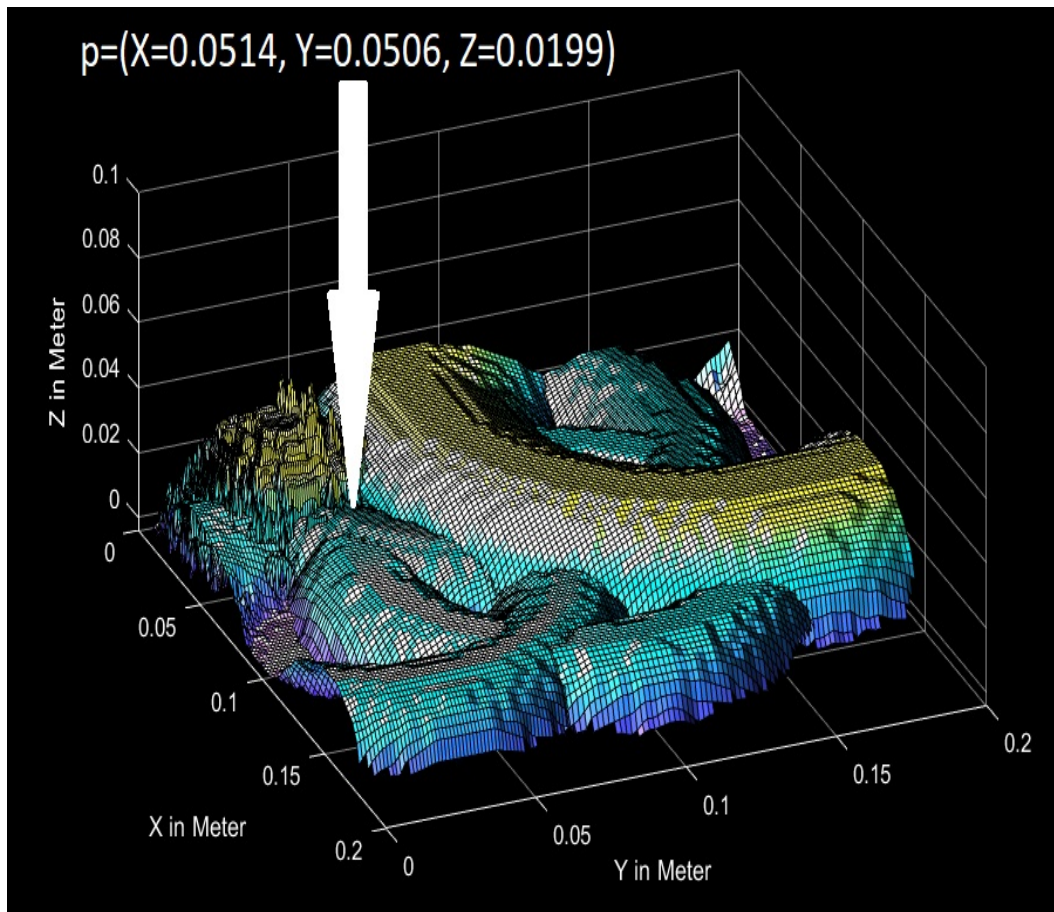


Figure 3.30: All the pre-calculated surfaces (due to the measurements of the mutual inductance) whose intersection leads to the localization of the receiver coil

Experiment	The real position of the receiver	The deduced position of the receiver	MAE
Experiment 1	X=5 cm, Y=5 cm, Z= 2 cm	X= 5.14 cm, Y=5.06 cm, Z= 1.99 cm	1 mm
Experiment 2	X=12 cm, Y=12 cm, Z= 4 cm	X= 11.97 cm, Y=12.06 cm, Z= 3.97 cm	4 mm
Experiment 3	X=6 cm, Y=5 cm, Z= 5 cm	X=5.9 cm, Y=5.07 cm, Z= 5 cm	3 mm
Experiment 4	X =3 cm, Y =14 cm, Z = 9 cm	X =2.9 cm, Y =13.9 cm, Z = 8.9 cm	1 mm

Table 3.4: Experimental results for localization.

repeated the process for other arbitrary positions in the volume of interest. By repeating the process for each position we want to see if we are able to localize the receiver coil position successfully.

Table 3.4 shows the results.

As one can see, the results are very close to the real positions. For estimating the error, the Mean Absolute Error (MAE) is used according to Eq.4.29

$$MAE = \frac{\sum_{i=1}^n |y_i - x_i|}{n} \quad (3.10)$$

where::

- the y_i is the deduced values of position (that is the deduced X, Y and Z coordinates in each experiment)
- x_i the real values of position (that is the actual X, Y and Z coordinates in each experiment)
- n is the number of coordinates for each position which in our case is three.

What is the source of this error?

One could think of following reasons:

1. The pre-calculated matrix for each configuration (that is the mutual inductance between the transmitter and the receiver when receiver is in different positions) was calculated using a MATLAB code that we developed using the quasi-static approximations. This calculation (though for practical reason is good enough) it is not completely accurate. We could use the commercially available software (like Maxwell Ansys) to enhance the pre-calculated matrix for each configuration and reduce the errors.
2. Dividing the volume of interest into grid of discrete points. As the volume of interest is divided into grid of denser points, the accuracy of localization will increase. However increasing the size of 3D grid of points will increase the size of required memory and it makes the algorithm to take more time to be performed.
3. The pre-calculated matrix for each configuration is calculated for idealized circular coil

as receiver and as transmitter. For doing the measurement, we fabricate such circular coil for the receiver and the transmitter. However this fabrication is not ideal. This means (in mapping) we compare the non ideal circular coils to ideal circular coils. This creates an error.

4. In any measurement there is certain inaccuracy (due to noise, inaccuracy of our measuring devices like VNA,...).

It should be mentioned that the accuracy of the measured mutual inductance plays an important role in the precision of the localization; the more accurate one could measure the mutual inductance the more precise one could localize.

Those are the source of errors.

As we said we performed this code in MATLAB. However we did not use any special function of MATLAB and the code could be performed in any micro controller for realistic application. But here we report some of the feature of the algorithm performance in MATLAB. Depending on the precision of the grid in which the volume of interest is divided, the algorithm will take different time to accomplish it. In the experiments, the algorithm took between 2 and 6 seconds to accomplish all computations, which can be considered as real time system. A computer with 64 GB RAM and a CPU of 3.2 GHz was used. With a micro controller with less memory and computational power this time should be more and like always an optimization between required minimum accuracy and time of performing the algorithm is required.

In addition, this method needs data storing capability. The data to be stored (which depends on the size of the volume of interest and the choice of spacing of points in 3D grid) for the practical system need not to be very large. In this study it was only 9 MB. The time necessary to localize the receiver coil as we said also depends on the above parameters and for a practical system it could be short time. In this study it was a few seconds.

The algorithm cannot predict how many coils are necessary to determine uniquely the position of the receiver. However, it starts by taking the intersection between 2 coils, if the algorithm finds more than one position, it takes the intersection between 3 coils, and continuing until the detected position is unique. In present experimental work, if the intersection between all of the 9 coils is performed and the position is still not unique, the algorithm cannot localize the receiver. However, in the experiments, we never faced such situation, and 4 or 5 coils were always enough for tag localization.

3.5 REDIRECTING THE MAGNETIC FIELD BY CHANGING THE CONFIGURATION OF THE TRANSMITTER BASED ON THE LOCALIZED RECEIVER AND EXPERIMENTAL RESULTS

After performing localization, the obtained information about the position of the receiver could be used to enhance the performances of IPT systems by beamforming.

Each coil of the grid of the transmitter could be excited individually by:

- (1) applying current into it in clockwise direction.
- (2) applying current into it in anticlockwise direction.
- (3) it could be simply disconnected.

Those are the three possible excitations of each coil and if the grid of transmitter has N coils, the grid could be excited in 3^N different ways and each of these 3^N different excitations will create a different magnetic field pattern in the volume of interest. Lets call each of these possible excitation of the transmitter one of its configuration (in transmitting mode). The magnetic field corresponding to one configuration of the transmitter is different from the magnetic field corresponding to another configuration of the transmitter. Consequently certain configurations of the transmitter are more suitable for certain positions of the receiver. Fig. 3.31 shows this.

To choose one configuration among these 3^N possibilities in a systematic way, one could divide the volume of interest into a set of sub volumes as shown in Fig. 3.32. The localization of the receiver performed previously helps to choose the configuration maximizing the magnetic flux in a sub volume in which the receiver is localized. The proper excitation of the grid of transmitters that gives rise to an optimal magnetic field for each sub volume is predetermined and stored in a table in the controlling system of the transmitter. This will increase the required memory of controlling system of the transmitter but not by too much. The size of this table depends on the number of sub volumes of the volume of interest and the number of coils in the transmitter. In our work we have 36 sub volumes. That means we have a table that assigns to each one of these 36 sub volumes a certain Transmitter's coils configuration.

Part of this table is shown in Fig. 3.33.

The way by which we determine which excitation of the transmitter (that is which coils are connected with certain direction of current, and which coils are disconnected) is determined by the method of magnetic beamforming explained in the previous chapter.

To summarize; the process appears in 6 steps:

1. The transmitter starts by being in localization mode.
2. It performs the localization algorithm as explained earlier.
3. The receiver location in the volume of interest is determined.
3. Based on this result now the transmitter knows in which sub volume the receiver is.
4. From the stored table, it can choose the configuration that creates the most suitable magnetic field for the sub volume in which the receiver was localized. This is the power transferring mode.
5. The transmitter stays in the power transferring mode for a while, then transmitter returns to the localization mode again to count for the possibility of the receiver moving and changing its position in the volume of interest.
6. The process continue in a cyclic way.

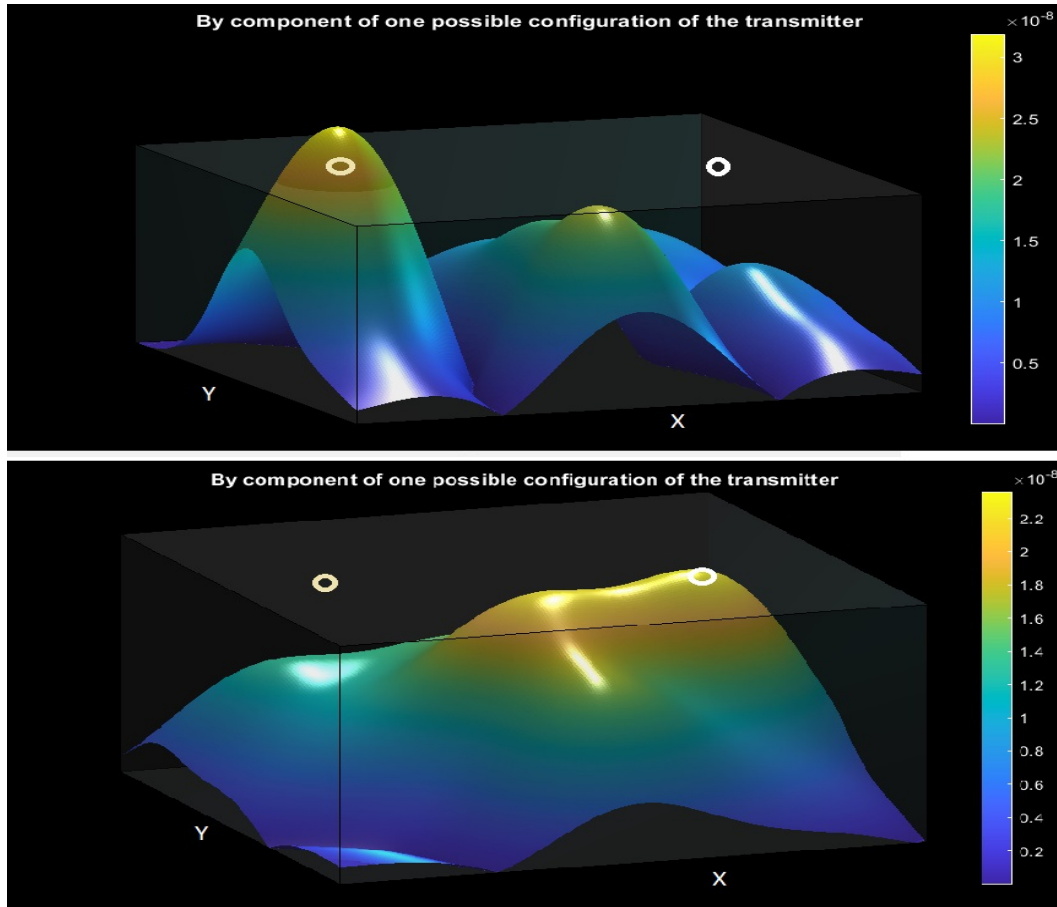


Figure 3.31: Two different configurations of transmitter lead to a magnetic field with different distributions in volume of interest. The upper part shows the magnetic field distribution of a configuration suitable for case in which the receiver is in the position shown by yellow circle and not suitable for case in which the receiver is in the position shown by white circle. The lower part shows the opposite (suitable for position shown by white circle and not yellow circle). Here the precise positions of the circles are not important and we just want to show the dependency of the magnetic field distribution in the volume of interest on the transmitter configuration.

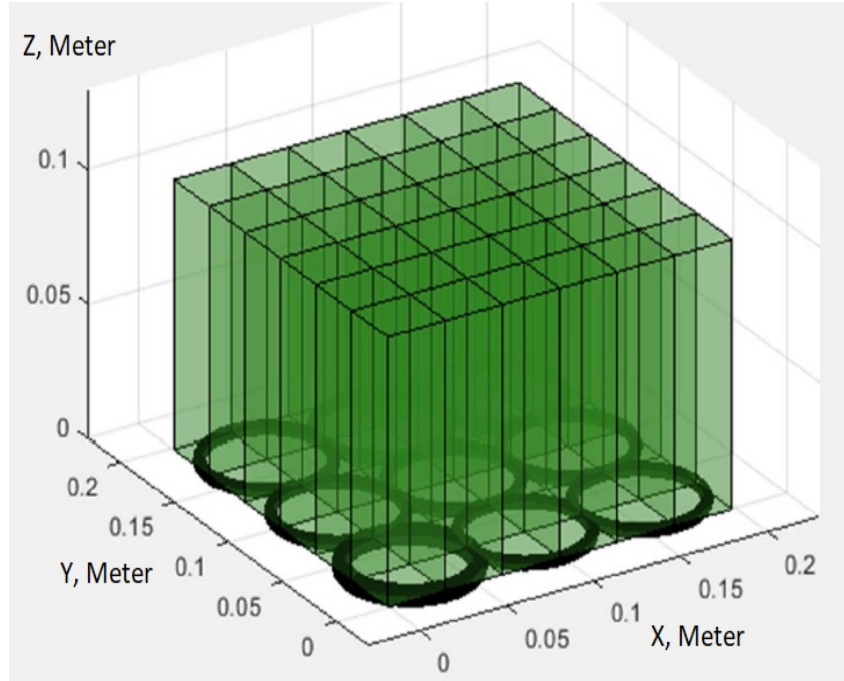


Figure 3.32: The volume of interest is divided into sub volumes (green voxels). Depending on the result of localization of the receiver, a configuration of transmitter is selected corresponding to the magnetic fields that add constructively in a sub volume in which the receiver was found.

the configuration that creates the most suitable magnetic field for the	Coil #1	Coil #2	Coil #3	Coil #4	Coil #5	Coil #6	Coil #7	Coil #8	Coil #9
sub volume #1	C	C	D	C	C	D	D	D	D
sub volume #2	D	C	C	D	D	D	D	D	D
sub volume #3	C	C	C	C	D	D	D	D	D

Figure 3.33: Part of the configuration table which is stored in the controlling system of the transmitter. "C" means connected, and "D" means disconnected.

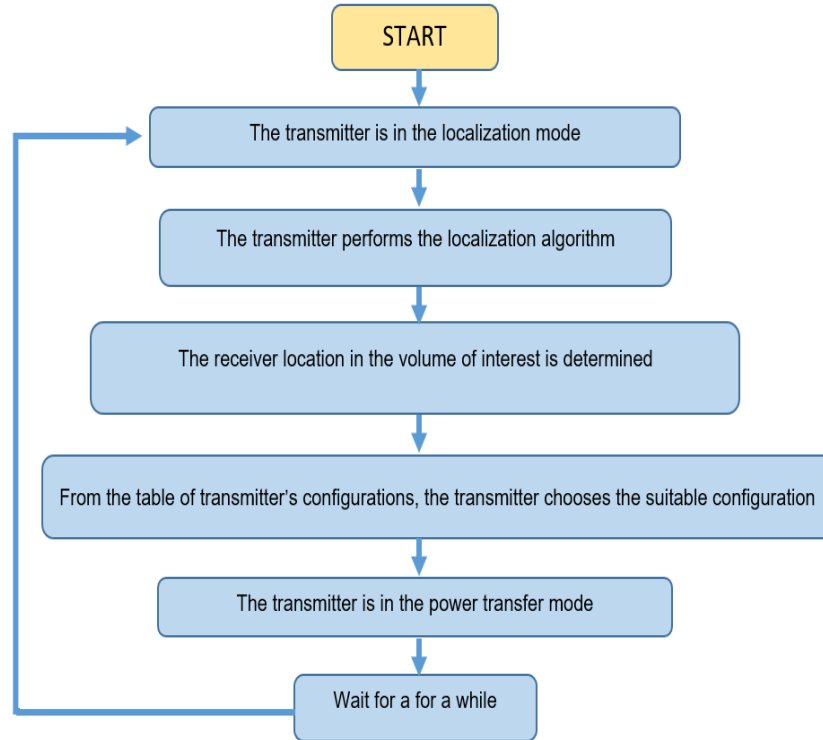


Figure 3.34: The chart for the process of localization and power transfer.

Fig. 3.34 shows the flowchart of this process.

For the experimental demonstration, the receiver was placed at different arbitrary positions. The goal is to control the direction of the magnetic field generated by the transmitter to add constructively in the position of the receiver. In two instance of previous section tests for localization, the receiver was at the positions and localized positions shown in the table 3.5

Experiment	The real position of the receiver	The deduced position of the receiver
Experiment 2	X=12 cm, Y=12 cm, Z= 4 cm	X= 11.97 cm, Y=12.06 cm, Z= 3.97 cm
Experiment 3	X=6 cm, Y=5 cm, Z= 5 cm	X=5.9 cm, Y=5.07 cm, Z= 5 cm

Table 3.5: Experimental results for localization that we will use for magnetic beam steering.

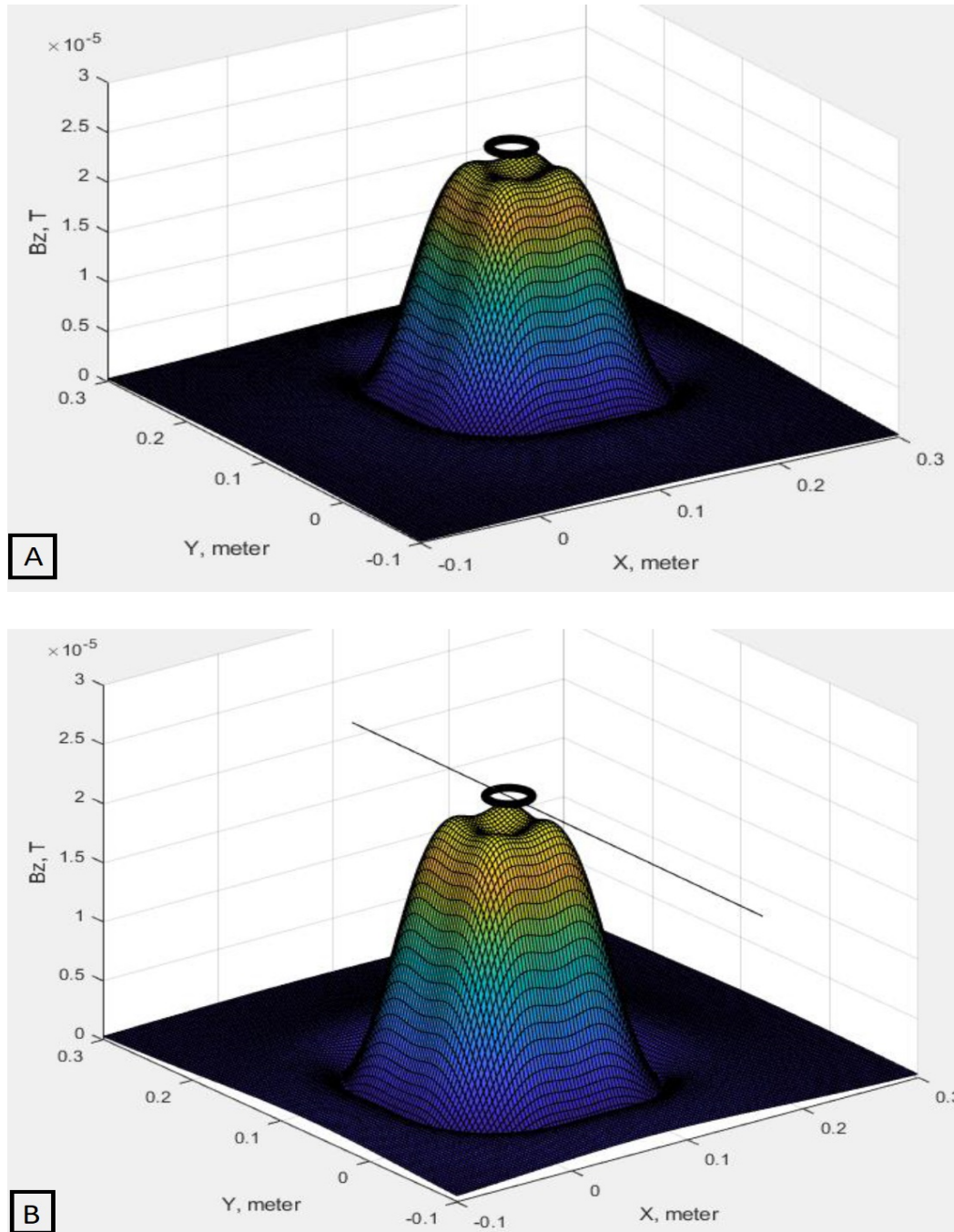


Figure 3.35: Calculation for z component of the magnetic for two different configurations of the transmitter suitable for (A panel) when the receiver is at the position $X = 12 \text{ cm}$, $Y = 12 \text{ cm}$, $Z = 4 \text{ cm}$ and (B panel) when the receiver is at the position $X = 6 \text{ cm}$ and $Y = 5 \text{ cm}$, $Z = 4 \text{ cm}$. The maximum of the generated field (z component) takes place at the position of the receiver. The black line in (B panel) is used to indicate the path along which measurement will be performed (shown in Fig.3.36) to compare the experimental results to the calculated results shown here.

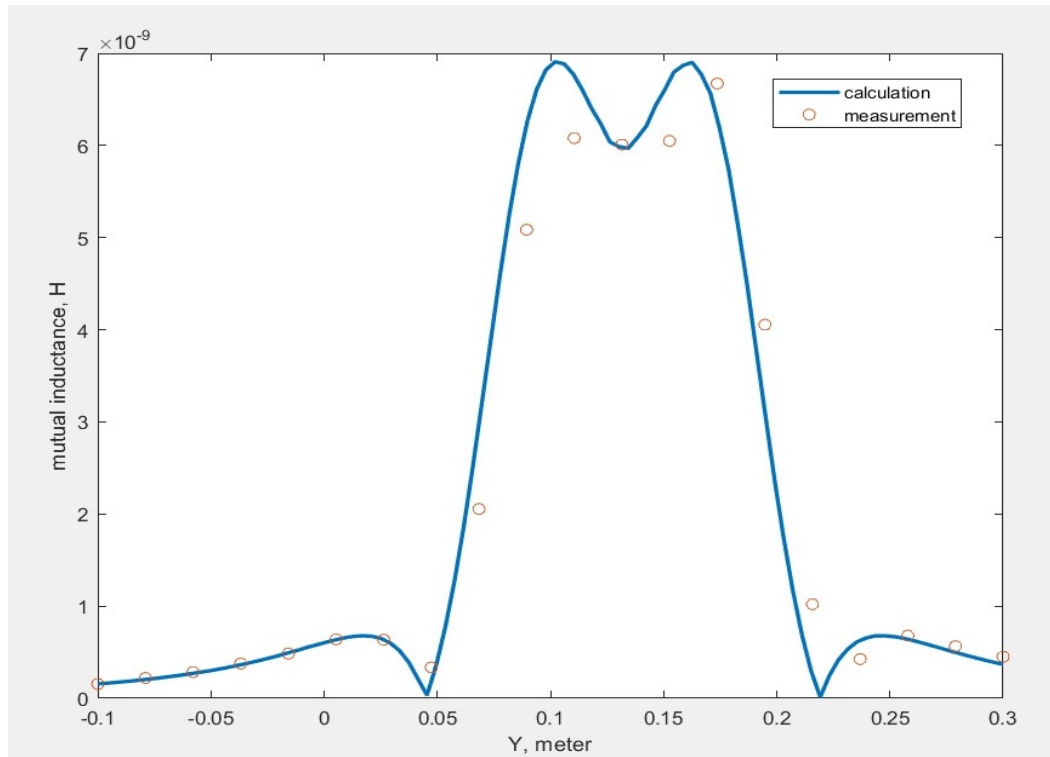


Figure 3.36: Mutual inductance along the black line shown in Fig. 3.35. This line extends from point (X=6 cm, Y=-1 cm, Z=4 cm) to point (X=6 cm, Y=30 cm, Z=4 cm). The mutual inductance increases where the receiver is positioned and falls down in other locations.

For testing the beam forming performance of the system, these two points are chosen as the position of the receiver and the goal is to produce a magnetic field which is suitable for them by choosing certain configuration for the transmitter.

For the moment the interest is just in the Z component of the field because of the assumption that the receiver is in XY horizontal plane and only the Z component contributes to the mutual inductance.

Fig. 3.35 shows the calculation of the perpendicular z-component of magnetic field, for two different configurations, each one is suitable to one of the locations of the receiver, explained above. The configuration of the transmitter is different depending on the location of the receiver, in a way that it guarantees there is a sufficient mutual inductance between the transmitter and the receiver. It shows that for two different positions of the receiver the peak of the field tracks the position of the receiver.

Fig. 3.36 shows the measured values for the mutual inductance for a configuration of transmitter which is suitable for the case where the receiver is in the position X = 6 cm, Y = 5 cm, Z = 4 cm (for which the calculation of the magnetic field is shown in B panel of the Fig.3.35). As one can see, the calculated and the measured values are close enough (the errors vary from 10% at its maximum to a negligible value at its minimum) to show the applicability of the algorithm for positioning and subsequently redirecting the magnetic field toward the position of the receiver (beam forming).

3.6 CONCLUSION

In this chapter a new algorithm, to the best knowledge of the authors, was investigated for localization in near field suitable for inductive power transfer or other applications which are using IPT (like LF and HF RFID and NFC).

Simulations were done by using a specific MATLAB code and its applicability was demonstrated by running a set of experiments.

The experimental results show that the algorithm operates as expected and it is possible to localize the receiver depending on its magnetic mutual coupling with the transmitter. If the same procedure is performed continuously, one could track dynamically the movement of the receiver.

It was assumed that the receiver is in an unknown position but always parallel to the transmitter. This assumption was made for the sake of simplicity and does not affect the algorithm principle and utility.

The algorithm could be modified for localizing a receiver in a more general situation in which the receiver could have any arbitrary orientation.

After localization also it was shown how the knowledge about the receiver location could be used to enhance the magnetic coupling between the transmitter and the receiver: by means of a switch-able grid of coils to steer the magnetic field properly towards the receiver.

This beam forming approach allows to increase the mutual inductance between the transmitter and the receiver and to increase the efficiency of such inductive power transfer systems. The algorithm in its current state is capable of localizing one receiver in the volume of interest and could be improved to localize more than one receiver as a perspective of this work.

At the end, it should be mentioned that the aim of this chapter was to show the feasibility of the idea of using different mutual inductances between the receiver and different coils of transmitter for localization of the receiver. Measurements of the mutual inductance between the receiver and the transmitter were completed by using a VNA, having access to both the transmitter and the receiver as a two-port network.

However, this is not a realistic scenario. In real world applications there is no access or control upon the receiver. The next step of our work is to adapt the current algorithm to measure the mutual inductance between the transmitter and the receiver only by having access to the transmitter, which is the case in practice.

The main difference here will be how to measure the mutual inductance between the transmitter and the receiver by just having access to the transmitter.

Is it possible to measure the mutual inductance in this way accurately enough to perform the algorithm? Or the measured mutual inductance by just having access to the transmitter could not be precise enough for the algorithm to be performed?

So now our next question is how to move from two-port network in measuring the mutual inductance, to one-port network for measuring the mutual inductance.

In next chapter we will see that this transition towards a more realistic system is possible indeed and we just need to add another elements to our transmitter to be able to deduce the mutual inductance from only the input impedance of the transmitter without need to have any access to the receiver.

Chapter 4

ONE PORT RECONFIGURABLE COIL GRID FOR RECEIVER LOCALIZATION IN INDUCTIVE POWER TRANSFER

4.1 INTRODUCTION

The main subject which was discussed in the previous chapter was the realization of a transmitter antenna (a grid of coils) supplied by an algorithm which enables the transmitter to localize receiver and sequentially steering the magnetic field toward the receiver.

The algorithm depends on the measuring of the mutual inductance between the transmitter and the receiver.

However in that chapter, we being more interested in showing that the method could localize the receiver in principle. We assumed that we have access to both receiver and transmitter. Hence the measurement of the mutual inductance was performed by connecting both transmitter and the receiver to a VNA.

This is clearly not practical. In this chapter we will try to address this problem.

The goal of this chapter is to arrive at a more practical system in which we could localize the receiver by having no access or control on it at all. The only thing that we have access to is the transmitter. This is completely a practical scenario.

In this case our circuit will be modelled by one port network, unlike the model in the previous chapter in which we model the circuit by a two ports network. In this chapter we will see that changing from two ports to one port network requires transmitter resonance in the frequency range of operation, using magnetically coupled resonator structures. This will take us to the magnetically coupled resonator which is widely used in today's state of

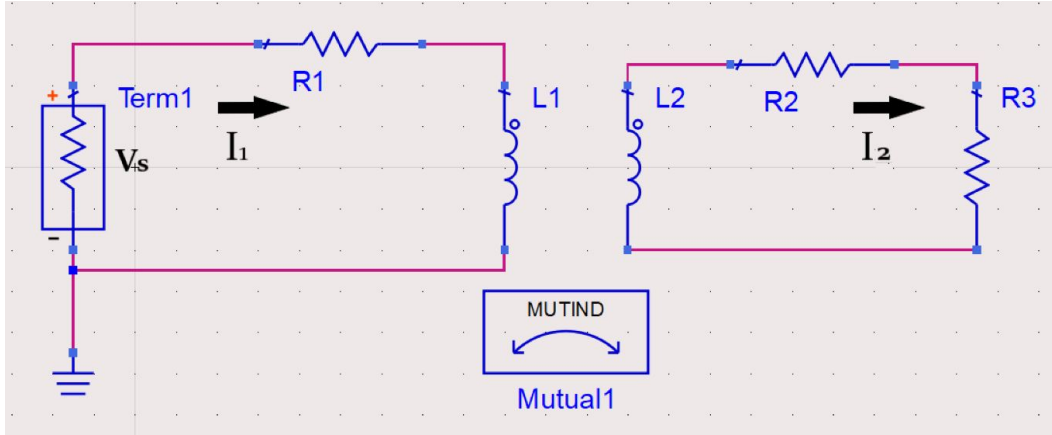


Figure 4.1: The $L1$ and $R1$ are respectively the inductance of the transmitter and the resistance of the transmitter, the $L2$ is the inductance of the receiver, the $R2$ is the resistance of the receiver, $R3$ is R_{LOAD} which is the load connected to the receiver and the M (labeled as MUTIND and Mutual1) is the mutual inductance between the transmitter and the receiver. I_1 and I_2 are the currents in loop 1 and loop 2, and V_s is the voltage applied to the port 1, shown by Term1.

art in WPT.

So we will replace the simple magnetically coupled transmitter-receiver system to a magnetically coupled system which will allow us to move from two ports network to a one port network.

In one port network we will find it sufficient to deduce the mutual inductance only from measuring the input impedance of the transmitter antenna circuitry.

We also will show that, this algorithm is consistent with the presently in-use systems in RFID and WPT and the capability of localization could be added to the presently in-use systems by adding simple modification to them.

We will start by explaining some modifications we have to perform on the algorithm explained in the previous chapter. After that we will continue by simulation and finally we will perform the required experiments to validate the algorithm and our method in new one port network set up.

4.2 MAGNETICALLY COUPLED RESONATOR

Consider the schematic in Fig. 4.1. It represents the simplest model of two magnetically coupled inductors (say two coils) as one port network. In this one port network configuration, we only have access to the transmitter port, meaning that we can measure the current through it, the voltage across it or equivalently its impedance.

In Fig. 4.1 the $L1$ and $R1$ are respectively the inductance of the transmitter and the resistance of the transmitter, the $L2$ is the inductance of the receiver, the $R2$ is the resistance of the receiver, R_{LOAD} is the load connected to the receiver and the M is the mutual inductance between the transmitter and the receiver.

$L1$, $R1$, $L2$, $R2$ and R_{LOAD} are not variable, and that means they are not affected by the relative positioning between the receiver and the transmitter. We already know their values.

What we don't know is the M, the mutual inductance between transmitter and the receiver which is a variable that changes based on the relative positioning between the receiver and the transmitter. We could measure the voltage and the current in the transmitter side but not on the receiver side. Our point is to drive from what we already know (L_1 , R_{L1} , L_2 , R_{L2} and R_{LOAD}) and what we could measure (the current and the voltage in transmitter side), the value of the mutual inductance M.

We start by writing the equation for each loop. For loop 1 in Fig. 4.1, we have:

$$V_s = I_1 R_1 + I_1 j\omega L_1 - I_2 j\omega M \quad (4.1)$$

For loop 2 we have:

$$0 = -j\omega M I_1 + (R_2 + j\omega L_2 + R_{LOAD}) I_2 \quad (4.2)$$

If we now simplify by defining Z_{11} and Z_{22} to be:

$$Z_{11} = \frac{V_s}{I_1} = R_1 + j\omega L_1 \quad (4.3)$$

$$Z_{22} = R_2 + j\omega L_2 + R_{LOAD} \quad (4.4)$$

we get:

$$V_s = Z_{11} I_1 - j\omega M I_2 \quad (4.5)$$

$$0 = -j\omega M I_1 + Z_{22} I_2 \quad (4.6)$$

The input impedance of the transmitter is the ratio of the voltage applied to it to the current it drives from voltage source, $Z_{in} = \frac{V_s}{I_1}$, if we solve equations 4.5 and 4.6 for getting this ratio we get:

$$Z_{in} = \frac{V_s}{I_1} = Z_{11} - \frac{(j\omega)^2 M^2}{Z_{22}} \quad (4.7)$$

We are interested in deducing the value of M from the equation 4.7. We note in equation 4.7, that the input impedance is simply Z11 if the coupling is reduced to zero. Z11 is independent of M and it is constant and not of much of use for us.

As the coupling increases from zero (increase in M), the input impedance differs from Z11 by an amount $\frac{\omega^2 M^2}{Z_{22}}$. It is this part which depends on M and could be useful for us.

So we are going to neglect Z_{11} for the moment and concentrate on the second term in equation 4.7 which is relevant to our work: Lets call it ΔZ .

If we substitute for Z_{22} in equation 4.7 and rationalize it we get (we are assuming that R_{Load} is resistive):

$$\Delta Z = \frac{\omega^2 M^2 (R_2 + R_{Load})}{(R_2 + R_{Load})^2 + \omega^2 L_2^2} - j \frac{\omega^3 M^2 L_2}{(R_2 + R_{Load})^2 + \omega^2 L_2^2} \quad (4.8)$$

Indeed, we have the following values for the components:

$$R_2 = 120 \text{ m } \Omega$$

$$L_2 = 1 \text{ } \mu \text{ H}$$

$$L_1 = 1 \text{ } \mu \text{ H}$$

$$R_{Load} = 100 \text{ } \Omega$$

and chose the frequency of operation to be 125 kHz, to see the behaviour of the real part and imaginary part of the ΔZ as a function of M. These are shown in Fig. 4.2 and 4.3.

From figures 4.2 and 4.3 one can see that the change in input impedance is very small to be measured.

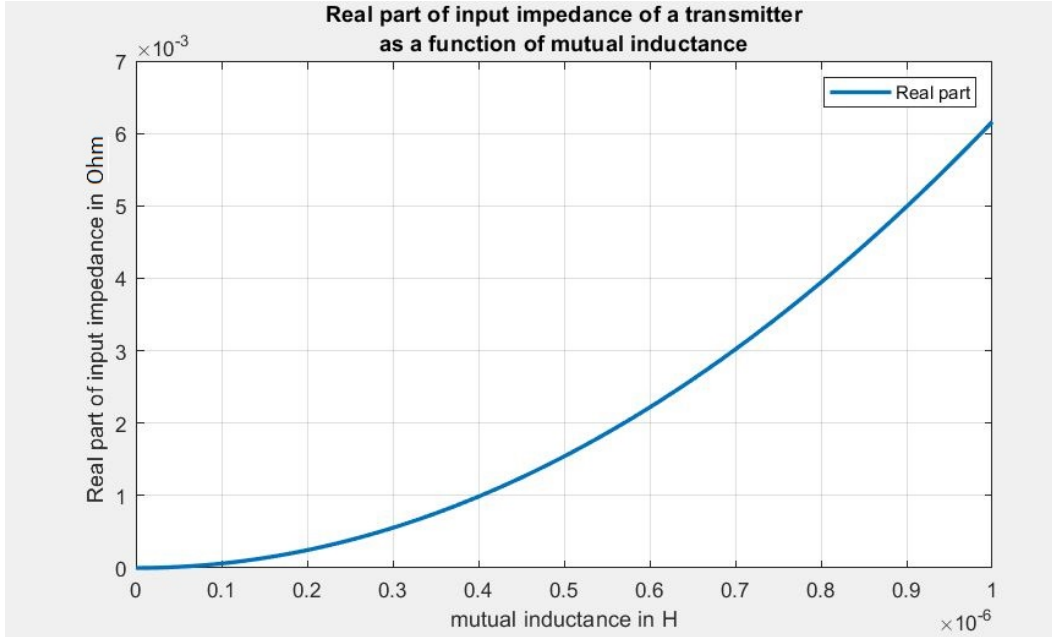


Figure 4.2: Simulation of real part of input impedance of a transmitter as a function of mutual inductance. The mutual inductance runs from zero to its maximum value of 1 μH . One can see that the change in input impedance is very small to be measured.

Paying more attention to the equation 4.8, suggests how the change in input impedance could be improved. The first term in equation 4.8:

$$\frac{\omega^2 M^2 (R_2 + R_{Load})}{(R_2 + R_{Load})^2 + \omega^2 L_2^2} \quad (4.9)$$

must be positive. When we express the impedance as a complex number, it is understood from circuit theory that the real part of the impedance is related to the energy which will be consumed (by whatever device that we are assigning the impedance to) and the imaginary part is related to the energy which will be stored (by whatever device that we are assigning the impedance to).

From the vantage point of the source of energy connected to the transmitter, this increase in the real part of impedance is equivalent to the increase of energy consumption of the transmitter .

But the transmitter has not changed (with or without coupling it is the same transmitter). So where this increased consumed energy goes? The only place for this energy to go is the receiver. This means if we increase the transmitted energy to the receiver, we will increase the change of impedance of the transmitter as it is seen by the source of energy. We want to increase the change of impedance so it became measurable in the limits of the sensitivity of our measuring devices (later we will see it is a VNA).

How to increase this transmitted energy? It is a well known fact in physics that the energy transmitted the best between two systems (here the transmitter and the receiver) when these two systems resonate.

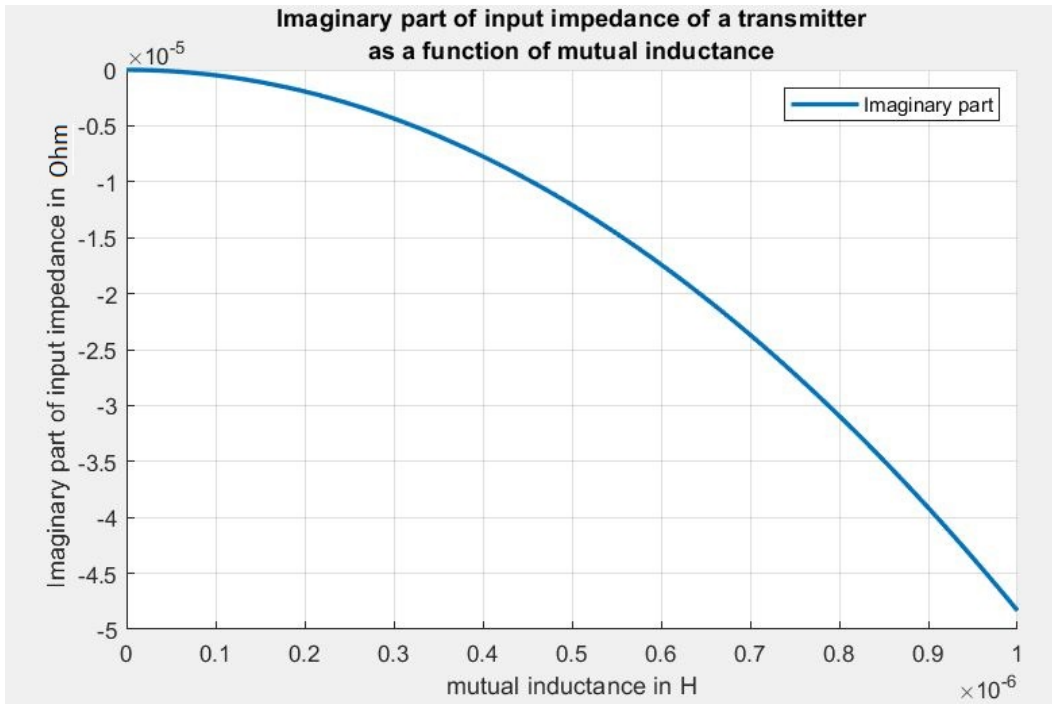


Figure 4.3: Simulation of imaginary part of input impedance of a transmitter as a function of mutual inductance. The mutual inductance runs from zero to its maximum value of $1\mu\text{H}$. One can see that the change in input impedance is very small to be measured.

This fact give rise to the concept of magnetic resonance coupling in WPT. The transmitter and the receiver could be considered as two coupled oscillators. The coupling is due to mutual inductance between them.

Magnetic resonance coupling is a method of wireless power transfer by making the transmitter resonance frequency and receiver resonance frequency the same (tuning them).

The magnetic resonance is chosen in WPT system because of its efficiency of power transferring. When power is transmitted from the transmitter to the receiver, it is seen from the transmitter point of view as a change in its input impedance. To see this, we replace the schematic shown in the Fig.4.1, with the schematic shown in the Fig.4.4.

In the Fig.4.4 L1 is the transmitter's coil self inductance, L2 is the receiver's coil self inductance. C1 is the capacitor in the transmitter side and the C2 is the capacitor in the receiver side. R1 is the stray resistance of the transmitter and RL is the load connected to the receiver and it includes the stray resistance of the receiver coil.

It should be mentioned that this is one of four general possible approaches to make the transmitter-receiver system resonates. These four topologies are:

1. Series – Series transmitter-receiver magnetic resonance coupling.

In which the transmitter coil is brought to resonance by adding a capacitor in series to it, and the same thing for the receiver coil.

2. Series – Parallel transmitter-receiver magnetic resonance coupling.

In which the transmitter coil is brought to resonance by adding a capacitor in series to it, and the receiver coil is brought to resonance by adding a parallel capacitor to it.

3. Parallel – Series transmitter-receiver magnetic resonance coupling.

In which the transmitter coil is brought to resonance by adding a capacitor in parallel to it, and the receiver coil is brought to resonance by adding a series capacitor to it.

4. Parallel – Parallel transmitter-receiver magnetic resonance coupling.

In which the transmitter coil is brought to resonance by adding a capacitor in parallel to it, and the receiver coil is brought to resonance by adding a parallel capacitor to it.

For the sake of demonstration we are going to chose the fourth topology in which the transmitter is a parallel resonance circuit and the receiver also is also a parallel resonance circuit. Though these topologies sometimes show different behaviour in different situation for our work, These differences are not important and they are the same.

To analyse the input impedances of the circuit shown in Fig.4.4, we start by applying the Kirchhoff voltage law to each loop, from the fifth loop on the right (the loop with RL) back to the first loop on the left (the loop with voltage source).

For the fifth loop we have equation 4.10. Solving this equation for I5, and substitute it in the equation for loop four gives equation 4.11. Solving this equation for I4, and substitute it in the equation for loop three gives equation 4.12. Solving this equation for I3, and substitute it in the equation for loop two gives equation 4.13. Now we have to substitute I2 from this equation in the equation for first loop than divide it by I1 to get the input impedance.

This gives us the equation 4.14 and equation 4.15 for the input impedance. This is the impedance seen by the voltage source.

This input impedance is a function of all parameters of the schematic shown in Fig.4.4: R1, C1,L1, M, L2, C2, RL and the frequency of operation.

To see the behaviour of this function we fix the value of each component as follows:

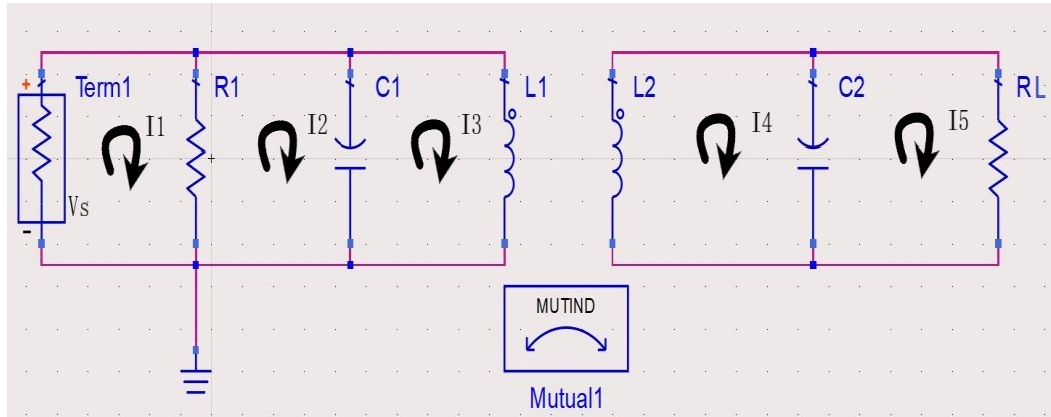


Figure 4.4: Parallel – Parallel transmitter-receiver magnetic resonance coupling schematic. V_s is the applied voltage and I_1 , I_2 , I_3 , I_4 and I_5 are the currents in each loop.

$R_1=5$ Ohm
 $C_1=1.62$ μ F
 $L_1=1$ μ H
 $C_2=1.62$ μ F
 $L_2=1$ μ H
 $R_L=100$ Ohm

Then we plot the input impedance as a function of the two other parameters, namely mutual inductance (M) and the frequency.

Because we chose the self inductance of the transmitter and receiver coils to be 1 μ H, the mutual inductance between them could not be more than 1 μ H. So we change the mutual inductance in its possible range between 0 H and 1 μ H. For frequency we sweep between 1 kHz and 400 kHz.

Input impedance is a complex number and have two parts, real part and imaginary part. The result for real part is shown in Fig.4.5 and the result for imaginary part is shown in Fig.4.6.

Here we can see the phenomena of frequency splitting.

When the mutual inductance is zero, the transmitter and the receiver are uncoupled oscillator. The transmitter acts as a single oscillator with resonance frequency determined by the values of L_1 and C_1 . But when the mutual inductance is not zero, the transmitter-receiver acts like two coupled oscillators with two degrees of freedom.

From the theory of wave and oscillation (mention book) we know that having two degrees of freedom is equivalent of having two normal modes of oscillation.

The frequency of oscillation of these two normal modes is depending on the coupling factor (here mutual inductance).

When the transmitter-receiver oscillates in the frequency of one of the normal modes, it resonates.

In this case the reactive parts of input impedance due to the inductor and the capacitor cancel each other and we see a rise in real part of the input impedance and vanishing to zero of the imaginary part of the input impedance of the transmitter-receiver system (for

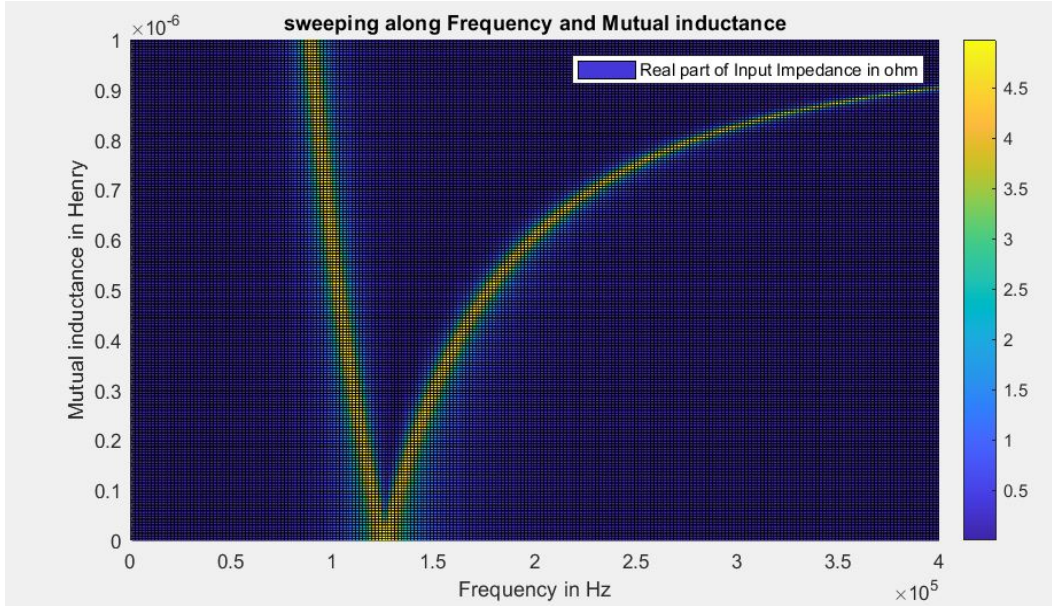


Figure 4.5: The real part of the input impedances of the circuit in Fig.4.4 as a function of the mutual inductance(M) and the frequency. This result shows what is known as frequency splitting.

parallel topology).

That is why we have a pick in the resonance frequency in Fig.4.5 and a zero in the resonance frequency in Fig.4.6.

To see this better, we fix the value of mutual inductance to four different values from minimum possible ($M=0$) to maximum possible ($M=1 \mu\text{H}$) and sweep along frequency. This is equivalent to see the variation of input impedance along a line parallel to frequency axis with fixed value of M .

Fig.4.7 to Fig.4.10 show this result. ¹

¹This phenomena of change in resonance frequency as a function of coupling between the transmitter and receiver, itself could be used as a method of deducing the mutual inductance between the transmitter and receiver. This will need an ability to sweep along a range of frequencies, then by calculating the shift of resonance frequency one can deduce M . However sweeping frequency needs more complicated circuitry and what we are going to propose is an easier method for deducing mutual inductance.

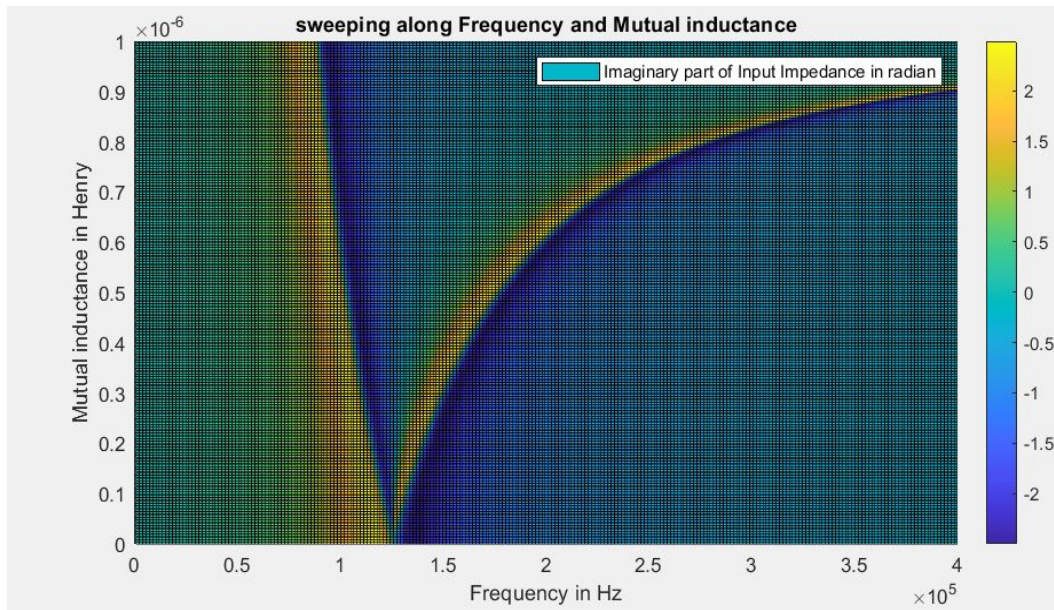


Figure 4.6: The imaginary part of the input impedances of the circuit in Fig.4.4 as a function of the mutual inductance(M) and the frequency. This result shows what is known as frequency splitting.

$$I_5 \text{RL} + \frac{(I_4 - I_5) \text{j}}{2 C_2 f \pi} = 0 \quad (4.10)$$

$$\pi I_4 L_2 f 2\text{j} - \pi I_3 M f 2\text{j} - \frac{\left(I_4 + \frac{L_4 (-1 + \pi C_2 \text{RL} f 2\text{j})}{4 \pi^2 C_2^2 \text{RL}^2 f^2 + 1} \right) \text{j}}{2 C_2 f \pi} = 0 \quad (4.11)$$

$$\pi I_3 L_1 f 2\text{j} + \frac{(I_2 - I_3) \text{j}}{2 C_1 f \pi} + \frac{4 I_3 M^2 f^2 \pi^2 (4 \pi^2 C_2^2 \text{RL}^2 f^2 + 1)}{(2 \pi C_2 \text{RL} f + 1\text{j}) (4\text{j} C_2 L_2 \text{RL} \pi^2 f^2 + 2 L_2 \pi f - \text{RL} \text{j})} = 0 \quad (4.12)$$

$$-R_1 (I_1 - I_2) - \frac{\left(I_2 + \frac{I_2 \text{j}}{2 C_1 f \pi \left(\pi L_1 f 2\text{j} - \frac{1\text{j}}{2 C_1 f \pi} + \frac{4 M^2 f^2 \pi^2 (4 \pi^2 C_2^2 \text{RL}^2 f^2 + 1)}{(4\text{j} C_2 L_2 \text{RL} \pi^2 f^2 + 2 L_2 \pi f - \text{RL} \text{j})} \right) \right) 1\text{j}}{2 C_1 f \pi} = 0 \quad (4.13)$$

$$Z_{in} = \frac{2 \pi R_1 f (4\text{j} C_2 \text{RL} \pi^2 M^2 f^2 + 2 \pi M^2 f - 4\text{j} C_2 L_1 L_2 \text{RL} \pi^2 f^2 - 2 L_1 L_2 \pi f + L_1 \text{RL} 1\text{j})}{D} \quad (4.14)$$

$$D = R_1 \text{RL} + 4 M^2 f^2 \pi^2 - 4 L_1 L_2 f^2 \pi^2 - 4 C_1 L_1 R_1 \text{RL} f^2 \pi^2 - 4 C_2 L_2 R_1 \text{RL} f^2 \pi^2 - 16 C_1 C_2 M^2 R_1 \text{RL} f^4 \pi^4 + 16 C_1 C_2 L_1 L_2 R_1 \text{RL} f^4 \pi^4 + \pi L_2 R_1 f 2\text{j} + \pi L_1 \text{RL} f 2\text{j} + C_1 M^2 R_1 f^3 \pi^3 8\text{j} + C_2 M^2 \text{RL} f^3 \pi^3 8\text{j} - C_1 L_1 L_2 R_1 f^3 \pi^3 8\text{j} - C_2 L_1 L_2 \text{RL} f^3 \pi^3 8\text{j} \quad (4.15)$$

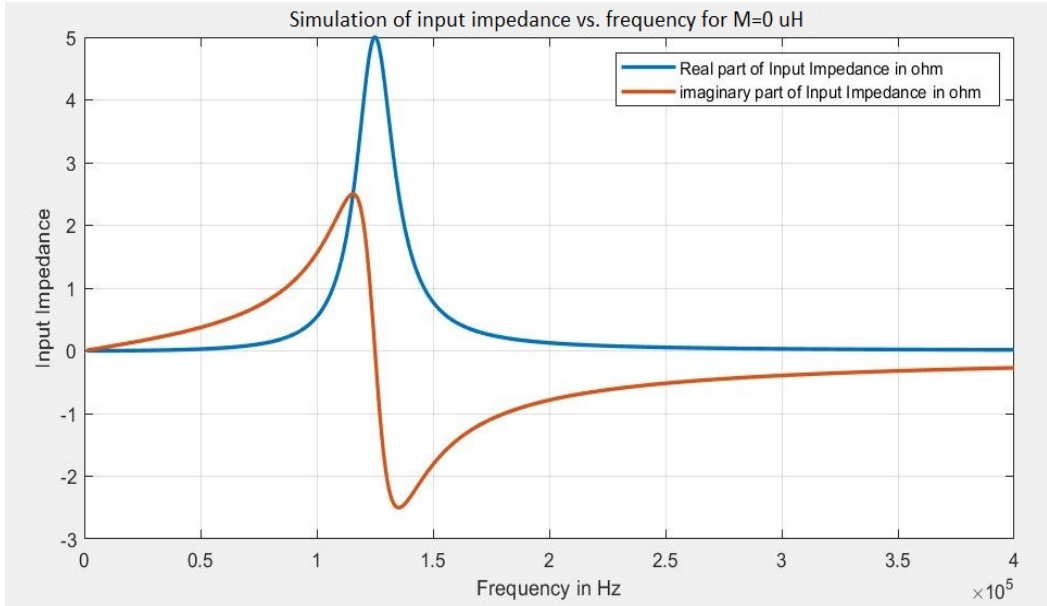


Figure 4.7: The input impedances of the circuit in Fig.4.4 as a function of frequency with $M=0 \mu\text{H}$.

The frequency splitting in general should be avoided in WPT. When it happens it means that the system does not resonate at the frequency of operation and it will resonate at another frequency and the system which does not work at resonant frequency is not very efficient in power transfer as we mentioned earlier.

However, in reality it always happen but if it does not shift the resonant frequency from the frequency of operation too much, it could be neglected.

When the peak (or zero) of the input impedance changes its position as frequency changes, it means if we fix the frequency of operation we will have variation of input impedance as variation of the mutual inductance only. To see this variation, we take the derivative of equations 4.14 in respect to mutual inductance (M) and fixing all other parameters and we get equation 4.16 for real part and equation 4.17 for imaginary part of variation of input impedance.

Fig. 4.11 shows these results. As one can see the change in input impedance as mutual inductance change is large and it should be measurable. Another important thing to notice is that, the change in input impedance is higher when the mutual inductance is small (namely when the transmitter and the receiver are weakly coupled) and when coupling is strong, the input impedance change is small. This is a good feature. It means that the transmitter and the receiver don't have to be too close to each other and that is good because if we assume that the transmitter and the receiver have to be very close to each other, there will no be no point in localization!

However what we have in Fig. 4.11 is the variation of the input impedance not its actual value that we are going to measure. The large variation necessary does not mean measurable change in input impedance. The effect of large variation could be cancelled by very small value of input impedance to start with. Fig. 4.12 shows the real part and the imaginary

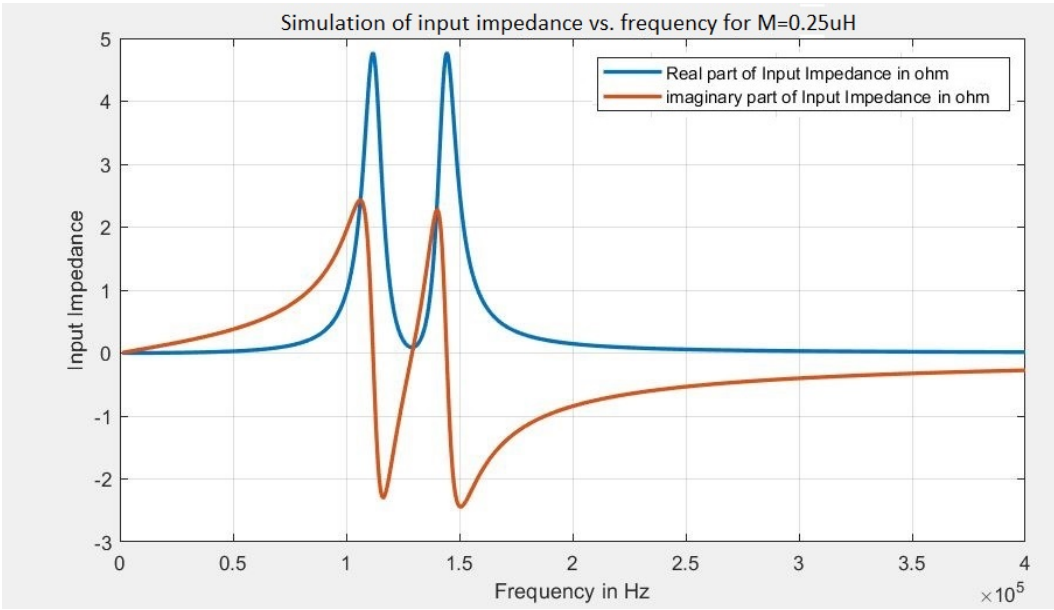


Figure 4.8: The input impedances of the circuit in Fig.4.4 as a function of frequency with $M=0.25 \mu\text{H}$.

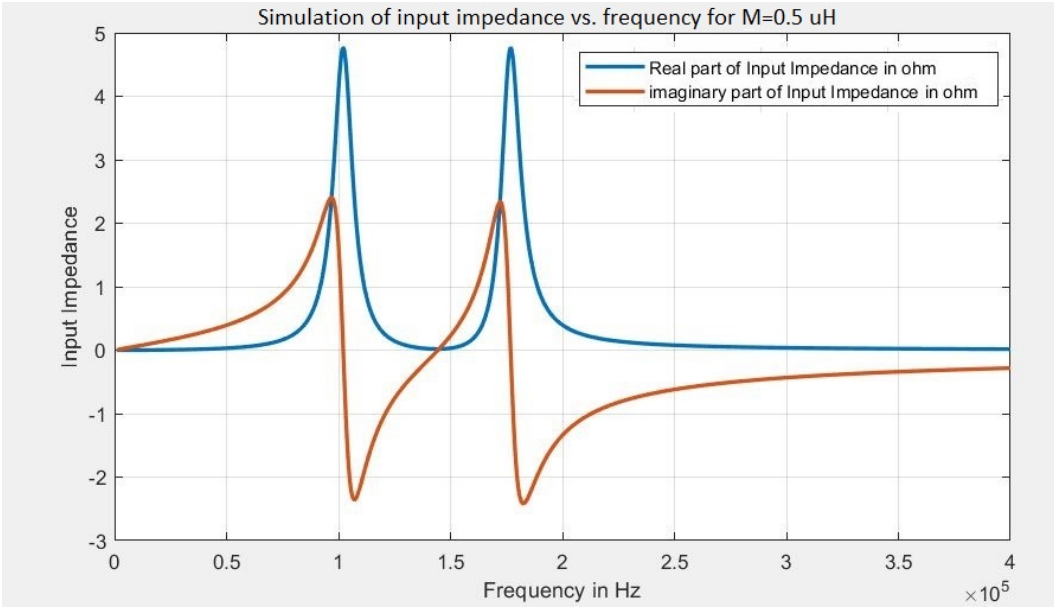


Figure 4.9: The input impedances of the circuit in Fig.4.4 as a function of frequency with $M=0.5 \mu\text{H}$.

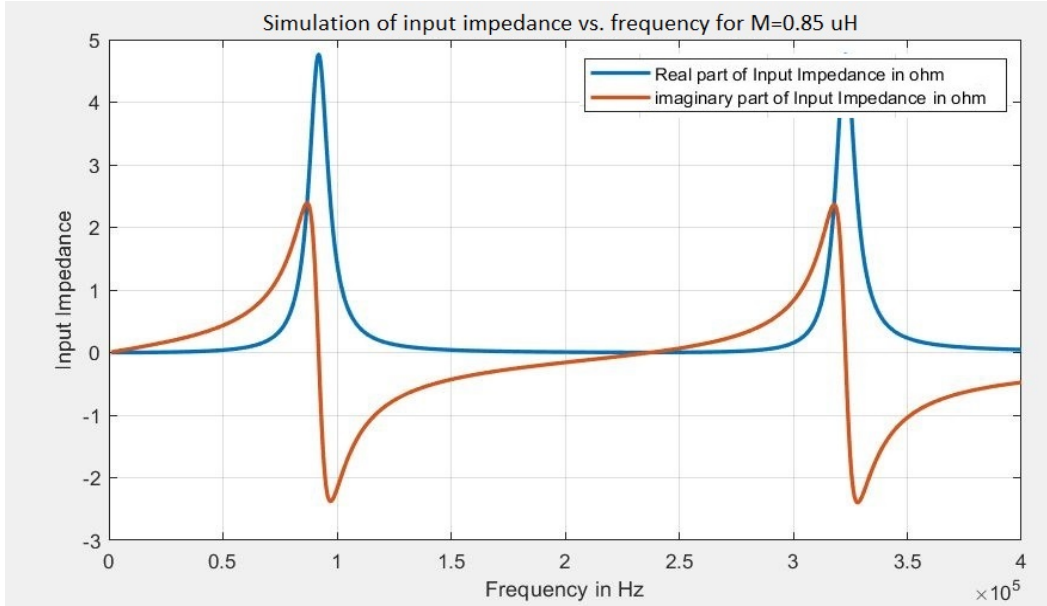


Figure 4.10: The input impedances of the circuit in Fig.4.4 as a function of frequency with $M=0.85 \mu\text{H}$.

part of the input impedance as a function of M .

The Fig. 4.12 and Fig. 4.13 should be compared to the the Fig. 4.2 and Fig. 4.3. Here one can see clearly that having resonating circuits changes the input impedances largely.

In the case of non-resonant circuit this variation was not easily measurable (given the sensitivity of available impedance meter and noise floor) but in the case of resonant circuit it is easily measurable.

Now that we know it is possible to measure the variation of input impedance as a result of change in mutual inductance we want to make sure that our algorithm is compatible and integrable with the existing protocol and standards. Though there are different standards and protocols, in near field wireless magnetic coupling, all these protocols and standards share the same principles. For that matter we should have a closer look at a realistic system (WPT or RFID) which employs the magnetic coupling in its operation. This is the content of the newt section.

$$\begin{aligned}
 \frac{dZ_{Real}}{M} &= \frac{6.5e + 20M (1.0e + 8M^2 + 7.0e - 8)}{(5.0e + 14M^2 + 0.62)^2 + (8.2e + 13M^2 + 0.058)^2} - \frac{6.2e + 12M (5.0e + 14M^2 + 0.62)}{(5.0e + 14M^2 + 0.62)^2 + (8.2e + 13M^2 + 0.058)^2} \\
 &+ \frac{7.8e + 14M (8.2e + 13M^2 + 0.058)}{(5.0e + 14M^2 + 0.62)^2 + (8.2e + 13M^2 + 0.058)^2} - \frac{3.9e + 21M (7.9e + 5M^2 - 7.9e - 7)}{(5.0e + 14M^2 + 0.62)^2 + (8.2e + 13M^2 + 0.058)^2} \\
 &3.9e + 6 (1.0e + 8M^2 + 7.0e - 8) \frac{(8.2e + 13M^2 + 0.058) (2.0e + 15M (5.0e + 14M^2 + 0.62) + 3.3e + 14M (8.2e + 13M^2 + 0.058))}{((5.0e + 14M^2 + 0.62)^2 + (8.2e + 13M^2 + 0.058)^2)} \\
 &+ \frac{3.9e + 6 (5.0e + 14M^2 + 0.62) (7.9e + 5M^2 - 7.9e - 7) (2.0e + 15M (5.0e + 14M^2 + 0.62) + 3.3e + 14M (8.2e + 13M^2 + 0.058))}{((5.0e + 14M^2 + 0.62)^2 + (8.2e + 13M^2 + 0.058)^2)} \quad (4.16)
 \end{aligned}$$

$$\begin{aligned}
 \frac{dZ_{Imag}}{M} &= \frac{3.9e + 6 (1.0e + 8M^2 + 7.0e - 8) (5.0e + 14M^2 + 0.62) (2.0e + 15M (5.0e + 14M^2 + 0.62) + 3.3e + 14M (8.2e + 13M^2 + 0.058))}{((5.0e + 14M^2 + 0.62)^2 + (8.2e + 13M^2 + 0.058)^2)} \\
 &- \frac{7.8e + 14M (5.0e + 14M^2 + 0.62)}{(5.0e + 14M^2 + 0.62)^2 + (8.2e + 13M^2 + 0.058)^2} - \frac{6.2e + 12M (8.2e + 13M^2 + 0.058)}{(5.0e + 14M^2 + 0.62)^2 + (8.2e + 13M^2 + 0.058)^2} \\
 &- \frac{6.5e + 20M (7.9e + 5M^2 - 7.9e - 7)}{(5.0e + 14M^2 + 0.62)^2 + (8.2e + 13M^2 + 0.058)^2} - \frac{3.9e + 21M (1.0e + 8M^2 + 7.0e - 8)}{(5.0e + 14M^2 + 0.62)^2 + (8.2e + 13M^2 + 0.058)^2} + \\
 &\frac{3.9e + 6 (8.2e + 13M^2 + 0.058) (7.9e + 5M^2 - 7.9e - 7) (2.0e + 15M (5.0e + 14M^2 + 0.62) + 3.3e + 14M (8.2e + 13M^2 + 0.058))}{((5.0e + 14M^2 + 0.62)^2 + (8.2e + 13M^2 + 0.058)^2)} \quad (4.17)
 \end{aligned}$$

4.3 Integrability of the localization algorithm in in-use standards

Though there are different protocols and standards regarding the operation of near field wireless power transfer and near field RFID, like frequency of operation, required data bandwidth and so on, the underlying physical principle are the same. In following discussion in this section in order to make the main idea clear, we talk specifically about HF RFID ISO 14443-Type A standard as a concrete example, but the same idea holds truth for other HF RFID, LF RFID and near field magmatic resonance wireless power transfer.

This system is composed of a transmitter and a passive receiver. In the context of RFID the receiver sometimes is called tag. Passive means there is no any source of energy in the tag and all the energy required for its operation is carried to it by the mechanism of power transfer.

The schematic in Fig.4.14 shows a generic antenna circuitry of a transmitter used in the near field magnetic coupling. In an specific applications there may be other elements that should be added to full fill the requirements demanded by certain standard, like:

- Adding an external resistor to reduce the quality factor of the antenna in order to achieve the required band- width for data communication in RFID.
- Having a bandpass filter (instead of the low pass filter shown in the schematic) for the electromagnetic compatibility. and some other requirement.

But the generic antenna circuitry remains as it is shown in the schematic. The schematic could be divided in four parts shown in Fig.4.15.

Those 4 parts are:

1. The inductor antenna, responsible of generating the magnetic field for magnetic coupling. In general the Q factor of this coil is high, so depending on the required bandwidth for data communication due to different protocols and standards probably one needs to add external resistor (not shown in the schematic).
2. The matching and resonance circuitry provides a maximum (or at least an acceptable level) of power transfer from the energy source or TX (IC pin which drives the antenna coil) to the antenna at the frequency of operation. When both transmitter (shown in Fig.4.15) and the receiver (not shown here) resonate at the same frequency, the efficiency of the system enhances significantly. That's why matching and resonance circuitry is an important part of the antenna circuitry.
3. The electromagnetic compatibility filter. Though EMC filter in not an essential part for us, it is required by most of the protocols and standards.
4. The receive circuit. The antenna coil is used for both transmitting and receiving data in half duplex mode. The RX pin of the IC is connected to the antenna coil, so a voltage is coupled back into the Rx input, this receive circuitry assures that this voltage does not exceed the maximum voltage accepted by the RX pin.

The receiver in wireless power transfer (or the tag in RFID application) is a passive device with no on-board battery or any other source of energy. The power is transmitted by mutual induction, where the time varying magnetic field created by the transmitter antenna induces an electromotive force into the receiver antenna and in doing so supplying the receiver chip with energy. In applications like RFID the transmitter is often referred to as reader, in wireless power transfer some times it is referred to as sender. Here the terms transmitter, sender and reader are used interchangeably, the term receiver or tag also are used interchangeably).

The schematic in Fig.4.16 shows a generic circuitry of a receiver used in the near field mag-

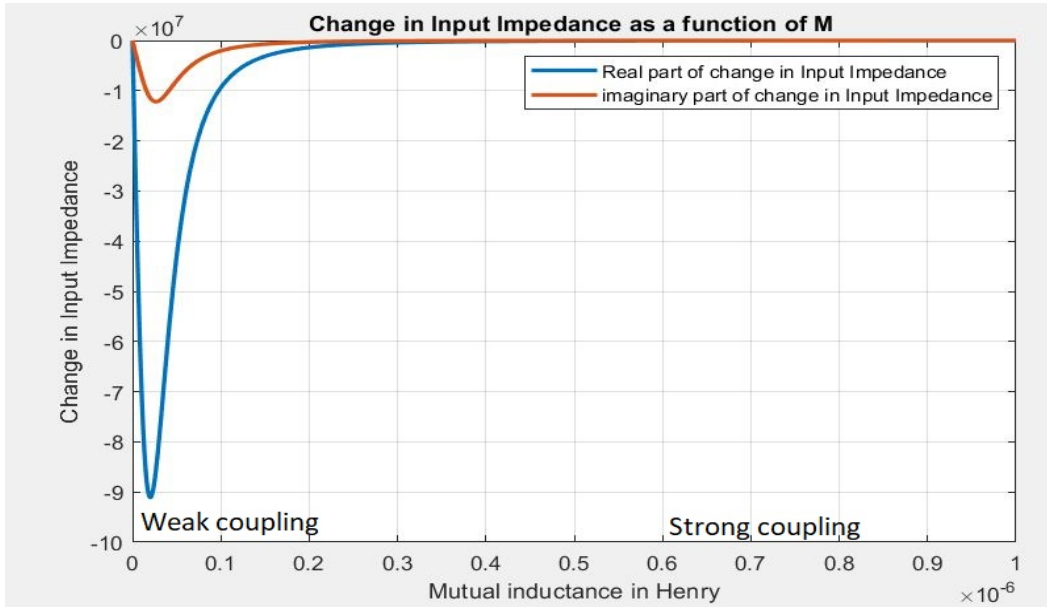


Figure 4.11: Variation of input impedance, real part and imaginary part, as a function of the mutual inductance (M). These values becomes negative because the value of input impedance reduces. Weak coupling is when the M is small, and the strong coupling is when M is high.

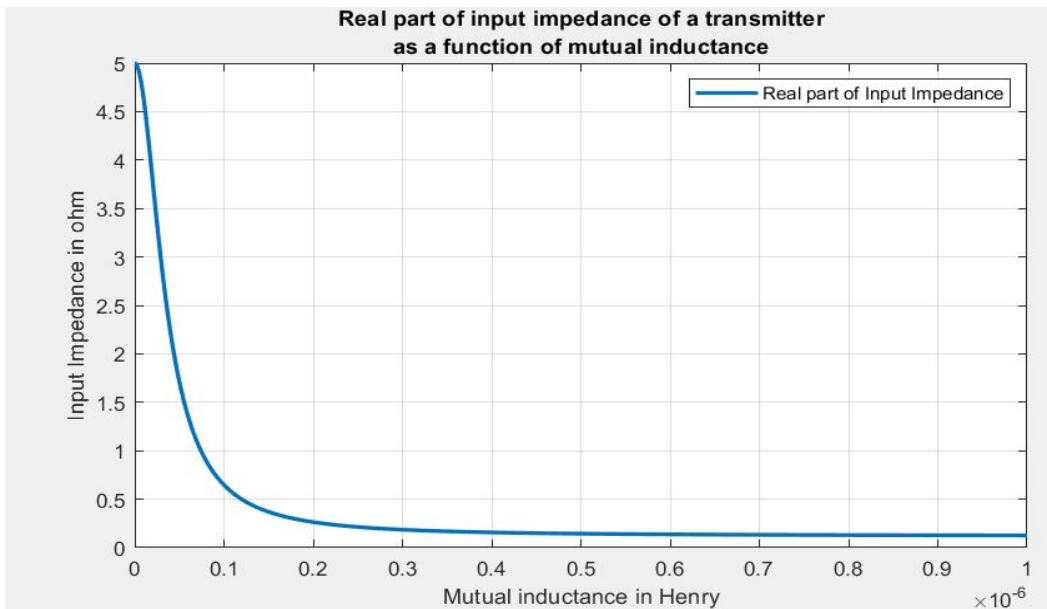


Figure 4.12: Real part of the input impedance of the circuit shown in Fig.4.4, as a function of M. Here the frequency is fixed at 125 kHz.

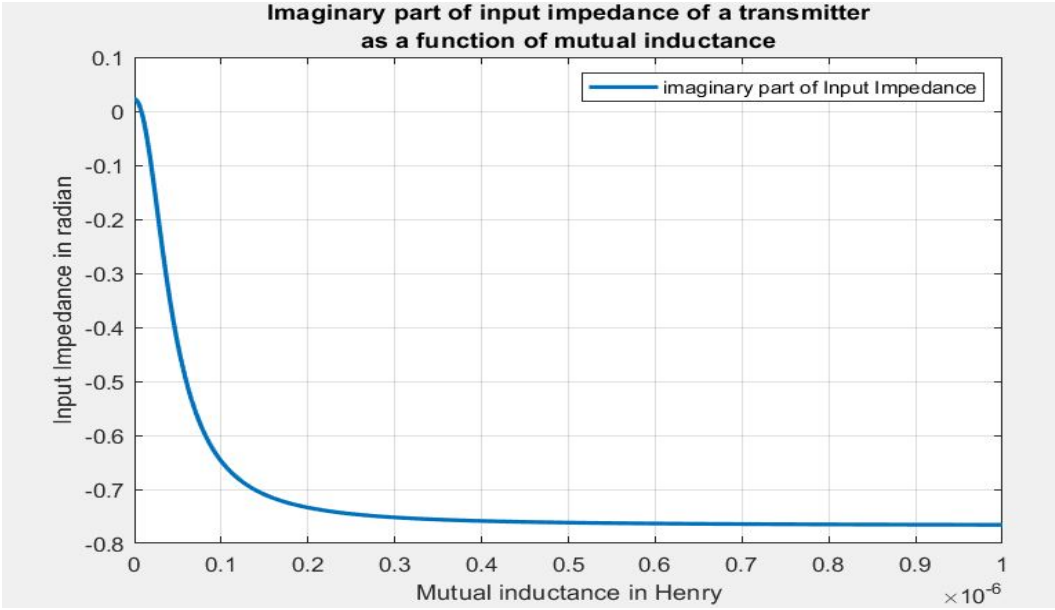


Figure 4.13: The imaginary part of the impedance of the circuit shown in Fig.4.4, as a function of M . Here the frequency is fixed at 125 kHz..

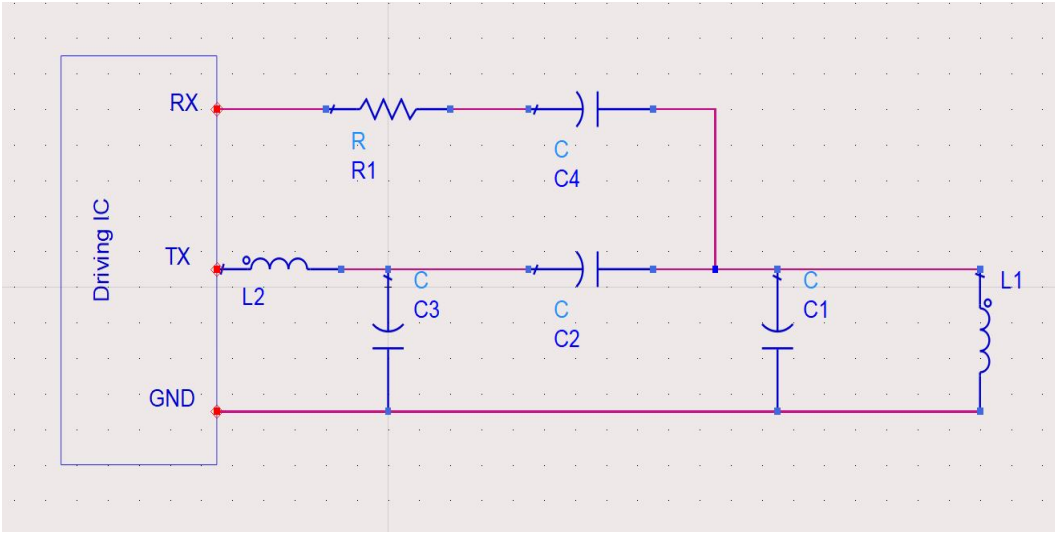


Figure 4.14: A generic antenna circuitry used in the near field magnetic coupling.

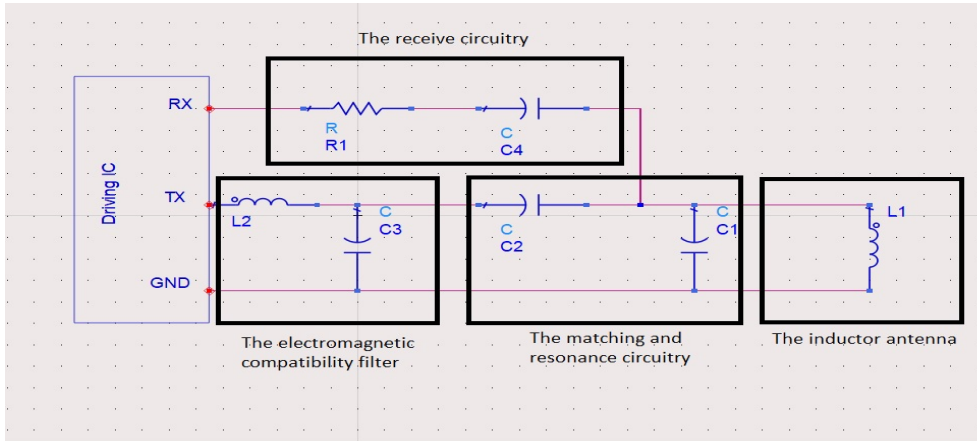


Figure 4.15: A generic antenna circuitry used in the near field magnetic coupling divided into four parts.

netic coupling. The schematic could be divided in three parts (Fig.4.16):

1. The inductor antenna which acts as a receiver antenna. The magnetic field generated by the transmitter antenna induces a voltage in this receiver antenna.
2. The resonance capacitor makes the receiver to resonate at the same frequency as the transmitter and as it was mentioned before, this significantly enhances the efficiency of the power transfer and data communication.
3. The load, which contains a circuitry for rectifying the signal and to convert it into DC signals. In magnetically coupled RFID communication, this DC signal provides necessary energy for the receiver IC to switch between two lodes according to data stored in it (load modulation). From circuit point of view it could be regarded as a variable resistor which alter between tow different values. For wireless power transfer when the emphasize is on the transmitted power more than data communication, the load could be regarded as a single resistor.

In HF RFID ISO 14443-Type A standard (which we are going to take as our example) the frequency of operation is 13.56 MHz. To show the main steps included in the process of power and data transfer, we explain the process in steps:

1. The IC that drives the transmitter is a current source which apply an alternative current of 13.56 MHz to the transmitter coil. Fig.4.17 shows the voltage that this current creates across the transmitter coil.
2. This alternative current creates an alternative magnetic field which induces an alternative voltage in the tag's coil.
3. This voltage is rectified and the tag IC is activated when the operating voltage is reached.
4. To transfer data between the transmitter and the receiver, a half-duplex communication scheme is used. The transmitter starts the communication. The data transmission from the transmitter to the receiver uses a 100% ASK modulation. Fig.4.18 shows such signal.
5. The data transmission from the tag back to the transmitter uses the principle of load modulation. The tag is designed as a resonance circuitry and consumes energy generated

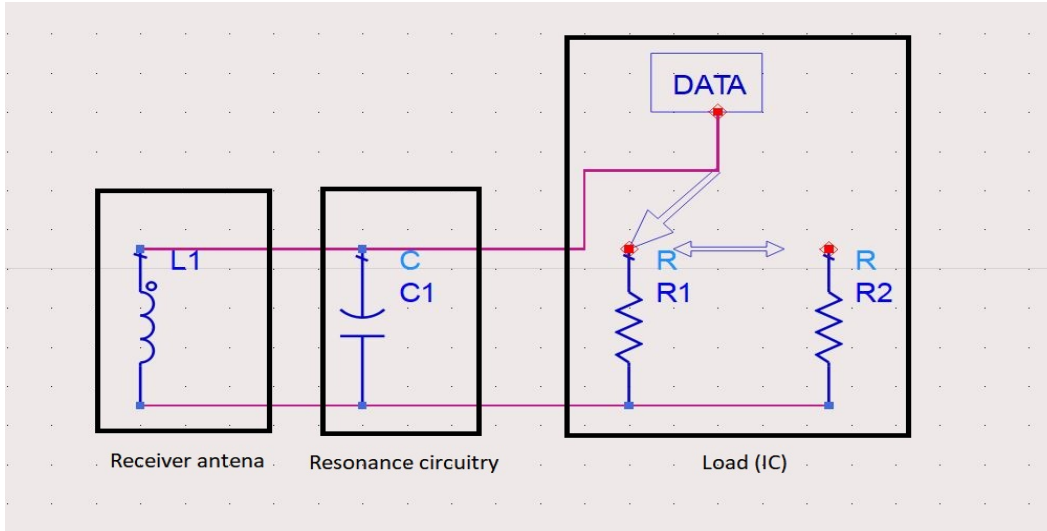


Figure 4.16: A generic receiver circuitry used in the near field magnetic coupling.

by the transmitter. This energy consumption has a feedback effect as a voltage drop on transmitter side. This effect is used to transfer data from the tag back to the transmitter by changing the load in the tag card IC. This is an On-off keying.

Fig.4.19 shows the feedback effect of this On-off keying as a voltage drop on transmitter side.

Here we just mentioned the main parts of energy and data transfer between the transmitter and the receiver. There are much more details which are irrelevant to our work such as specific data coding used by the transmitter and so on that we neglect because they are irrelevant to our work.

The data sent by the tag is extracted in transmitter side by noticing the variation of the voltage across the transmitter coil between two values, as a result of On-off keying performed by the tag. This is all what is important for the transmitter IC and not these two values themselves. The point is: These values between which the voltage varies are determined by how strong is the magnetic coupling between the transmitter and the receiver. To our best knowledge all the systems in use today just track this variation and they neglect the values between which the voltage varies.

What we propose is this: Beside tracing their alternation (which is useful for communication) if we track these values themselves, they could be used for localization.

These values could be used for determining the mutual inductance between the transmitter and tag, and after that, the mutual inductance between the transmitter and tag could be used for localization as we explained in the previous chapter.

CHAPTER 4. ONE PORT RECONFIGURABLE COIL GRID FOR RECEIVER LOCALIZATION IN INDUCTIVE POWER TRANSFER

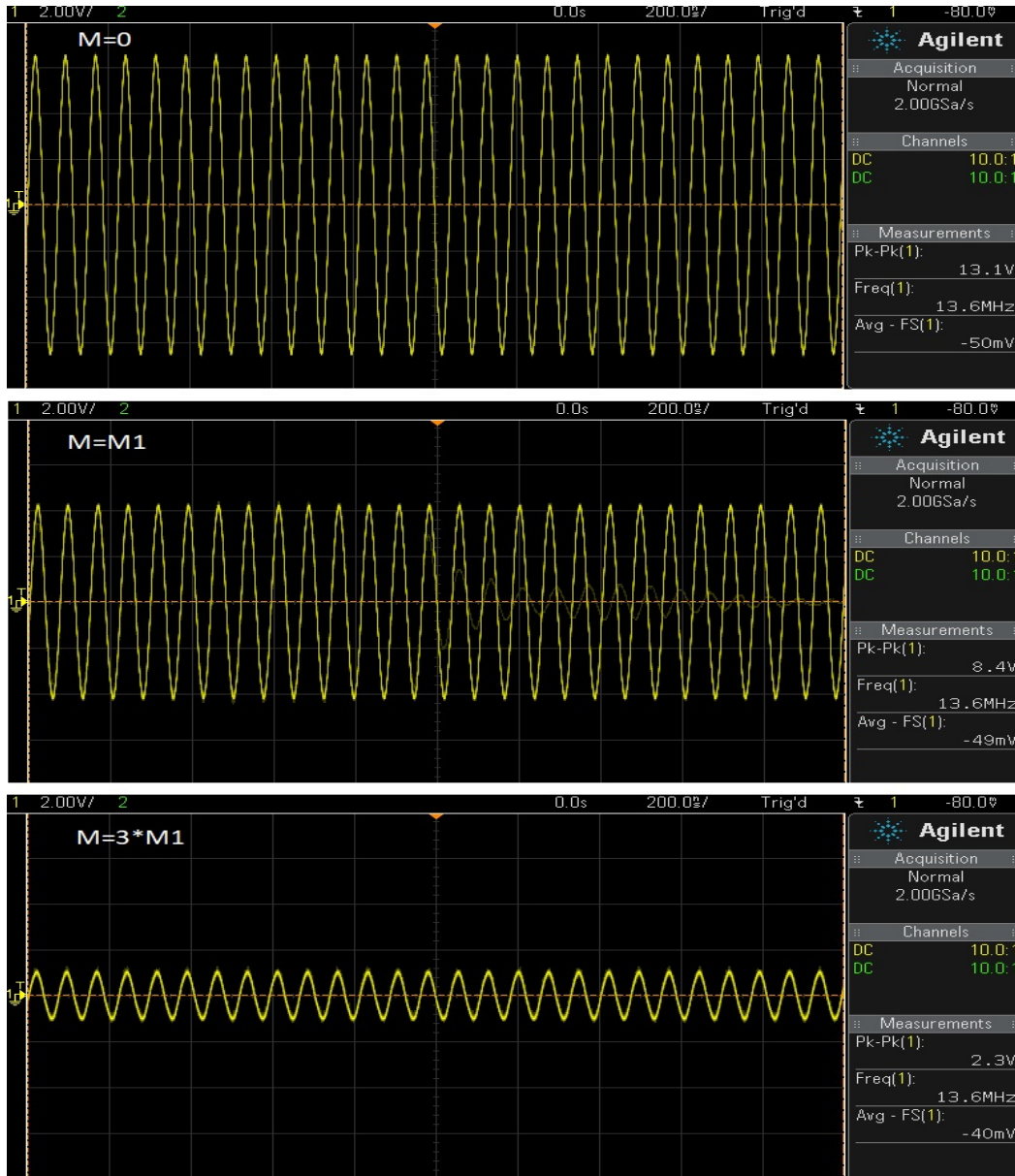


Figure 4.17: The Tx pin in Fig.4.15 is a current source. This current drives the transmitter. In these images the transmitter is in energy transmitting step. The voltage across the transmitter coil depends on the mutual inductance between transmitter and receiver. As the mutual inductance increases, for the same applied current, the voltage across the transmitter drops. The different voltages across the transmitter coil for different mutual inductances are what in-use protocols neglect and is what we use for deducing the mutual inductance. This measurement is performed on a HF RFID reader compatible with ISo 14443 Typ A standard using Agilent DSO-X 2002A oscilloscope.

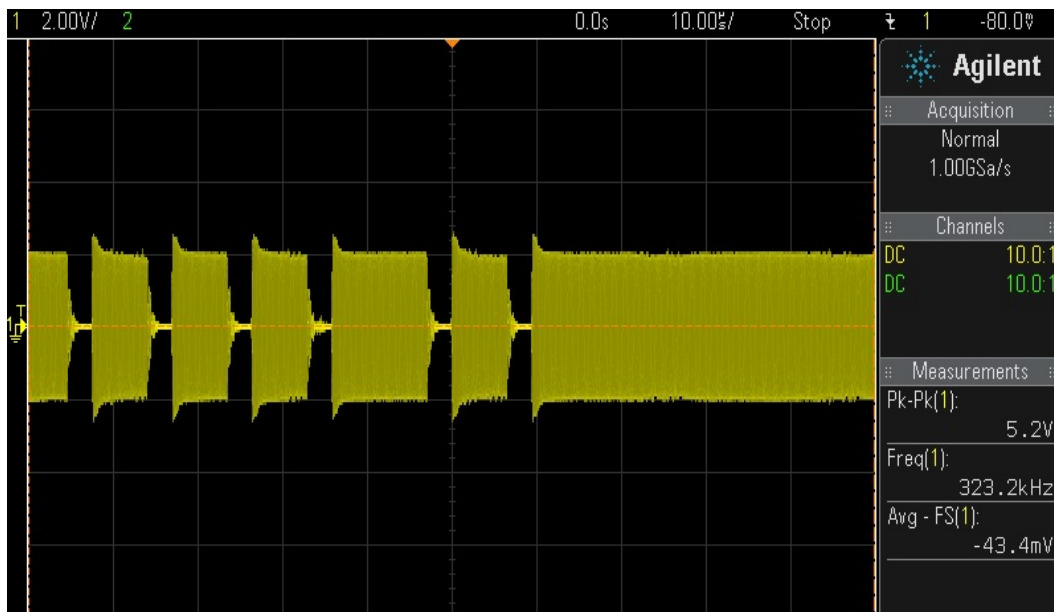


Figure 4.18: The transmitter starts the communication. The data transmission from the transmitter to the receiver uses a 100% ASK modulation. Here we show the signal for just one value of M . If the value of M changes, the signal keeps its shape, but the peak to peak values will change. This measurement is performed on a HF RFID reader compatible with ISO 14443 Typ A standard using Agilent DSO-X 2002A oscilloscope.

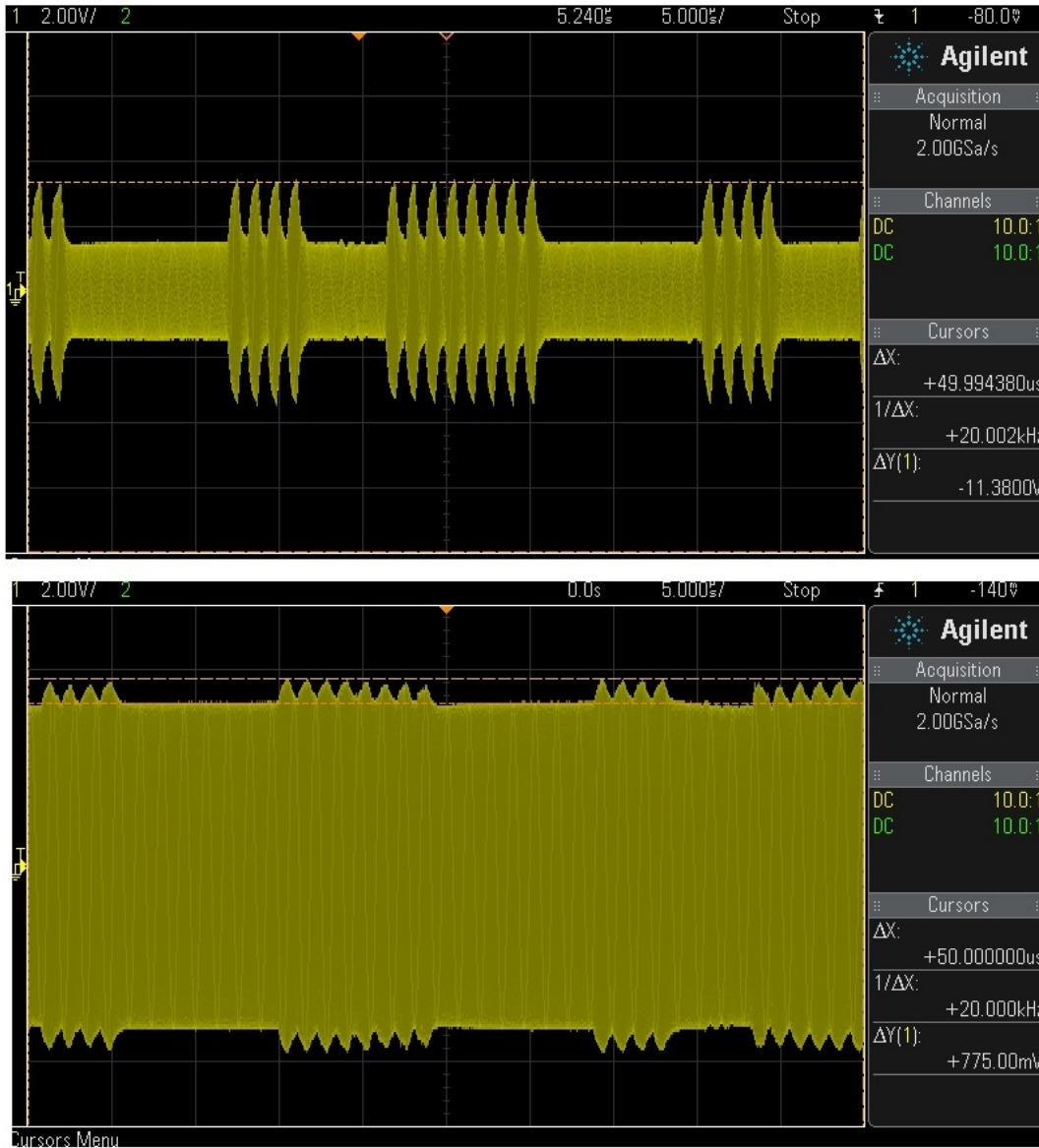


Figure 4.19: The data transmission from the tag back to the transmitter uses the principle of load modulation. This has a feedback effect as a voltage drop on transmitter side. For different coupling (different M) the signal keeps its shape, but the peak to peak values will change. The in-use protocols only pay attention to the variation of this voltage to translate it into 0s or 1s (depending on certain coding) and the peak to peak value itself is neglected. It is this peak to peak value that we are going to use for localization method. This measurement is performed on a HF RFID reader compatible with ISO 14443 Typ A standard using Agilent DSO-X 2002A oscilloscope.

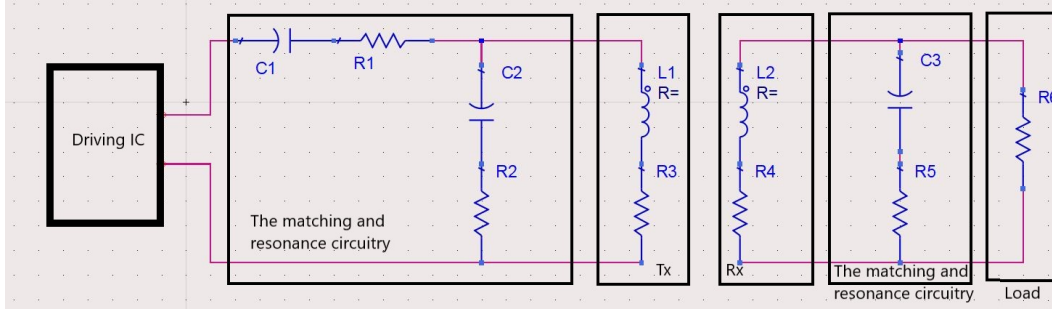


Figure 4.20: Transmitter antenna circuitry and receiver antenna circuitry that we are going to use has the main part of Fig.4.15 which is the matching and resonance circuitry part without getting us into unnecessary complication (like EMC) which are irrelevant to our work.

4.4 LOCALIZATION BY MEASURING THE INPUT IMPEDANCE

What we learned in the previous section is that the method that we proposed in chapter three, could be integrated in the in-use system just by measuring the voltage across the transmitter coil. That is the voltage at the Rx pin in Fig.4.15. For localization beside monitoring the variation of the voltage at the Rx pin (which is what is done by in-use protocols), the value of this voltage itself, should also be measured.

When we measure this voltage (the current provided by the current source in TX pin in Fig.4.15 is known) we are effectively measuring the input impedance of the transmitter antenna circuitry (shown in Fig.4.15).

When the input impedance is measured (by measuring the voltage at Rx pin in Fig.4.15 and dividing it by known current that we applied to the circuit), and the values of all other components of the transmitter antenna circuitry are known we should be able to deduce the mutual inductance between the transmitter and the receiver coils.

For doing it in practice, we will use somehow more simple transmitter antenna circuitry that have the main part of Fig.4.15 which is the matching and resonance circuitry part. In doing so we are not losing any generality and what we will do next, could be done as well for the schematic in Fig.4.15 or for any other schematic. However for the sake of simplicity and convenience we use the schematic in Fig.4.20 as our transmitter antenna circuitry and the receiver circuitry.

Our task now is to have a relation between the impedance seen by the driving IC that runs the circuit (that is the input impedance) and the mutual inductance between the transmitter coil and the receiver coil. When we have such relation, by measuring the input impedance we can deduce the value of M, assuming that we know the values of other components.

We start by the schematic in Fig.4.21 which has 4 loops with current I_1 , I_2 , I_3 and I_4 in each loop:

For the forth loop we have:

$$I_4 R_L - (I_3 - I_4) \left(R_3 - \frac{1j}{C_3 W} \right) = 0 \quad (4.18)$$

CHAPTER 4. ONE PORT RECONFIGURABLE COIL GRID FOR RECEIVER
 LOCALIZATION IN INDUCTIVE POWER TRANSFER

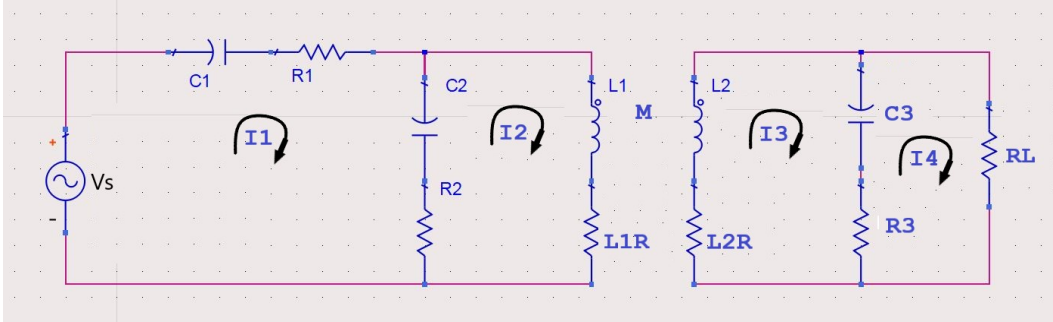


Figure 4.21: Transmitter antenna circuitry and receiver antenna circuitry that we are going to use. We want the relation between M and the input impedance of this circuit.

or

$$I_4 = \frac{I_3 \left(R_3 - \frac{1j}{C_3 W} \right)}{R_3 + R_L - \frac{1j}{C_3 W}} \quad (4.19)$$

We continue in this manner for each loop, each time we substitute equation for current from previous loop in the equation of next loop to eliminate it and we get equation 4.20 to equation 4.25. As we expect in last equation for Z_{in} we get read of all currents and voltages and it is just a function of different components of the circuit.

$$I_3 (L_2 R + L_2 W 1j) + \left(R_3 - \frac{1j}{C_3 W} \right) \left(I_3 - \frac{I_3 \left(R_3 - \frac{1j}{C_3 W} \right)}{R_3 + RL - \frac{1j}{C_3 W}} \right) - I_2 M W 1j = 0 \quad (4.20)$$

$$I_3 = \frac{I_2 M W 1i}{L_2 R + L_2 W 1i - \left(\frac{R_3 - \frac{1i}{C_3 W}}{R_3 + RL - \frac{1i}{C_3 W}} - 1 \right) \left(R_3 - \frac{1i}{C_3 W} \right)} \quad (4.21)$$

$$-(I_1 - I_2) \left(R_2 - \frac{1j}{C_2 W} \right) + I_2 (L_1 R + L_1 W 1j) + \frac{I_2 M^2 W^2}{L_2 R + L_2 W 1j - \left(\frac{R_3 - \frac{1j}{C_3 W}}{R_3 + RL - \frac{1j}{C_3 W}} - 1 \right) \left(R_3 - \frac{1j}{C_3 W} \right)} = 0 \quad (4.22)$$

$$I_2 = -(I_1 - I_2) \left(R_2 - \frac{1j}{C_2 W} \right) + I_2 (L_1 R + L_1 W 1j) + \frac{I_2 M^2 W^2}{L_2 R + L_2 W 1j - \left(\frac{R_3 - \frac{1j}{C_3 W}}{R_3 + RL - \frac{1j}{C_3 W}} - 1 \right) \left(R_3 - \frac{1j}{C_3 W} \right)} = 0 \quad (4.23)$$

$$-V_s + I_1 \left(R_1 - \frac{1j}{C_1 W} \right) + \left(R_2 - \frac{1j}{C_2 W} \right) \left(I_1 - \frac{I_1 \left(R_2 - \frac{1j}{C_2 W} \right)}{L_1 R + R_2 + L_1 W 1j - \frac{1j}{C_2 W} + \frac{M^2 W^2}{L_2 R + L_2 W 1j - \left(\frac{R_3 - \frac{1j}{C_3 W}}{R_3 + RL - \frac{1j}{C_3 W}} - 1 \right) \left(R_3 - \frac{1j}{C_3 W} \right)}} \right) = 0 \quad (4.24)$$

$$Z_{in} = R_1 - \frac{1i}{C_1 W} - \left(\frac{R_2 - \frac{1i}{C_2 W}}{L_1 R + R_2 + L_1 W 1i - \frac{1i}{C_2 W} + \frac{M^2 W^2}{L_2 R + L_2 W 1i - \left(\frac{R_3 - \frac{1i}{C_3 W}}{R_3 + RL - \frac{1i}{C_3 W}} - 1 \right) \left(R_3 - \frac{1i}{C_3 W} \right)}} - 1 \right) \left(R_2 - \frac{1i}{C_2 W} \right) \quad (4.25)$$

To test the algorithm of localization in the case of one port network (having only access to the transmitter) we start by fabricating a transmitter and a receiver according to the schematic given in the Fig.4.20.

The following values for each component are chosen. These values for capacitors are chosen to have a resonance at 125 kHz and a matching to 50 Ohm output impedance of the output from VNA that we are using for measurement (the stray resistances : R1, R2 and R3 of each capacitor are unavoidable). The values of transmitter coil inductance and the receiver coil inductance are chosen to be realistic values (the stray resistances : L1R and L2R of each coil are unavoidable). These values are:

$$\begin{aligned}
 C1 &= 10.07 \quad \text{nF} \\
 R1 &= 124 \quad \text{m-}\Omega \\
 C2 &= 109.82 \quad \text{nF} \\
 R2 &= 14.19 \quad \text{m-}\Omega \\
 L1 &= 13.68 \quad \mu\text{H} \\
 L1R &= 217.3 \quad \text{m-}\Omega \\
 L2 &= 5.16 \quad \mu\text{H} \\
 L2R &= 124 \quad \text{m-}\Omega \\
 C3 &= 300 \quad \text{nF} \\
 R3 &= 5.7 \quad \text{m-}\Omega \\
 RL &= 680 \quad \Omega
 \end{aligned}$$

(We started by commercially available capacitors, then we calculated what value of inductance is needed so we will have a resonator at 125 kHz, then we used simulation to find the diameter and number of turns in each coil to have desired inductance)

When we put these values of component in the equation 4.25 we get:

$$\begin{aligned}
 Z_{inReal} &= \frac{130.0 (1.6e + 12 M^2 + 0.23)}{(1.6e + 12 M^2 + 0.23)^2 + (1.9e + 12 M^2 - 0.85)^2} \\
 &+ \frac{0.33 (1.9e + 12 M^2 - 0.85)}{(1.6e + 12 M^2 + 0.23)^2 + (1.9e + 12 M^2 - 0.85)^2} + 0.14
 \end{aligned} \tag{4.26}$$

$$\begin{aligned}
 Z_{inImag} &= \frac{0.33 (1.6e + 12 M^2 + 0.23)}{(1.6e + 12 M^2 + 0.23)^2 + (1.9e + 12 M^2 - 0.85)^2} \\
 &- \frac{130.0 (1.9e + 12 M^2 - 0.85)}{(1.6e + 12 M^2 + 0.23)^2 + (1.9e + 12 M^2 - 0.85)^2} - 140.0
 \end{aligned} \tag{4.27}$$

With equations 4.26 and 4.27 at hand we have three unknown, Z_{inReal} , Z_{inImag} and M, two of them are easily measurable: Z_{inReal} , Z_{inImag} . That give us two equations with one unknown: M. This is more than enough for deducing M.

It is very important that one knows the correct values of the parameters making the circuit. If these components values are not measured accurately before running the algorithm and have real values rather than values that we used to get equations 4.26 and 4.27 (or any equation like equations 4.26 and 4.27), these error will show themselves as error in determining M and that will lead to wrong localization.

To determine how the accuracy of localization is effected by the inaccuracy of measuring the values of these component, we can take the derivative of the equation 4.25 in respect to each parameter and see the variation of each of these parameters on the input impedance. Because we think we measured these values accurately enough this step is not necessary here.

CHAPTER 4. ONE PORT RECONFIGURABLE COIL GRID FOR RECEIVER LOCALIZATION IN INDUCTIVE POWER TRANSFER

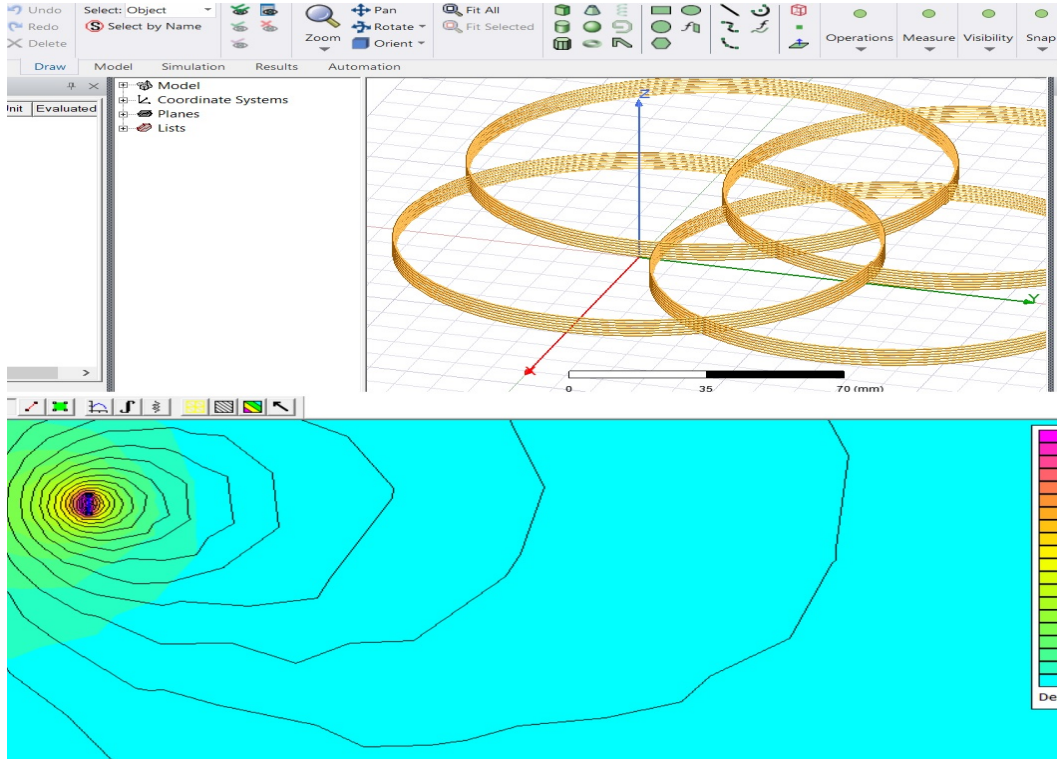


Figure 4.22: To design an inductor coils for the transmitter and the receiver that matches the capacitance of these commercially available capacitors and resonates at 125 kHz and be matched to 50 Ω we used software like FEEM (below) and Q3D Ansys (above)[26] [27].

The capacitors (as their values show) are standard commercially available capacitors. To design an inductor coils for the transmitter and the receiver that matches the capacitance of these commercially available capacitors and resonates at 125 kHz and be matched to 50 Ω we used software like FEEM and Q3D Ansys. Some simulation are shown in Fig.4.22.

We ended up with transmitter and the receiver coils having property shown in table 4.4 at the frequency of operation (which is 125 kHz)

When we put these values in the schematic in Fig.4.22, we end up with the complete circuitry for the transmitter-receiver schematic shown in Fig.4.23.

Fig.4.24 shows the fabrication of a transmitter antenna and the fabrication of a receiver antenna.

The volume of interest for testing the algorithm of localization in one port condition is consisting of a cuboid of the following dimensions:

$$\Delta x = 25cm$$

$$\Delta y = 19cm$$

$$\Delta z = 15cm$$

We use a grid of six identical transmitter coils placed underneath the volume of interest. We assign the origin of the coordinate system in a way that the center of each transmitter coil have the coordinates shown in table 4.4.

CHAPTER 4. ONE PORT RECONFIGURABLE COIL GRID FOR RECEIVER LOCALIZATION IN INDUCTIVE POWER TRANSFER

Coil	Radius	number of turns	Resistance
Transmitter	63.42 mm	7 turns	217.3 m- Ω
Receiver	49.4 mm	5 turns	124 m- Ω

Table 4.1: Properties of the transmitter(s) and the receiver.

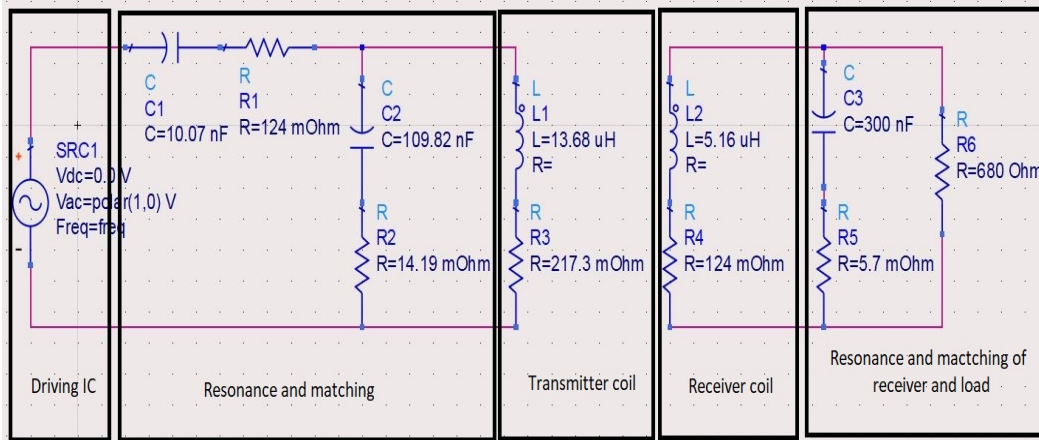


Figure 4.23: The complete circuitry for the transmitter-receiver schematic .

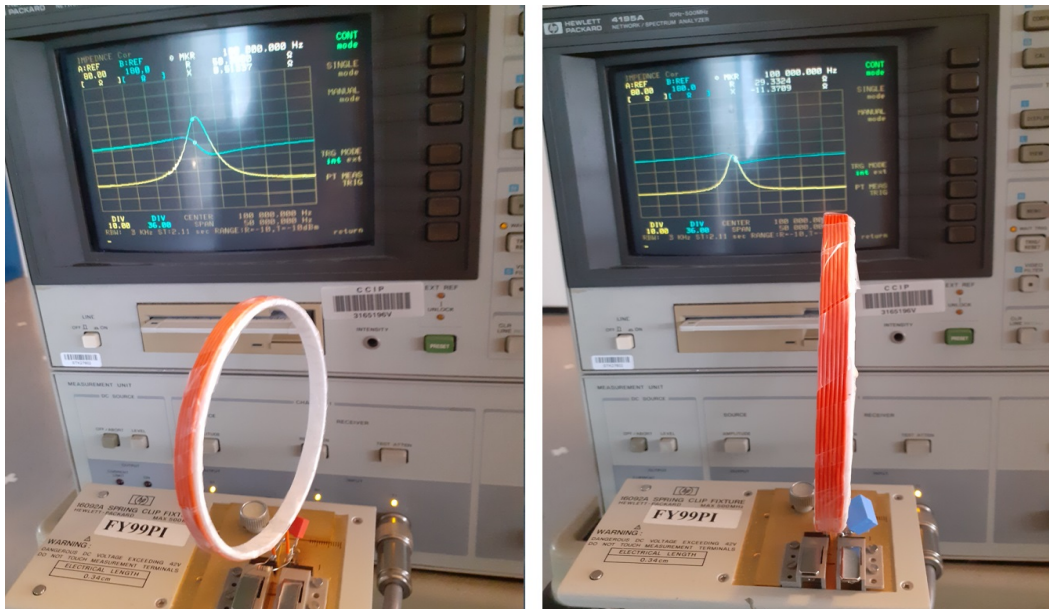


Figure 4.24: The fabrication of the transmitter antenna (right) and the fabrication of a receiver antenna (left). As we can see in the background of the picture both of them are tuned to resonate at 125 kHz. Measurements made by HP 4195.

CHAPTER 4. ONE PORT RECONFIGURABLE COIL GRID FOR RECEIVER
LOCALIZATION IN INDUCTIVE POWER TRANSFER

Coil	X coordinate	Y coordinate
The coil number 1 in Fig. 4.25	0 cm	0 cm
The coil number 2 in Fig. 4.25	63 cm	0 cm
The coil number 3 in Fig. 4.25	0 cm	63 cm
The coil number 4 in Fig. 4.25	63 cm	63 cm
The coil number 5 in Fig. 4.25	126 cm	0 cm
The coil number 6 in Fig. 4.25	126 cm	63 cm

Table 4.2: Coordinates of each coil of the transmitter. Z coordinates for all coils could not be the same because they will intersect. However they are placed as close as possible to $Z=0$, in a range of (-2.5 cm, 2.5 cm).

Fig. 4.24 shows the positions of the transmitter coils and the volume of interest.

What we are going to do is to put the receiver in a known position of the volume of

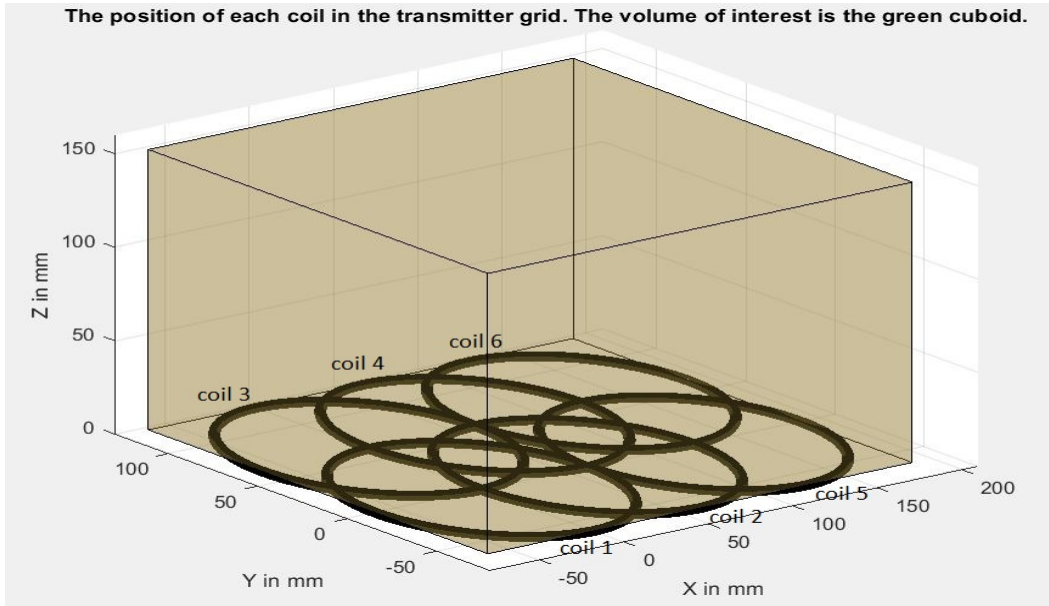


Figure 4.25: The position of each transmitter coil in the volume of interest. The position of these coils depends on the The volume of interest. The choice of position of each coil is made in a way that guarantee that they cover all the volume of interest. The volume of interest is a cuboid shown in brown.

interest, then we want to recover this position just by measuring the input impedance of the transmitter antenna. This is the first step in which the transmitter antenna localize the receiver.

Based on the location of the receiver (found in the first step) the transmitter performs the beam steering to increase the efficiency of the system. We explained this process (localization and beam steering) in the previous chapter in detail.

The only difference is that we moved from non realistic two ports set up (in which we should have access to both transmitter and the receiver) to realistic one port set up (in which we only need to have access to transmitter).

The beam steering will not be effected in this new case and it will be performed exactly in the same way it was described in the previous chapter, so we will not repeat it here. Most steps in localization also will be similar so we will explain them briefly in some steps and not in details.

1. The volume of interest is divided into 3D grid of points as following:

- 53 points along X axis with 4.7 mm spacing between each.
- 40 points along Y axis with 4.7 mm spacing between each.
- 48 points along Z axis with 3.1 mm spacing between each.

The number of points and the spacing between them is chosen arbitrary in our case but in practice they are chosen based on required accuracy of localization and the memory and

computational power available of controlling mechanism which drives the transmitter and perform the localization algorithm.

2. The mutual inductance between each coil of the transmitter (each coil of the transmitter has a known position in the volume of interest mentioned in the table 4.4) and the receiver coil is calculated as if the receiver center was to be at any of the points of the 3D grid mentioned above. This is the pre-calculated mutual inductance matrix which was mentioned in previous chapter. Each coil of the transmitter has its own pre-calculated mutual inductance matrix.

3. We put the receiver center in the known location of $X=73$ mm, $Y=24$ mm and $Z=78$ mm in the volume of interest (according to the coordinate given in table 4.4). Our goal is to deduce this position by running our algorithm.

4. The localization process is initiated by choosing a configuration of the transmitter in which all the coils are disconnected except coil number 1. This means in this configuration the transmitter is consisted only of coil number 1. Lets call it configuration 1.

5. We measure the input impedance of the antenna circuitry. This is the input impedance seen by the driving IC shown in Fig.4.23. For doing so the IC just needs to measure the voltage and from its known current (because it is basically a current source) the input impedance is deduced.

6. We find the input impedance in this specific example to be:
 $Z=43.9-17.6j$

7. We put this input impedance in the equation 4.25. All the values in equation 4.25 are known, except M , we solve it for M and we get, $M=0.205 \mu\text{H}$. It should be mentioned that we actually getting two answers from solving equation 4.25. It is reasonable because in this equation what appears in square of M not M itself. The two answers are complex conjugate of each other. We just take the positive imaginary part as M .

8. This value of the mutual inductance is compared with the pre-calculated mutual inductance matrix of the coil 1 (corresponding to the configuration 1 of the transmitter) and all the possible positions of the receiver that would lead to the same measured mutual inductance in the volume of interest are determined. There are 4507 such possible positions. Fig.4.26 shows the results.

9. The answer is not unique (localization is not performed). To reduce further more the number of possible positions and find the real position of the receiver, the configuration of the transmitter is changed. We disconnect the coil number 1 and connect only coil number 2. Now we are in a configuration in which the transmitter is consisting of only coil number two. Lets call it the configuration (2) of the transmitter.

10. We measure the input impedance of the antenna circuitry when the antenna is in the configuration 2.

11. We find the input impedance to be:

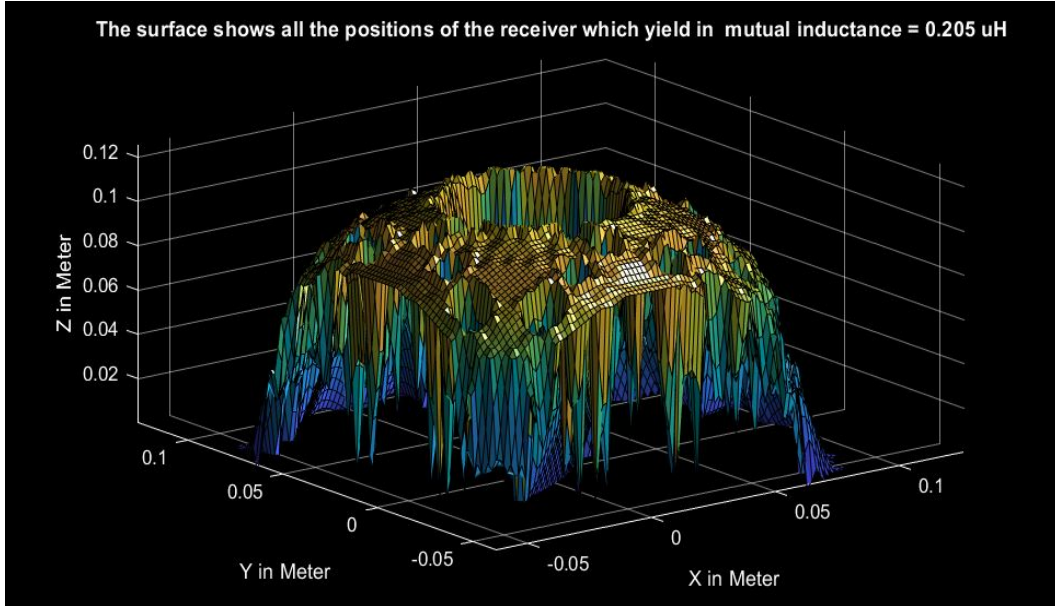


Figure 4.26: The measured value of mutual inductance ($M=0.205 \mu\text{H}$) could be a result of any position of receiver belonging to the surface shown here. The color just shows the Z component of the possible locations.

$$Z=41.1-66.13j$$

12. We put this input impedance in the equation 4.25 and we solve it for M and we get, $M=0.417 \mu\text{H}$.

13. This value of the mutual inductance is compared with the pre-calculated mutual inductance matrix of the coil 2 (corresponding to the configuration 2 of the transmitter) and all the possible positions of the receiver that would lead to the same measured mutual inductance in the volume of interest are determined. There are 3617 such possible positions. Fig.4.27 shows the results.

14. The real position of the receiver should belong to both surfaces shown in Fig.4.26 and Fig.4.27, so we take their intersection. There are 118 points that belong to both surfaces, shown in Fig.4.28.

15. The last step hugely reduced the number of possible positions of the receiver but it is still a large set of number (containing 118 different positions). To reduce it more we again change the configuration of the transmitter. We disconnect the coil number 2 and connect only coil number 3. Now we are in a configuration in which the transmitter is consisting of only coil number 3. Lets call it the configuration (3) of the transmitter.

16. We measure the input impedance of the antenna circuitry when the antenna is in the configuration 3.

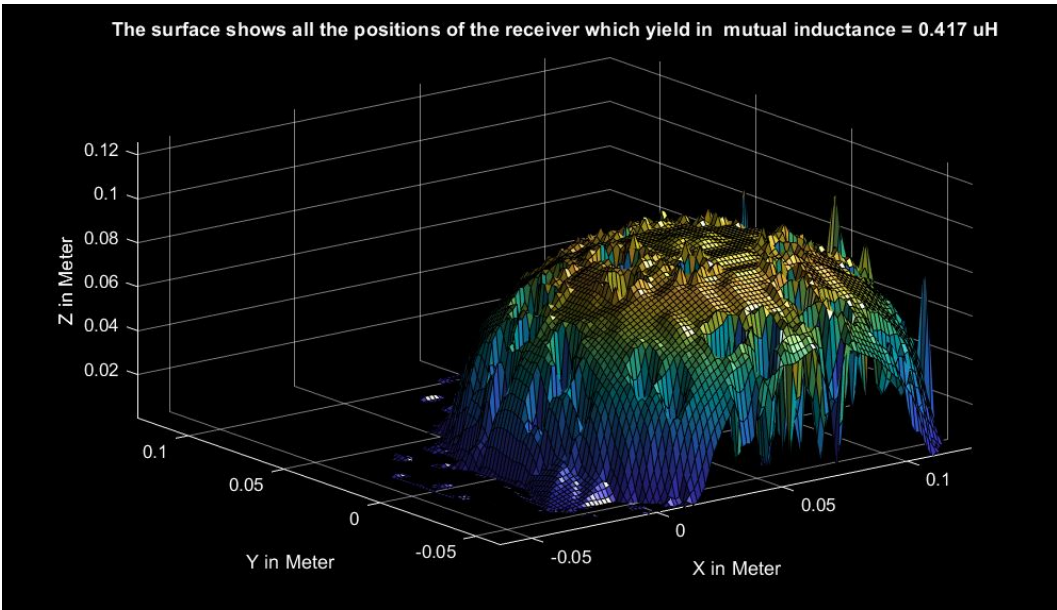


Figure 4.27: The measured value of mutual inductance ($M=0.417 \mu\text{H}$) could be a result of any positions of receiver belonging to the surface shown here.

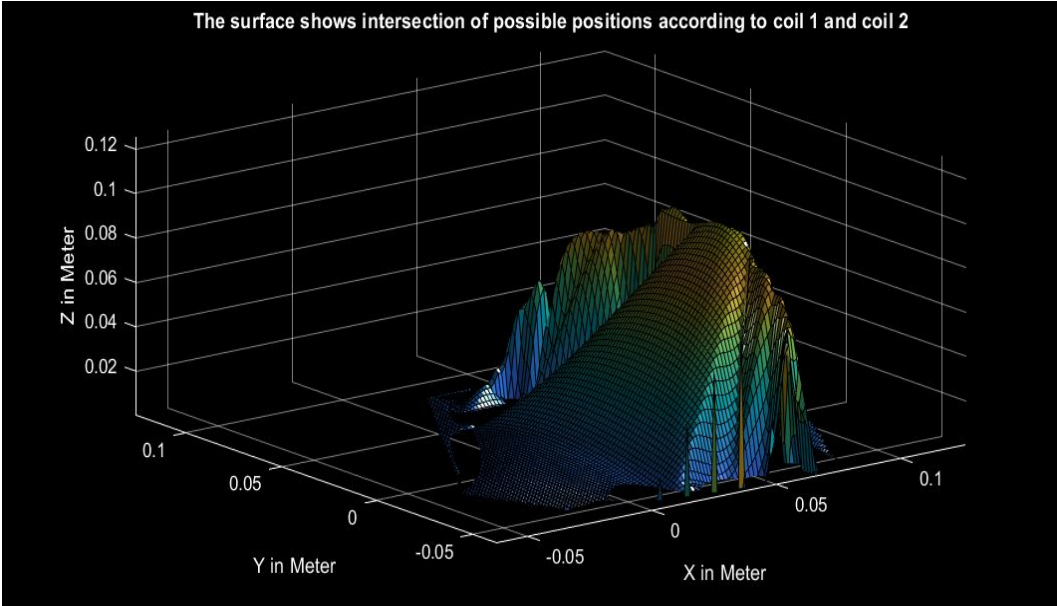


Figure 4.28: The surface shows the intersection of possible positions according to coil 1 and coil 2.

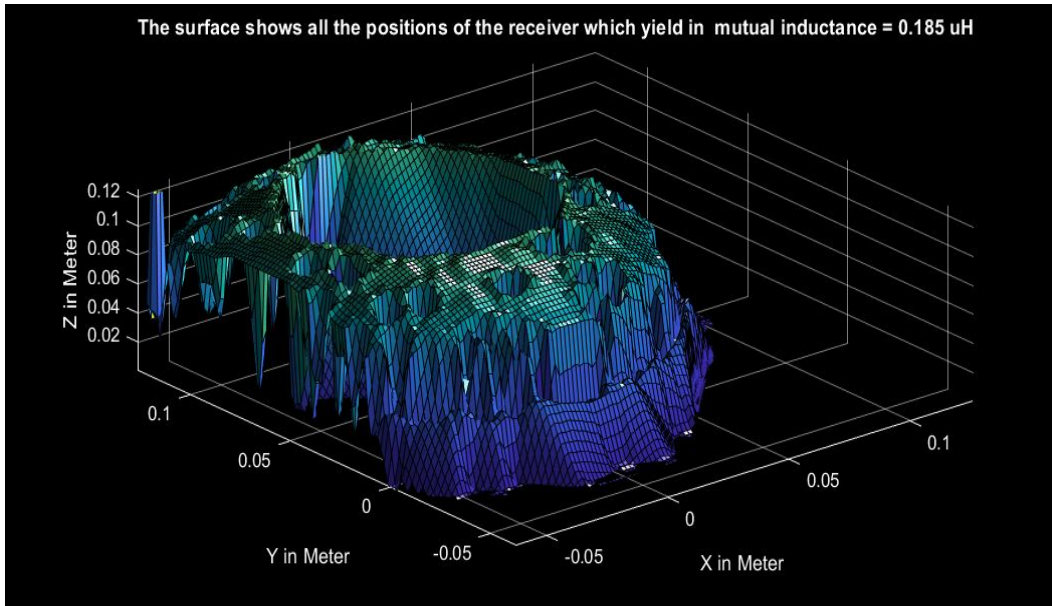


Figure 4.29: The measured value of mutual inductance ($M=0.185 \mu\text{H}$) could be a result of any positions of receiver belonging to the surface shown here.

17. We find the input impedance to be:
 $Z=43.3-13.14j$

18. We put this input impedance in the equation 4.25 and we solve it for M and we get, $M=0.185 \mu\text{H}$.

19. This value of the mutual inductance is compared with the pre-calculated mutual inductance matrix of the coil 3 (corresponding to the configuration 3 of the transmitter). There are 4222 such possible positions. Fig.4.29 shows the results.

20. The real position of the receiver should belong to both surfaces shown in Fig.4.28 and Fig.4.29, so we take their intersections. There are just 3 possible positions that belong to both surfaces. They are:

- $X=0.0740$ $Y=0.0339$ $Z= 0$
- $X=0.0760$ $Y=0.0362$ $Z= 0$
- $X=0.0693$ $Y=0.0268$ $Z= 0.0866$

21. Though last steps reduced the number of possible positions to just 3, and the X and Y component in all three possible positions are close but there is a big difference in Z component. One possible position is in $Z= 8$ cm and two others in $Z=0$ cm. To decide which one is the answer we disconnect the coil number 3 and connect only coil number 4. Now we are in a configuration in which the transmitter is consisting of only coil number 4. Lets call it the configuration (4) of the transmitter.

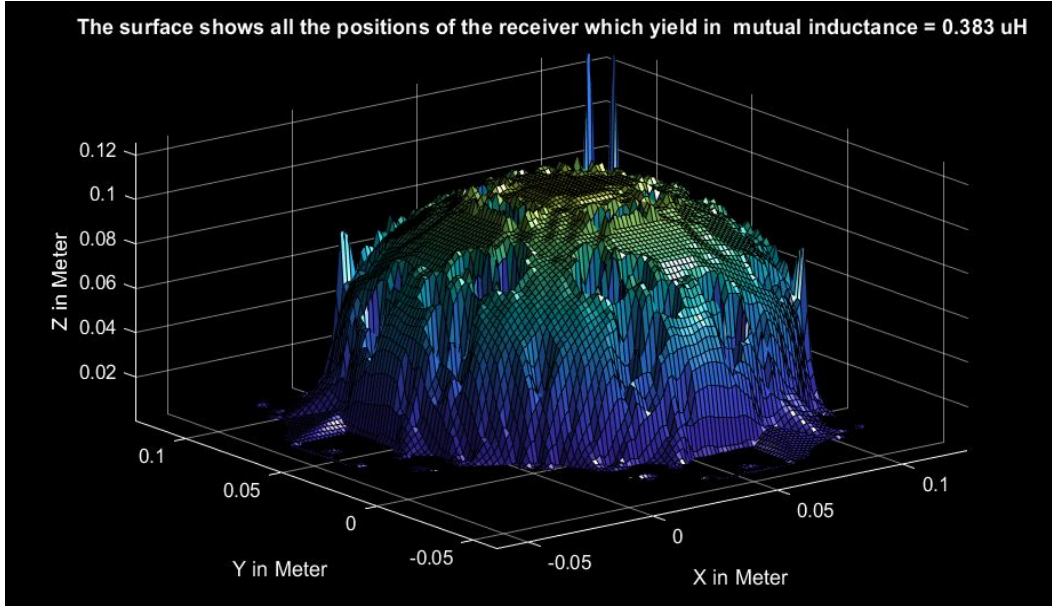


Figure 4.30: The measured value of mutual inductance ($M=0.383 \mu\text{H}$) could be a result of any positions of receiver belonging to the surface shown here.

22. We measure the input impedance of the antenna circuitry when the antenna is in the configuration 4.

23. We find the input impedance to be:
 $Z=42.45-59.13j$

24. We put this input impedance in the equation 4.25 and we solve it for M and we get, $M=0.383 \mu\text{H}$.

25. This value of the mutual inductance is compared with the pre-calculated mutual inductance matrix of the coil 4 (corresponding to the configuration 4 of the transmitter). There are 3508 such possible positions. Fig.4.30 shows the results.

26. The real position of the receiver should belong to the surfaces shown in Fig.4.30 and the three positions we get in step 20. So we take their intersection. There are just 1 possible positions that belong to both and it is:

- $X=0.0693$ $Y=0.0268$ $Z= 0.0866$ (meter)

27. This is a unique answer and could not be reduced more. The localization is completed.

If we compare this position that we found through our algorithm to the real position of the receiver, we find them to be close. However there are some errors. To estimating the error, the mean absolute error (MAE) is used according to:

CHAPTER 4. ONE PORT RECONFIGURABLE COIL GRID FOR RECEIVER
LOCALIZATION IN INDUCTIVE POWER TRANSFER

Experiment	The real position of the receiver	The deduced position of the receiver	MAE	MAE normalized to the receiver diameter
Experiment 1	X=73 mm, Y=24 mm, Z= 78 mm	X= 69 mm, Y=26 mm, Z= 87 mm	5 mm	5%
Experiment 2	X=40 mm, Y=30 mm, Z=67 mm	X= 41 mm, Y=29 mm, Z=76 mm	3.6 mm	3.6%
Experiment 3	X=0 mm, Y=40 mm, Z= 50 mm	X=-7 mm , Y=41 mm, Z= 59 mm	5.6 mm	5.6%
Experiment 4	X =92 mm, Y =21 mm, Z = 99 mm	X =82 mm, Y =30 mm, Z = 109 mm	9.6 mm	9.6%

Table 4.3: Experimental results for localization.

$$MAE = \frac{\sum_{i=1}^n |y_i - x_i|}{n} \quad (4.28)$$

Where::

- the y_i is the deduced values of position (that is the deduced X, Y and Z coordinates in each experiment)
- x_i the real values of position (that is the actual X, Y and Z coordinates in each experiment)
- n is the number of coordinates for each position which in our case is three.

We put the receiver in the location (X=73 mm, Y=24 mm and Z=78 mm), and the algorithm we performed localized the receiver to be at (X=69.3 mm, Y=26.8 mm and Z=86.6 mm). The mean absolute error (MAE) is:

$$MAE = \frac{\sum_{i=1}^n |y_i - x_i|}{n} = \frac{|(73 - 69.3)| + |(24 - 26.8)| + |(78 - 86.6)|}{3} = 5mm \quad (4.29)$$

To put this error in perspective we normalize it in respect to the diameter of the receiver which is 100 mm, and we get normalized MAE to be 5%.

To make sure that we were not just lucky in getting results and the algorithm is reliable, we repeated the process for other arbitrary positions in the volume of interest. By repeating the process for each position we want to see if we are able to localize the receiver coil position successfully. Table 4.4 shows the results.

What is the source of the error in the localization?

In the previous chapter in localization in two ports network we mentioned some of the sources of this error. Here in localization in one port network those previously mentioned

sources of errors are also again sources of errors and we will not repeat them here again. The new source of error (which increases the error) is the inaccuracy in the numeric values of components constituting the transmitter antenna circuitry and the receiver circuitry. Though these component are measured carefully before fabricating the circuits, this measurement is not perfect (like all other measurements) and has some inaccuracy. When these inaccurate values are substituted in equation 4.25 they affect the calculated M as a function of input impedance. Beside this, during the fabrication and connecting different elements we create stray capacitors which in turn affect the deduced M . The error in deduced M translates itself in error in localization.

However, even with these errors still the localization could be performed with acceptable accuracy as we can see from table 4.4.

We also should mention the time that the algorithm takes to be performed. In our case we used MATLAB software to perform the algorithm, but we did not used any specific MATLAB function. So it could be implemented and programmed easily in any micro controller. Calculating the pre-calculated mutual inductance is time consuming. But it is a task which should be performed just once before starting the algorithm, So the time it takes is not important.

The memory required to store each of these pre-calculated mutual inductance of course depends on the size of volume of interest and the 3D grid that we are using, for each point in the volume of interest the pre-calculated mutual inductance will have one entry. In this example the required memory for each pre-calculated mutual inductance was 500 kB. The time of performing the algorithm itself also depends on the size of volume of interest and the 3D grid and the speed of the computer or the micro controller that run the code. In this example, we used a computer with processor of 2.30 GHz speed and 8 GB memory. The average execution time was two seconds. When a certain micro controller is given one should reduce the size of the 3D grid to keep the algorithm an algorithm which executes in real time. This of course will reduce the resolution of localization. This is an inescapable trade off.

4.5 CONCLUSION

In this chapter we extended and completed the algorithm that we introduced in the previous chapter. In previous chapter we implement our algorithm to a two ports network. That is same thing as saying we have access to both transmitter and the receiver. Having access to the transmitter is simple but having access to the receiver is not practical in most realistic situations. In this chapter, we showed that if we add resonance and matching parts to the transmitter antenna and the receiver antenna, it becomes possible to deduce the value of mutual inductance between the transmitter and the receiver from measuring the input impedance of the transmitter without any need to access the receiver. The deduced value of mutual inductance could be used for performing the localization algorithm as it was explained in previous chapter. Simulations were done by using a MATLAB code and its applicability was demonstrated by running a set of experiments. The experimental results show that the algorithm operates as expected.

If the same procedure is performed continuously, one could track dynamically the movement of the receiver.

We assumed that there is just one receiver in the volume of interest. If we want to extend it to the case in which we have more than one receiver in the volume of interest (say two receivers) one should change the pre-calculated mutual inductance matrix for each transmitter coil to contain all combination of all possible positions of two receivers in the volume of interest. This will require some modification of the algorithm (and more required memory for the controlling part of the transmitter). But we could not say it for sure. It could be one of the prospective at this point.

It was assumed that the receiver is in an unknown position but always parallel to the transmitter. This assumption was made for the sake of simplicity. The algorithm could be modified for localizing a receiver in a more general situation in which the receiver could have any arbitrary orientation.

We should mention that the algorithm could be easily integrated in presently in-use system to add to them (if it is required) the ability of localization.

At the end it should be mentioned that we performed simulations and experiments for certain arbitrary size of volume of interest for the sake of demonstrations. In real life scenario, the volume of interest depends on the application on hands and it should be given to us in prior.

However the algorithm could be adapted to any required size of volume of interest if the size of the transmitter coils and the number of such transmitter coils which makes the transmitter grids, are chosen in appropriate way. The algorithm is easily scalable and it could be applied to much larger volume of interest which we examined here, because the small volume of interest makes fabrication and simulation more convenient.

Extending the volume of interest to larger scale and examining the algorithm in larger scale could be another perspective of this work and the next step.

CONCLUSION

In This work we tried to address the problem of IPT deficiency due to mutual inductance deficiency between the receiver and the transmitter.

The first method we proposed, was based on the TLAs (Twisted Loop Antenna) that could be considered as an array of coils. Different structures of TLA indeed create different pattern of electric current. In its turn different patterns of electric current, create different patterns of magnetic fields. Therefore it gives us a way for controlling the magnetic field by controlling which TLA is excited and which TLA is not excited.

This method is very well known for far-field radiation, and we applied it to near-fields.

The same method could be used to increase the range of wireless power transfer. The idea of using array-like structure to increase the efficiency of power transfer was proposed earlier, however, we here followed a new approach and proposed an application of this principle, namely a system which guarantees power transfer regardless of misalignment between sender and receiver. The simulation was performed followed by measurements. Measurements showed good agreement between calculation and the measured values for the mutual inductances, which confirms the feasibility of the method. However if there are a few receivers or even just one of them (for example for wireless charging of robots, cars, drones,...) though the method still should work, but it does not seem to be a very efficient approach. The reason is that the effective mutual inductance the receiver coil will have in this method is the average of mutual inductances the receiver coil have in each step.

This happens because if in one step we have a magnetic field which creates suitable mutual inductance for the receiver, that magnetic field will change in the next step and in this new step the magnetic field is not necessarily suitable any more and the receiver should wait till the repetition of the configuration that generates suitable magnetic field.

If there is a few receivers or just even one receiver, it is not any more an efficient way.

A better possible solution is to have some kind of localization. When the localization is done, the magnetic field could be steered in a way which is optimal for the particular position and the orientation of the receiver.

It should be mentioned that though we here mentioned localization as a method for enhancing magnetic coupling, the ability of localization by itself is an interesting subject to be considered.

For doing so we proposed an algorithm based on measuring the mutual inductance between the transmitter and the receiver. In this case the transmitter is a grid of circular coils. But the idea is general and could be applied to other kind of transmitter grid as well. The measured mutual inductance between the transmitter and receiver could be used for localization of the receiver. This method needs a priori knowledge about the volume of interest. This is a region around the transmitter in which the receiver could be localized. We also need to calculate what we called the pre-calculated matrix of mutual inductance.

Simulations were done by using a specific MATLAB code and its applicability was demonstrated by running a set of experiments.

The experimental results show that the algorithm operates as expected and it is possible to localize the receiver depending on its magnetic mutual coupling with the transmitter. If the same procedure is performed continuously, one could track dynamically the movement of the receiver. It was assumed that the receiver is in an unknown position but always parallel to the transmitter. This assumption was made for the sake of simplicity and does not affect the algorithm principle and utility. The algorithm could be modified for localizing a receiver in a more general situation in which the receiver could have any arbitrary orientation, and this modification will be one of the perspective of this work. However this assumption is not a real limitation.

The real limitation comes from considering more than one receiver. The algorithm in its current state is capable of localizing one receiver in the volume of interest. If we want to localize more than one receiver, we should calculate the pre-calculated mutual inductance matrix for each coil of the transmitter and all combination of the receiver in their different possible position. As the number of receivers is few the code could be generalized to deal with these situations. But increasing the number of receivers will increase the required memory and computational power of the system and it will stop to be applicable (or at least not in the real time). This is a real limitation and overcoming it is another one of the perspective of this work. But one should remember that in case of having a number of distributed receivers in the volume of interest, the proposed method in chapter 2 becomes more relevant and in this case the localization probably is not necessary.

After localization also it was shown how the knowledge about the receiver location could be used to enhance the magnetic coupling between the transmitter and the receiver: by means of a switchable grid of coils to steer the magnetic field properly towards the receiver. This beam forming approach allows to increase the mutual inductance between the transmitter and the receiver and to increase the efficiency of such inductive power transfer systems.

Until this point we were working with a two ports network. That is same thing as saying we have access to both transmitter and the receiver. Having access to the transmitter is simple but having access to the receiver is not practical in most realistic situations. In our next step we showed that if we add resonance and matching parts to the transmitter antenna and the receiver antenna, it becomes possible to deduce the value of mutual inductance between the transmitter and the receiver from measuring the input impedance of the transmitter without any need to access the receiver. The deduced value of mutual inductance could be used for performing the localization algorithm as it was explained earlier. In this case also, simulations were done by using a MATLAB code and its applicability was demonstrated by running a set of experiments. The experimental results show that the algorithm operates as expected.

In both cases we have some error in localization. As one expect the error in the one port network to be more than error in two port networks. However even with this error the method seems to localize the receiver in more or less acceptable accuracy. This accuracy could be controlled to match the required accuracy for concrete applications.

Bibliography

- [1] Traian E. Abrudan et al. “Distortion Rejecting Magneto-Inductive Three-Dimensional Localization (MagLoc)”. In: *IEEE Journal on Selected Areas in Communications* 33.11 (2015), pp. 2404–2417. DOI: 10.1109/JSAC.2015.2430518.
- [2] Traian E. Abrudan et al. “Underground Incrementally Deployed Magneto-Inductive 3-D Positioning Network”. In: *IEEE Transactions on Geoscience and Remote Sensing* 54.8 (2016), pp. 4376–4391. DOI: 10.1109/TGRS.2016.2540722.
- [3] Johnson I. Agbinya. *Wireless Power Transfer 2nd Edition*. 2016.
- [4] Mohd Yazed Ahmad and Ananda Sanagavarapu Mohan. “Novel Bridge-Loop Reader for Positioning With HF RFID Under Sparse Tag Grid”. In: *IEEE Transactions on Industrial Electronics* 61.1 (2014), pp. 555–566. DOI: 10.1109/TIE.2013.2245617.
- [5] Mohd Yazed Ahmad and Ananda Sanagavarapu. “Multiple-bridge-loop reader antenna for improved positioning and localisation”. In: *Electronics Letters* 48 (Aug. 2012), pp. 979–980. DOI: 10.1049/e1.2012.1930.
- [6] Megdouda Benamara et al. “A Twisted Loop Antenna to enhance HF RFID detection for different tag positioning”. In: *2016 10th European Conference on Antennas and Propagation (EuCAP)*. 2016, pp. 1–5. DOI: 10.1109/EuCAP.2016.7481810.
- [7] Zhang Bin and Hao Xiao-hong. “Modeling and analysis of wireless power transmission system via strongly coupled magnetic resonances”. In: *2014 International Conference on Mechatronics and Control (ICMC)*. 2014, pp. 70–75. DOI: 10.1109/ICMC.2014.7231519.
- [8] Joaquin J. Casanova, Zhen Ning Low, and Jenshan Lin. “A Loosely Coupled Planar Wireless Power System for Multiple Receivers”. In: *IEEE Transactions on Industrial Electronics* 56.8 (2009), pp. 3060–3068. DOI: 10.1109/TIE.2009.2023633.
- [9] Joaquin J. Casanova, Zhen Ning Low, and Jenshan Lin. “Magneto-Inductive Waveguide”. In: *Electronics Letters* 38.8 (2002), pp. 371–373. DOI: 10.1049/e1:20020258.
- [10] Luca Catarinucci et al. “Smart RFID Antenna System for Indoor Tracking and Behavior Analysis of Small Animals in Colony Cages”. In: *IEEE Sensors Journal* 14.4 (2014), pp. 1198–1206. DOI: 10.1109/JSEN.2013.2293594.
- [11] Matthew J. Chabalko and Alanson P. Sample. “Three-Dimensional Charging via Multimode Resonant Cavity Enabled Wireless Power Transfer”. In: *IEEE Transactions on Power Electronics* 30.11 (2015), pp. 6163–6173. DOI: 10.1109/TPEL.2015.2440914.

- [12] Bang-Jun Che, Fan-Yi Meng, and Qun Wu. “An omnidirectional wireless power transmission system with controllable magnetic field distribution”. In: *2016 IEEE International Workshop on Electromagnetics: Applications and Student Innovation Competition (iWEM)*. 2016, pp. 1–3. DOI: 10.1109/iWEM.2016.7504898.
- [13] Bo H. Choi et al. “A Novel Source-Side Monitored Capacitive Power Transfer System for Contactless Mobile Charger Using Class-E Converter”. In: *2014 IEEE 79th Vehicular Technology Conference (VTC Spring)*. 2014, pp. 1–5. DOI: 10.1109/VTCSpring.2014.7023151.
- [14] Bo H. Choi et al. “Six Degrees of Freedom Mobile Inductive Power Transfer by Crossed Dipole Tx and Rx Coils”. In: *IEEE Transactions on Power Electronics* 31.4 (2016), pp. 3252–3272. DOI: 10.1109/TPEL.2015.2449290.
- [15] Samuel R. Cove et al. “Improving Wireless Power Transfer Efficiency Using Hollow Windings With Track-Width-Ratio”. In: *IEEE Transactions on Power Electronics* 31.9 (2016), pp. 6524–6533. DOI: 10.1109/TPEL.2015.2498638.
- [16] Ashok Das. *Lectures on Electromagnetism*. 2013.
- [17] Daniel M. Dobkin. *The RF in RFID*. 2008.
- [18] Klaus Finkenzeller. *RFID HANDBOOK*. 2010.
- [19] Dany Fortin-Simard et al. “Accurate passive RFID localization system for smart homes”. In: *2012 IEEE 3rd International Conference on Networked Embedded Systems for Every Application (NESEA)*. 2012, pp. 1–8. DOI: 10.1109/NESEA.2012.6474010.
- [20] M. Grzeskowiak et al. “Sub-coil in reader antenna for HF RFID volume detection improvement”. In: *2017 IEEE International Conference on RFID Technology Application (RFID-TA)*. 2017, pp. 134–139. DOI: 10.1109/RFID-TA.2017.8098871.
- [21] M. Grzeskowiak et al. “Sub-coil in reader antenna for HF RFID volume detection improvement”. In: *2017 IEEE International Conference on RFID Technology Application (RFID-TA)*. 2017, pp. 134–139. DOI: 10.1109/RFID-TA.2017.8098871.
- [22] Marjorie Grzeskowiak et al. “Distributed Diameter Subcoil Twisted Loop Antenna in Nonradiative WPT”. In: *IEEE Antennas and Wireless Propagation Letters* 17.1 (2018), pp. 4–7. DOI: 10.1109/LAWP.2017.2767020.
- [23] Marjorie Grzeskowiak et al. “Distributed Diameter Subcoil Twisted Loop Antenna in Nonradiative WPT”. In: *IEEE Antennas and Wireless Propagation Letters* 17.1 (Jan. 2018), pp. 4–7. DOI: 10.1109/LAWP.2017.2767020. URL: <https://hal-centralesupelec.archives-ouvertes.fr/hal-01691560>.
- [24] Sherif Hekal, Ahmed Allam, and Adel B. Abdel-Rahman and Ramesh K. Pokharel. *Compact Size Wireless Power Transfer Using Defected Ground Structures*. 2019.
- [25] <https://getcorp.com/>.
- [26] <https://www.ansys.com>.
- [27] <https://www.femm.info/wiki/HomePage>.
- [28] <https://www.mikroe.com/rfid-reader-board>.
- [29] <https://www.nilase.top/products.aspx?cname=iphone+x+wireless+charging+coil&cid=106&xi=1&xc=22>.
- [30] <https://www.wirelesschargingcoil.com/wireless-charging-solution/>.

- [31] Hao Hu and Stavros V. Georgakopoulos. “Analysis and design of broadband Wireless Power Transmission system via conformal Strongly Coupled Magnetic Resonance”. In: *WAMICON 2014*. 2014, pp. 1–4. DOI: 10.1109/WAMICON.2014.6857760.
- [32] S. Y. Hui. “Planar Wireless Charging Technology for Portable Electronic Products and Qi”. In: *Proceedings of the IEEE* 101.6 (2013), pp. 1290–1301. DOI: 10.1109/JPROC.2013.2246531.
- [33] S. Y. R. Hui, Wenxing Zhong, and C. K. Lee. “A Critical Review of Recent Progress in Mid-Range Wireless Power Transfer”. In: *IEEE Transactions on Power Electronics* 29.9 (2014), pp. 4500–4511. DOI: 10.1109/TPEL.2013.2249670.
- [34] Jackson. *Classical Electrodynamics*.
- [35] Abbas Jamalipour and Ying Biand. *Wireless Powered Communication Networks*. 2019.
- [36] Sangyeong Jeong et al. “Analytical investigation of optimal wireless power transfer topology for electric vehicles”. In: *2015 IEEE PELS Workshop on Emerging Technologies: Wireless Power (2015 WoW)*. 2015, pp. 1–5. DOI: 10.1109/WoW.2015.7132836.
- [37] Olutola Jonah, Stavros V. Georgakopoulos, and Manos M. Tentzeris. “Orientation insensitive power transfer by magnetic resonance for mobile devices”. In: *2013 IEEE Wireless Power Transfer (WPT)*. 2013, pp. 5–8. DOI: 10.1109/WPT.2013.6556868.
- [38] Marian P. Kazmierkowski, Rafał M. Miskiewicz, and Artur J. Moradewicz. “Inductive coupled contactless energy transfer systems - a review”. In: *2015 Selected Problems of Electrical Engineering and Electronics (WZEE)*. 2015, pp. 1–6. DOI: 10.1109/WZEE.2015.7394025.
- [39] Kyungtae Kim, Han-Joon Kim, and Ji-Woong Choi. “Magnetic beamforming with non-coupling coil pattern for high efficiency and long distance wireless power transfer”. In: *2017 IEEE Wireless Power Transfer Conference (WPTC)*. 2017, pp. 1–4. DOI: 10.1109/WPT.2017.7953869.
- [40] S. Kisseleff, I. F. Akyildiz, and W. Gerstacker. “Beamforming for Magnetic Induction Based Wireless Power Transfer Systems with Multiple Receivers”. In: *2015 IEEE Global Communications Conference (GLOBECOM)*. 2015, pp. 1–7. DOI: 10.1109/GLOCOM.2015.7417006.
- [41] Steven Kisseleff, Ian F. Akyildiz, and Wolfgang H. Gerstacker. “Throughput of the Magnetic Induction Based Wireless Underground Sensor Networks: Key Optimization Techniques”. In: *IEEE Transactions on Communications* 62.12 (2014), pp. 4426–4439. DOI: 10.1109/TCOMM.2014.2367030.
- [42] Mitchell Kline et al. “Capacitive power transfer for contactless charging”. In: *2011 Twenty-Sixth Annual IEEE Applied Power Electronics Conference and Exposition (APEC)*. 2011, pp. 1398–1404. DOI: 10.1109/APEC.2011.5744775.
- [43] Byunghun Lee and Yaoyao Jia. “Wirelessly-Powered Cage Designs for Supporting Long-Term Experiments on Small Freely Behaving Animals in a Large Experimental Arena”. In: *Electronics* 9 (Nov. 2020), p. 1999. DOI: 10.3390/electronics9121999.
- [44] Eun S. Lee et al. “Six Degrees of Freedom Wide-Range Ubiquitous IPT for IoT by DQ Magnetic Field”. In: *IEEE Transactions on Power Electronics* 32.11 (2017), pp. 8258–8276. DOI: 10.1109/TPEL.2017.2691063.

- [45] Jianchao Li et al. “Electromagnetic Induction Position Sensor Applied to Anti-Misalignment Wireless Charging for UAVs”. In: *IEEE Sensors Journal* 20.1 (2020), pp. 515–524. DOI: 10.1109/JSEN.2019.2940925.
- [46] Deyan Lin, S. Y. Ron Hui, and Cheng Zhang. “Omni-directional wireless power transfer systems using discrete magnetic field vector control”. In: *2015 IEEE Energy Conversion Congress and Exposition (ECCE)*. 2015, pp. 3203–3208. DOI: 10.1109/ECCE.2015.7310110.
- [47] Deyan Lin, Cheng Zhang, and S. Y. Ron Hui. “Mathematic Analysis of Omnidirectional Wireless Power Transfer—Part-II Three-Dimensional Systems”. In: *IEEE Transactions on Power Electronics* 32.1 (2017), pp. 613–624. DOI: 10.1109/TPEL.2016.2523506.
- [48] Deyan Lin, Cheng Zhang, and S. Y. Ron Hui. “Mathematical Analysis of Omnidirectional Wireless Power Transfer—Part-I: Two-Dimensional Systems”. In: *IEEE Transactions on Power Electronics* 32.1 (2017), pp. 625–633. DOI: 10.1109/TPEL.2016.2523500.
- [49] Deyan Lin, Cheng Zhang, and S. Y. Ron Hui. “Power and efficiency of 2-D omni-directional wireless power transfer systems”. In: *2015 IEEE Energy Conversion Congress and Exposition (ECCE)*. 2015, pp. 4951–4958. DOI: 10.1109/ECCE.2015.7310358.
- [50] Liu X, Ho WC, Hui SYR, Chan WC (2011) *Localized charging, load identification and bidirectional communication methods for a planar inductive battery charging system*. U.S. Patent 7 915 858, 29 Mar 2011.
- [51] Alicia Triviño-Cabrera and José M. González-González and José A. Aguado. *Wireless Power Transfer for Electric Vehicles: Foundations and Design Approach*. 2020.
- [52] Erik Marinissen et al. “Contactless testing: Possibility or pipe-dream?” In: Apr. 2009, pp. 676–681. DOI: 10.1109/DATE.2009.5090751.
- [53] Andrew Markham et al. “Magneto-Inductive Tracking of Underground Animals”. In: *Proceedings of the 8th ACM Conference on Embedded Networked Sensor Systems*. SenSys ’10. Zürich, Switzerland: Association for Computing Machinery, 2010, pp. 365–366. ISBN: 9781450303446. DOI: 10.1145/1869983.1870025. URL: <https://doi.org/10.1145/1869983.1870025>.
- [54] Mehrnoush Masihpour and Johnson I Agbinya. “Cooperative relay in Near Field Magnetic Induction: A new technology for embedded medical communication systems”. In: *2010 Fifth International Conference on Broadband and Biomedical Communications*. 2010, pp. 1–6. DOI: 10.1109/IB2COM.2010.5723612.
- [55] Iker Mayordomo et al. “An Overview of Technical Challenges and Advances of Inductive Wireless Power Transmission”. In: *Proceedings of the IEEE* 101.6 (2013), pp. 1302–1311. DOI: 10.1109/JPROC.2013.2243691.
- [56] SangCheol Moon et al. “Analysis and design of wireless power transfer system with an intermediate coil for high efficiency”. In: *2013 IEEE ECCE Asia Downunder*. 2013, pp. 1034–1040. DOI: 10.1109/ECCE-Asia.2013.6579235.
- [57] CLAYTON R. PAUL. *INDUCTANCE Loop and Partial*. 2010.
- [58] Venugopal Prasanth and Pavol Bauer. “Distributed IPT Systems for Dynamic Powering: Misalignment Analysis”. In: *IEEE Transactions on Industrial Electronics* 61.11 (2014), pp. 6013–6021. DOI: 10.1109/TIE.2014.2311380.

- [59] Nannapaneni Narayana Rao. *Elements of Engineering Electromagnetics*. 2018.
- [60] Chun T. Rim and Chris Mi. *Wireless Power Transfer for Electric Vehicles and Mobile Devices*. 2017.
- [61] Alanson P. Sample, David T. Meyer, and Joshua R. Smith. “Analysis, Experimental Results, and Range Adaptation of Magnetically Coupled Resonators for Wireless Power Transfer”. In: *IEEE Transactions on Industrial Electronics* 58.2 (2011), pp. 544–554. DOI: 10.1109/TIE.2010.2046002.
- [62] Naoki Shinohara. *Wireless Power Transfer*. 2018.
- [63] Imura Takehiro. *Wireless Power Transfer Using Magnetic and Electric Resonance-Coupling Techniques*. 2020.
- [64] Nam Ha-Van and Chulhun Seo. “Analytical and Experimental Investigations of Omnidirectional Wireless Power Transfer Using a Cubic Transmitter”. In: *IEEE Transactions on Industrial Electronics* 65.2 (2018), pp. 1358–1366. DOI: 10.1109/TIE.2017.2733470.
- [65] Dongyang Wang et al. “Enabling multi-angle wireless power transmission via magnetic resonant coupling”. In: *2012 7th International Conference on Computing and Convergence Technology (ICCCT)*. 2012, pp. 1395–1400.
- [66] *Wireless Power Consortium (2012) [Online]*. <http://www.wirelesspowerconsortium.com>.
- [67] Lei Yang et al. “Accurate and Efficient Object Tracking Based on Passive RFID”. In: *IEEE Transactions on Mobile Computing* 14.11 (2015), pp. 2188–2200. DOI: 10.1109/TMC.2014.2381232.
- [68] Zhao-Hong Ye et al. “Energy Efficiency Analysis of U-Coil Wireless Power Transfer System”. In: *IEEE Transactions on Power Electronics* 31.7 (2016), pp. 4809–4817. DOI: 10.1109/TPEL.2015.2483839.
- [69] Cheng Zhang, Deyan Lin, and S. Y Hui. “Basic Control Principles of Omnidirectional Wireless Power Transfer”. In: *IEEE Transactions on Power Electronics* (2016).
- [70] Jiantao Zhang, Chunbo Zhu, and C.C. Chan. “A wireless power charging method for Automated Guided Vehicle”. In: *2014 IEEE International Electric Vehicle Conference (IEVC)*. 2014, pp. 1–5. DOI: 10.1109/IEVC.2014.7056153.
- [71] Zhen Zhang et al. “Wireless Power Transfer—An Overview”. In: *IEEE Transactions on Industrial Electronics* 66.2 (2019), pp. 1044–1058. DOI: 10.1109/TIE.2018.2835378.
- [72] Wenxing Zhong and Dehong Xu and Ron Shu Yuen Hui. *Wireless Power Transfer*. 2020.
- [73] Wenxing Zhong and Dehong Xu and Ron Shu Yuen Hui. *Wireless Power Transfer*. 2020.
- [74] Qi Zhu et al. “Field Orientation Based on Current Amplitude and Phase Angle Control for Wireless Power Transfer”. In: *IEEE Transactions on Industrial Electronics* 65.6 (2018), pp. 4758–4770. DOI: 10.1109/TIE.2017.2767556.

ABSTRACT

Inductive Power Transfer) is an approach based on magnetic coupling to realize a WPT (Wireless Power Transfer) system. In applications using IPT as a mean for transferring power, like RFID, it is of great interest to have a free positioning system, meaning without or at least fewer constraints on relative positioning and orientation between the sender and the receiver. One of the problems which face the free positioning WPT by using IPT is the great sensitivity of the system to lateral and orientational misalignment between the sender and the receiver of power. This could hugely reduce the efficiency of the whole system for certain lateral and orientational misalignments, resulting in null points for the coupling coefficient, therefore no power transfer in general or no detection in case of RFID (Radio Frequency Identification). Another subject related to IPT is the ability to localize the receiver. The ability of the transmitter to localize the receiver could be interesting for applications such as IoT (Internet of Things).

In Qi standards for wireless power transfer, the localization is performed by using a coils array. Here the resolution of localization is equal to the diameter of the coils in the transmitter array. Decreasing the diameter of coils in transmitters increases the resolution of localization but also reduces the range of power transfer. This is an inevitable trade-off. In this work we tried to address these problems.

RESUME

L'IPT (Inductive Power Transfer) est une approche basée sur le couplage magnétique pour réaliser un système WPT (Wireless Power Transfer). Dans les applications utilisant l'IPT comme moyen de transfert de puissance, comme la RFID, il est très intéressant d'avoir un système de positionnement libre, c'est-à-dire sans ou au moins avec moins de contraintes sur le positionnement et l'orientation relatifs entre l'émetteur et le récepteur. Ces contraintes sont là pour garantir une inductance mutuelle non nulle (ou un déficit d'inductance mutuelle). L'un des problèmes auxquels est confronté le WPT à positionnement libre en utilisant l'IPT est la grande sensibilité du système au désalignement latéral et d'orientation entre l'émetteur et le récepteur de puissance. Dans ce travail, nous essayons de résoudre le problème du transfert de puissance inductif (TPI) dû au manque d'inductance mutuelle entre le récepteur et l'émetteur.

La première méthode que nous proposons est basée sur les TLA (Twisted Loop Antenna) qui peuvent être considérées comme un réseau de bobines. La deuxième méthode que nous proposons est d'avoir une sorte de localisation. Lorsque la localisation est effectuée, le champ magnétique peut être dirigé de manière optimale pour la position et l'orientation particulières du récepteur. Il convient de préciser que, bien que nous ayons mentionné ici la localisation comme méthode d'amélioration du couplage magnétique, la capacité de localisation en elle-même est un sujet intéressant à considérer.